HARDNESS AND ADHESION OF THIN METALLIC FILMS

by

Robert M. Hill, A.R.C.S.T.

A Thesis

Submitted for the Degree of Doctor of Philosophy

in the Faculty of Science

University of Glasgow

April, 1958

ProQuest LLC.
789 East Eisenhower Parkway
P.O. Box 1346
Ann Arbor, MI 48106 – 1346

ACKNOWLEDGEMENTS

The author would like to acknowledge his indebtedness to Professor James S. Rankin, B.Sc., Ph.D., A.R.C.S.T.,M.I.Mech.E.,F.Inst.P., and to all the members of the Staff of the Department of Natural Philosophy of the Royal College of Science and Technology, Glasgow. In particular he would like to thank Mr. J.W.Sharpe,M.A., F.Inst.P., for the use of the electron microscope, Mr. M.Hamilton and the Staff of the Workshop for their assistance, and Mr. C.Weaver, B.Sc.,M.I.R.E.,A.R.T.C., A.M.I.E.E., for the use of the High Vacuum equipment and laboratory, and particularly for his continued assistance and encouragement. He would also like to acknowledge the receipt of maintenance grants from the Cross Trust, the Caird Trust and the Department of Scientific and Industrial Research.

ABSTRACT

The nature of the increased adhesion of evaporated reflecting films by the pre-deposition of a substrate layer of another metal has been investigated. The ageing of the films at room temperature and at 120°C. has been studied and the mechanism of the increased adhesion appears to be one of interdiffusion at the metallic interface and the formation of a transition structure. The structure of the best adhesion promoter, chromium, has been investigated using an extension of Schopper's theory of ellipsoidal particles.

C O N T E N T S

CONTENTS (Cont'd.)

CONTENTS (Cont'd.)

CONTENTS (Cont'd.)

CONTENTS (Cont'd.)

CHAPTER 1

INTRODUCTION

(a) Thin Films

The preparation of solid thin films by the technique of vacuum evaporation has become of increasing importance, particularly on an industrial scale. The process of vacuum evaporation consists of raising the temperature of a thermally stable material in vacuo in such a manner that the vapour pressure of the material becomes greater than the residual air pressure and evaporation takes place. The vapour condenses onto suitable surfaces surrounding the evaporating source. There can be little oxidation at the low pressure at which this is carried out, The free path of the residual molecules is generally considerably greater than the vacuum chamber dimensions, thus there will be little risk of molecular collisions in the evaporating beam on a large scale, and the majority of the condensing molecules will have arrived directly from the source. This gives a means of depositing on practically any given surface, that does not out-gas under vacuum, a metallic film which contours the surface perfectly. Such films can be used to determine the structure topography as in multiple beam

interferometric investigations and as front surface mirrors.

The production of such mirrors has been carried out for some time, a notable example being the large mirror at the Mount Palomar Observatory, but, unfortunately, for industrial uses the adhesions of such coatings to their backing plates is poor. The condensing plates are commonly made of glass because of the degree of surface finish that can be obtained and of the two metals commonly used as reflectors, aluminium and silver, the former has the better adhesion to glass. It has been known for some time that the adhesion of such coatings could be increased by the prior deposition of some materials that had themselves good adhesion to the backing. It has been suggested that chromium was such a metal and an earlier investigation has shown this to be the case[1].

(b) Previous Work

Adhesions of Films

The increases in adhesion produced by an under-layer were first measured in a quantitative way by Heavens[1]. A scratching device was used in which a pointer with a spherical tip was drawn across the surface of the reflecting film. The adhesion of the reflecting film where it had been deposited directly onto the glass itself

was first measured, then similar measurements were taken for the same film where it had been deposited on top of an initial evaporated layer of chromium and the difference between these two values was taken as a measure of the increase in adhesion. The actual measurement recorded was the load on the pointer required to just remove the films. Reflecting films of aluminium, silver and gold were investigated. The thicknesses of the chromium films were varied in the range 0-500A and graphs constructed of the increases in adhesion against the thickness of the substrate material. These are shown in Fig. 1.

The films were prepared in a vacuum of better than 10^{-4} mm. of mercury from high purity metal samples. No details were given for the time lapse between evaporation and measurement, which must have at least been some minutes, as the specimens would have to be removed from the evaporating chamber. Microscope slides were used as condensing plates; they were cleaned with a detergent and subjected to a glow discharge under vacuum for several minutes. On to each substrate film a reflecting film was evaporated until it was just opaque, the thickness of such a film being, for aluminium, 800-1,000A.

An investigation by electron diffraction was undertaken on similar films by Collins[2]. It was found

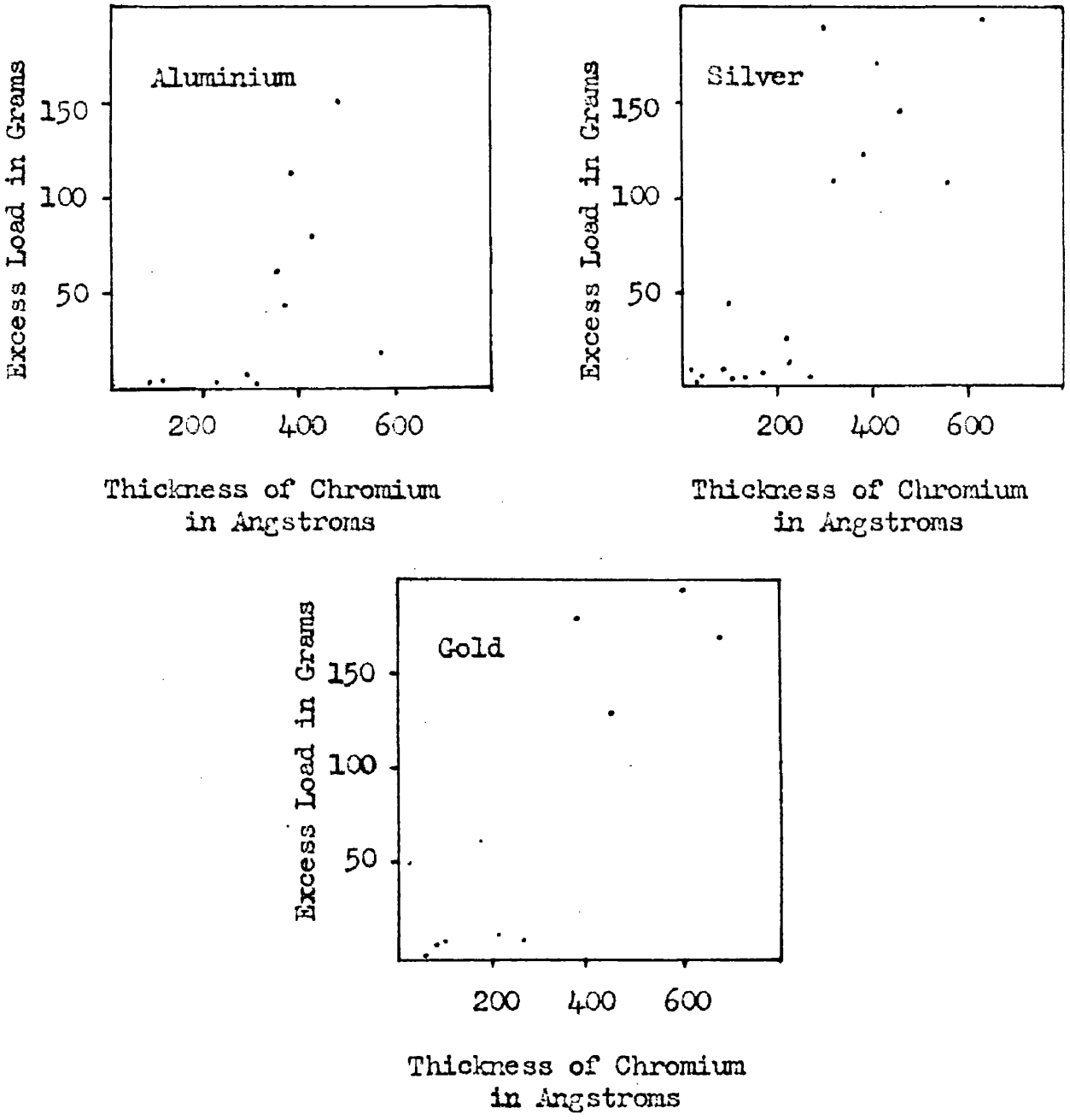

Fig.1. Heavens' Graphs of Adhesion against Thickness of Chromium Film.

Reproduced from J. de Physique Vol.11, 1950, p355.
13, 1952, p658.

that the structure of the films depended on the rate of evaporation. The faster evaporated films tended to show preferential orientation on the glass condensing plate, but when evaporated onto the chromium substrate no orientation was found. This was taken as evidence by Heavens and Collins[3] that there was being formed at the interface with the first monolayers of the reflecting film an embryo of different orientation from that in which the reflecting film preferred to grow. The conflict in growth forms then resulted in an un-oriented surface layer. Thus the adhesion was said to be due to an oriented overgrowth effect.

It was suggested that the steps apparent in the graphs in Fig. 1 were due to the formation of a critical thickness of the substrate at which the structure became continuous enough to support the embryo. The (110) plane of chromium having a structure fitting the (110) plane of aluminium with a low degree misfit, making it suitable for overgrowth phenomena to take place. However, Collins could not find any trace, by electron diffraction, of a change in the properties of chromium in the thickness region of 300A. Heavens, however, did find that when air was admitted into the vacuum chamber after evaporating the chromium and before evaporating the aluminium, there was

little increase in adhesion. This was considered to be due to the unsuitability of the oxidised surface of chromium as a support for the overgrowth. Assuming that the thicker films of chromium supported an oriented overgrowth, the small adhesions obtained for the thinner films could then be caused by these films forming as an aggregated layer which would not give the continuous structure required for orientation in the aluminium films.

Adhesion Measurements

Other methods of measuring the adhesion of evaporated films have been used[4,5]. These primarily give a measure of the resistance to marr of the specimen. Instead of a rounded tip either rubber, steel wool, or cotton wool has been rubbed across the film. The number of rubbing cycles, or the load, required to remove the film, or to increase the transmission of the film by a fixed amount, has been taken as the measurement of the adhesion. Such devices give only qualitative measurements, cause burnishing, and can hardly be used for such extensive examinations as those carried out by Heavens. The Scotch Tape[6] method has been favoured by a number of investigators. This consists of pressing onto the surface of a film a length of adhesive Scotch Tape, then stripping the tape

off. The fraction of the film also removed is taken as the adhesive measurement. This, however, does not allow comparative measurements to be made accurately, and indeed only shows up the weakly adherent areas in a particular deposit. Where the adhesions of a film are strong no measurement is possible as none of the film can be removed.

(c) Scope of Present Work

The work presented in this thesis can be divided into two sections, first an extension of the earlier work carried out by Heavens, then investigations into the nature of the transition layer between the metal films, and into the structure of films of the best adhesion promoting material - chromium.

Heavens' method of adhesion testing was used to investigate the adhesions obtained for a larger range of substrate layer metals. Aluminium was generaly taken as the reflecting film material, but silver, gold and copper were also used. A number of the transition metals were taken as the substrate materials, the only metal from outside this group being lead. After the films had been evaporated and the adhesion values measured, it was found that age-hardening effects became noticeable. This was investigated for the complete range of specimens and graphs

of adhesion/thickness of substrate layer were constructed for the initial adhesions, and the values obtained after ageing. It was found that the best adhesion increases were obtained for a substrate layer metal and a reflecting film metal which could form an alloy system containing a large number of thermally stable phases at low temperatures. However, where there was present in the alloy system an intermetallic compound of such high energy of formation that it could freeze out directly from the liquid phase on cooling, there appeared to be a decrease in the adhesions of films of that system, particularly for the thicker substrate layers. Adhesion/time curves were prepared and were found to be in agreement with those expected theoretically for age-hardening phenomena at the metallic interface.

For two of the systems an electron diffraction investigation was undertaken to try to show the nature of the transition region between the metal films, but transmission specimens had to be used and, consequently, the method of investigation limited the resolving power of the diffraction method. For the two systems investigated, however, transition structures were obtained that were not direct extensions of the lattice structures of the metals comprising the evaporated films. These could only be

formed if the parent metals interdiffused to some extent. The nature of the diffusion process in alloying metal systems has not been fully interpreted at present, but the result of such a diffusion process would be the formation of the thermally stable phases in the alloy system.

The alloy systems of the metals used in the investigation were examined and it was found that the adhesions obtained were dependent on the type of transition structure formed at the interface, deduced from equilibrium diagrams. For some of the specimens a loss in reflectivity at the reflecting surface was noticed. This made it essential that the reflectivities of the reflecting surfaces of the substrated specimens should be measured during ageing. On ageing, the reflectivities of the majority of the specimens showed similar changes to those obtained for the reflecting film when deposited by itself without a substrate film, but for one or two specimens there was a definite reduction in the reflecting power due to the penetration of the substrate film material through the thickness of the reflecting film.

The structure of chromium films was investigated by a new optical technique, and for the thinnest films were found to be comprised of very small metallic particles surrounded by a thin layer of oxide. The oxide film

appears to be formed as the films are condensing since evidence of its presence was found in the first layers of films which were too thick to allow oxidation inside the film once it was formed. The presence of this oxide layer was detectable in the thinnest films by electron diffraction. The thicker films, however, could be regarded as being formed of two layers, the original deposit possessing the properties of the bulk material described above, and subsequent layers having almost bulk properties.

CHAPTER 2

APPARATUS

(a) Introduction

The evaporation of metallic films requires that pressures of the order of 10^{-4} mm. of mercury should be obtained. Pressures in this range can easily be reached using metal pumping systems and oil diffusion pumps. These require no liquid air cooling and thus are simpler to use than mercury vapour pumps. The vacuum equipment used in the preparation of the specimen slides is described in this Chapter, as are the adhesion testing apparatus and the method of measuring the thickness of the evaporated substrate film while still under vacuum. The thicknesses of the reflecting films were kept constant by monitoring during evaporation and ceasing the evaporation when the films were just becoming opaque.

(b) Vacuum Equipment

The vacuum apparatus formed one self-contained unit. A rotary pump in the base acted as the backing and roughing pump for the system, with an oil diffusion pump mounted directly below the evaporating chamber and connected to it through a flap valve. A large pyrex

bell jar was used as the evaporating chamber. The water vapour in the system was removed by a P_2O_5 trap mounted on the vacuum side of the rotary pump.

The steel base plate of the chamber was ground flat, and the bell jar was sealed to it by means of a rubber ring of L section. Inside the chamber the base-plate had been drilled with a number of counter-bored holes. These could be sealed by metal plugs and rubber 'O' rings. Most of the plugs were hollow and sealed into them were heavy electrodes to carry the heater current, light electrodes for the H T. gas discharge, ionisation and Pirani gauges and a leak tube. A pair of the plugs carried rotating shafts using modified Wilson seals, one of these was used for rotating the slide carrier and the other for the evaporating shutter. The slide carrier can be seen in Fig. 2; it could be rotated so that the condensing slide would occupy any one of a number of positions. The first of these, on the half of the bell jar not used for evaporation, was so arranged that the complete slide was exposed to the gas discharge used for the final cleaning. After cleaning and out-gassing of the heaters, the slide carrier was rotated until it was directly above the first heater. In this position one end and the middle of the slide had the substrate film material deposited onto it.

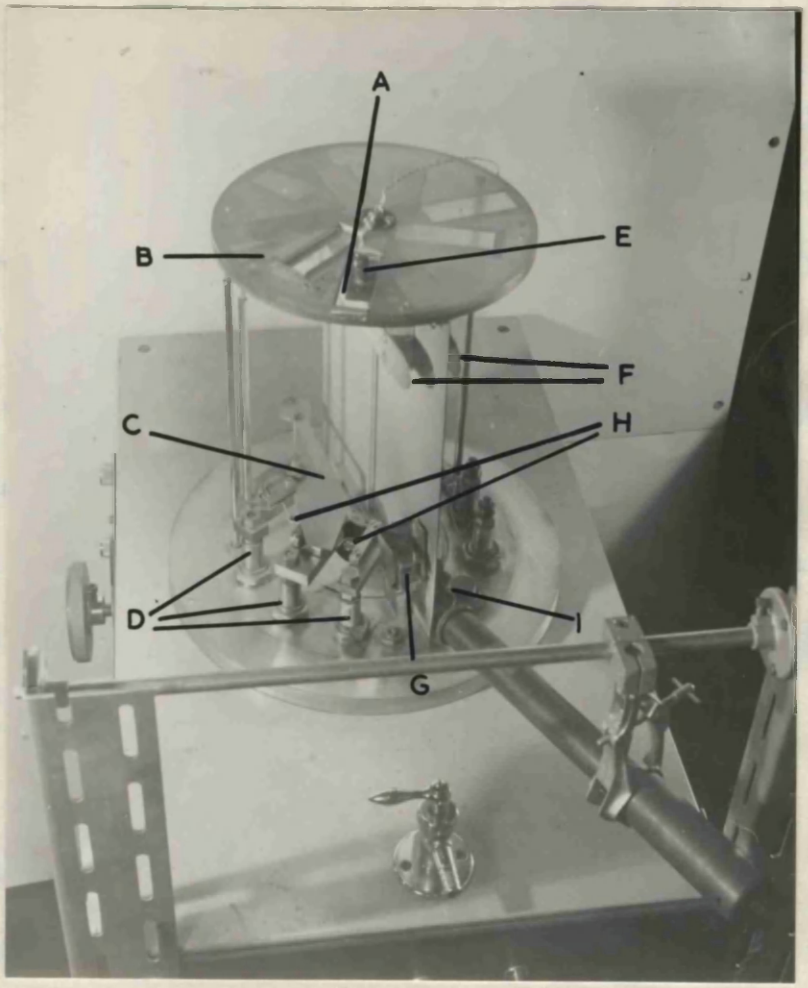

Fig.2. The Evaporating Chamber

A - Condensing Plate
B - Slide Carrier
C - Evaporating Shutter
D - Heater Electrodes
E - Barrier Photo-cell
F - Gas Discharge Electrodes
G - Reflecting Prism
H - Evaporation Sources
I - Drive Mechanism for the Slide Carrier.

Further rotation allowed the other end and the middle to be coated with the reflecting film. The heavy currents required for the evaporation processes were obtained from mains transformers, the current output being regulated by means of a Variac transformer across the primary. The pressure inside the evaporating chamber was always obtained before evaporation commenced by means of an ionisation gauge and no evaporation was carried out at pressures in excess of 5×10^{-5} mm. Hg.

(c) Thickness Determination

The thickness of a thin evaporated film is completely dependent on the method of measurement. Two principal thicknesses on any one film can generally be measured, the weight thickness d_w, and the apparent thickness, d_o, being obtained by optical measurements. The weight thickness is defined as the thickness of an equal weight of bulk material of the same surface area. Neither of these gives a true representation of the film as the structure is generally aggregated and not in nearly as regular a form as the bulk metal would be. Due to the presence of voids within the film, and to the effective reduction of the density of the film, the weight thickness represents practically the smallest value possible. The

apparent thickness, d_o, can be taken as about the maximum value of thickness possible. A truer representation of the actual height of the aggregate particles can be obtained by interferometric measurements[7].

In all the work described here, unless note is made specifically to the opposite, when the thickness of a substrate material is given, it is the weight thickness that is being referred to. It was found convenient to measure the thickness of the substrate films in vacuo before deposition of the reflecting film. A barrier type photocell was mounted directly above the condensing plate and the optical transmission of each film to a parallel beam of 'white' light was obtained. From this the thickness was determined by means of the calibration curves in Fig. 3. These were constructed by evaporating a series of test slides for each material consisting of the substrate film only. The transmission of these films was noted then the films were removed from the vacuum and immediately measured on a microbalance. The thicknesses, d_w, were calculated assuming bulk density. In the optical investigation on chromium described later, the optical thicknesses were many times greater than d_w. The ratio of d_w/d_o was given the symbol 'q' and the value of q was less than 0.4.

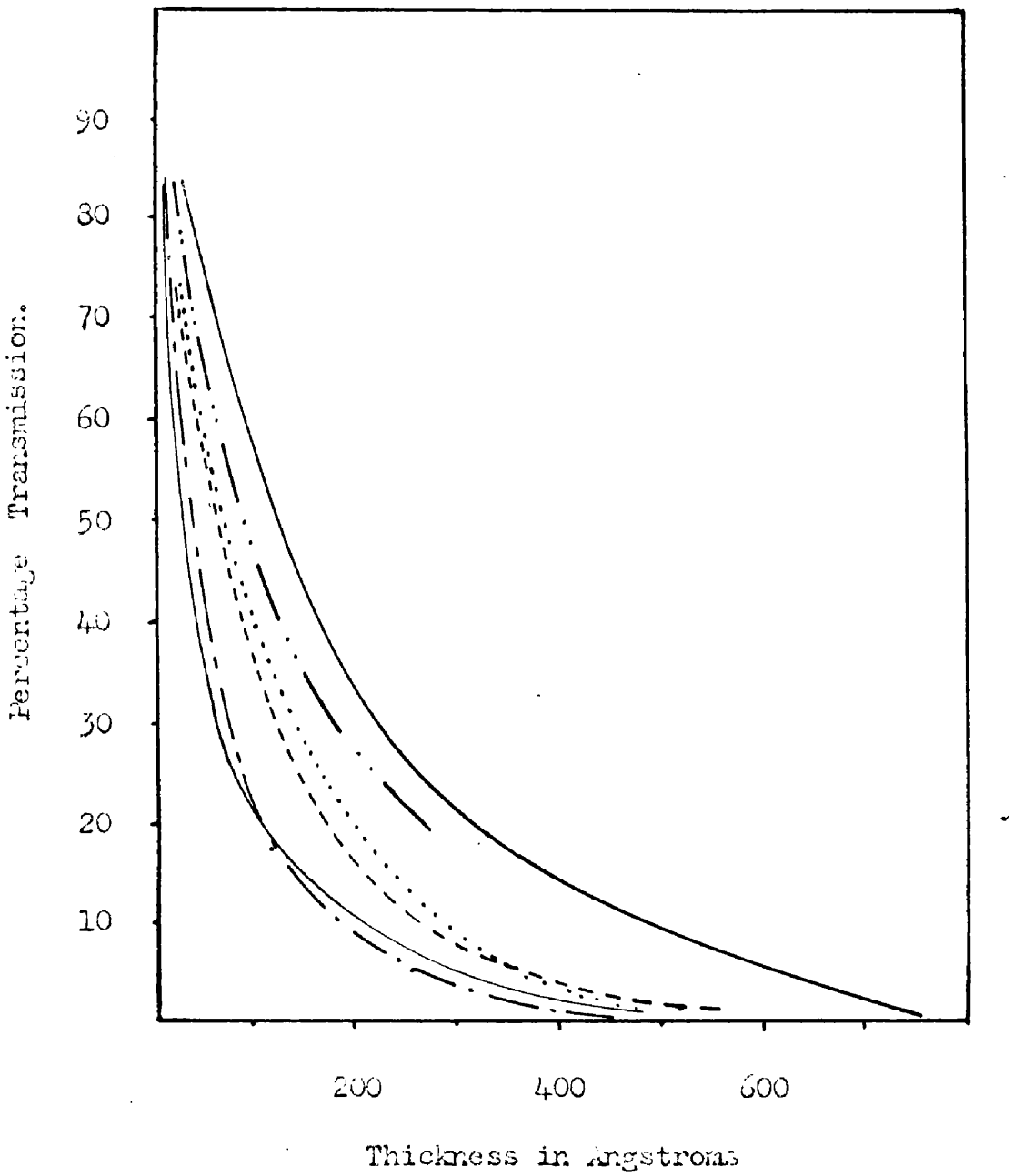

Fig.3. Calibration Graphs for Thickness of Substrates.

Chromium ——— Manganese — · — · —

Nickel ····· Iron ————

Cobalt — · · — Lead - - - - - -

In order to reduce the number of variable parameters the thicknesses of the reflecting films were kept at about the same value for each specimen. For convenience, this thickness was chosen as that at which transmission just becomes zero. This is the simplest constant value to obtain and gives film thicknesses of the order of 1,000A. The upper limit of the substrate thickness is limited theoretically at the same point, but practically, in order to make the transmission reasonably accurately measurable, it was found necessary to cease the evaporation at transmissions of about one per cent. This limited the thickness of such films to less than 700A.

(d) Adhesion Testing

The adhesion of the films were measured on a device similar to that used by Heavens[1]. This consisted of drawing over the surface of the film a hardened steel pointer of known tip radius, on which the load could be varied. The load on the pointer required to just remove the film from its condensing plate was taken as a measure of the adhesion to the film. When a substrate layer had been evaporated onto the condensing surface first, it was found that the value was altered and that a greater or less load on the pointer was required to remove the film.

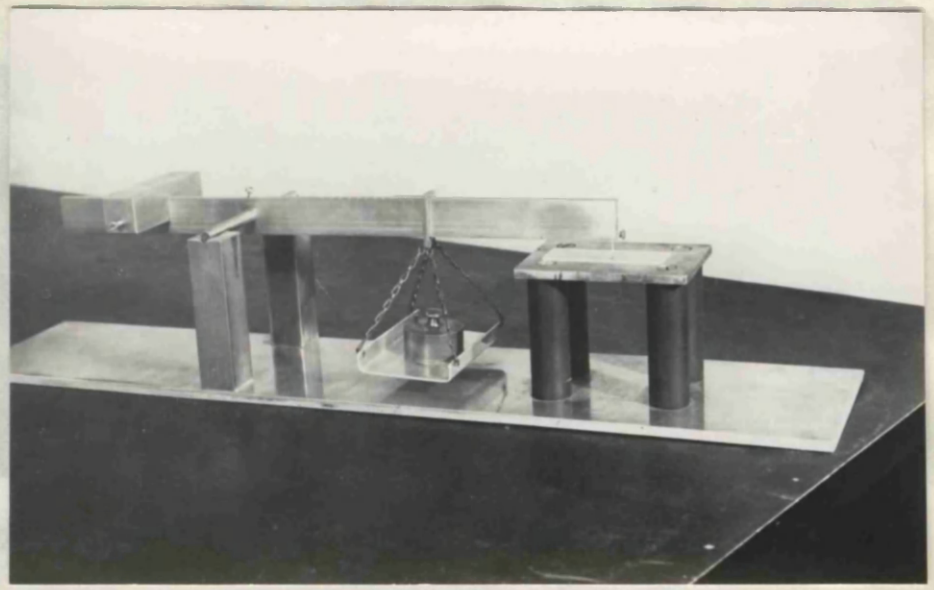

Fig.4. General View of the Adhesion Testing Apparatus

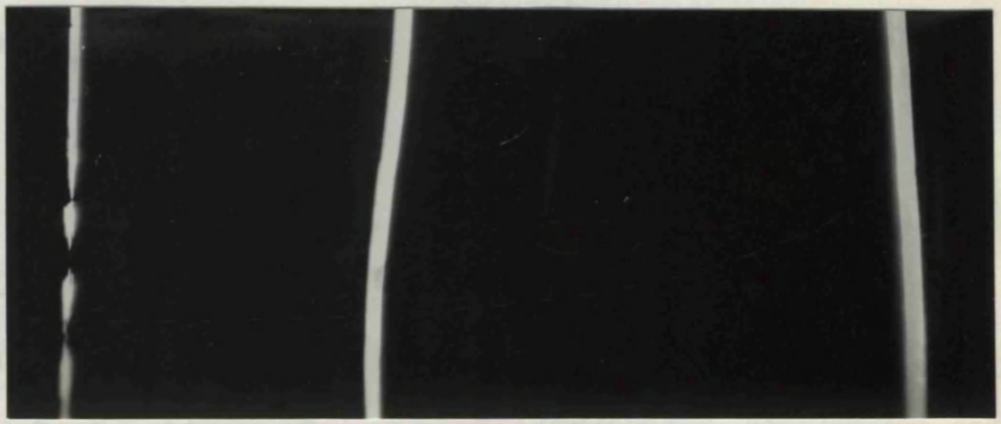

20gms. 22gms. 24gms.

(a) Aluminium film on glass condensing plate.

Adhesion value 22gms.

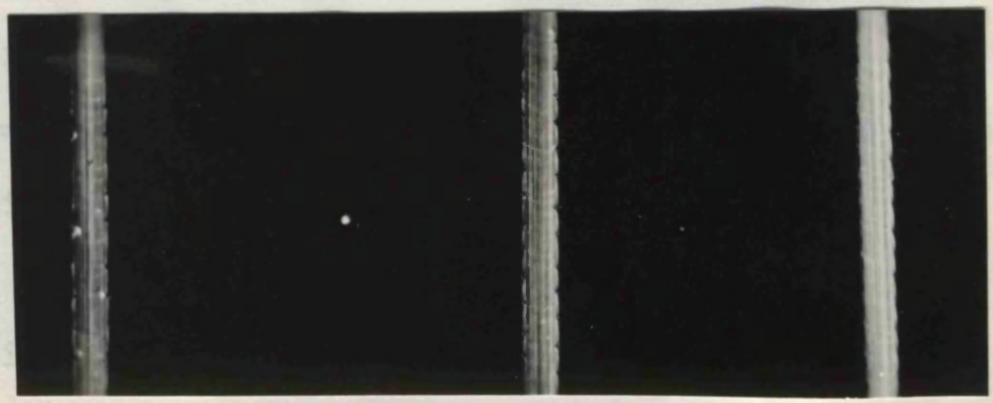

425gms. 450gms. 475gms.

(b) Aluminium film on glass, with a substrate layer of 286A of Chromium.

Adhesion value 475gms.

Fig.5. Typical scratches for a reflecting film with, and without, a substrate layer. 80^{x} magn.

The difference between the values of adhesion for a single film, and when the substrate layer was interposed, was taken as the increase or decrease in adhesion obtained by substration.

Hardened steel gramophone needles were used as the testing points. By means of a projection microscope the diameters of the tips of a large number of these were measured as 0.06 mm. $\pm$ 0.01 mm. A diagram of the measuring apparatus is given in Fig. 4. The main beam was pivoted on steel knife edges, and the weight pan was mounted exactly midway between these and the pointer. The position of the counter weight could be adjusted so that the beam would come to rest with the probe tip exactly the thickness of a microscope slide above the support table. As the measure of adhesion the vertical load on the pointer was taken, i.e. half the actual load in the pan.

Three typical scratches are shown in Fig. 5a. The weight increment between them is 2 gm., and the film was aluminium. For the lowest weight it can be seen that the film has been incompletely stripped while, for the other two, the stripping is clean and even. The lowest value at which this takes place, i.e. 22 gm. was taken as the adhesion value of this film. A second series of

scratches for the same film is given in Fig. 5b. For this specimen, however, a substrate layer of chromium was interposed. Here the adhesion increments are 25 gm. and the adhesion value 475 gm. This gives, for this film, an increase in adhesion due to an underlayer of 286A of chromium, of 453 gm.

(e) Preparation of Slides

Soda glass microscope slides were used as condensing plates throughout this investigation. These were carefully cleaned before mounting in the evaporating chamber. The slide was first scrubbed with cotton wool dipped in Teepol, a detergent liquid, then washed clean with hot water and dried roughly with more cotton wool. Complete drying was carried out with a well laundered linen cloth. The slides were then polished with lens tissue until no breath figures[8] were obtained. Care was taken during this process so that the condensing surfaces of the slide would not become contaminated through handling. They were touched as little as possible and, when necessary, only at the ends for on these regions no adhesion measurements were taken.

After placing them in the slide carrier the slides were subjected to a glow discharge cleaning process. An

H.T. discharge was passed through the chamber for fifteen minutes at a pressure of 0.01 mm. of mercury. This is said to strip from the surface adsorbed water and leave it perfectly clean[8]. On one occasion the films were evaporated onto an unbombarded slide and the adhesion was found to be much poorer. This slide was then discarded.

In order to increase the purity of the metals used a shutter was interposed between the slide and the heater. Before evaporation commenced the heater was raised to the evaporating temperature with the shutter in place. The heater and its charge were kept at this temperature until the more volatile impurities had evaporated and been caught by the shutter. The shutter was then swung out of the way and the evaporation allowed to commence. The process was stopped by replacing the shutter. Some earlier work was undertaken without the shutter and the adhesions of the metallic films in this case were found to be much less than when the shutter was used.

(f) Evaporation Sources

The evaporation sources can be classified into two types, those formed from sheet metal, and those wound from metal wire. For the latter process tungsten wire

was used, either a plain wire 1 mm. in diameter or a stranded wire formed from three thinner pieces, having the same external size. Molybdenum sheets were used for the other types. In Table I are listed the types of heater used for each evaporation and the material. The metal samples were either in the form of a thin wire or roughly crystalline. The crystals were ground down to give a coarse powder that could be packed into the basket type of heater to give a good thermal contact between the heater and the metal. The wire materials were wound round a former to give a roughly spherical ball shape that fitted into the type of heater used.

(g) Evaporation of Alloys

In some experiments a chromel alloy was used instead of pure metal to produce an underlayer.

A method of determining the rates of evaporation of the components of an alloy system has been devised by Dushman[9]. If we let the mass evaporated per unit area in unit time be given by the Langmuir equation, then

$$E = kP\,(M/T)^{\frac{1}{2}} \qquad (2.1)$$

where P is the vapour pressure at a temperature $T^{o}K$, M a mol of the substance evaporated and k is a constant.

TABLE I

Metal	Form of Metal	Type of Heater	Heater Material	Ease of Evaporation
Aluminium	1 mm. wire	Basket	1 mm. Stranded Tungsten	++
Chromium	Small chips	Basket	1 mm. Tungsten	+
Cobalt	Small chips	Basket	1 mm. Tungsten	--
Copper	Thin sheet	Boat	Molybdenum Sheet	+++
Gold	.013" wire	Basket	1 mm. Tungsten	++
Iron	.015" wire	Basket	1 mm. Tungsten	+
Lead	2 mm. sheet	Boat	Molybdenum Sheet	+++
Manganese	Small chips	Basket	1 mm. Tungsten	++
Nickel	.2 mm. wire	Basket	1 mm. Stranded Tungsten	-
Silver	.5 mm. wire	Boat	Molybdenum Sheet	+++
Chromel	.015" wire	Basket	1 mm. Stranded Tungsten	++

Then if we consider an alloy of composition Wa/Wb by weight whose components are metals A and B, then it follows that in order to obtain a film of the same composition it is necessary that the rate of evaporation Ea/Eb must be equal to the original concentration of the alloy. From equation (2.1)

$$\frac{Ea}{Eb} = \frac{Pa}{Pb}\left(\frac{Ma}{Mb}\right)^{\frac{1}{2}} \qquad (2.2)$$

where Pa and Pb are the partial vapour pressures of the components, and Ma and Mb their molecular weights. If, however, Raoult's Law is considered applicable to the system, and it is used to determine the partial vapour pressures of the components, it can be shown that the molecular fraction of a solvent V in a solution S is given by

$$X_V = P_S/P_V \qquad (2.3)$$

where P_S is the vapour pressure of the solution and P_V that of the solute.

Applying this result to equation (2.2) for our system, we find

$$\frac{Ea}{Eb} = \frac{Xa}{Xb}\frac{Pa}{Pb}\left(\frac{Ma}{Mb}\right)^{\frac{1}{2}} \qquad (2.4)$$

where Pa and Pb are the vapour pressures of the pure metals A and B.

It follows from this that

$$\frac{Ea}{Eb} = \frac{Wa}{Wb}\frac{Pa}{Pb}\left(\frac{Mb}{Ma}\right)^{\frac{1}{2}} \qquad (2.5)$$

From the values Dushman tabulates for the quantities $P/M^{\frac{1}{2}}$ the evaporation rates of a chromel alloy of composition 80/20 nickel-chromium can be calculated.

$$\frac{E_{Cr}}{E_{Ni}} = \frac{6.58}{2.16}\frac{10^{-2}}{10^{-4}} \cdot \frac{20}{80} \qquad (2.6)$$

$$= 63$$

Thus the film formed by evaporation of the alloy is mainly chromium. If, however, the evaporation were carried out at a temperature just below the evaporating temperature for chromium in the vacuum then there would be a preferential distillation of the nickel component as the melting point of that metal at normal atmospheric pressure is less than the melting point of chromium. Care has thus to be taken when evaporating this type of alloy that the temperature of the vapour source is high enough to allow the components to evaporate freely.

CHAPTER 3

THEORY OF METALS

(a) Introduction

In this chapter ~~is~~ are described a number of separate but related topics on the structure and properties of alloys, the ageing mechanism in alloys, and the oxidation of metals. The structures of the metals used in this investigation are given as are the type of phase reactions expected between each reflecting metal and substrate metal pair. One section describes the theory of the formation of oriented overgrowths so that Heavens' results may be fully considered.

(b) Structural Properties of Alloy Systems

The conditions for the equilibrium of any alloy system in which the temperature and the pressure are fixed is that a function of the temperature, pressure, and composition, called the thermodynamic potential should be a minimum. Expressed in terms of elementary functions this becomes

$$\phi = U - TS + pV$$

where U is the internal energy, T the absolute temperature,

S the entropy, p the pressure and V the volume of the system. Generally pV is small and can be neglected. When this takes place the thermodynamic potential does not differ from the free energy, F, where

$$F = U - TS$$

The condition of equilibrium is then called the principle of least free energy.

If it were possible to calculate the free energy of an alloy from a knowledge of the characteristics and composition of its component metals then we would know the complete phase structure of any alloy, of any composition, and at any temperature. However, we are unable to do this, and it is only possible to predict results from very general principles. Experimentally the structures of most binary alloys have been investigated and the results assembled in the form of equilibrium, or phase, diagrams. These give the range of composition and temperature in which every phase structure of the alloy system is stable. The diagrams represent in different ways each of the reactions that can take place and are thus built up from a small number of elemental forms.

For the simplest system of two metals that are completely soluble in each other in the solid state the

free energy curves for both the solid and liquid states are of a simple U form (Fig. 6a) with one minimum value of free energy at some value of concentration. The phase diagram of such a system can be constructed from the interaction of these curves as the temperature of the system is decreased. The form of the equilibrium diagram obtained can be seen in Fig. 6b. However, in order to know the stable phases at low temperatures it is only necessary to know the form of the solid free energy curve[10]. It can be shown that where there is a minimum in the free energy curve there will be a stable phase. Thus the system represented by Fig. 7 has four stable phases, the α, β, γ and the δ. If common tangent lines be drawn to these minima curves then the structure of an alloy whose composition lies beneath one of these lines will be a mixture of the stable phases at the ends of the tangent lines. The extent of each stable phase is given by the concentration range lying between the points of contact on each minimum.

Where a chemical compound is formed between two metals the minimum will represent a very low free energy, and be strongly peaked. As the concentration deviates from the stochiometric value the free energy will rise rapidly; this has the effect of making the concentration ranges of intermetallic compounds very limited. When such

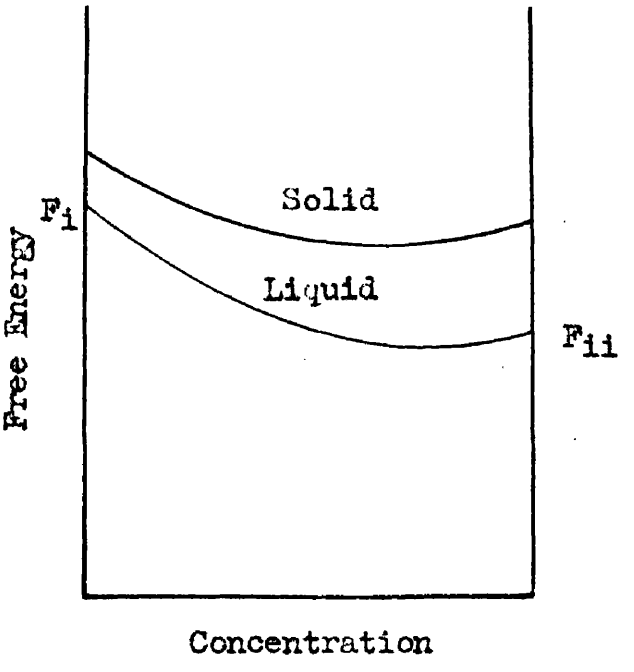

(a)

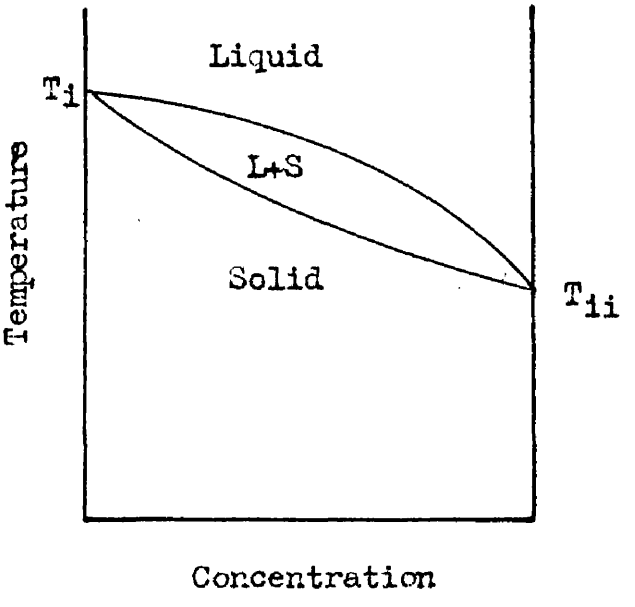

(b)

Fig.6. Free Energy and Equilibrium Diagrams for a Miscible Alloy.

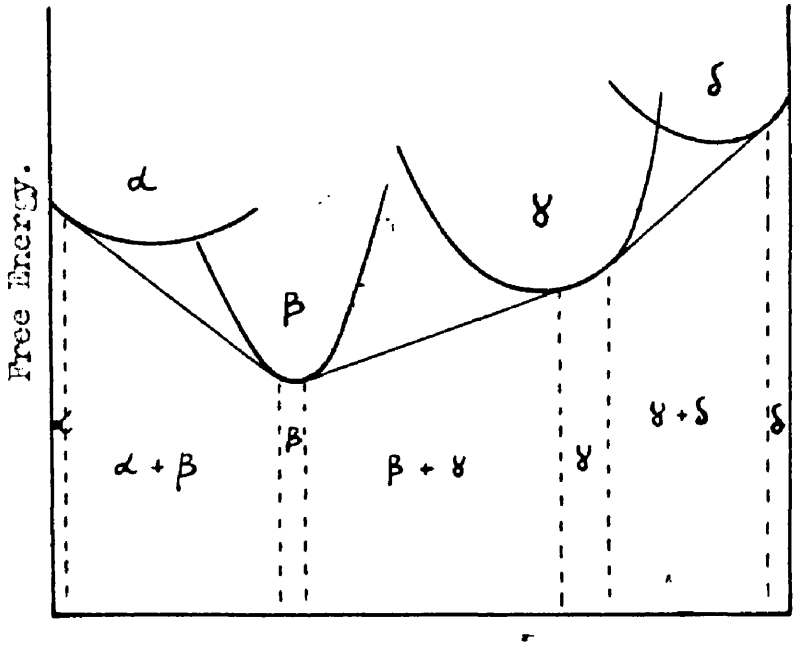

Fig.7. Free Energy Curve for an Alloy forming Intermediate Phases.

a compound is formed from the liquid phase directly maxima are obtained in both the solidus and liquidus curves of the phase equilibrium diagrams, and such a system denotes a large decrease in the free energy at that concentration. Intermediate phases can also be obtained by peritectic reactions; the type of free energy and phase diagrams obtained for these systems are given in Fig. 8.

The structure of an alloy must by its very nature control, to a considerable extent, the physical properties of the alloy. In a weak solid solution the presence of the foreign atoms will obstruct the flow and movement of dislocations, thus causing the hardness of the system to increase. The hardness will still tend to increase as we increase the proportion of our foreign atoms until the structure, assumed to be completely miscible, becomes related more to the foreign atoms than the original ones. We now have a structure of foreign atoms in which the original atoms are causing an increase in hardness. As the composition of the original metal decreases so will the hardness until we reach a pure metal structure. This suggests that for the completely miscible system we could expect a simple parabolic type of hardness/concentration curve. Such a result has been obtained experimentally.[11]

If, however, we consider the hardness of an alloy

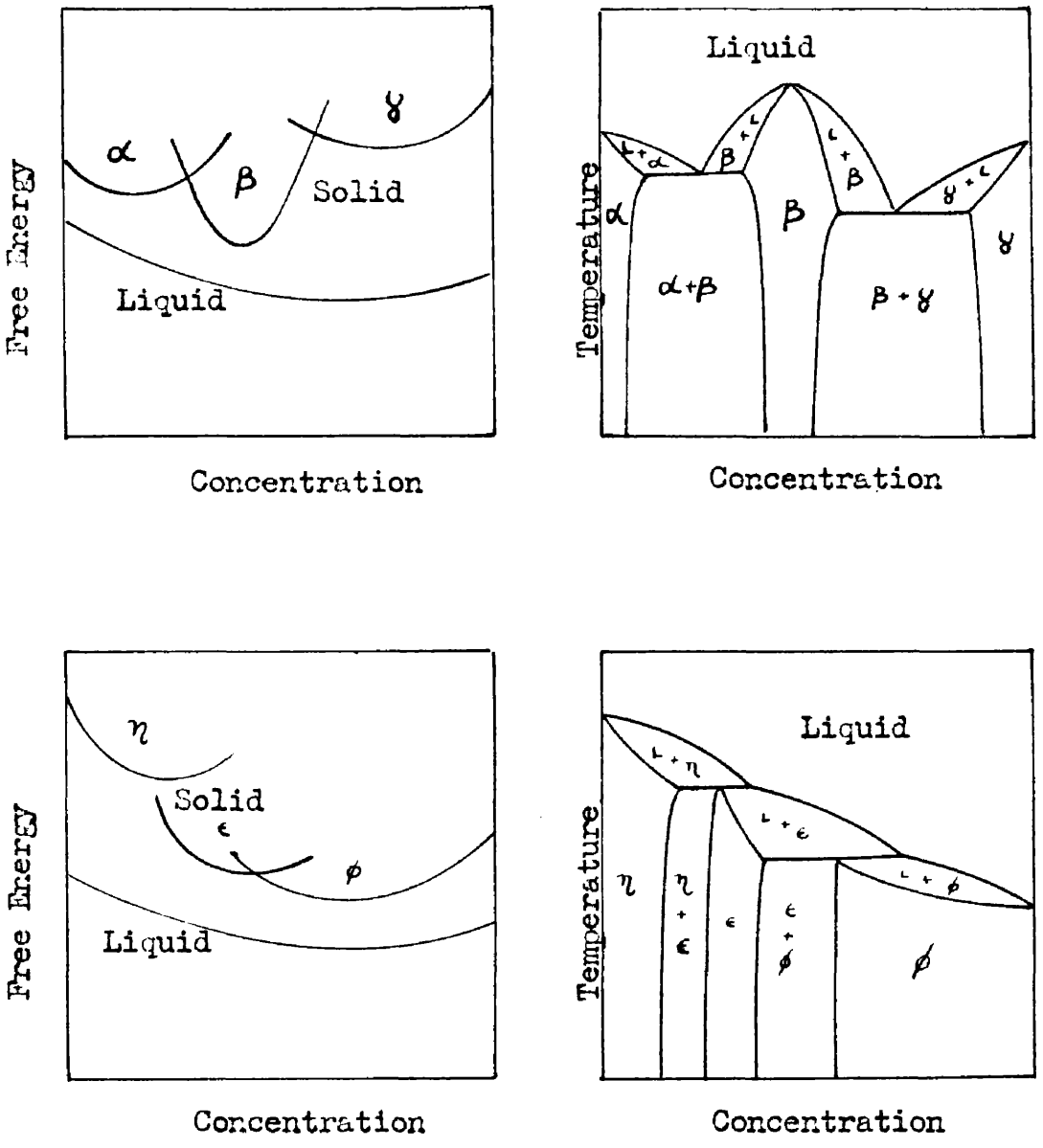

Fig.8. Free Energy Curves and Equilibrium Diagrams for Eutectic and Peritectic Alloy Systems.

system in which a phase region exists, then in that region there would be a high degree of order and the hardness, or rather the resistance to flow, would decrease to a particular value dependent on the structure and its degree of homogeneity. This has also been experimentally shown[12], Fig. 9. The hardness of the silver magnesium alloy system was investigated by the Brinell indentation method, and the electrical conductivity of the same specimens were also measured, the conductivity of an alloy being another very sensitive structural property. For the system investigated an intermetallic compound AgMg was formed, and in the region of 50/50 atomic composition the hardness decreased and the conductivity increased. The hardness of the compound at its minimum value, however, was still three times that of either of the constituent metals.

(c) Description of Alloy Systems

The systems of metals investigated in this work can be divided into three categories from the type of phase diagrams that they form.

(i) Completely Miscible Systems. The completely miscible systems investigated were the aluminium/lead, and the silver/chromium. The equilibrium diagrams[13] for each of these systems are given in Fig. 10a. For these

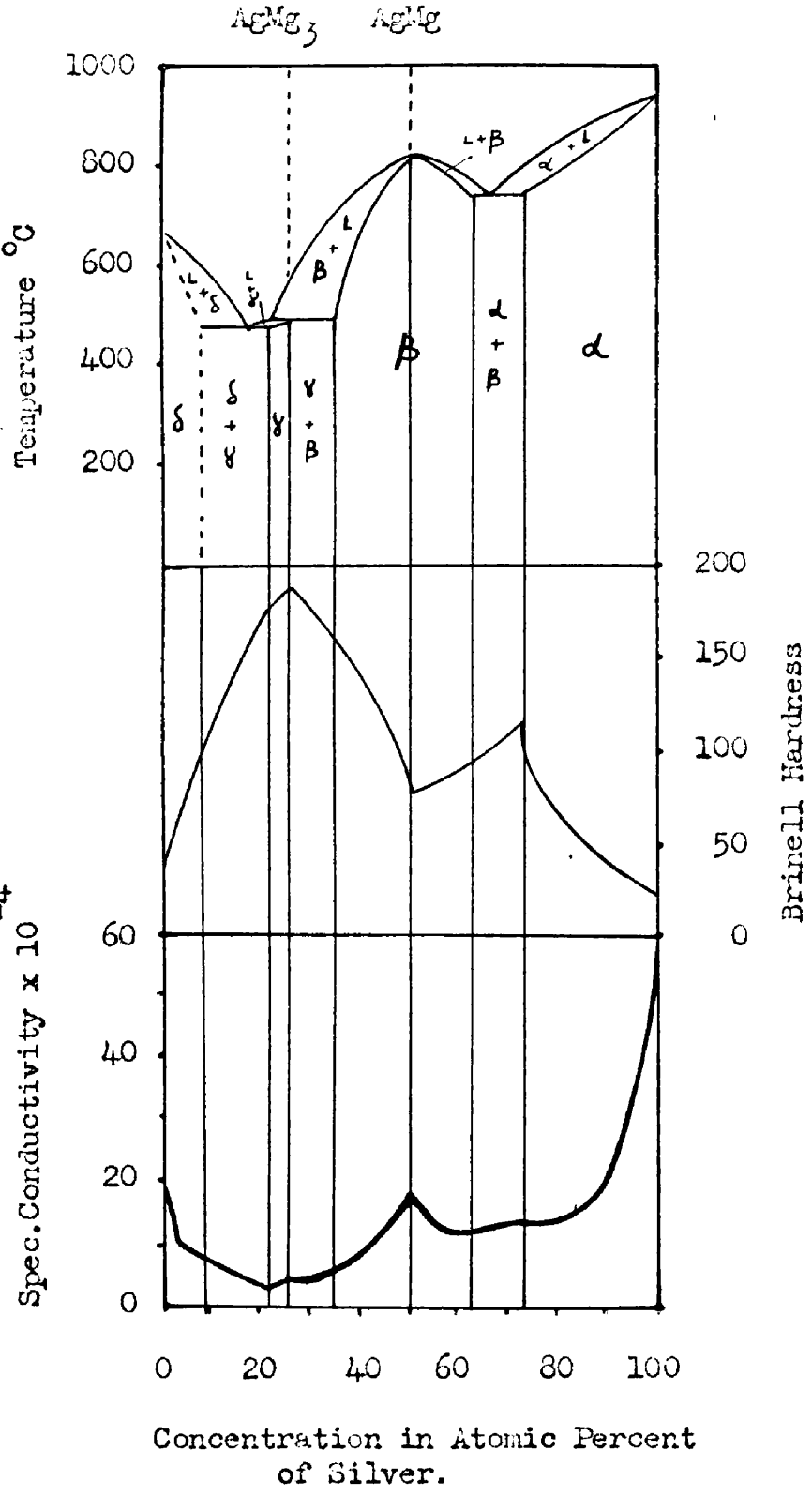

Fig.9. Variation of Conductivity and Hardness with Alloy Composition - C.H.Desch.

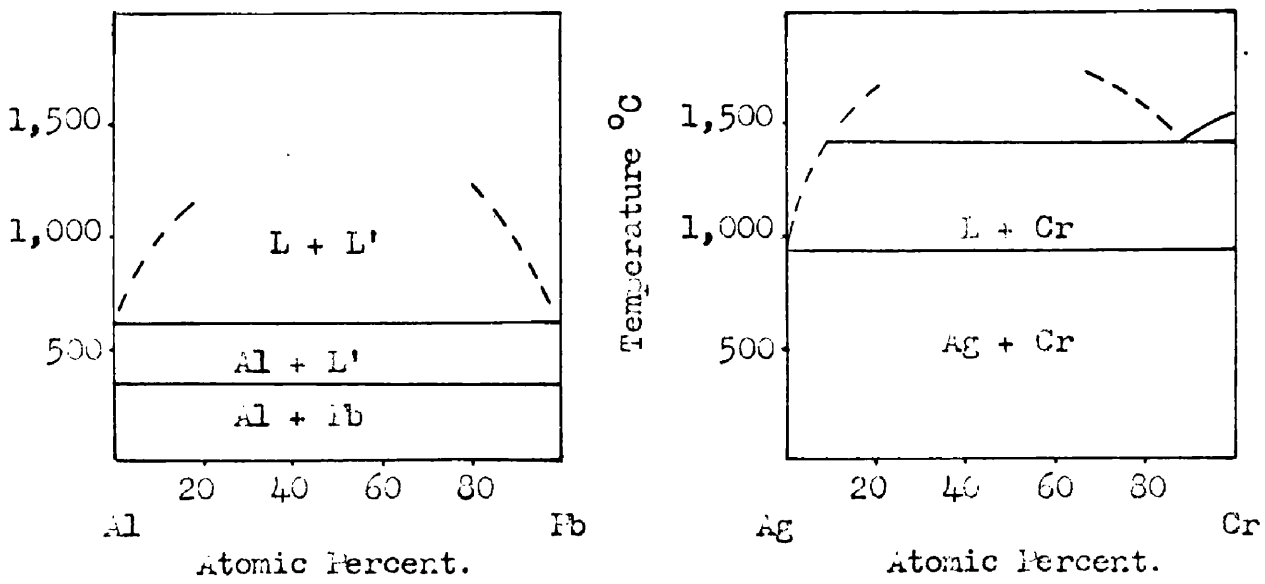

Fig.10(a). Equilibrium Diagrams; Systems Aluminium-Lead

Silver-Chromium

alloys the free energy curve will show a single minimum, and the hardness/composition curve a maximum. The requirements usually necessitated for miscible systems, i.e. that the constituent metals should have approximately the same structure, and the same atomic diameter is similar to the conditions required for oriented overgrowth. Investigation of a number of metal systems that were known to form such overgrowths showed that the systems did, in general, have simple phase diagrams. In the cases in which there was not complete miscibility there was usually miscibility over a wide range of composition. Table II lists the structure, spacing and atomic radius of the metals used. The atomic radii listed in the table are the distance of closest spacing in the elemental lattice structure; this it is thought[14] represents a truer atomic diameter than those suggested by Goldsmith and Pauling[15].

(ii) Partially Miscible Systems. Examples of this type of system were the gold/chromium, the copper/chromium and the silver/lead. For these systems the free energy curve will have two minima. The common tangent between these representing the concentration range of the mixed phases. This type of system is usually obtained for metal pairs that have similar structure but little mutual solubility. From the equilibrium diagrams (Fig. 10b) it can be

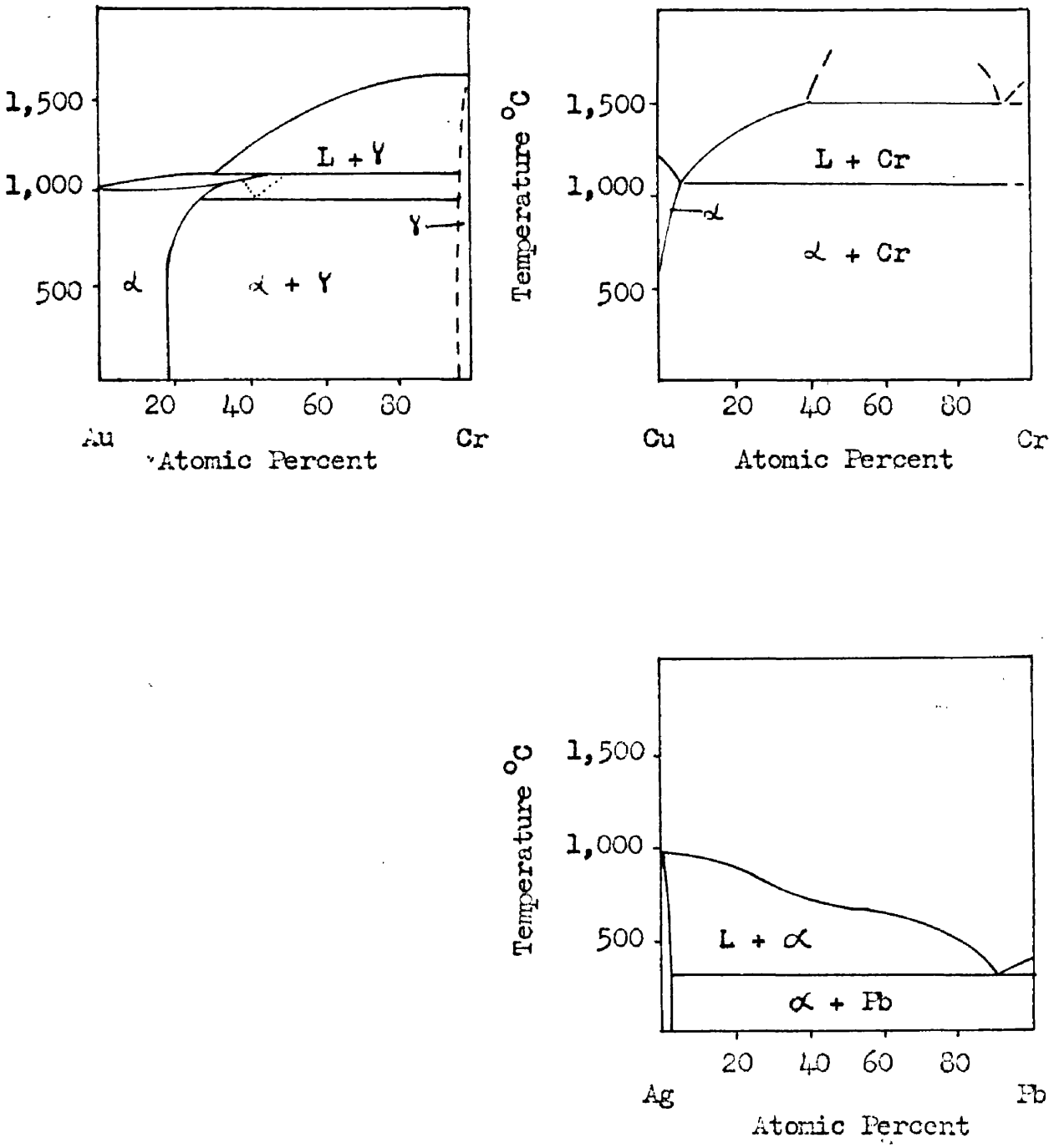

Fig.10(b). Equilibrium Diagrams; Systems Gold-Chromium

Copper-Chromium

Silver-Lead

TABLE II

Metal	Structure	a_o in Angstroms	c_o in Angstroms	Interatomic Distance in Angstroms
Aluminium	F.C.C.	4.045	-	2.86
Chromium	B.C.C.	2.879	-	2.49
Cobalt	C.P.H. stable below 400°C.	2.514	4.105	2.55
Copper	F.C.C.	3.608	-	2.55
Gold	F.C.C.	4.070	-	2.88
Iron	B.C.C.	2.861	-	2.53
Lead	F.C.C.	4.940	-	3.50
Manganese	Irregular structure based on cubic.			
Nickel	F.C.C. stable below 20°C.	3.517	-	2.49
	C.P.H. stable above 20°C.	2.64	4.32	2.64
Silver	F.C.C.	4.078	-	2.88

seen that the first of these systems has limited solubility at each end of the alloy systems, but that the last two have one of the components in solution with a solid solution.

(iii) Intermediate Phase Systems. This group can be subdivided into three. Those systems that form an intermetallic compound directly from the liquid state with a low free energy, those that form one having a large free energy and the systems in which the metallic compound is formed during a peritectic reaction. In the first category we include the systems aluminium/nickel and aluminium/cobalt, in the second, aluminium/iron and aluminium/manganese, while the third was represented by aluminium/chromium. All of these metal pairs form a large number of intermediate phases, i.e. the last system shows nine phases in all. Although such systems are generally formed from components that have no common structural features it should be noted that there is a strong agreement between the atomic dimensions in the (110) planes of aluminium and chromium. The spacing of the aluminium structure is 4.045 x 2.858A while that of chromium is 4.080 x 2.879A.

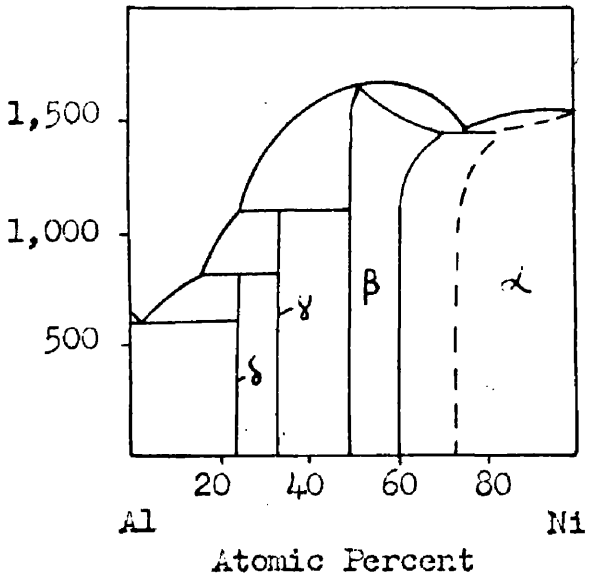

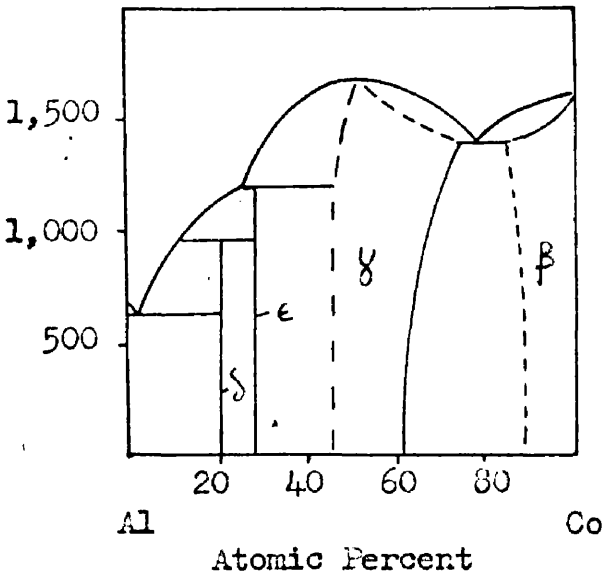

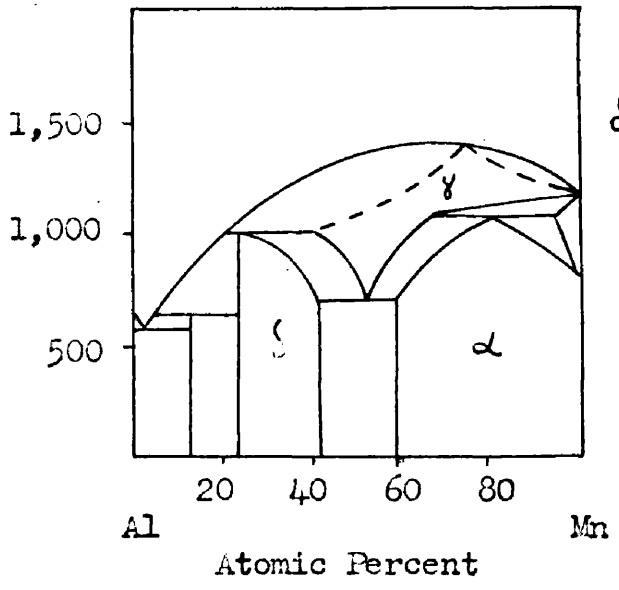

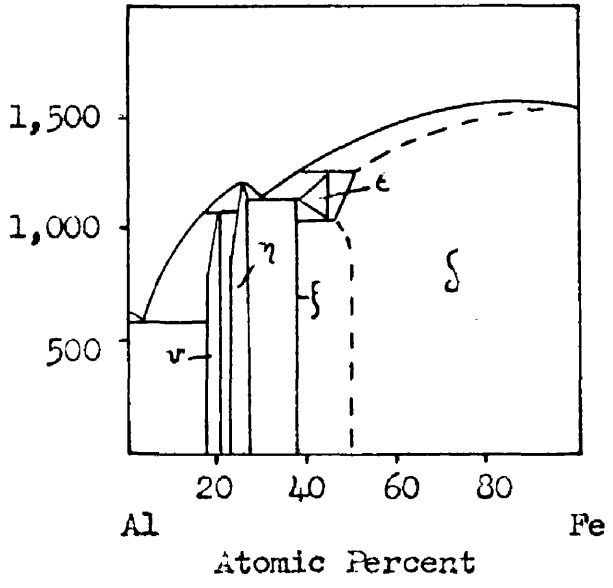

Fig. 10(c).

Equilibrium Diagrams

Systems Aluminium-Nickel
Aluminium-Cobalt
Aluminium-Manganese
Aluminium-Iron
Aluminium-Chromium

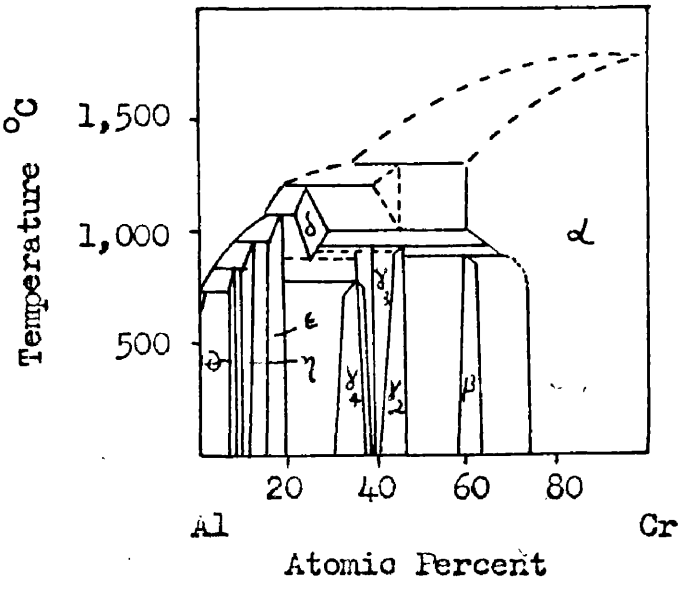

(d) Age-Hardening in Alloy Systems

In the past many theories of age-hardening in metallic alloys have been put forward[16-18]. Present work[19] indicates that the phenomenon is one primarily of coherent phase precipitation and the resulting strains set up in the parent lattice structures. When a metallic solid solution precipitates it forms a new phase, generally another solid solution of differing composition from the parent one, and a depleted matrix. Two types of precipitate are recognised, coherent and incoherent. The former are those for which there is some degree of fit between the parent lattice and that of the precipitate. In order to obtain a precipitate of this form it is usually necessary for the precipitated particles to adopt a metastable structure, or to strain the lattice in such a way as to reduce the degree of mismatch. This is followed by a slow release of the coherency strains, and possible the completion of the precipitation process to give the final particle structure. Incoherent precipitates, for which there is no continuity of lattice, have, however, been found to arrange the growth of their structures in such a way as to reduce the discontinuity at the interface region to as little as possible. In this process of precipitation and release of strain, it is generally

believed, lies the cause of age-hardening.

The process of precipitation can only take place where there has been suitable nucleation. Incoherent precipitates require some discontinuity of structure to form nuclei, and those that are formed have to grow by random migration of suitable structural elements to a certain minimum size before the growth process can begin[20]. From the very nature of the coherent structure it can be seen that less rigorous conditions are required for nucleation and growth.

As the precipitated particles increase in size and number the depleted parent solution approaches the equilibrium value of concentration. However, due to the appreciable surface energy[21] of the incoherent particles, and to the strain energy of the coherent, a quasi-equilibrium is often set up. Once this point has been reached the earlier form of growth stops, and it has been suggested a new form takes over, necessitating a completely new form of nucleus and, it was further suggested, that this would give rise to the double and multiple ageing peaks that have been experimentally obtained.

It is impossible to measure the velocities of these reactions, but they must be allied to the diffusion equation, where

$$D = A.e^{-Q/RT}$$

This requires that a decrease in temperature T will involve a rapid decrease in the diffusion constant D, making the reactions very temperature sensitive in the low temperature range.

This form of ageing is comparable experimentally with the theory of age-hardening proposed by Gayler[22] in 1937. Gayler considered that a diffusion process allowed the formation of molecules of the precipitate, still in solution with the parent solid solution; as the molecules grew the structure of the parent matrix could no longer contain them and a precipitation phenomena took place. The essential points about these phenomena were that the formation of molecules was associated with an increase in hardness, and the precipitation with a decrease. From the standpoint of the new theory we can see that Gayler's molecules are equivalent to the precipitation stage, and Gayler's precipitation process to the release of the coherency strains. The apparent appearance of the precipitate in two different places in the theory is due to the more advanced microscopical techniques now in use. Gayler constructed a diagrammatic representation of the hardness/time curves for a complete range of ageing temperatures: this is reproduced in Fig. 11. This set of curves is still applicable and ageing curves such as

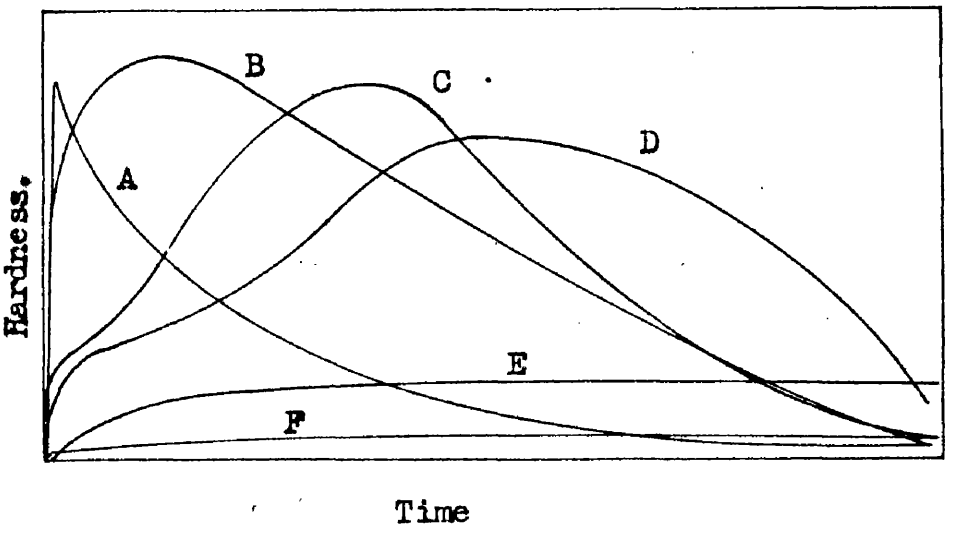

Fig.11. Gayler's Agehardening Curves.

Curve A - Upper Rate Limit of Ageing.

Curve B - Second Stage of Ageing, Slight Indication of First Stage.

Curve C - First and Second Stage both Apparent.

Curve D -

Curve E - First Stage of Ageing, Slight Indication of Second Stage.

Curve F - Lower Rate Limit of Ageing.

Reprinted from J. Inst. Metals, Vol.60, 1937, p249.

these have been obtained for most age-hardening alloy systems. The curve described by Gayler as the result of the first stage of ageing only (E. Fig. 11) can be described now as due entirely to simple precipitation, with no release of stress. This is the type of hardness curve that we might expect from ageing an incoherent alloy. Curve B on the other hand shows the effect of a precipitation/quasi-equilibrium/re-arrangement process.

From the diffusion equation noted earlier we can replace the temperature range by a range of diffusion velocities. Thus, if we can measure the form of the age-hardening graphs, at the same temperature, for a large number of metal pairs we might expect to obtain some, if not all, of the forms of the curves of Fig. 11.

(e) Orientation in Overgrowths

Condensing films can grow in one of two ways, either as solid aggregates or as stable monolayers. If the energy of the condensing atoms is high they will have a high mobility on the condensing surface and tend to cluster together to form three dimensional groups, these are called aggregates. Lower energy atoms will tend to form more continuous structures. In either case, the structure of the base material can influence the form of

growth by offering preferential atom sites to the initial deposit. If there is a strong energy bond between the atoms of the film and those of the condensing surface then the condensing atoms will take up these positions and grow with its structure regularly oriented to that of the base material.

A relationship between the influence of the base and the mutual adhesion was experimentally determined by Finch and Sun[23] in 1936. They stated that the substrate nearly always affects the deposit, when it does not the adhesion of the deposit is poor . A measure of the interaction between base and film can be obtained by measuring the amount of induced orientation in the film when evaporated onto the base. Most films on an amorphous substrate are deposited with one particular plane parallel or perpendicular to the substrate face; however, when deposited on a crystalline substance there may be a completely different, or even no, orientation present. The amount of enforced orientation, or the lack of it, can be taken as a measure of the interaction.

Crystal orientations are formed by interaction between one atomic layer and the next, and for a new structure to be oriented it is necessary to have strong orientation in the first monolayer, as well as a low

mobility. The first monolayer then must be of regular atomic pattern and if the orientation is to be induced the atomic pattern must be regulated by the base onto which it is formed. It is usual to call this layer the 'embryo' of the structure.

If the deposit were to have exactly the same structure and interatomic distances as the base it would be expected that the atoms of the embryo would take up equivalent positions to the atoms of the base. Such a growth has been obtained[24] for copper electrically plated onto a copper crystal. It has been found[25], however, that equivalent positions are taken up with suitable structures even with a misfit of nine per cent, where the degree of misfit is expressed as $(b-a)/a$, a and b being the corresponding lattice spacings. With a higher degree of misfit the number of dislocations formed at the interface rises rapidly and the embryo no longer becomes characteristic of the substrate, any orientation effects are lost within the thickness of a few monolayers. Ionic substrates can induce orientation by nature of the stronger adhesion bonds with an even greater misfit[26] between the lattice dimensions: fourteen per cent has been found. The effects of ionic substrates have been investigated by Rhodin and[27], Wellems[28], while Frank and Van der Merwe[29] have deduced

theoretically that a misfit of fourteen per cent is generally allowable if the activation energy for generation of dislocations be taken into account.

Near equality of spacing is not enough, however, to ensure that one substance will form an embryo on another[30]. It has been suggested[29] that in order to obtain embryo formation on a suitable substrate facet it is necessary to have some irregularities either steps or cracks along which the growth can originate. If the surface were perfectly smooth then the initial growth might take the form of a number of very small clusters of atoms occupying the preferential lattice sites, but having no correlation one with the other. We might thus form a growth in which one particular plane would be parallel to the substrate and the other two principal planes in any direction. Such a structure is said to have fibre orientation.

A theoretical approach to oriented overgrowths has been established by Rhodin[27], and shown to give results of the correct order of magnitude, assuming Van der Waal's forces. The graph of percentage orientation against substrate temperature obtained by Rhodin for aluminium on a number of substrate materials is given in Fig. 12. For each base temperature the lowest vapour pressure of the metal at which condensation could take place was

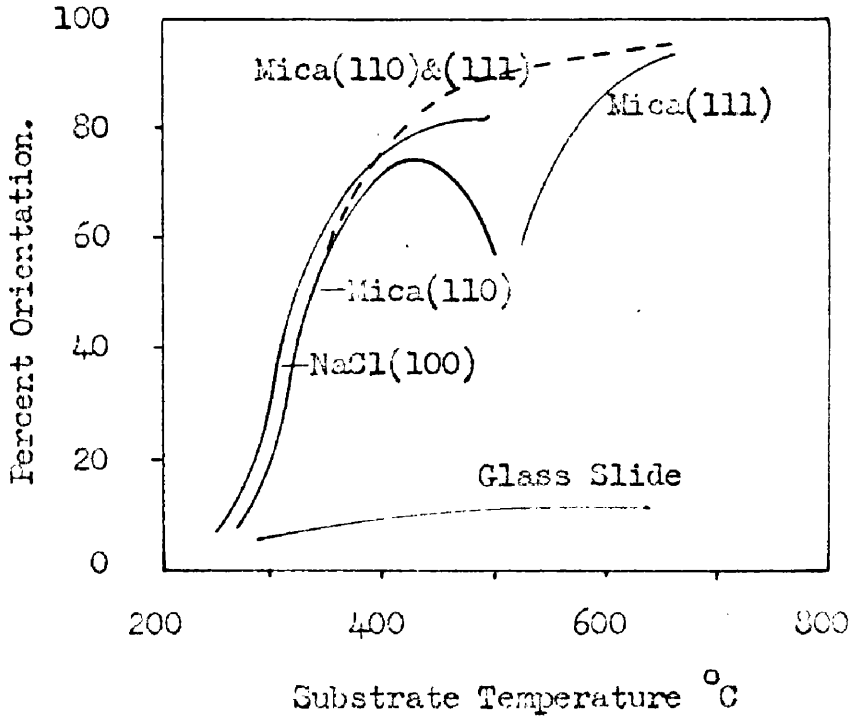

Fig.12. Rhodin's Graph of Substrate Temperature to Percentage of Orientation in Aluminium Films

determined, and a pressure/temperature relationship was suggested

$$p = a.e^{-A/RT}$$

where p = pressure of metal vapour,

a = a constant, insensitive to temperature,

T = the absolute temperature of the substrate,

A = an energy term characteristic of the film and substrate.

It has been shown by Wood[31], Estermann[32] and Semenoff[33] that

$$A = E + \Delta$$

where E is the adhesive energy of binding of the metal and substrate, and Δ the binding energy of the metal atoms in the first monolayer. That is to say, the characteristic energy of the metal film. Rhodin showed that the orientation increased with E, but if Δ was larger than E the film was relatively independent of the substrate and there was little orientation. The values of E are of the same order of magnitude as Van der Waal's forces between a single atom and an infinite plane surface. Thus, the initial embryo can act as the base for an overgrowth continuing its orientation if the interatomic binding of the condensing atoms is not stronger than their binding to

the substrate. A classification of a number of ionic substrates for aluminium is given by Rhodin and the theoretical classification agrees with a fair degree of accuracy to that determined experimentally. Appleyard[34] has based another method of classification on the Lennard-Jones theory of adsorption. The surface of the substrate is regarded as being made up of a series of potential troughs and hills, over the atom spaces and the atom sites. These may, or may not, act as barriers to the movements of atoms on the surface, depending on the kinetic energies of the atoms and the latent heat of evaporation of the metal from itself, Lm. If La is the latent heat of evaporation of the metal from the substrate, and if $La > Lm$ no surface motion can take place, and a monatomic surface film will be formed. If $La < Lm$ and $La \gtrsim 1ev$, then at low temperatures a limited mobility is given to the atoms and stable coherent films will be formed. If $La << Lm$ then surface motion can take place at any temperature and the surface will be formed of solid aggregates. Aluminium, gold and copper on glass fall into the second of Appleyard's categories according to Pickard and Duffendack[35]. Electron microscopical studies[36-37] have shown that chrome, nickel, cobalt, iron, manganese, lead, silver and copper on glass condense on the form of

aggregates and these are separated by interstices much smaller than the size of the particles. This shows that these metals also fall into the second of Appleyard's classifications.

Thus we see that the substances used as substrate materials, chromium, nickel, cobalt, iron, manganese and lead, form films that are relatively continuous, and have some possibility of supporting oriented overgrowths. From the published results of orientation in metallic deposits, there is little evidence to show whether with the systems we are investigating oriented overgrowths are obtained or not. Copper has been found to be suitable as a substrate for the growth of oriented films of electro-deposited chromium[38], the (111) plane of the copper lattice being the substrate face, and the chromium growing with its (110) plane parallel to this.

The effect of chromium as substrate to aluminium, silver and gold, has been investigated for vacuum prepared specimens by Collins[2] as described in Chapter 1. He found that the metal films when evaporated onto glass had a definite orientation of their own. But when they were evaporated onto the already prepared chromium film no orientation in the upper film was visible. It was suggested that this was evidence of the formation of an embryo in the upper film of different orientation from the habitual

growth of the film material. However, as the same result was obtained for all the metals, whether they were evaporated onto a slowly evaporated film of chromium which had no orientation, or whether they were evaporated onto a quickly evaporated film of chromium which had the (110) plane parallel to the surface, and as the misfit between the (110) planes of chromium and aluminium, silver and gold is less than one per cent, this result does not appear to be very conclusive.

(f) Oxidation of Metallic Films

The rate of growth of an oxide film is usually given as obeying a parabolic law,

$$x^2 = k.t \qquad (3.1)$$

where x is the thickness of the oxide film at time t, and k is a constant dependent on the conditions of oxidation. The value of k can be calculated on the basis of diffusion of the reacting substances through the oxide layer, and

$$k = 2.D_i (f_2 - f_1) \qquad (3.2)$$

where D_i is the cation diffusion coefficient, and f_1 and f_2 the fraction of defects at the metal-oxide and oxide-oxygen boundaries, respectively.

Cases have been found in which the growth follows a logarithmic law of this type,

$$x = a.\log(1 + bt) \qquad (3.3)$$

An explanation of this type of growth has been given by Evans[39]. It is based on a mechanism involving repeated cracking and healing of the surface of the film.

A possible mechanism for the growth of the oxide layer on aluminium has been suggested by Mott[40]; it is based on the formation of an electric field in the oxide layer. If oxygen atoms are absorbed on the surface of the oxide film they will form vacant energy levels for electrons, as in Fig. 13a. Electrons passing through the oxide film will set up a field, by forming negative ions, on filling these levels. A state of quasi-equilibrium will be obtained, Fig. 13b, where a constant potential difference V is set up across the film. The electric field strength will be given by

$$F = V/x$$

Fig. 13c shows the potential energy of an ion as it leaves the metal and passes into the oxide. The point A represents the position of an ion in the metal and the position B an interstitial place in the oxide. The energy W is then the difference in energy of an ion in the two positions, U is the activation energy required to move the ion in either direction.

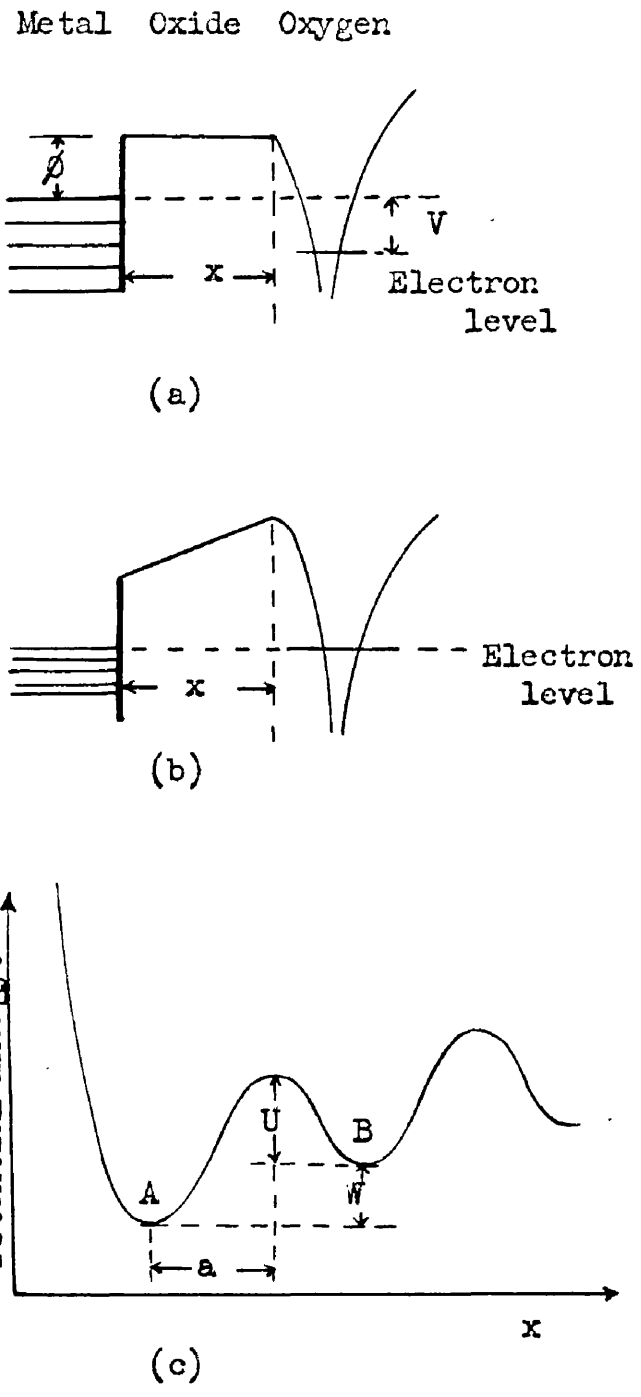

Figs.13(a,b&c) Oxidation of a Metallic Surface.

If p is the probability that position B is occupied, then the probability of an ion jumping from A to B in unit time is

$$\nu.e^{-(W + U)/kT} \tag{3.4}$$

ν being the frequency of atomic vibration, assuming it to be constant and the same at A and B. The probability of a jump from B to A in unit time is

$$\nu.p.e^{-U/kT} \tag{3.5}$$

Thus p can be obtained, for steady conditions, by equating (3.4) and (3.5), i.e.

$$p = e^{-W/kT} \tag{3.6}$$

In a field of strength F the current flow will be

$$N.epvF$$

where N is the number of interstitial positions per unit volume in the oxide and v the mobility of an ion. If the temperature is large, so that p is small and the barrier in Fig. 13c is depressed by aeF, the probability of an ion jumping from A to B in unit time is

$$\nu\, e^{-(W + U - aeF)/kT} \tag{3.7}$$

The probability of jumping back before jumping on again

is negligible and the number of ions crossing unit area in unit time is then

$$n\nu e^{-(W + U)/kT} . e^{aeF/kT} \qquad (3.8)$$

where n is the number of ions at the ends of layers of unit area.

$$\text{i.e.} \quad \frac{dx}{dt} = n\nu e^{-(W + U)/kT} . e^{aeV/kTx} \qquad (3.9)$$

This gives a more rapid initial growth than the parabolic law, which is followed by a more rapid fall off.

Verwey[41] has deduced that 'a' is of the order of 10A, and U + W for aluminium 1.8eV. Although 'n' is not known it has been suggested that about one atom in a hundred would be ready to jump from the metal into the metallic oxide. Then the number of layers of metal atoms which pass through the oxide in unit time are

$$0.01\ e^{-W'/kT}\ e^{x'/x} \qquad (3.10)$$

where $W' = W + U$ and $x' = aeV/kT$.

If ν is taken as 10^{12} and an insignificant rate is when one layer passes into the metal oxide in 10^8 sec., then the thickness at which growth stops is given by

$$\exp.(W' - aeF)/kT \approx 10^{18} \qquad (3.11)$$

i.e. $x = eaV/(W' - 45kT)$.

Thus a critical temperature T_o is obtained, below which the oxide films have a limiting thickness and

$$T_o = W'/45k = 300^oC \text{ for aluminium} \qquad (3.12)$$

and

$$x = (eaV/W').(1 - T/600)^{-1} \qquad (3.13)$$

At room temperature this gives, for the limiting thickness, a value of 20A, and at 120°C, 30A, when eV/W' is taken to be unity. However, Hass and Scott[42] have measured the thickness of the oxide film after it had reached its limiting value at room temperature as 45A. They found that this limiting thickness could be increased by increasing the temperature of ageing. This is in agreement with the theory evolved and suggests that a value of two might be a better value to choose for eV/W'. This would then give as the limiting thicknesses 40A for room temperature ageing and 60A when ageing took place at 120°C.

Difficulty is found in obtaining the time factor for the rate of growth of the oxide layer. If an approximation is made to the parabolic law, then accepting that the film grows to the limiting thickness of 40A, at 20°C, in 31 days we can find the constant k of equation (3.1),

where x is the thickness of the oxide layer and t the time of growth. This gives

$$k = x^2/t$$

$$= 5.94 \times 10^{-20} \text{ cm.}^2/\text{sec.}$$

The form of this parabolic growth is represented in Fig. 14; this graph also shows the forms of growth given by equations (3.9), as can be seen for both the ageing temperatures the thickness rises initially much faster than for the parabolic form, but slows down to a more decisive limiting value.

Evidence to support this form of growth has been obtained by Hass[43] who states that he found that films of aluminium grew an oxide film of thickness of 15-20A almost immediately after evaporation. The formation of an oxide film with time has been investigated[44] by weighing a specimen of pure aluminium after it had been stripped of its oxide film. Weight measurements were made during the formation of a new oxide layer: the results are graphed in Fig. 15. The specimen used had a surface area of 100 sq.cm. and if the film were purely amorphous Al_2O_3 then the weight increase corresponds to a film 100A thick. If the film were $Al_2O_3.2H_2O$ then the weight increase is equivalent to a film 135A thick. The

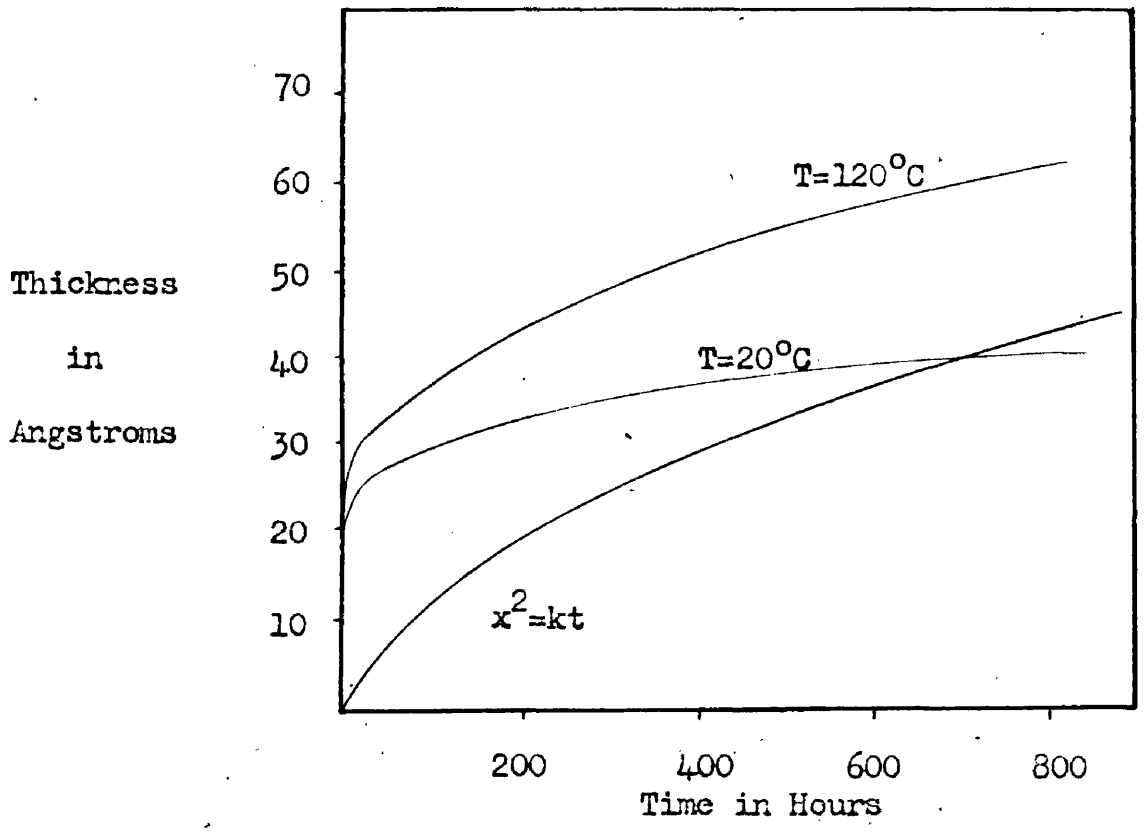

Fig.14. Theoretical oxidation curves.

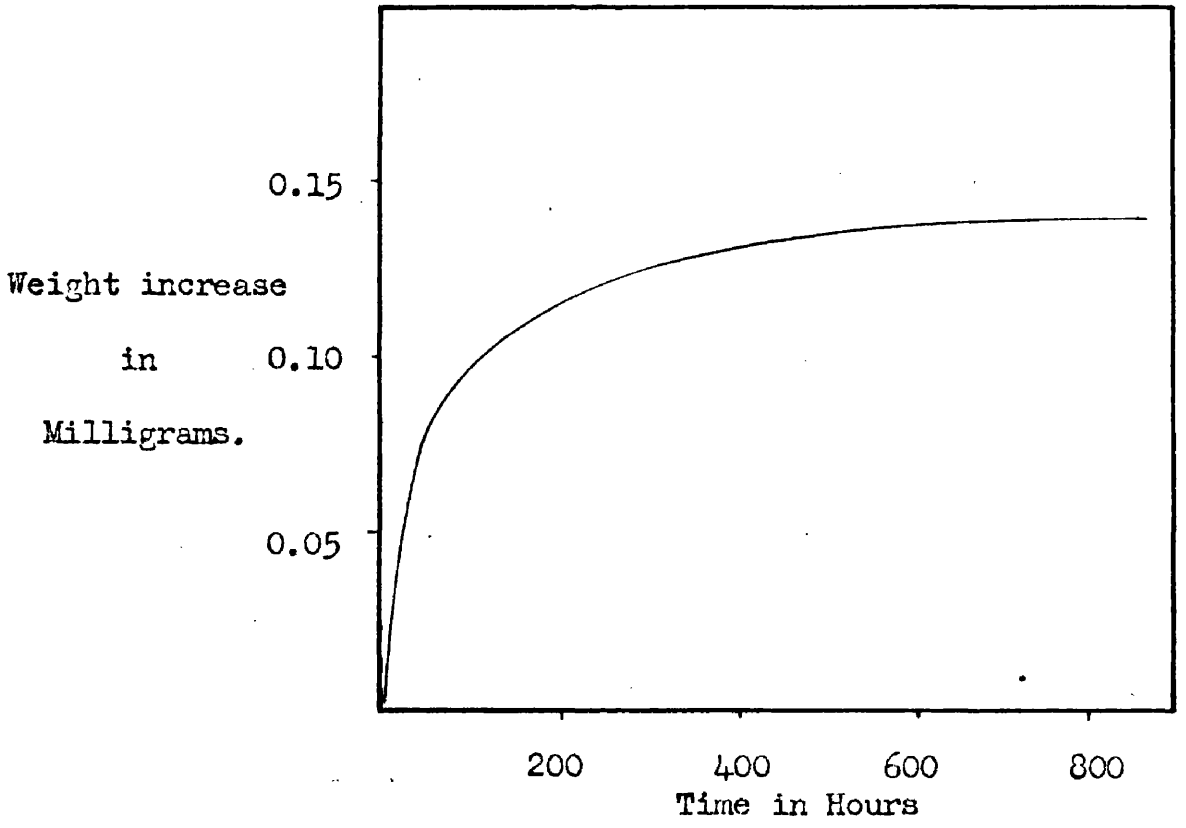

Fig.15. Vernon's oxidation by weight curve.

discrepancy in the results may be due to experimental factors; however, the shape of the curve is interesting as it lies between the theoretical 'electric field' curve and the pure parabolic type.

The growth of an oxide layer on silver has not received so much attention as that of aluminium as the oxide film is not so tenacious and protective. However, in Fig. 16, the experimental results[45] of an investigation carried out on the metal are given. In the graph are also shown the results for films of oxide on copper and iron. The oxide films here are thicker than those of either silver or aluminium, and the semi-protective nature of them has been investigated fully[46]. When copper and iron are oxidised at advanced temperatures the oxide film formed is thick and tends to blister from the surface of the metal; this allows more oxidation and the process becomes one of continual chemical attack. However, when the films are grown slowly at low temperatures they tend to contour closely the underlying surface and assist the formation of a protective coating. No experimental results in this lower temperature range were found for the other metals investigated. It is probable that chromium, like aluminium, grows a very protective coating; the oxidation rate at high temperatures is known to be[47] like aluminium, parabolic. Lead oxidises readily giving

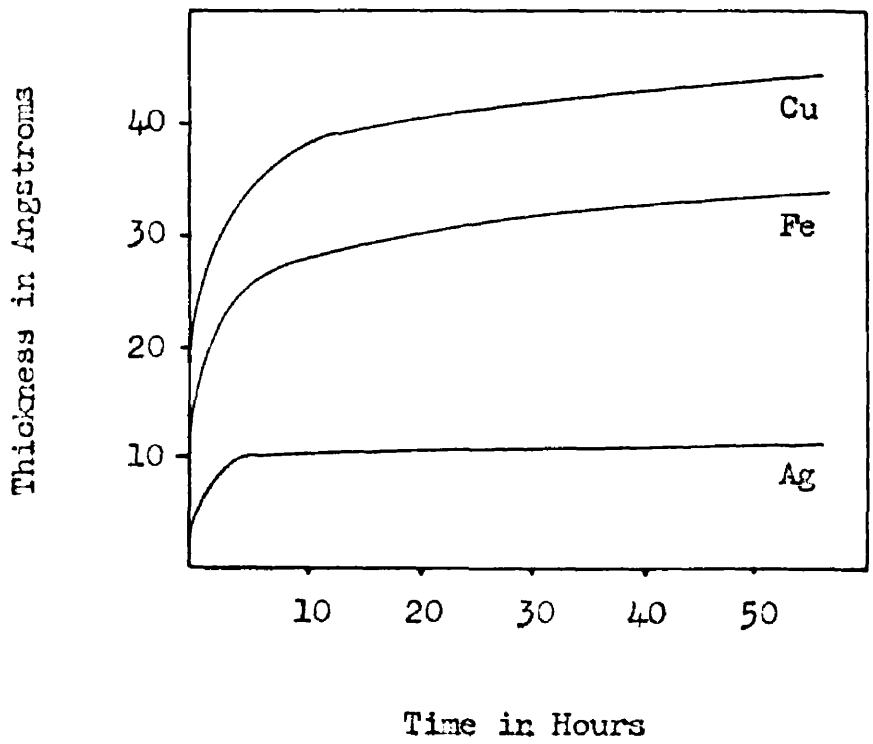

Fig.16. Oxidation Curves for Copper, Iron and Silver.

an oxide that adheres strongly to the surface of the metal. Nickel and cobalt have the same oxidation reaction but cobalt oxidises at a rate 25 times as high as that of nickel[45]. These metals, as well as manganese, oxidise with a parabolic law at high temperatures. The form of reaction at low temperatures is not known but it is expected that it will be similar to that of aluminium and copper.

CHAPTER 4

RESULT OF AGE-HARDENING INVESTIGATION

(a) Presentation of Results

The metal pairs investigated have been grouped together in the same way as they were in Chapter 3(c), by the type of equilibrium diagram that alloying the materials would give. For each of the metal pairs a number of slides were prepared as described earlier, and the changes in scratch values for the films were measured during the ageing periods, which lasted three weeks for specimens aged at room temperature, and three days for those ovened at 120°C. On each of the specimens it was possible to measure the adhesion of the substrate film to the glass alone without the upper film, the substrate film with the reflecting film on top, and the adhesion of the reflecting film when evaporated by itself onto the glass condensing plate. From the batch of slides prepared for each system a representative pair were chosen, one that had been aged at 20°C. and one at 120°C. It is the results of these specimens which are given in graphical form in the following pages. The specimens were chosen as being representative of the types of reactions obtained for each system and temperature and thus the thicknesses of the substrate films

are not the same for all the specimens. The adhesion values obtained were found to vary with the thickness of the substrate; the form of this variation is described in detail in the following Chapter.

In each of the diagrams are graphed the adhesions to the condensing plates, not only of the substrated films but also the individual metal films. The increase in adhesion obtained for each specimen can then be obtained by subtracting from the adhesion value of the compound film that of the reflecting film alone. Using this method of presentation it can be clearly seen how the ageing of the substrate layer and the reflecting film affect the compound film. For some of the systems investigated the adhesion of the double films was less than those of the reflecting films to the glass; this gives a negative increase in adhesion. Occasionally some of the films were found to be so strongly bonded to the glass that there was a tendency for the glass to chip before the scratch value was reached. This generally held for loads in excess of 800-1,000 gm. The values obtained in this region, and above, are thus only approximate.

(b) Age-Hardening in Single Metal Films

The single metal films generally aged in a parabolic or logarithmic form. Ageing in these films

cannot be due to precipitation phenomena as the metal samples used were pure and there was no possibility of subsidiary phase precipitation. The ageing, however, could be caused by three distinctly different types of phenomena, and is probably dependent on each to some degree.

If the scratch value of the film is principally dependent on the adhesion of the film to its substrate then the increase in adhesion must be caused by a reaction at the metal-glass interface. At this interface there will be some form of bonding between the regular structure of the metal and the highly irregular structure of the glass as large adhesion values were encountered. It has been suggested that the bonding of the metals to the glass is due to the formation in the glass of a surface layer of hydroxyl ions[8], and that the metal replaces the hydrogen atoms from this surface layer, forming a strong chemical bond. If this is so the increase in adhesion will be due to diffusion of the metal into suitable positions in the glass structure, increasing the number of adhesion bonds. This theory is supported by the evidence that the substances showing the best adhesion to glass are the metals that readily form oxides.

If the film structure has been deposited in the form of aggregates it is possible that some areas of the

glass might not be in contact with the metal film and the increase in adhesion could then be due to diffusion of the metal within the film filling up the vacant surface bonds. From the vast increases in adhesion obtained on ageing it is unlikely that this could account completely for the ageing.

As the scratch test is dependent to some extent on the actual cohesion of the films then the process could be one of diffusion in the film only. It is known that metal films condense from the vapour with a large number of vacant lattice sites and dislocations[48]. Random migration of the lattice atoms would aid the reduction of the free energy of the system to its minimum value. The vacancies would thus tend to diffuse outwards to grain boundaries, or if no grain boundaries were present, to positions of suitable stress concentration, there they would group together and assist break up of the film. The planes of maximum stress would form the most likely sites for the vacancies to migrate to and the dislocation paths to end at. Comparison with the increase in adhesion that could be expected from this method of ageing lead us to the conclusion that although this process might assist the hardening it could not control it. Thus it appears that the first theory suggested, that of diffusion into the glass structure itself, is the most likely.

If we consider the method used for measuring the adhesions of the specimens in detail we can see that the process can be taken as being composed of two parts, the probe and the specimen. In this particular investigation, the size of the probe has been kept constant by examining a large number of the tips of these under a microscope. They were found to be of practically constant diameter. However, the method of measuring adhesion is essentially a ploughing phenomenon and when the cohesional forces within the film are constant it gives a relative measure of the adhesion of a film. If the cohesion is not constant then the apparent adhesion values will be altered. This is the basis of the formation of the age-hardening curves which are described in the following sections.

The specimen can be considered as made up of a number of structural regions and the measured adhesion value of the film to be affected by the individual strengths of these regions. The factors involved are:

(1) Adhesion of substrate to condensing plate.

(2) Cohesion of substrate material.

(3) Adhesion of substrate film to alloy layer.

(4) Cohesion of alloy layer.

(5) Adhesion of reflecting film to alloy layer.

(6) Cohesion of reflecting film.

(7) Strength of a protective coating on the surface of the reflecting film.

The most important of these are undoubtedly (1), (2), (4) and (6). The adhesions (3) and (5) can be considered as part of the alloy layer and, indeed, if a true transition structure is obtained there will be no sharp boundaries from either of the metals into the transition layer. The quantities (1) and (2) are closely related and appear to be inseparable, for a good adhesion in a single film appears to be obtained for a material that has a high cohesional strength. This is in agreement with the theory that the adhesion is caused by diffusion of the metal atoms into the glass structure.

The presence of a hard surface layer could increase the resistance of the film to marr; this, however, would tend to show up more in the other methods of adhesion testing, described in Chapter 1. The loads used in this investigation are enough to cause plastic flow in the reflecting metal film which would give no support to a hard oxide film. The increase in adhesion of the single metal films are certainly not due to this cause as the time for oxidation and ageing are not comparative. Thus we are left with two principal factors to consider,

(a) Adhesion and cohesion of substrate film,

(b) Strength of interfacial layer.

The former of these is given by the shape of the adhesion curve for the single film of the substrate metal and the summation of the two must be the total adhesion results for the substrated film. The difference then gives the quantity 'b'. It can be seen from the results that this gives negative values for the strength of the interfacial layer as well as positive values.

(c) Intermediate Phase Systems

Five metal systems were investigated here and these have been sub-divided into three categories. Two alloy systems formed intermediate compounds with a high energy of formation, aluminium-nickel and aluminium-cobalt; two formed compounds with a large free energy, aluminium-iron and aluminium-manganese; and the last system formed all its compounds by peritectic reaction, aluminium-chromium. For all these systems aluminium was used as the reflecting film material and evaporated on to the others which formed the substrate films.

Aluminium-Nickel. The adhesion curves obtained for the adhesion of the aluminium films, Fig. 17, are representative

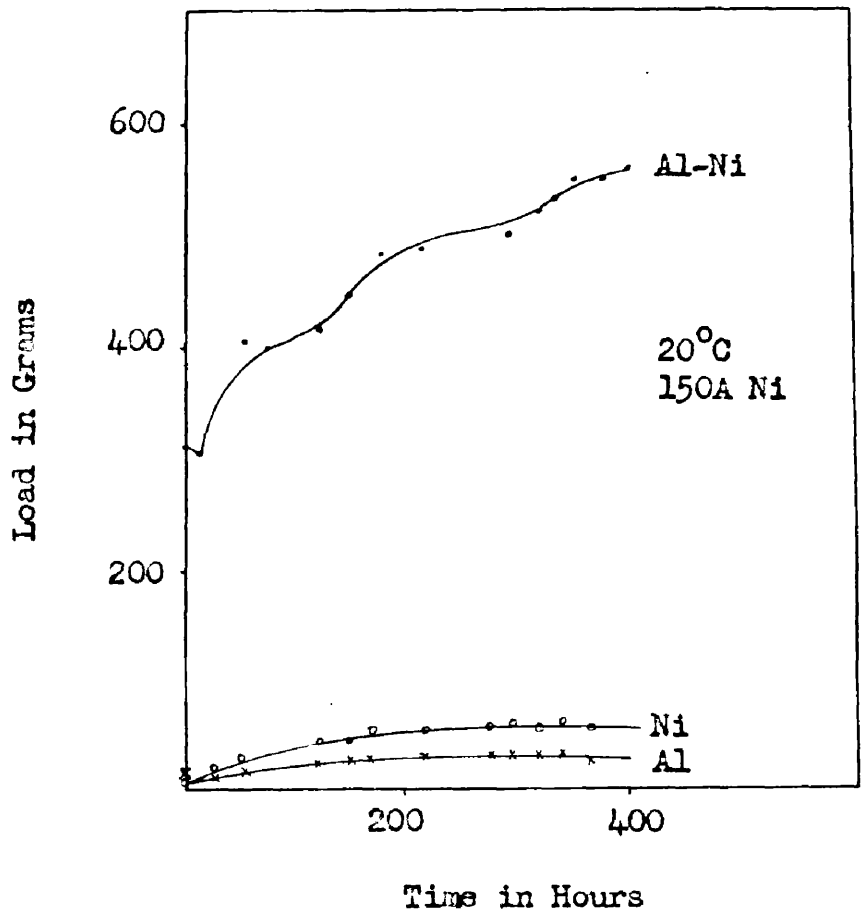

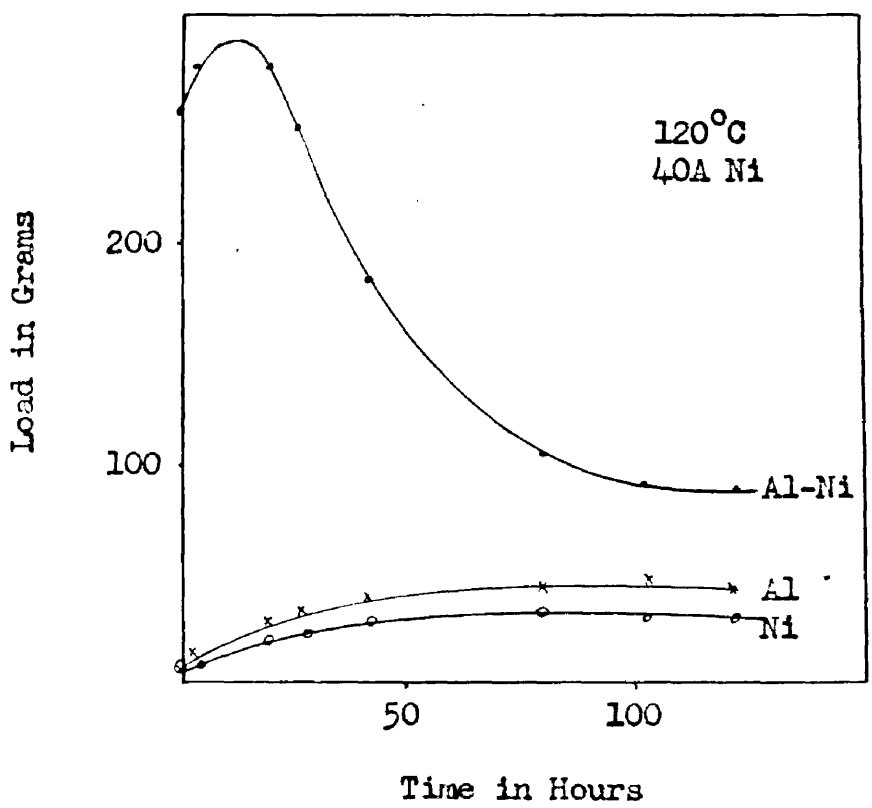

Fig.17. Ageing of Aluminium-Nickel Films at 20°C & 120°C

of all the films of aluminium investigated. The specimens increased their adhesions regularly in the manner previously described, reaching the maximum values in 200 hours at 20°C. and 20 hours at 120°C. The adhesions of the nickel films are comparable with the aluminium ones and the nature of the bonding appears to be, as suggested earlier, for both cases a diffusion process into the glass structure.

The substrated film, however, is extremely interesting. Here we have an excellent example of the multiple step ageing process expected from an alloy system containing a number of pure phases. The system nickel-aluminium has three of these, the cubic β phase NiAl, the $NiAl_2$, and the $NiAl_3$, as well as a solid solution of aluminium in nickel. The compound with the high energy of formation is the simple intermetallic compound NiAl. As shown in Chapter 3(c), the ageing curve represents the summation of the ageing processes that are forming the transition layer. As the precipitation structures change, so the hardness of the transition layer increases, as shown by the room temperature ageing curve. The ovened graph shows another example of the type of ageing outlined by Gayler. Here we can see that the rapid precipitation has allowed the adhesion to increase to its maximum within ten hours of the commencement of

ageing. The precipitation process has then allowed the stresses in the lattice to be eased and the hardness has decreased. This is the second period of age-hardening proper. The precipitated phase should be the β and this has been confirmed (see Chapter 6). The process will be entirely independent of the thickness of the substrate film once a certain minimum value has been reached. If, however, the thickness of the nickel is very small there might not be enough of it to form a compound layer of sufficient thickness to cause the precipitation stresses to be released. Thus it is possible that the adhesion of the compound film would give an adhesion value in excess of the specimen chosen here for thinner substrate films.

Aluminium-Cobalt. If the precipitation of the β phase of the system aluminium-nickel reduced the adhesion of the compound film of these materials, precipitation of the γ phase of the aluminium-cobalt system removed the adhesion completely. The adhesion of the ovened and the air hardened films can be seen in Fig. 18. The pure films of aluminium and cobalt aged as already described, but the compound films showed no adhesion to the condensing surface at all. From the phase diagrams of these analagous systems it can be seen that the γ phase has a slightly

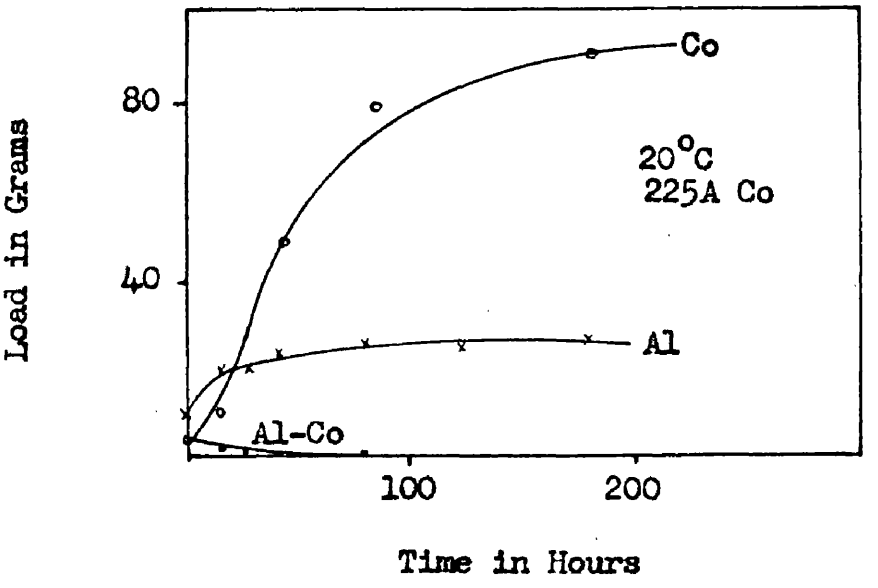

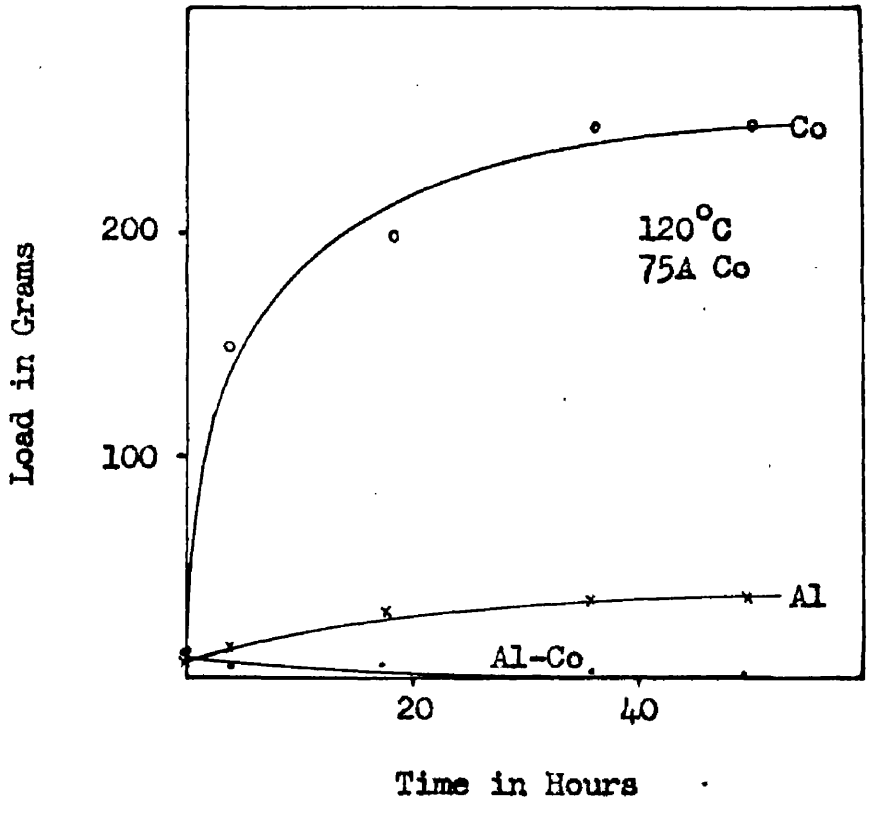

Fig.18. Ageing of Aluminium-Cobalt Films, 20°C & 120°C.

wider concentration range than the β NiAl, but the energy of formation appears to be about the same. Thicker films of aluminium substrated with nickel, however, showed the same decrease in adhesion as this relatively thin film of cobalt and aluminium.

Aluminium-Iron. Thin films of iron aged very rapidly and were much more tenacious than the metals that have been already described, Fig. 19. This is in agreement with the oxide theory of surface bonding as iron is more readily oxidised than aluminium, nickel or cobalt. The phase diagram of the aluminium-iron system shows that the concentration range in which the compounds are formed is very limited, and that each separate phase has an extremely narrow concentration region. The effect of this on the interfacial layer can be seen from the shapes of the ageing curves for the compound films. Both graphs show the form of curve already obtained for the nickel-aluminium film aged at 120°C. This follows directly from the narrowness of the transition region as very slight diffusion would be required to give large structural changes within the film. From the shape of the curves it would appear that the precipitation and release of strain processes have been obtained in both the specimens. Ageing at the elevated temperature has only increased the rate of the reaction.

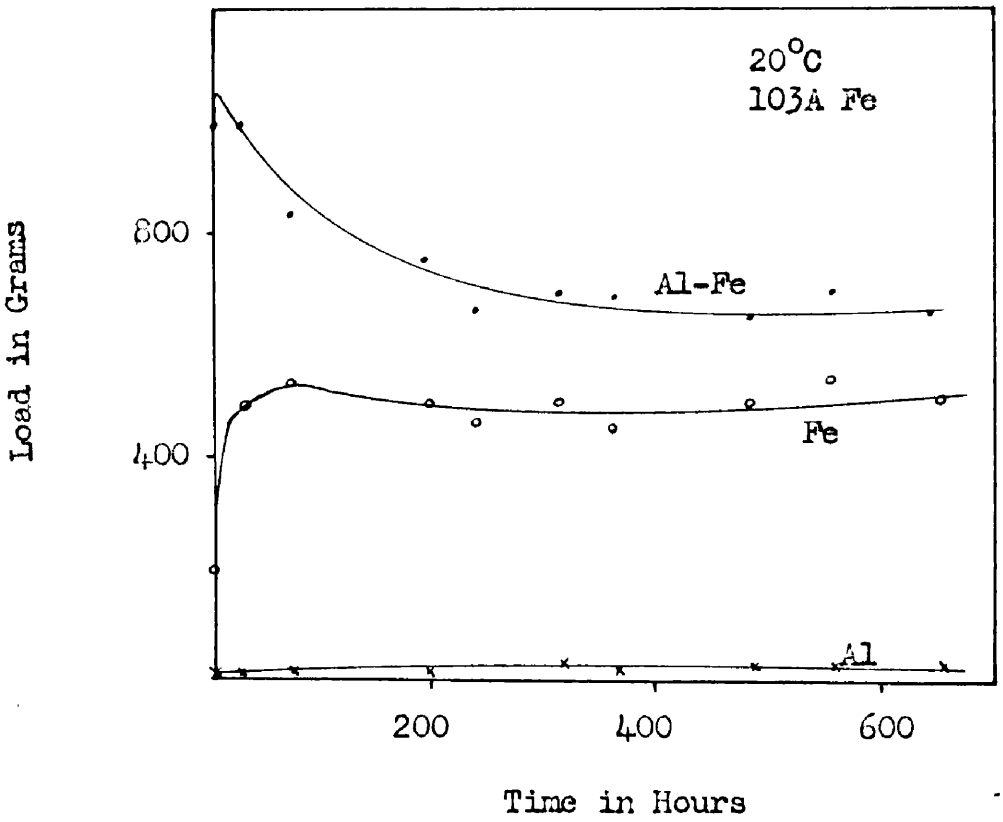

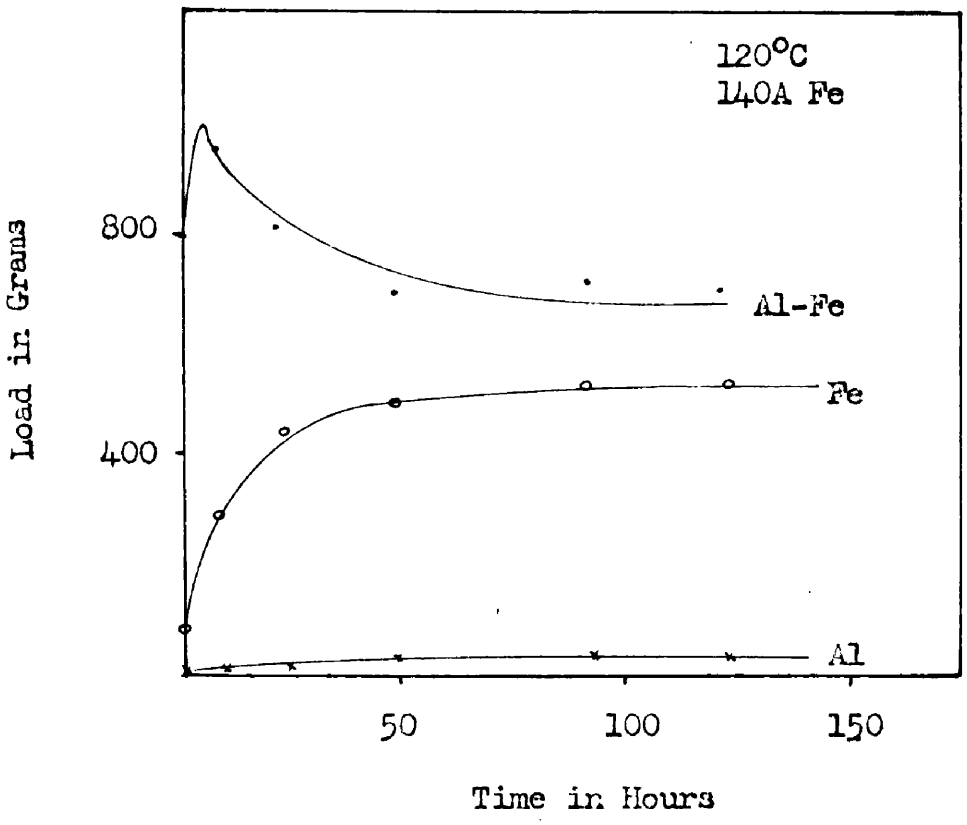

Fig.19. Ageing of Aluminium-Iron Films, 20°C & 120°C.

The initial and final values of adhesion appear to be fairly constant, suggesting that the process may be thickness independent. This could only be so if the transition region was only penetrating into the substrate film to a small depth.

Aluminium-Manganese. As Fig. 20 shows, similar results were obtained for the aluminium-manganese system. In both films, however, the original rapid increase appears to have taken place before the first measurement could be made and both films show only a decrease in the adhesion value with time. The lower temperature aged specimen gives a much slower rate of decrease reaching a final value larger than that of the specimen aged at the higher temperature.

The principal point of interest in the specimens of this system are the ageing curves for the manganese films. For both specimens, we have a pure metal film exhibiting the ageing habits of an alloy. The explanation of this is that manganese has three distinct structures, the α, the β, and the γ. The first of these is stable at room temperature, and the others are high temperature transformations. It is not known in which form manganese will condense from the vapour phase but it is possible that as the energy content of the condensing film is high

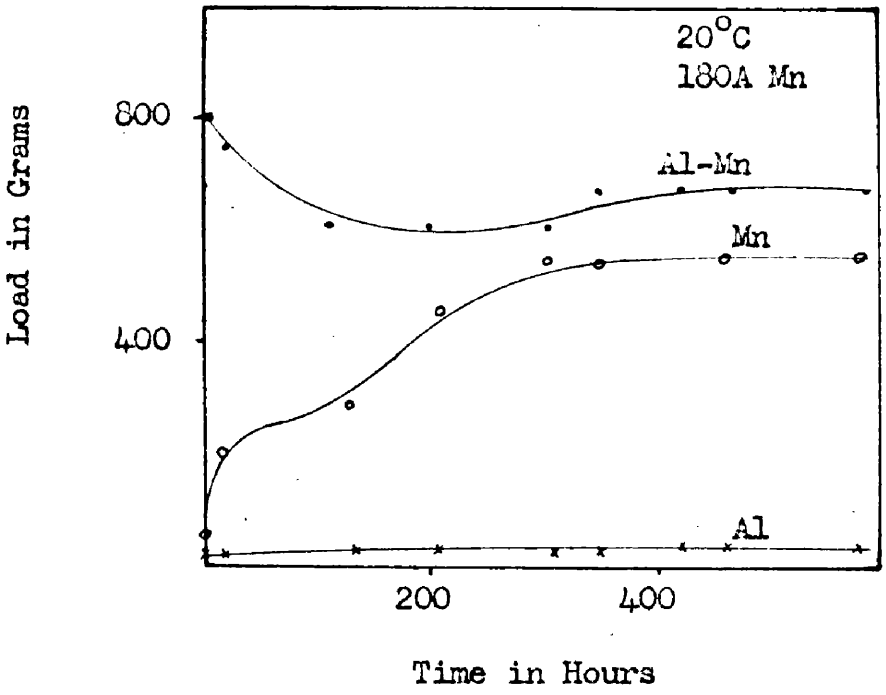

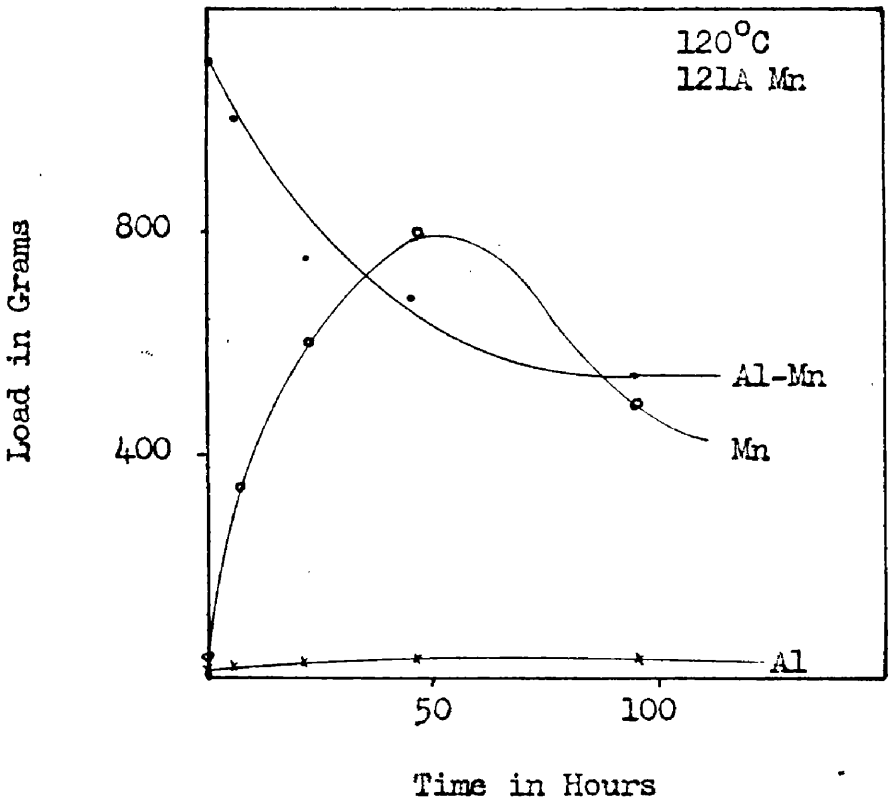

Fig.20. Ageing of Aluminium-Manganese Films, 20°C & 120°C.

that it might form one or other of the more irregular structures. Ageing at low temperatures will assist the transformation of these structures into the more stable α type. This will require nucleation of the new phase, and precipitation of the new structure will lead to the ageing phenomena obtained experimentally. The transformation appears to have had little effect on the adhesion of the compound film.

Aluminium-Chromium. This system showed the simpler form of substrate layer ageing curves, Fig. 21. The ageing of the compound film at the lower temperature was very similar to the adhesion curves for the manganese films. It can be seen that the ageing process is taking place as two distinct parts, both increasing the adhesion of the specimen. The equilibrium diagram for the system shows the presence of a large number of stable phases, none of them having such a high energy of formation that there would be a tendency to form one particular phase at the expense of the others, neither is there such a large region of solid solubility, nor such a small complex phase region as in the case of iron. From the ageing graphs it appears that the diffusion process is limited and that solid solutions are formed. The transition region then will be small, but not too small to cause interaction from the

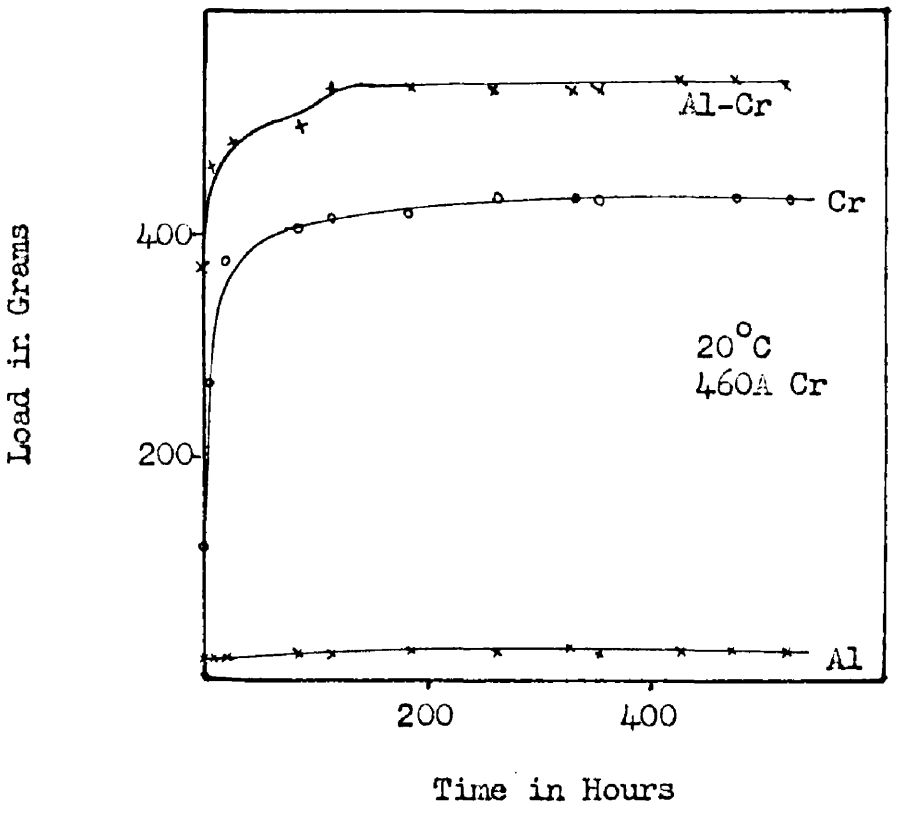

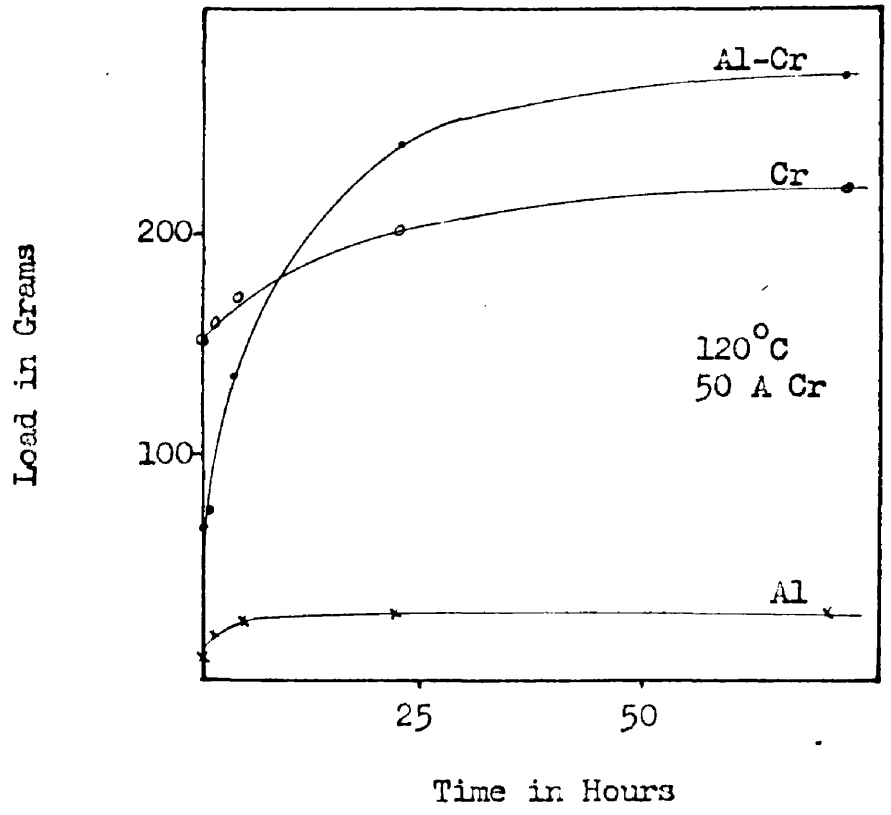

Fig.21. Ageing of Aluminium-Chromium Films, 20°C & 120°C

different phase boundaries. The raising of the ageing temperature causes both the ageing processes to follow on directly as expected.

For both these specimens the adhesion of the substrated film is greater than that of either of the substrate, or reflecting films. Thus it cannot be said that it is only the adhesion of the substrate that is affecting the adhesion of the substrated film. The rapid increase of adhesion in the first few hours suggests that when the films are first prepared the adhesion at the interface is very small, and the values initially obtained are not so much a measure of the adhesion of the actual metal pair as a measure of the time that has elapsed between evaporation of the first monolayer and the measurement of adhesion. This would seem to be true of the measurements made on the single metal films also. In particular, when results were being obtained for films of chromium, the film was found to be increasing its adhesion while being measured.

(d) Partially Miscible Systems

The metallic systems investigated here were the silver-lead, the gold-chromium, and the copper-chromium. The first and last of these are only slightly non-miscible,

lead being slightly soluble in silver, and chromium slightly soluble in copper at temperatures in excess of 500°C.

Silver-Lead. The adhesions of the silver-lead compound films are extremely dependent on the nature of the substrate layer. As films of lead appear to have a poor adhesion to the condensing plate, and as lead is a very soft metal this gives small adhesion values for the compound films. The presence of the silver layer can be seen as the loads required for the compound films are always greater than the corresponding values for the pure lead films. The results obtained for the pair of specimens are given in Fig. 22. The adhesions of the silver films are comparable with those of the films of aluminium.

"With this system there can be no doubt as to the formation of a transition region by diffusion, for in the specimen ovened at 120°C. the presence of lead could be clearly seen in the reflecting surface of the silver film. This means that the lead atoms must have diffused completely through the thickness of the silver film. The loss in reflectivity caused by this is described in detail in Chapter 10. The presence of the relatively mobile lead atoms in the silver structure would almost certainly cause the solid solution of lead in silver to be formed. This, however, would not bring about a precipitation process, and

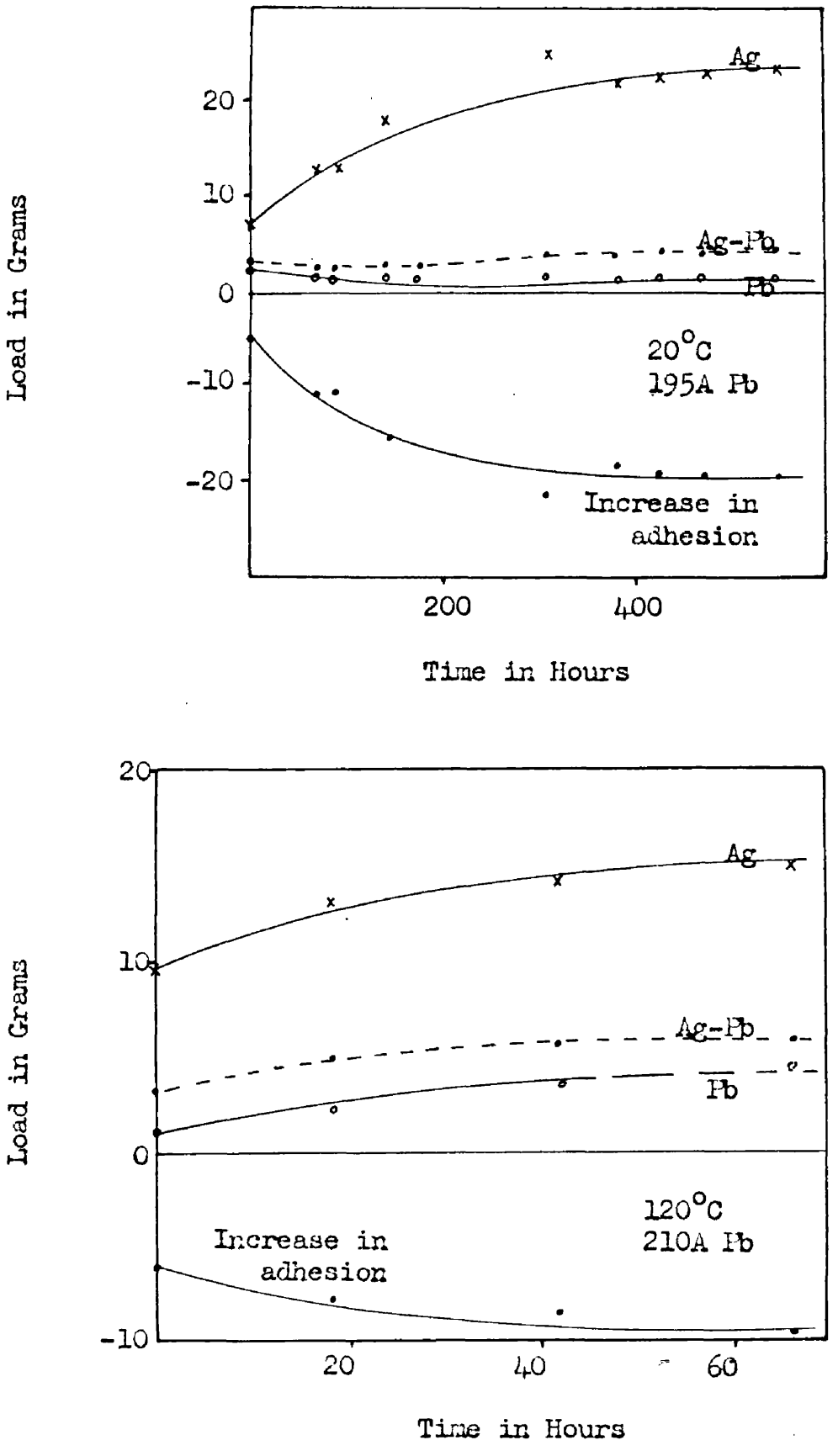

Fig.22. Ageing of Silver-Lead Films, 20°C & 120°C.

there would be no corresponding increase in the strength of the interfacial layer.

Using lead as a substrate difficulty was found in obtaining adhesion measurements over a period of time as the lead, particularly when ovened, appeared to be either evaporating away from the glass or forming a non-absorbing oxide. Because of this it became impossible to view the scratches and results could not be obtained for the later stages of ageing.

Gold-Chromium. Thin films of gold had a poor adhesion to the glass condensing surface. Being a noble metal it is not readily oxidised and thus would not be expected to show a high adhesion. However, the adhesions of the substrated films, Fig. 23, were excellent. The compound films show that the phase diagram of the metal system is more complex than for the last case, and indeed two miscible solid solutions are formed. Initially the compound films showed larger adhesion values than the corresponding substrate films. However, the specimen aged at room temperature gave the form of ageing curve already obtained for the aluminium-iron specimens. This must be due to the formation of the miscible solid solutions. As no great change in the reflectivity of the gold surface was noticed we may assume that the diffusion of gold and chromium was

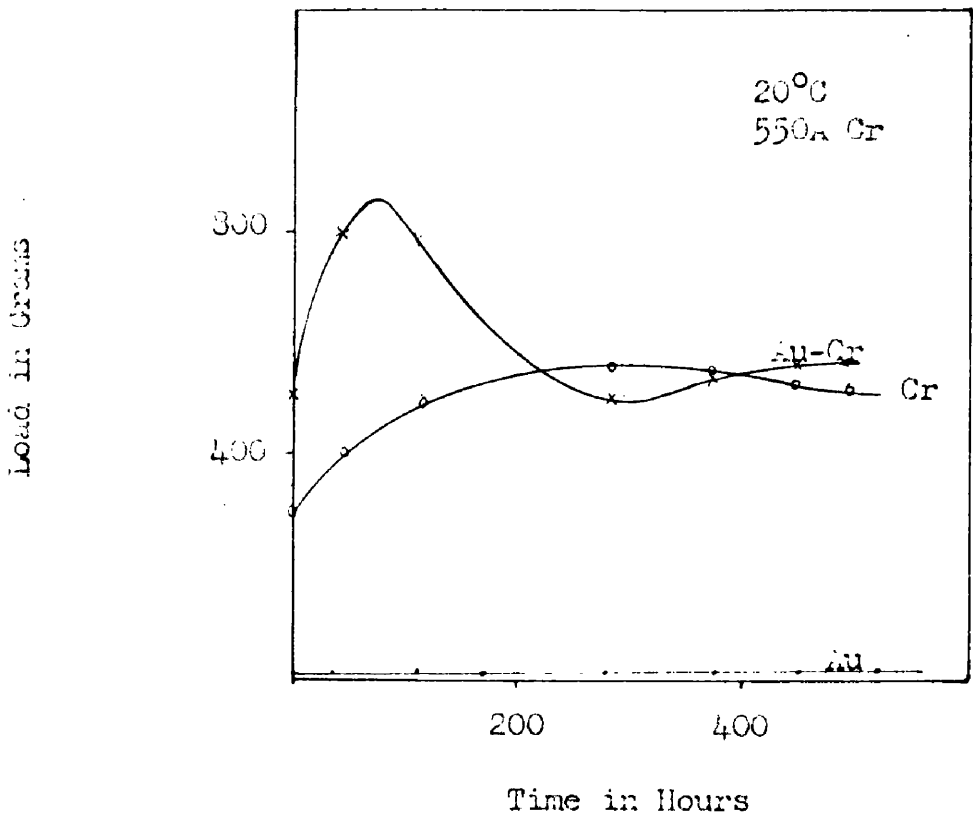

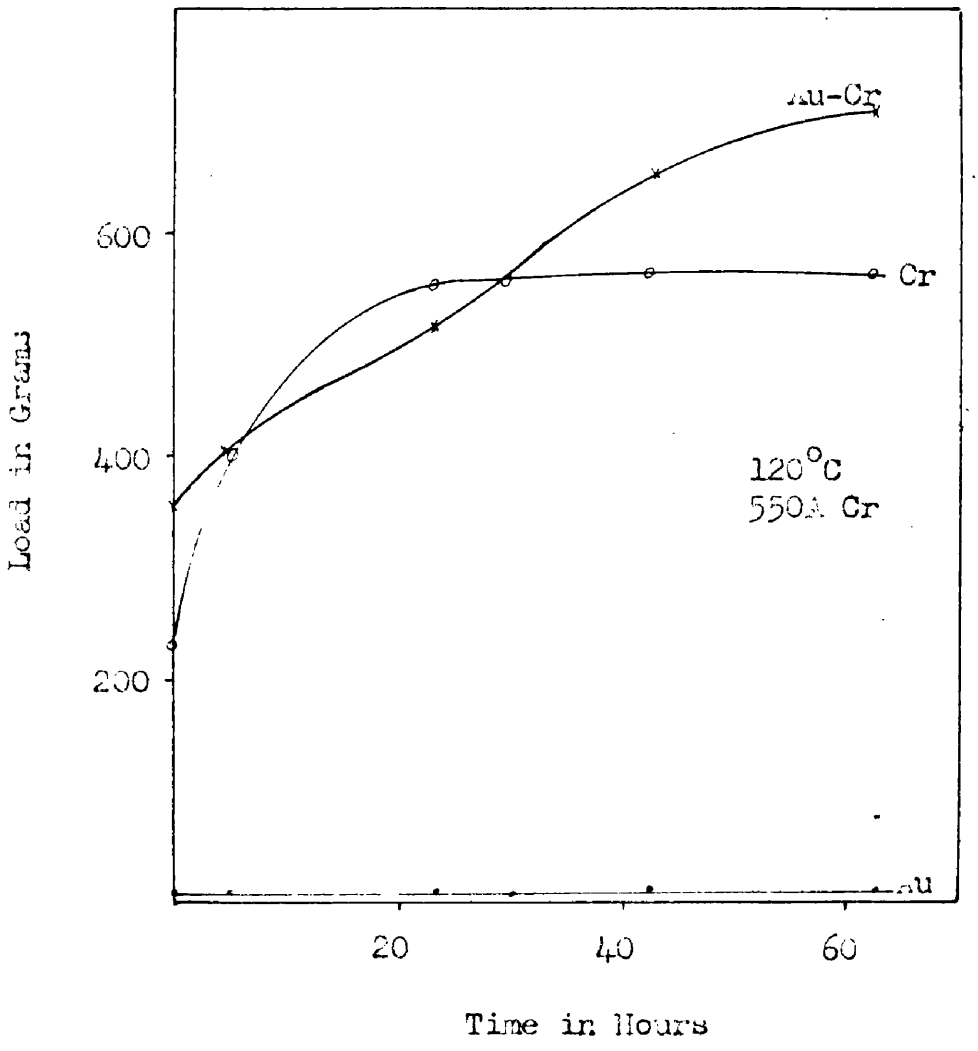

Fig.23. Ageing of Gold-Chromium Films, 20°C & 120°C.

limited. The solid solutions then would be formed within a very narrow region. This will allow strains to be set up which would increase the hardness of this region. If the stress concentration becomes greater than some particular value internal slip would take place and the hardness of the region would decrease.

If the same film were to be aged at an advanced temperature the mobility of the atoms would be increased; this would allow the formation of a buffer of the mixture of the miscible solid solutions to be formed between the phase boundaries. The stress will thus be lessened and if the concentration of stress stays below the critical value the interfacial layer will increase its hardness without causing slip to be generated. This could, of course, only take place where the cohesion of the substrate layer is great and it itself is strongly resisting distortion of the structure in the transition region.

Copper-Chromium. The phase diagram of this system is very similar to that of the silver-lead system, but the ageing curves, Fig. 24, are completely different. This is undoubtedly due to the greater cohesive strength of the substrate film material. Little age-hardening could be discerned in the copper films, but the adhesion value was as good as any of the reflecting film materials. If the

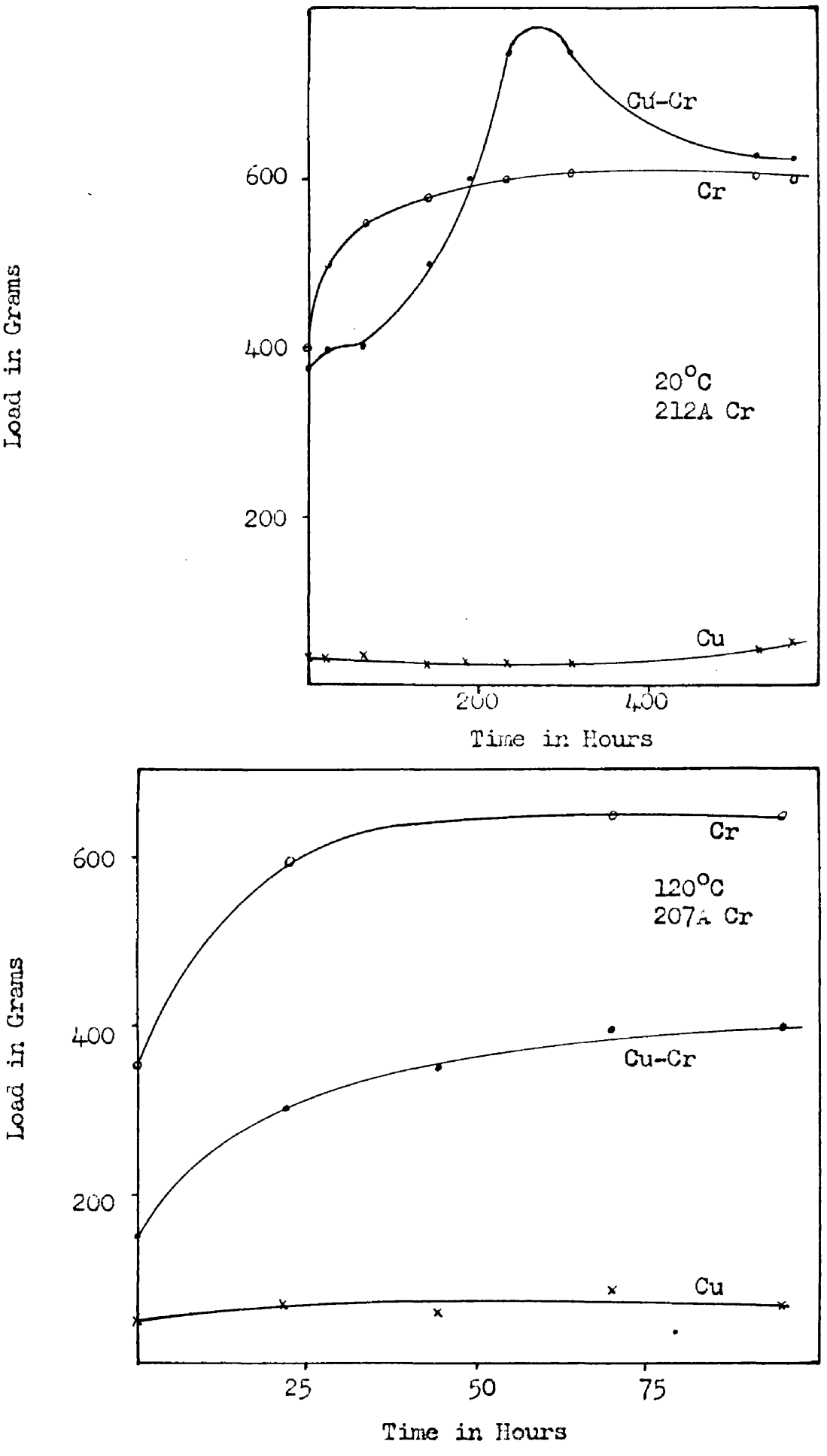

Fig.24. Ageing of Copper-Chromium Films, 20°C & 120°C.

adhesion is caused by the presence of a thin layer of oxygen between the metal film and the glass surface then copper, having a high rate of oxidation could, by a gettering action on the remaining gas in the vacuum chamber, form a complete layer of copper oxide before the metal began to condense[49]. Then whereas the other films increase their adhesion after deposition by diffusion of the oxide, the copper films would show a constant adhesion value.

This would also mean that underneath the substrated copper films there would be trapped a layer of chemically bonded oxygen forming an interfacial layer between the chromium substrate and the copper reflecting film. The metals, however, will probably diffuse right through this barrier and interact to give the solid solution. The process of diffusion will, however, form stresses in the oxide layer which would increase rapidly with the degree of penetration. With increasing stress the oxide would break up under a shearing action and the hardness of the layer would increase rapidly.

If, however, the action takes place at a temperature at which the copper atoms are relatively free to diffuse through the oxide layer then the copper will diffuse through readily and the oxide will become dispersed in the copper film without exceptionally high stresses being

set up. In this case, the solid solutions formed will give a further increase in the hardness by the process outlined by Desch[12]. As the stresses do not reach the value at which slip would occur there will be no peak in the age-hardening graph.

(e) Miscible Systems

Aluminium-lead and silver-chromium were the only miscible systems involved. At higher temperatures than those used for ageing there is a possibility of chromium being slightly soluble in silver.

Aluminium-Lead. The hardness results for the specimen of the compound film, aged at the lower temperature, Fig. 25, followed the pattern of the silver-lead specimens. The adhesion values were undoubtedly strongly influenced by the nature of the substrate material. It was obvious that the rate of diffusion of lead in aluminium was greater than that of lead in silver as the presence of lead on the reflecting surface of this specimen was quite noticeable, and for the silver specimens ageing at 120°C. was required before the depth of penetration of the lead atoms became comparable to the thickness of the reflecting film.

The other specimen for this system showed an

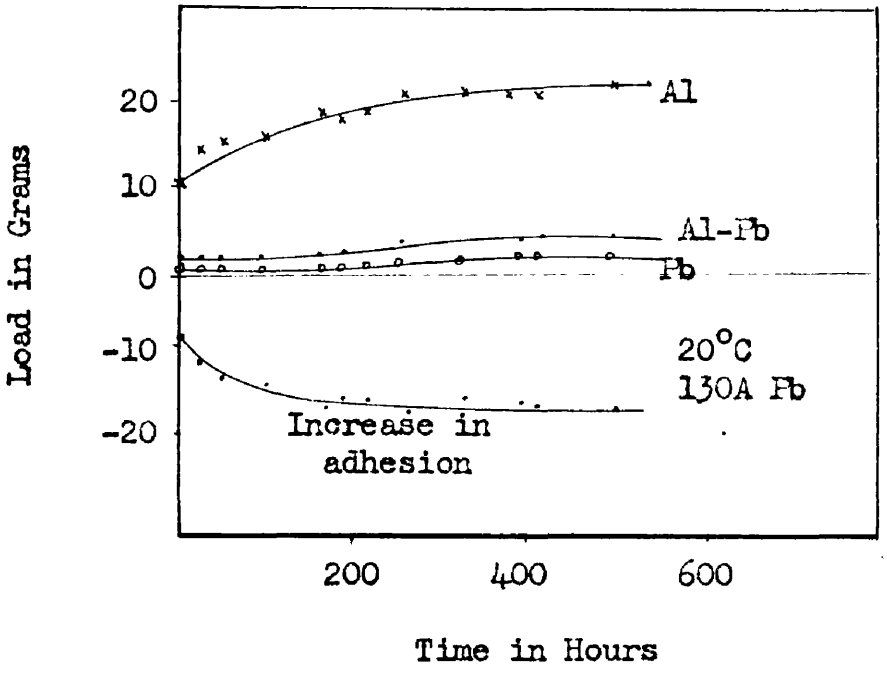

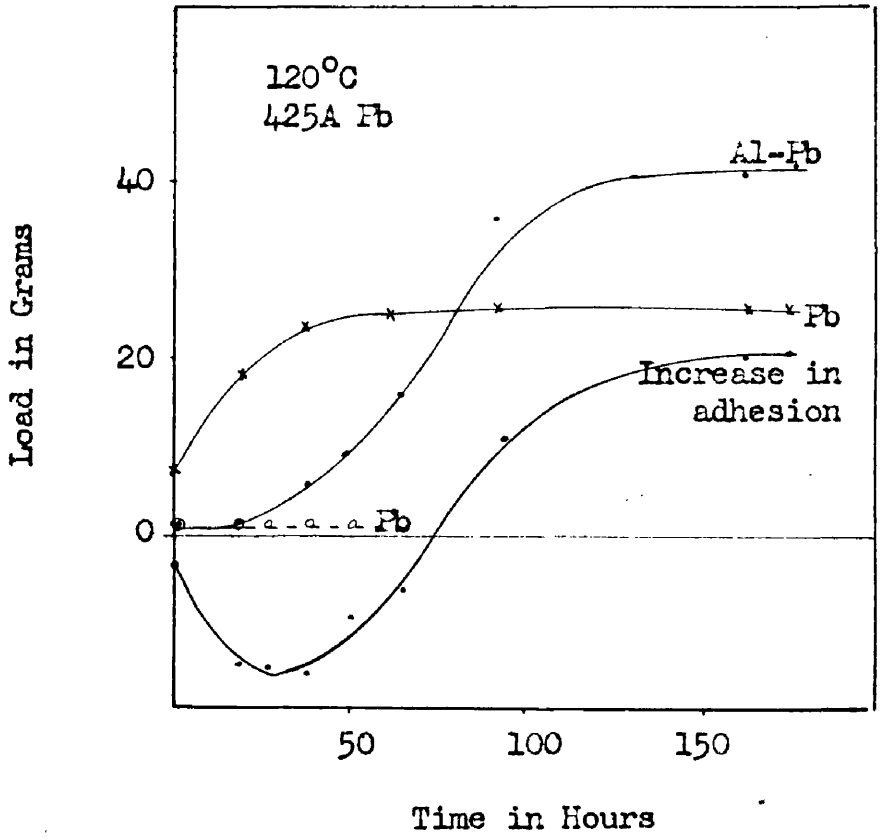

Fig.25. Ageing of Aluminium-Lead Films, 20°C & 120°C.

anomalous increase in adhesion. This was not accompanied by a corresponding increase in the adhesions of the single metal films, which behaved quite normally, nor was this type of ageing found in any of the silver-lead specimens. The reaction must be due to the increased rate of diffusion of lead in aluminium at 120°C. and it is suspected that it is caused by an oxidation process. This would require further investigation by other means in order to obtain accurate information on the complete composition of the film. Both aluminium and lead oxidise readily and the oxide of aluminium is extremely hard. Assuming that the reaction is an oxidation phenomena it will be completed relatively quickly in the thinner films, or rather those having a thinner substrate layer. Where, however, the lead thickness is large the reaction will probably not reach finality. We would thus expect there to be a critical value of thickness at which the hardness would reach a maximum value.

Silver-Chromium. The adhesion curves for this system are given in Fig. 26. The particular specimen of silver chosen for the 120°C. ageing showed a decrease in adhesion with time that was not generally found; however, the form of the compound film curve is representative of the other specimens of the system. The chromium graphs are excellent

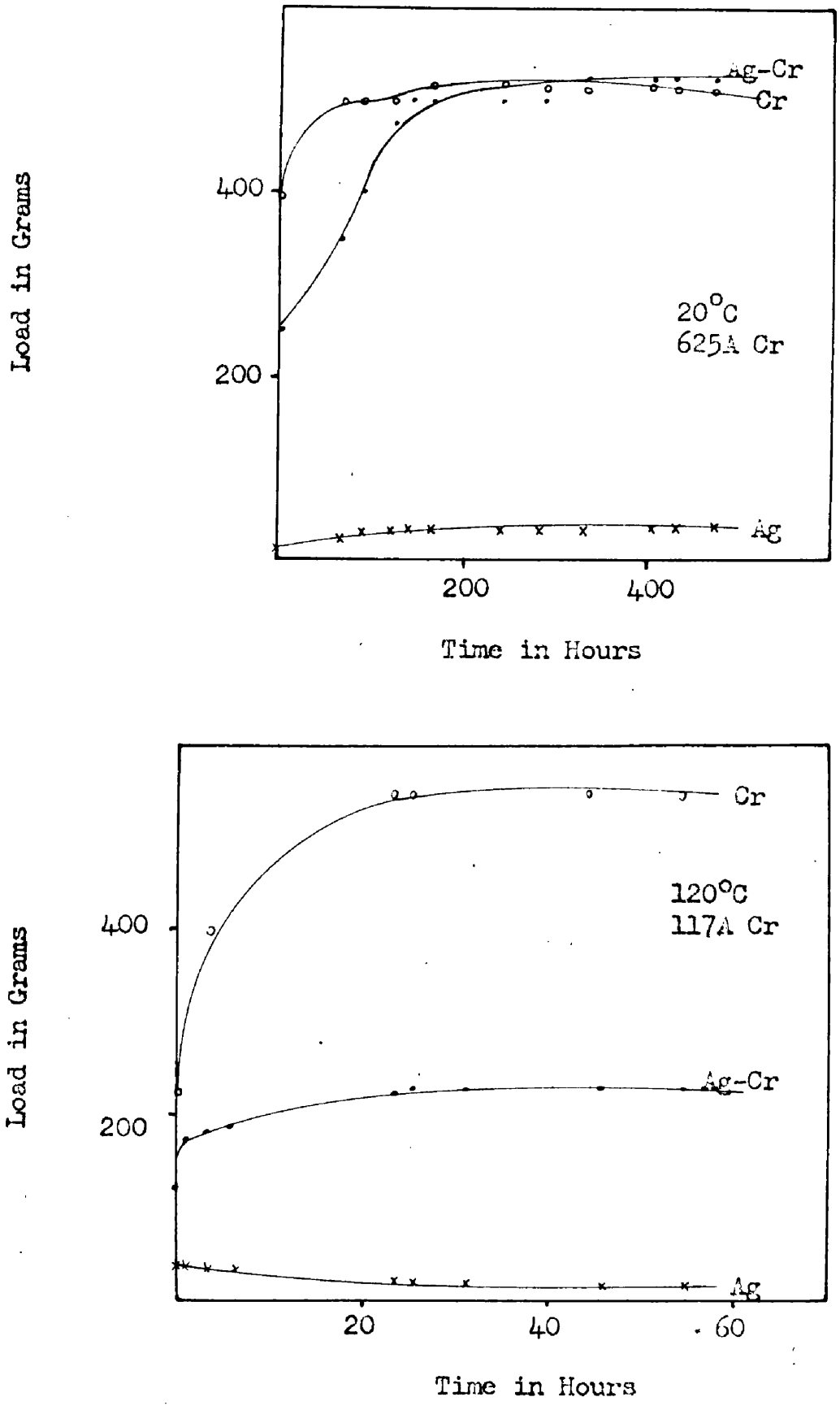

Fig.26. Ageing of Silver-Chromium Films, 20°C & 120°C.

examples of the types of ageing curves obtained for this metal. Chromium was an extremely consistent metal to work with as can be seen from the other systems in which it was used as the substrate layer.

Both compound films showed an initial adhesion value less than that of the substrate layer but the film aged at 20°C. increased its adhesion until it became slightly greater than that of the chromium film. When, however, from this value is taken away the adhesion of the silver film alone, the increase in adhesion appears to be equal to the adhesion of the chromium substrate layer. This suggests that the silver was actually peeling off the surface of the chromium and that the increase in adhesion was due entirely to the presence of the substrate. In a few of the films it was noticeable that the silver was peeling, leaving behind some of the chromium. However, as the scratch mark, when viewed under a microscope, was quite even this load was taken as the adhesion value of the film. The early part of the ageing curve, however, shows that the silver and chromium did not behave completely as independent layers and the high temperature ageing graphs showed that the adhesion of the compound film, in this case, is much less than that of the substrate.

As the two metals are entirely miscible there

can be no hardening at the interfacial layer and the adhesion of the substrated film appears to be completely controlled by the adhesion of the substrate film. Some interdiffusion is undoubtedly taking place, but under strain the silver layer peels off the chromium. Although fair adhesion values have been obtained it is possible that these films would not show such a good marr resistance as the other specimens.

(f) Discussion of Results

From the results described some broad generalities can be considered on the question of the adhesion of a metallic film when a metallic film of another material has been interposed between the film and the condensing plate.

(i) There is, for certain metal-substrate pairs, a high initial adhesion, as measured by the scratch test method. This adhesion can be greater than that of either of the single metal films to the condensing plate.

(ii) If the metals are allowed to remain at one temperature for a period of time then the value of the adhesion of both the single metal films and the compounded

films do not remain constant.

(iii) The changes found in the compounded films cannot be related directly to the changes in the single metal films forming the double layer.

From the first and last of these it would appear that the process must be one of mutual interaction at the interface. The process then, as discussed in detail for each particular pair, is equivalent to an alloying, and, from (ii) the resultant age-hardening. Here, however, instead of starting off with an alloy mixture we have initially the two components in intimate contact along a common boundary plane. The process is thus limited and dependent entirely on the rate of interdiffusion of the metallic components in one dimension. It is extremely unlikely, except for high rates of diffusion, that a perfectly homogeneous alloy layer will be formed. The more reasonable conclusion to draw is that there will be formed, at the interface, a transition region blending into the parent metal structures on either side. The stresses formed by this diffusion process will be concentrated in this transition region and, under certain circumstances, they will cause precipitation of an alloy phase from the solid solutions.

CHAPTER 5

RESULTS OF THICKNESS INVESTIGATION

(a) Presentation of Results

This chapter describes the results of the measurements made on a large number of specimens of each of the metallic systems described in detail in the preceding chapter. The slides were prepared having various thicknesses of substrate film, and the increase in adhesion obtained for each specimen is plotted against the thickness of the substrate layer. Measurements were made immediately after the specimens were removed from the evaporation unit and after the periods of ageing. As before, two ageing conditions were chosen: the first at room temperature for three weeks and the other, for specimens at 120°C., for three days. The results are plotted as increases in adhesion, that is, from the adhesion value of the compound film was subtracted the adhesion of the reflecting film of the same specimen to the same glass base. This does not give a direct measure of the strength of the interfacial layer which can be obtained by subtracting from the adhesion value of the compound film that of the substrate layer, but is more

representative of the durability and resistance to abrasion of the compound film as compared with the reflecting film alone.

The higher temperature ageing was investigated more thoroughly as it was felt that this would show up deleterious ageing effects that would only be noticeable in the specimens in which a lower rate of diffusion prevailed after a long period of ageing. In doing so we were following industrial practice in which aluminium reflecting films are ovened after evaporation.

(b) Adhesion of Single Metal Films

In the first of the specimens examined there appeared to be no regular variation in the adhesion of the single metal films forming the substrate and reflecting layers with their thickness, and thus no thorough investigation was carried out for these films. Some variation in adhesion was obtained for the more strongly bonded metal films, but this was probably due to a difference in the time lag between evaporation and measurement, for the adhesions of these films increased immensely just after evaporation. The period of time between evaporation and actual measurement was kept to a minimum, but even then it could not be less than about

three minutes. The greatest part of this was taken up in allowing air into the evaporation chamber. The adhesions of metal films for varying thickness and condensing surface material has been investigated by Benjamin[50], who reports that he found negligible changes in adhesion with thickness.

(c) Intermediate Phase Systems

Aluminium-Nickel. The specimens for this system already described in detail showed that when the films were aged at 20°C. there was a large increase in the hardness of the film due to an increase in the concentration of stress at the compound film interface. When aged at 120°C., however, the stress increased above the critical value and the resulting precipitation of the intermediate compound rapidly reduced the hardness of the interfacial layer. It can be seen from Fig. 27 that the latter process is dependent on the thickness of the substrate layer.

Initially the films showed a good adhesion and ageing at room temperature increased this. The thinner films when ovened, however, showed only a slight decrease in adhesion, presumably due to insufficient nickel content within the films to bring about the precipitation process,

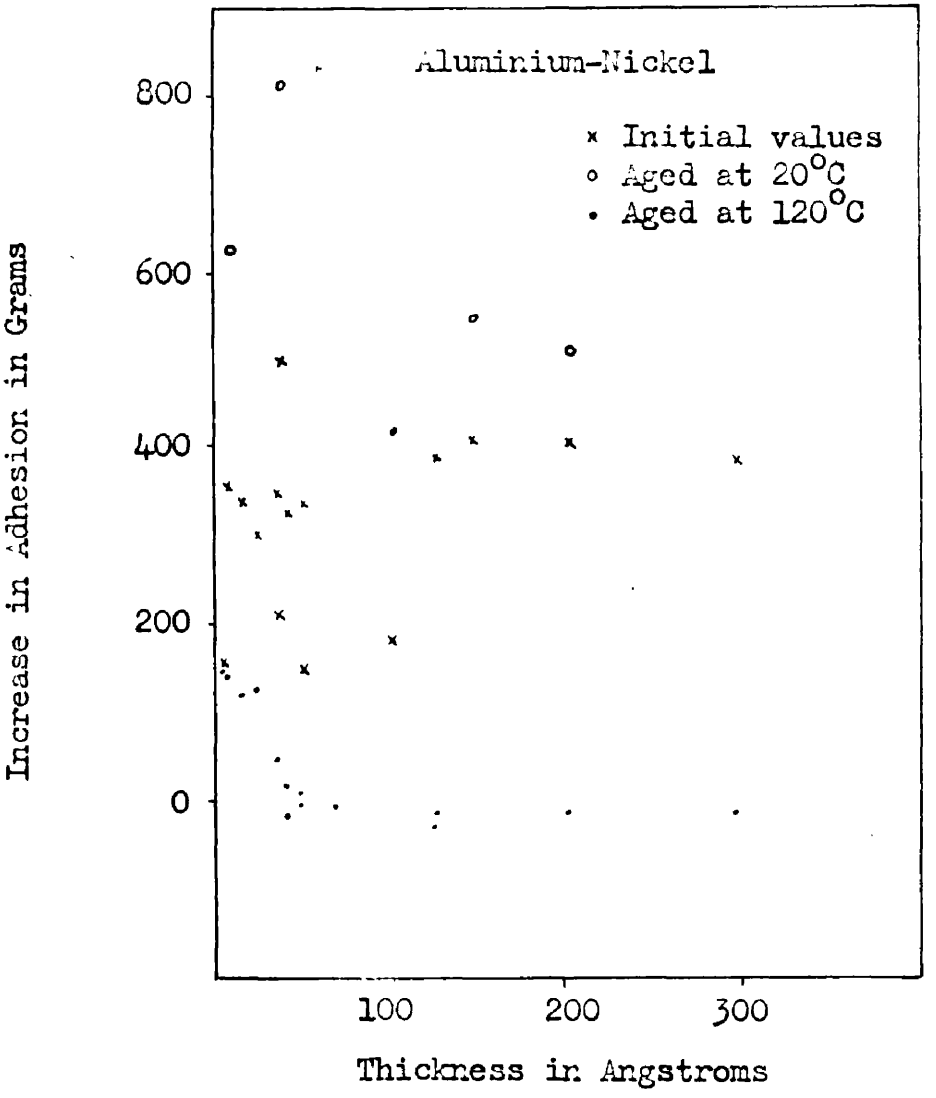

Fig.27. Increase in Adhesion/Thickness of Nickel Film.

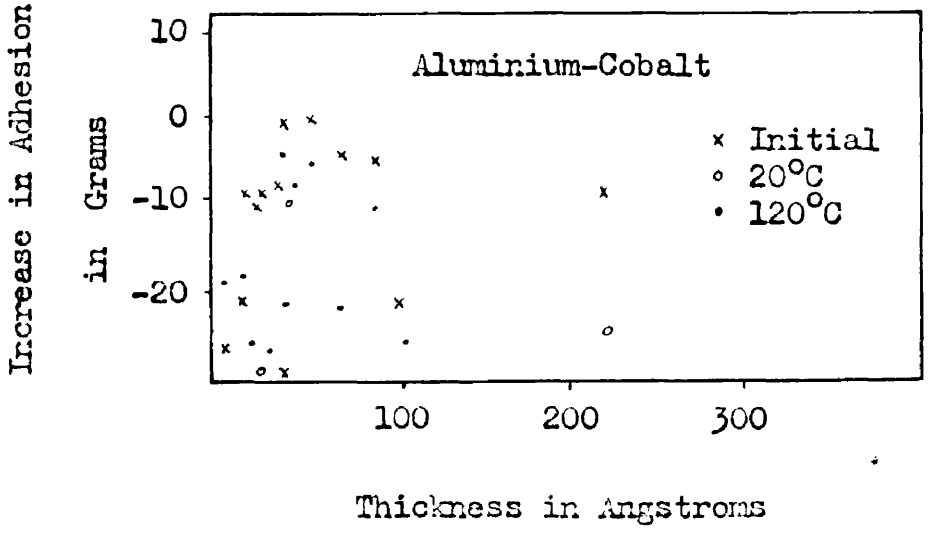

Fig.28. Increase in Adhesion/Thickness of Cobalt Film.

however, as the thickness of the nickel substrate layer increases the concentration of stress, and resultant precipitation increases and the adhesions become extremely small. It can be seen that about 75Å of nickel is required to bring about the precipitation phenomena and as the preferential compound is the β phase or NiAl compound, this would then require about the same thickness of aluminium to react with as the atomic volumes are approximately equal. The transition region would then be about 150Å thick.

The ovened hardened compound films whose thicknesses are in excess of 50Å certainly have an adhesion less than that of the single nickel films. This gives a negative value for the hardness of the interfacial layer and shows the extent of the precipitation process.

Aluminium-Cobalt. As before, similar results were obtained for this system, Fig. 28, as for the last, but the process appears to have been carried through at a far higher rate. Neither of the specimens chosen in the last chapter gave positive values for the increase in adhesion on substration and this is typical for almost the complete thickness range of the system. For two of the specimens the initial values were just positive, but after ageing they became negative. This peak in the graph occurred

at a thickness value of 40Å of cobalt. For all other thicknesses of substrate the adhesion decreased.

The peak which occurs for the aged films as well, in the graph against thickness of substrate, must be formed by the interaction of two types of ageing phenomena. Thicker films will give stress concentrations more than enough to cause precipitation, as was obtained for the thicker films in the aluminium-nickel system. In the thinner films diffusion of the aluminium atoms through the depth of the nickel film appears to be affecting the adhesion value of the substrate films; this type of reaction was not obtained previously, but cobalt is known to oxidise more rapidly than nickel and the aluminium atoms might be forming a complex with the cobalt oxide interface. This second reaction would become less effective as the thickness of the films increased, and as the precipitation reaction is proportional in some degree to the thickness of the substrate film, there will be between the two some substrate thickness at which the adhesion value should reach a maximum. This appears to hold for films 40Å thick.

Aluminium-Iron. For all thicknesses of substrate the adhesion values of compounded films of aluminium-iron were high. The values obtained show little change with the

thickness of the substrate layer, and are close to the value of loading at which shattering in the glass took place. The large scatter of results obtained, Fig. 29, is probably due to variations in the strengths of the glass microscope slides. Apparently the degree of penetration of aluminium into iron is small for there was only a slight decrease in the adhesion values of the thinnest iron film measured, which was about 20A thick. The phase diagram for the system shows that the intermetallic phases are grouped together near the aluminium end of the phase diagram, and that they are only formed over very limited concentration ranges. This would assist phase precipitation as little diffusion would be required to give the complete range of stable phases. There appears to be no evidence of the effect noticed for the thinner films of the last system of the diffusing aluminium atoms decreasing the adhesion between the glass surface and the substrate film.

Aluminium-Manganese. The results obtained for this system are so scattered that it is difficult to form any conclusions about the change of the adhesion values with thickness of substrate. Initially the increases in adhesion, Fig. 30, were good but they dropped as the specimens were aged. An unexpected thickness peak was obtained for the ovened

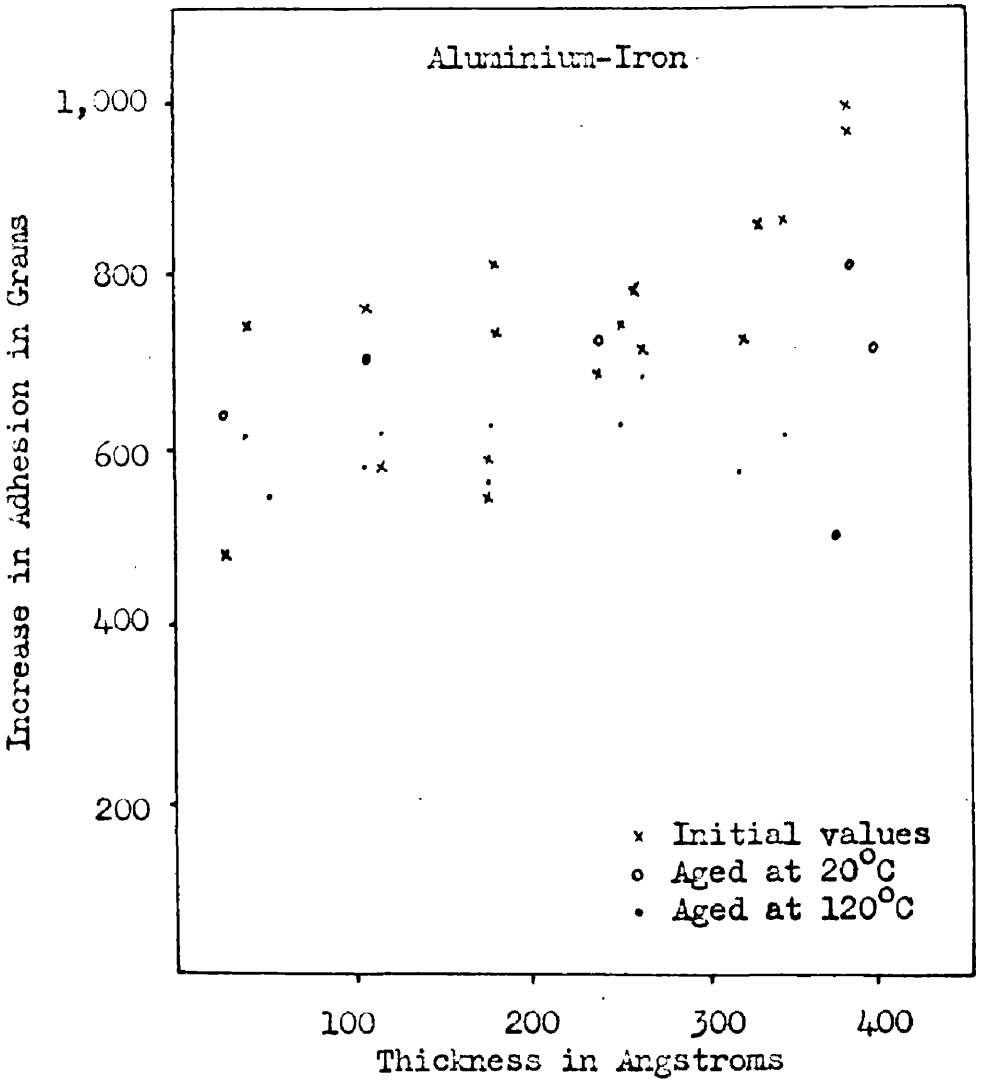

Fig. 29. Increase in Adhesion/Thickness of Iron Film.

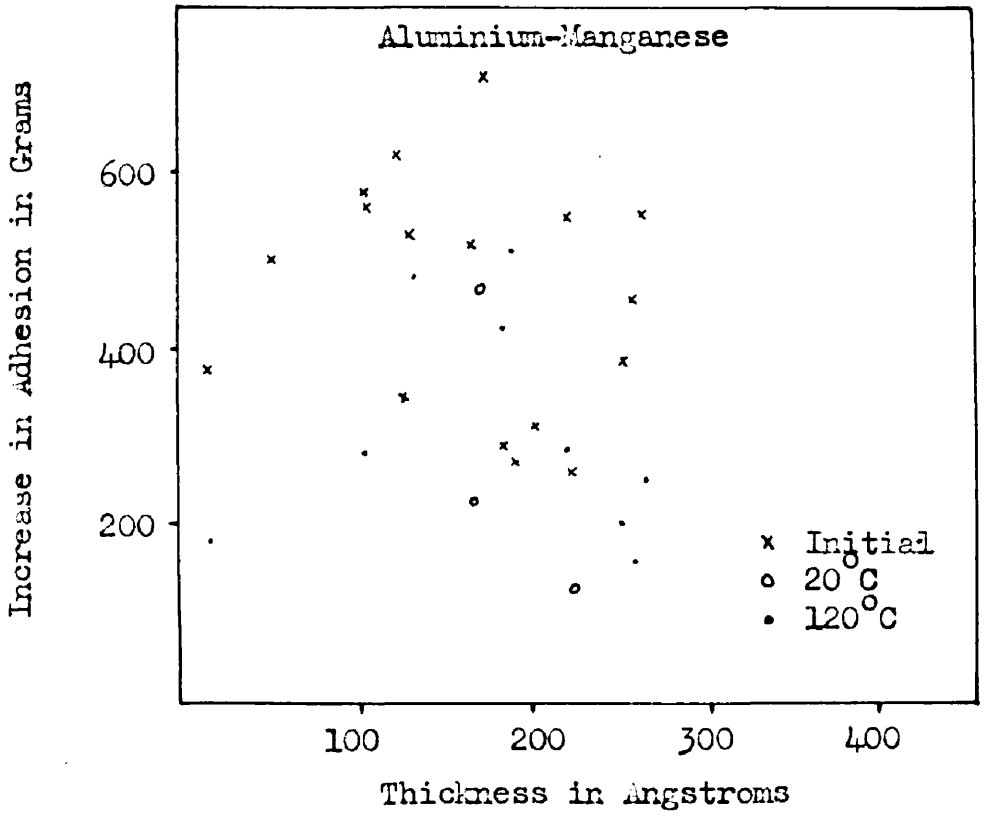

Fig. 30. Increase in Adhesion/Thickness of Manganese Film.

films at a substrate thickness value of 200A.

It had already been suggested that the decrease in adhesions on ageing was due to a reorganisation within the structure of the manganese films, Chapter 4(c). It is shown later that chromium films grow in two distinctly different types of aggregated structure. It is possible that the peculiar peak denotes a transition region in the type of structure being formed by the metallic atoms, or a particular degree of aggregation in the substrate films.

Aluminium-Chromium. The graph of adhesion against thickness of substrate for aluminium evaporated onto chromium is given in Fig. 31. The initial values show a slight difference from those obtained by Heavens[1] for the same system. The graph, however, still retains the peculiar step region at 300A. The adhesion values above this for the freshly evaporated specimens agree well with the results of the previous investigation, but the thinner values are no longer negligible. Ageing increases the adhesion of all the specimens but whereas the step is even more apparent in the oven hardened films, it has disappeared in the films aged at room temperature.

Heavens considered, as described in Chapter 1(b), that the step was caused by the deposition of the reflecting film on the thicker substrate films as an oriented overgrowth.

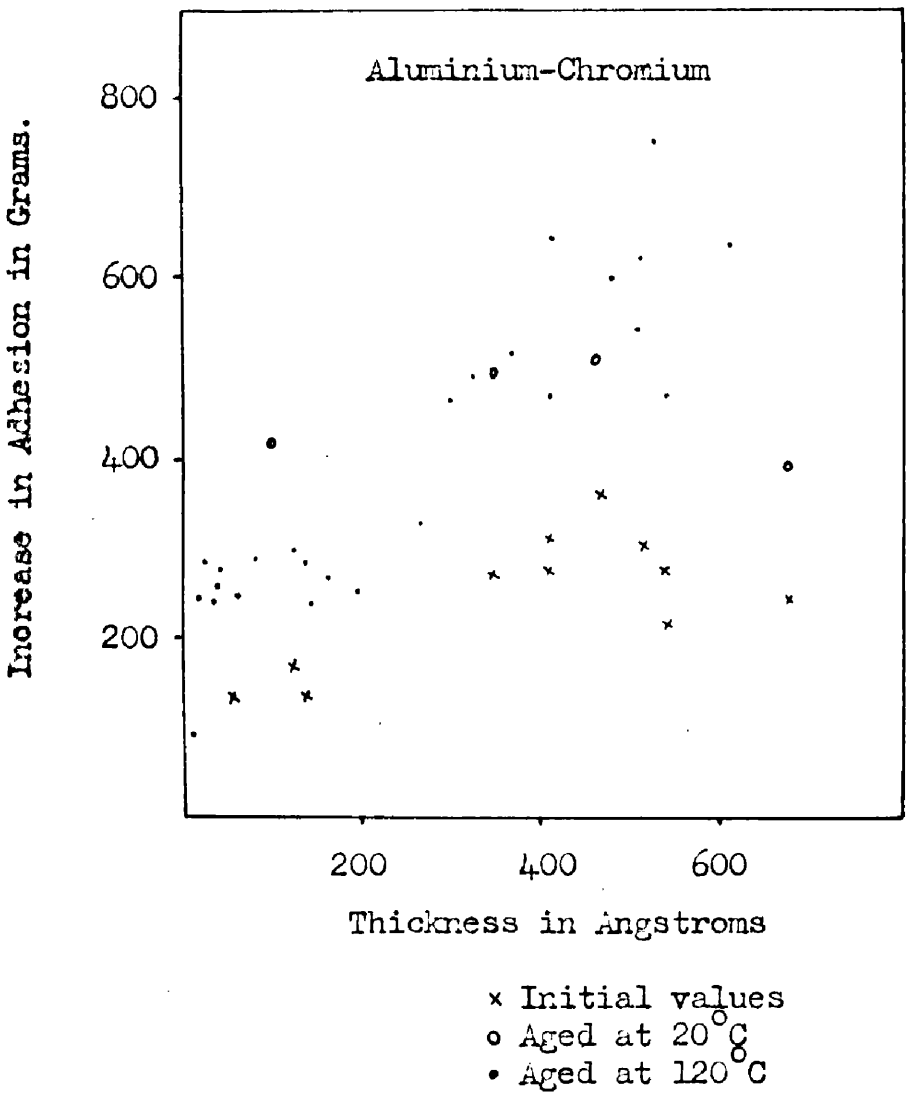

Fig.31. Increase in Adhesion/Thickness of Chromium Film.

For this to be possible the thicker films must be able to present to the condensing film a relatively large, unicrystalline, pure, chromium surface. However, chromium does not condense to give this type of film. The thinner films, and the initial deposit in the thicker ones, form very small aggregates[51] having the shape of ellipsoids of revolution with the unique axis perpendicular to the condensing surface. These particles appear to be surrounded by a thin layer of oxide which has been formed by a gettering action as the particles were deposited. As the thickness of the films increases the ellipsoids become more and more plate like until the surface is exhibiting bulk properties. If the thickness of the oxide layer is severely limited it would be possible, as Heavens suggests, that limited overgrowths could be formed on the thicker substrate films, but there would be no possible mechanism of increasing the adhesion of the reflecting films after deposition. The thinner films would be completely unsuitable as bases on which overgrowth could be formed, and yet large adhesion values were found for these films.

It is possible, however, to explain the presence of the step, not as the onset of a new growth form in the aluminium films, but as being caused by a difference in the type of diffusion between the chromium and the aluminium

films. Where the chromium layer is thin the diffusion of aluminium into chromium will be analogous to a grain boundary diffusion process, and as the particles are small it will be a simple matter for them to distort in such a way as to minimise the stresses set up by the diffusion process. Where, however, the aluminium atoms are faced with larger chromium particles the grain boundary type of diffusion will decrease in importance and the process will become one of interpenetration in one dimension. The high kinetic and thermal energies of the condensing atoms will assist both diffusion processes and give the initial values of adhesion. Ageing will increase the amount of strain in the thicker films as more and more aluminium will be allowed into solid solution. From the shape of the ageing curves it does not appear that the stress concentration in any of the films reached the critical value at which precipitation would be nucleated. In this system there is no preferential compound having a large energy of formation which would assist precipitation.

The diffusing atoms, however, will not be so mobile at the lower ageing temperature and the stresses set up in the larger chromium particles will be less than for those aged at 120°C.; however, for the same reason, the smaller particles will not be able to distort so readily and the stress in these films will increase. Thus the

lower temperature aged films showed after ageing a relatively constant hardness and the aged films an even more pronounced step region.

The ageing processes in the thicker films is similar to those already obtained for other systems, but with the thinner films the situation has become much more complex by the formation of the highly aggregated structure. It is possible that the peculiarities obtained for the system aluminium-manganese also have their basis in the growth process of the substrate film. An investigation into the change in structure of films of this metal would be required before a full knowledge of the adhesion process could be known. However, manganese is chemically similar to chromium and just as readily oxidised; thus the structure might be very similar to that obtained for the chromium films. In the alloy diagram for this system there is a compound with a slightly higher force energy than the component metals and this could well bring on precipitation in the thicker substrated films, which would decrease the hardness of the interfacial layer and lower the adhesion of these films.

(d) Partially Miscible Systems

Silver-Lead. The results for the silver-lead system are strongly influenced by the nature of the substrate film metal. Only for the thinnest specimen were positive adhesions recorded. The room temperature aged specimens showed larger decreases in adhesion after ageing than the oven aged ones. There can be no doubt as to the mobility of lead in silver as the ovened films all gave a very dull reflecting surface after they had been aged; this was not noticeable in the air hardened specimens. As lead is only slightly soluble in silver the ovening would probably form a relatively homogeneous alloy film. This, however, could be expected to give good hardness values and thus the adhesion of the films must be principally dependent on the adhesion of the base material to the condensing surface, but as lead oxidises quite readily it is surprising to record these low adhesion values. From Fig. 32 it can be seen that for the same thickness of lead film the adhesion of the air hardened specimen is less than that of the ovened one and, assuming that the actual adhesion values of the lead films are about the same in each case as we obtained earlier, then the difference in adhesion must be due to the thickness of the lead film which is not dissolved in the silver. Thus, on scratching, we could

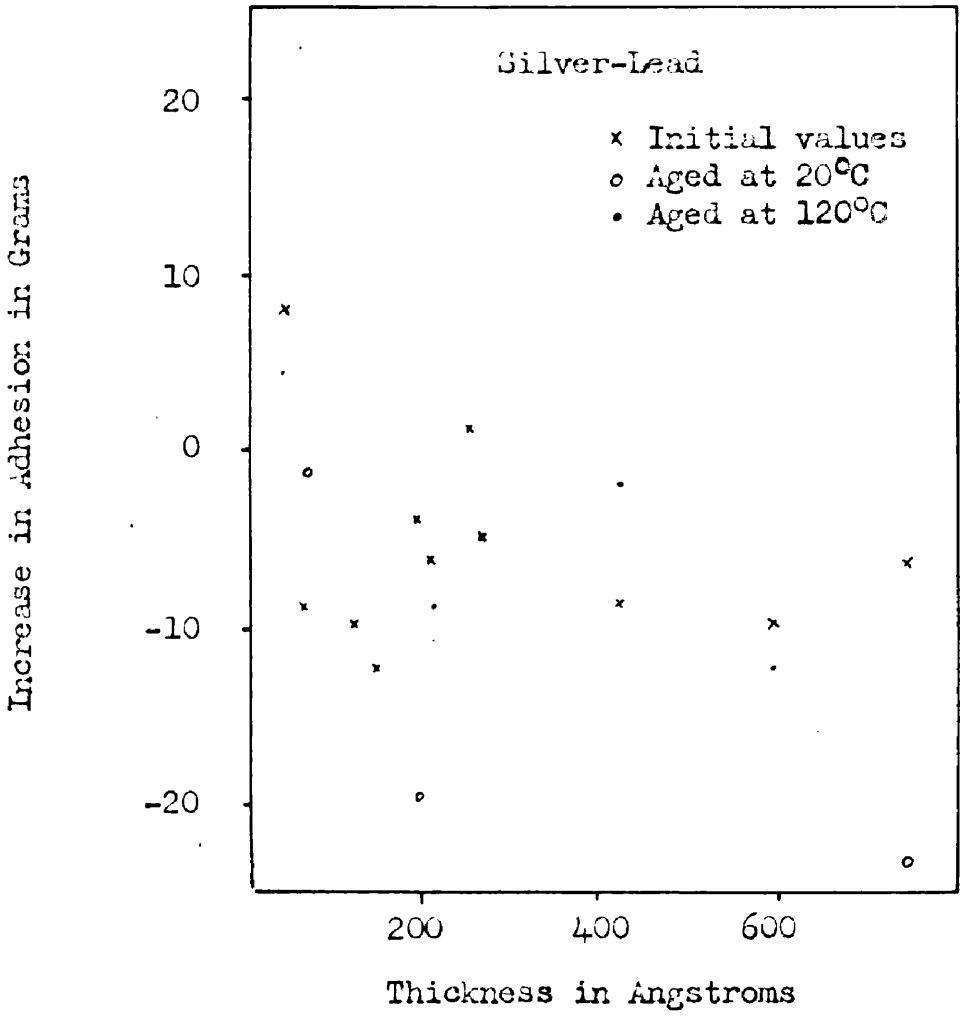

Fig.32. Increase in Adhesion/Thickness of Lead Film.

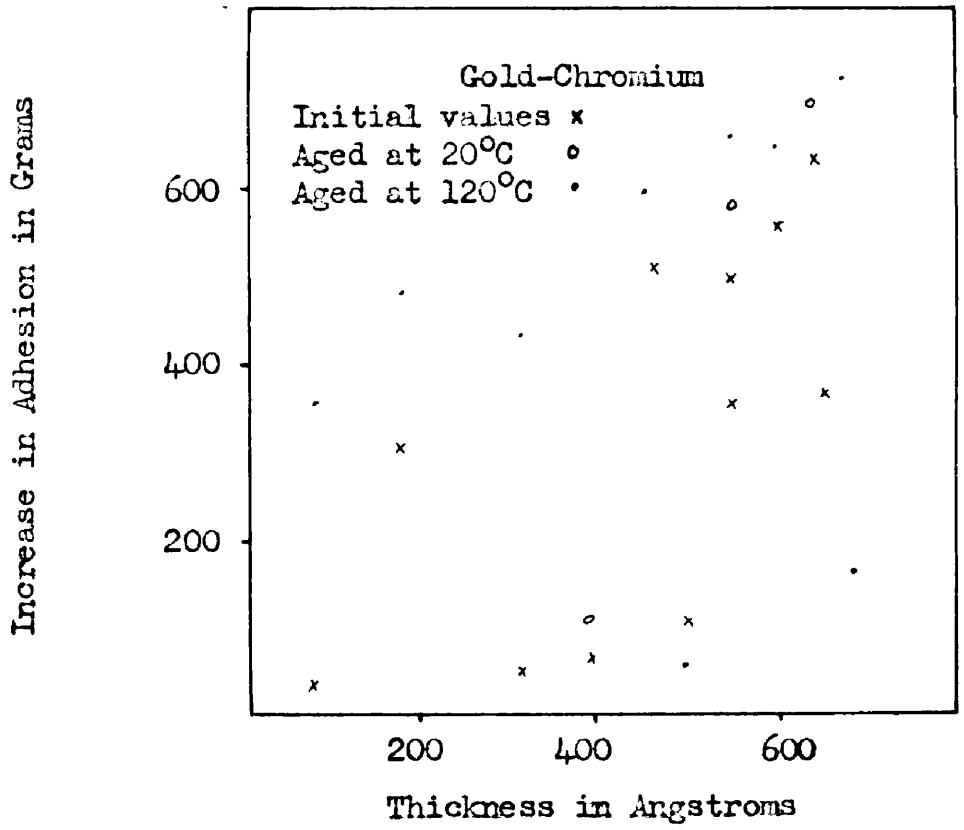

Fig.33. Increase in Adhesion/Thickness of Chromium Film.

be leaving at the glass interface a uni-molecular film of lead bonded directly to the glass. This would be untraceable by conventional methods of examination and would give the appearance of a perfectly clear scratch. If this is the case then the adhesion of the film is not so much dependent on the adhesion of the substrate film and the hardness of the interface as the cohesion or hardness of the substrate film material.

Gold-Chromium. The initial results for the gold-chromium system are in close agreement with those obtained by Heavens, the step, however, being obtained at 500Å, Fig. 33, and not 300Å as in the previous investigation. Little increase in adhesion was shown by the thinner substrated films immediately after evaporation, or after ageing at room temperature. This was caused by a tendency for the gold to strip away from the chromium substrate, which was particularly noticeable on the thinner films but did not occur on the thicker ones. No stripping was apparent for the films aged at 120°C. and at that temperature, the adhesions of the thinner films increased vastly.

Stripping at the metal interface would agree with the theory of interfacial stress that was suggested from the form of the ageing curves. Where no stripping takes place the stresses must be accommodated by localised

shearing within the thickness of the substrate. Not only a higher ageing temperature but also thicker substrate layers appear to allow this latter process to take place. It has already been suggested that the presence of the step when chromium is used as the substrate material indicates the change from ellipsoid particle growth to a more continuous layer of chromium, i.e. a change from diffusion along the grain boundaries to one through the actual depth of the particles. The second of these would certainly assist adhesion more than the first, and ageing at the advanced temperature would aid the latter process as the gold would diffuse into the body of the chromium particles from the grain boundaries.

Copper-Chromium. No actual adhesion values have been given for this system by Heavens and Collins although it was investigated. However, the increasesin adhesions were said to be independent of the substrate thickness. If this is so then it would certainly appear to be evidence in support of the theory of epitaxial overgrowth as chromium and copper have no directly fitting lattice planes. The results obtained in this investigation are given in Fig. 34 and it can be seen that although the results are highly scattered they are to some degree dependent on the thickness of the substrate layer. In particular, the

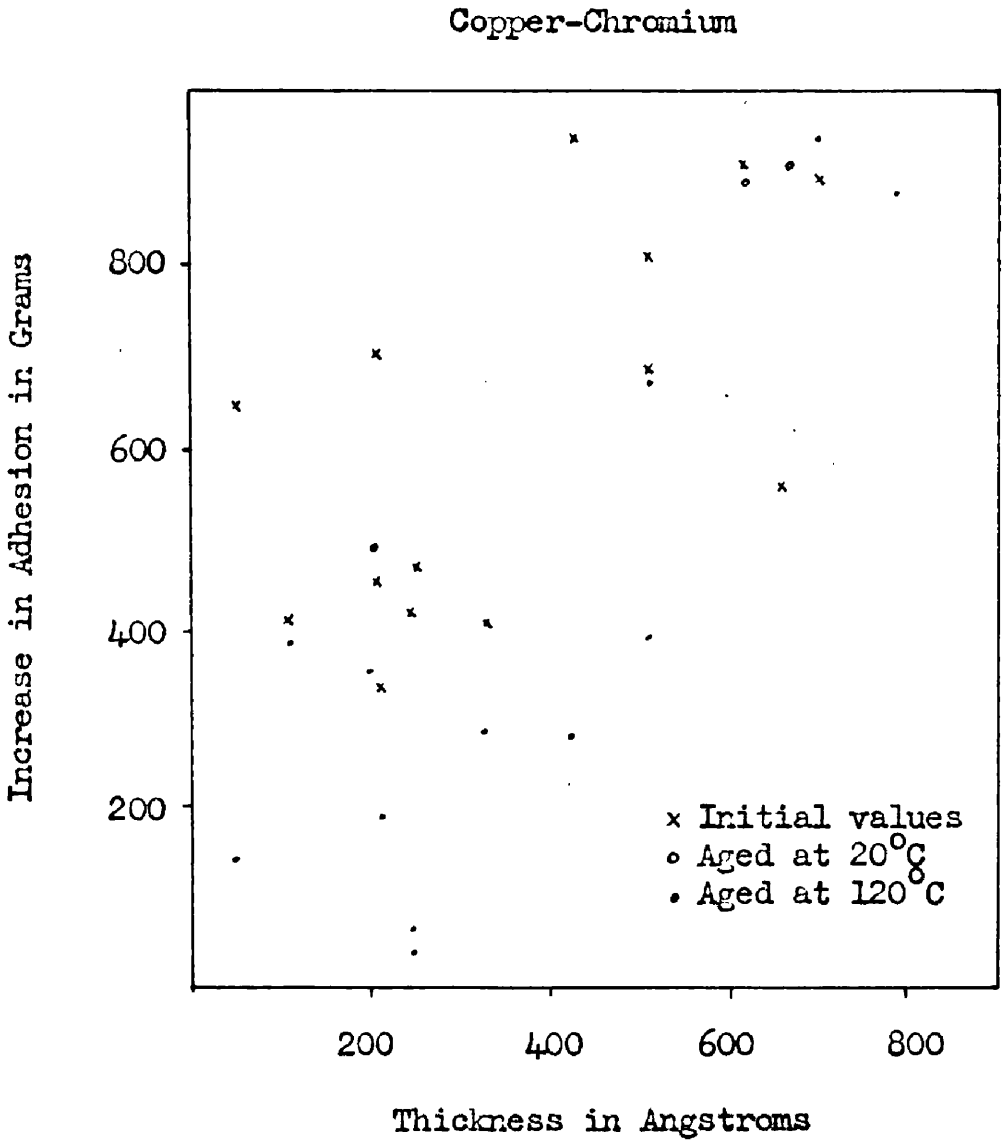

Fig.34. Increase in Adhesion/Thickness of Chromium Film

ovened films show a step similar to that obtained for both the systems already described in which chromium was used as the substrate material.

The scatter of results is undoubtedly initially due to the presence of the oxide layer at the metallic interface and, after ageing, to the degree to which the oxide has become dispersed in the ovened films. The initial values are only slightly dependent on the thickness of the substrate film, showing that the action is not, as was the case before, dependent on the structure of the films but on the extent of oxidation at the metallic interface. On ageing the hardness values become more structure sensitive as the diffusion process progresses, and the final result shows the step obtained for the other systems in which chromium was used as the substrate material.

(e) Miscible Systems

Aluminium-Lead. The anomalous behaviour of this system which was referred to in the preceding chapter can be clearly seen in the graph given in Fig. 35. Whereas the initial and low temperature aged values for the increases in adhesion were comparable with the results for the silver-lead system the ovened films gave positive values and a very prominent peak for a substrate layer thickness

of 150A. However, the use of lead as a substrate material could not be recommended as the lead diffused through all the films of aluminium for both types of ageing and gave diffuse, dull, reflecting surfaces.

As the alloy system is very similar to that of the only slightly non-miscible silver-lead system the positive adhesions must be caused by the differences between the nature of the two reflecting materials. The adhesions of silver and aluminium to the glass condensing plates were comparable and can be neglected as a source of the increase in adhesion. From the appearance of lead at the reflecting surface of the aluminium film almost immediately after evaporation we can say that the rate of diffusion of lead through aluminium is greater than that of lead through silver, but no great change in the reflectivity at the glass support was noticed for either system and thus it would appear that the diffusion rate of lead through the reflecting film materials is greater than that of aluminium or silver through lead.

It has already been suggested that the presence of a number of oxidised metallic particles distributed within the films could increase the hardness of the compound film, and as aluminium oxidises to a greater extent than silver we must take this feature into consideration. The

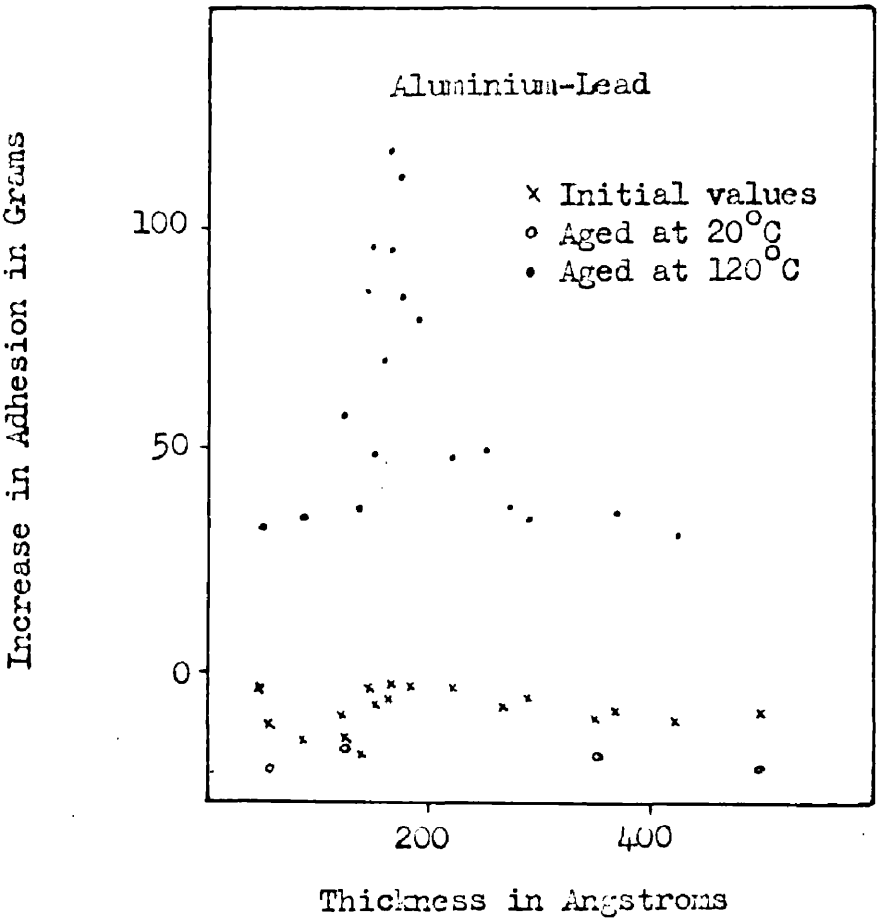

Fig.35. Increase in Adhesion/Thickness of Lead Film.

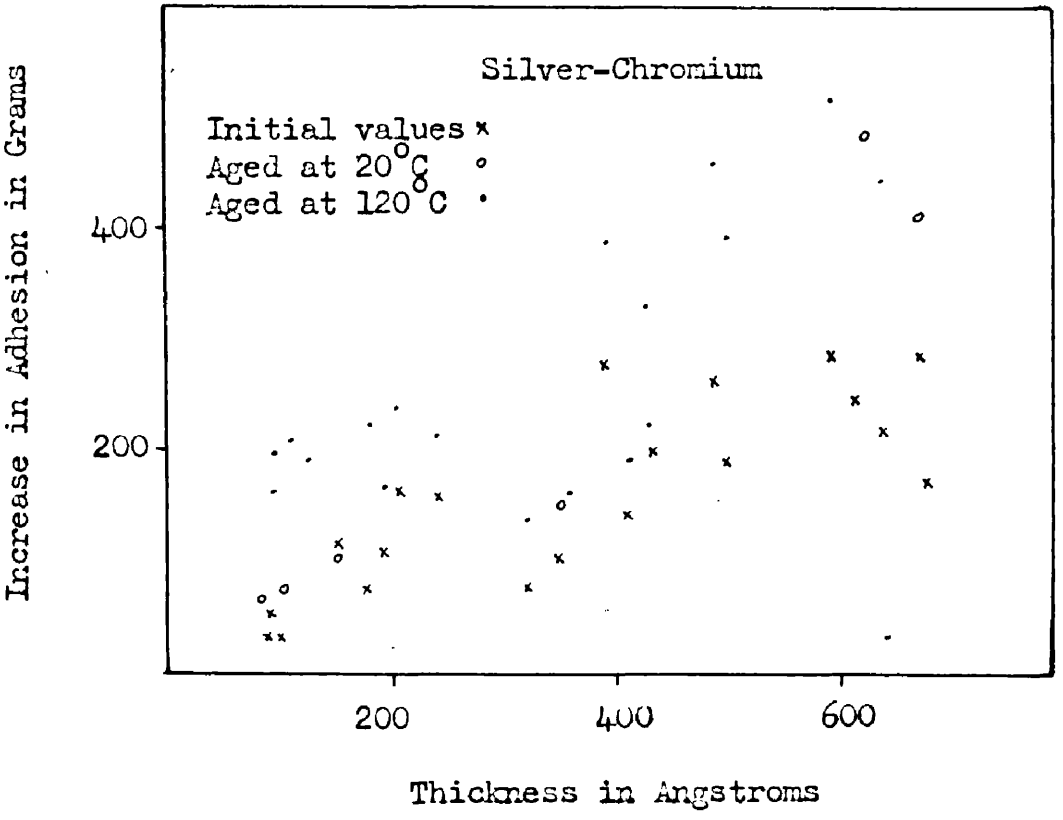

Fig.36. Increase in Adhesion/Thickness of Chromium Film.

poor adhesions of the silver-lead films was attributed not to the apparently poor adhesion of lead but to its poor cohesional energy, and it was suggested that the lead might well form a surface layer having good adhesion which, however, was unable to assist the overall hardness of the layers. This mechanism would hold good for the lower temperature ageing of our specimens and for the measurements made immediately after evaporation. However, in the low temperature range the diffusion constants are very temperature sensitive and raising the ageing to 120°C. increases the activity within the films greatly. We have to assume that for the thinner films the aluminium has, to some extent, diffused into the substrate layer. This would form a homogeneous mixture increasing the hardness by the process outlined by Desch[12]. It follows that as the thickness of the substrate layer increases and the relative concentration of lead in aluminium increases, the hardness of the mixture will also increase, the compound film being firmly bonded to the glass through the thin layer of lead oxide at the surface. However, the mean penetration of aluminium into lead will still be limited and after a certain thickness has been reached the adhesion will decrease as more and more pure lead will be left at the lead oxide interface. Random migration, however, will ensure that the fall off is relatively gradual, and that

the lead still contains some aluminium atoms which will increase its resistance to shear.

Silver-Chromium. As with the other chromium systems this graph, Fig. 36, shows a dependence on the thickness of the chromium substrate layer thickness, having a step in the region of 350A. Comparison with Heavens' results, Fig. 1, shows that the same differences have been obtained between these results and those of the earlier investigation, as was obtained for the system aluminium-chromium, i.e. non-negligible adhesions for the thinner films and a smoother transition region. Comparable values, however, were obtained between the measurements made immediately after evaporation and Heavens' values for the thicker range of substrates.

As there is no compound formation between the metals of this system, the process of age-hardening must be one purely of interdiffusion of the constituent metals resulting in stresses within the non-homogeneous interface region. The step being caused by the same difference in diffusion method as was described for the aluminium-chromium system. This system, however, is very similar to the aluminium-chromium within the temperature range we have been investigating, for in the discussion on specimens of the other system the conclusion was reached that the stress

concentration had not reached the critical value for precipitation and that the interface was existing in the form of a range of solid solutions; in this case no precipitation is possible and there is only one solid solution, but the hardness is attributable to the same cause.

(f) Alloy Substrate Material

As some difficulty was experienced in evaporating thick films of chromium, partially due to alloying of the molten metal with the tungsten heater, but mainly due to overheating of the glass bell-jar by radiant heat from the almost white hot tungsten basket, a chromium alloy was used in a further investigation. The alloy chosen was an alloy of composition 80/20 nickel and chromium respectively. As shown in Chapter 2(g) this evaporates off the chromium preferentially. The alloy is known commercially as Chromel, and the particular sample used was manufactured by Wiggin & Co., Birmingham, as electrical resistance wire, Brightray C.

Exactly the same investigation was carried out as in the previous cases. The ageing curves for the substrate films showed the double ageing form similar to those obtained for manganese. This indicates that some

nickel might have evaporated with the chromium, and as the melting point of nickel is much less than that of chromium a low source temperature would assist the evaporation of the more volatile component. Results were obtained using both aluminium and silver, and only ageing for three days at 120°C.; these are given in Fig. 37. The adhesions obtained are similar to those for the same reflecting films having chromium substrates except for the thinner films. Here the presence of the small nickel content appears to have assisted the adhesion of both silver and chromium. Nickel forms a partially miscible solid solution with silver, and as has already been shown, limited quantities of nickel can increase the adhesion of aluminium. The step has been completely eliminated from the graph, and the results, although scattered, are consistent.

(g) Discussion of Results

Considering the nature of the method used for adhesion testing, the results obtained are in good agreement with those obtained by Heavens. The principal difference is in the increase in adhesions of the thinner substrated films for the systems aluminium-chromium and silver-chromium. The results for the gold-chromium system agree extremely

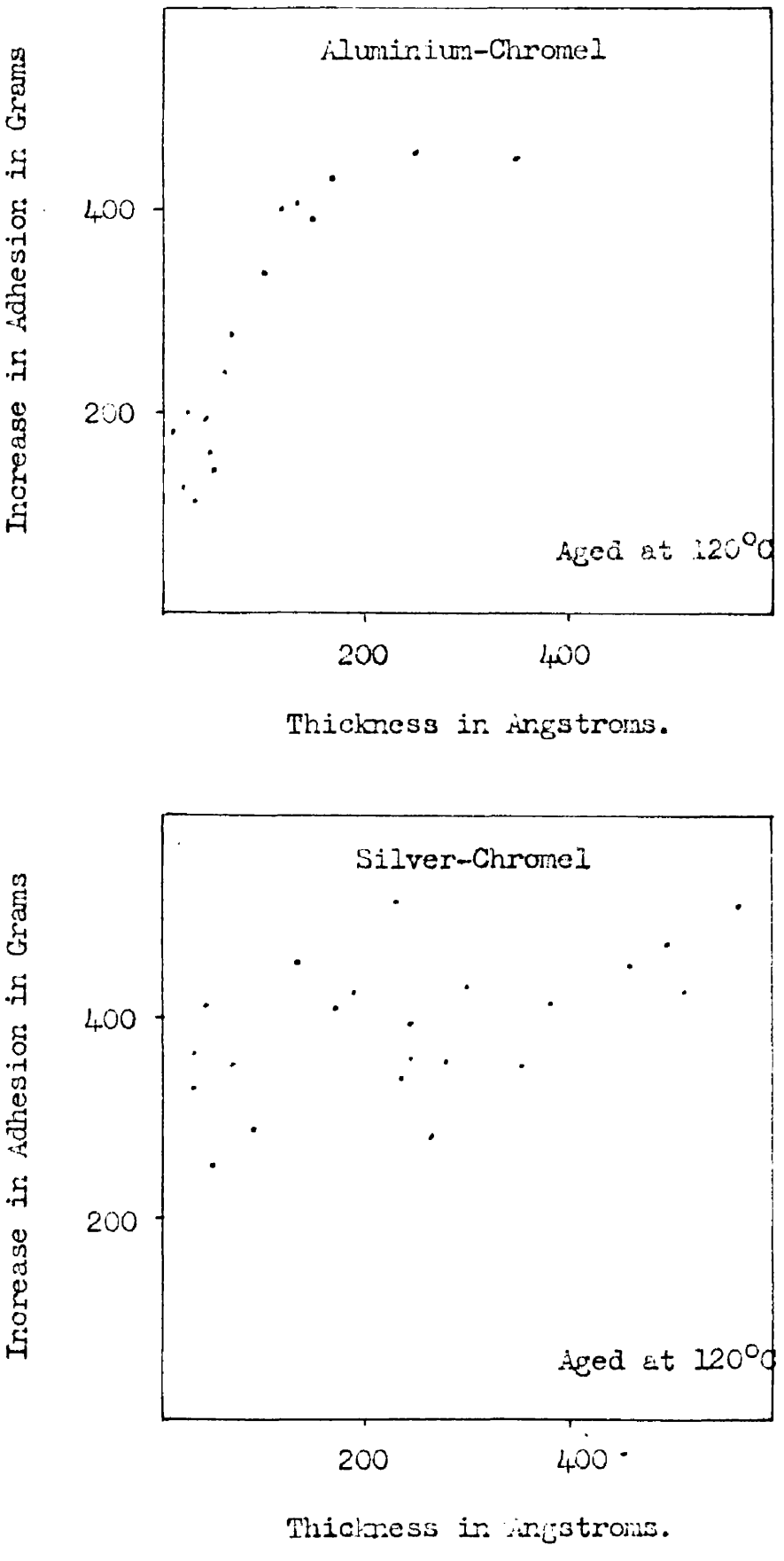

Fig.37. Increase in Adhesion/Thickness of Alloy Film.

well. The actual adhesion values in this investigation, however, are much larger than those given by Heavens, although they follow the same pattern. The same tip radius was used in both investigations, thus the difference cannot be due to a change in the width of the channel being torn out of the film, but may be due to some slight difference in the evaporation technique.

Good adhesions were obtained when silver and copper were substrated with chromium, and when aluminium was substrated with iron, manganese and chromium. These results show that one of the principal qualities required for a useful substrate material is a strong cohesion. From the nature of the adhesion/time graphs it would appear that the process is one of interdiffusion, and the apparently slower rate of diffusion of the transition metals suggests that the increase in adhesion is due largely to the formation of a hard compound layer at the interface. When, however, the structure of the substrate film is highly aggregated the formation of this compound layer takes place through a considerable thickness of the film. From the form of the graph of adhesion/thickness of substrate it would appear that there is a change in the structure of the majority of the substrate films at about 300-500Å thickness. It will be shown in Chapter 9 that, for chromium, this corresponds to a change in the degree of

aggregation and that the structure of the films, for smaller values of thickness, are highly aggregated. The possibility cannot be ignored that the aggregates act as a keying surface to the reflecting film, but in this case we would expect that as the size of the aggregate particles increased there would be a decrease in adhesion as the number of aggregate interstices decreased. That this was not found must be taken as evidence to show that the keying theory is not substantiated in practice.

The metallic systems possessing a large number of thermally stable phases would naturally expect to show age-hardening effects stronger than systems which were to a great extent miscible. The changes in the adhesions obtained for the nickel system are a good example of this. Where the amount of nickel is limited the adhesions are high, but for the thicker films they decrease rapidly. However, where the same films have been aged at a slightly lower temperature, thereby decreasing the rate and extent of the diffusion and, consequently, the precipitation process, large adhesions were obtained.

The chromium-nickel alloy, chromel, gives excellent adhesion values and would be most suitable to use commercially. As was shown in Chapter 2(g), the alloy evaporates chromium preferentially, but for the thinner

films, where possibly the source has been kept at a slightly lower temperature, the presence of some nickel content can be clearly seen.

CHAPTER 6

DIFFUSION IN THIN FILMS

(a) Introduction

While describing the age-hardening effects in the films in the preceding chapter, it was assumed that diffusion took place at the interface between the two metals. No conclusions were drawn, however, on the rates of the diffusion process, or its extent. In this present chapter is described the theory of diffusion as it applies to the type of system we are considering, and some electron diffraction investigations that were carried out in order to determine whether transition structures were being formed at the interface. Some work undertaken by other investigators is considered in detail and an estimate is made of the actual distances of interpretation for a few of the systems.

(b) Theory of Diffusion Process

One of the greatest experimental difficulties in making diffusion experiments is in placing the two components of the diffusing system into intimate contact. The technique of evaporation ensures that this is carried out; however, the limited thickness of the layers does not allow measurements to be made through the depth of the film

The changes in reflectivity at the surfaces have been used[52] in an attempt to measure the diffusion constants in films of zinc and gold. The investigators found that there was little difference between the values they obtained and those already known for the bulk materials. Electron Diffraction[52] and X-ray[53] measurements have also been made.

Let us consider the simple case of a perfect interface between the metals. We can then assume this to be a case of one dimensional diffusion, and at zero time, the condition at the interface can be represented by a diagram of the type shown in Fig. 38. After a time the concentration/displacement graph will become more like the t' curve, and after an infinite time the composition will be the same everywhere, and only dependent on the amounts of material originally present. We assume for simplicity that these are equal so that the homogeneous composition is 50/50. The series of curves that we have constructed are the normal concentration/time graphs for a single phase system of interdiffusing metals. If we let the diffusion constant of Me' into Me'' be D_I and that in the opposite direction D_{II}, then for the case we have constructed

$$D_I = D_{II} = \text{a constant},$$

Where $D_I \neq D_{II}$ conditions will be similar to those shown

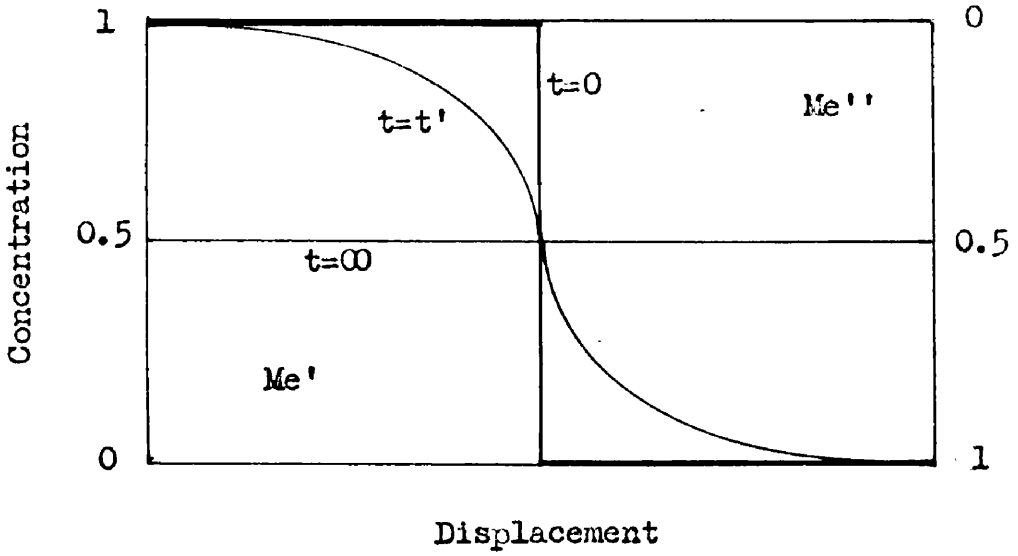

Fig.38. Diffusion of two Metals across a Boundary

Single Phase System

$D_I = D_{II}$

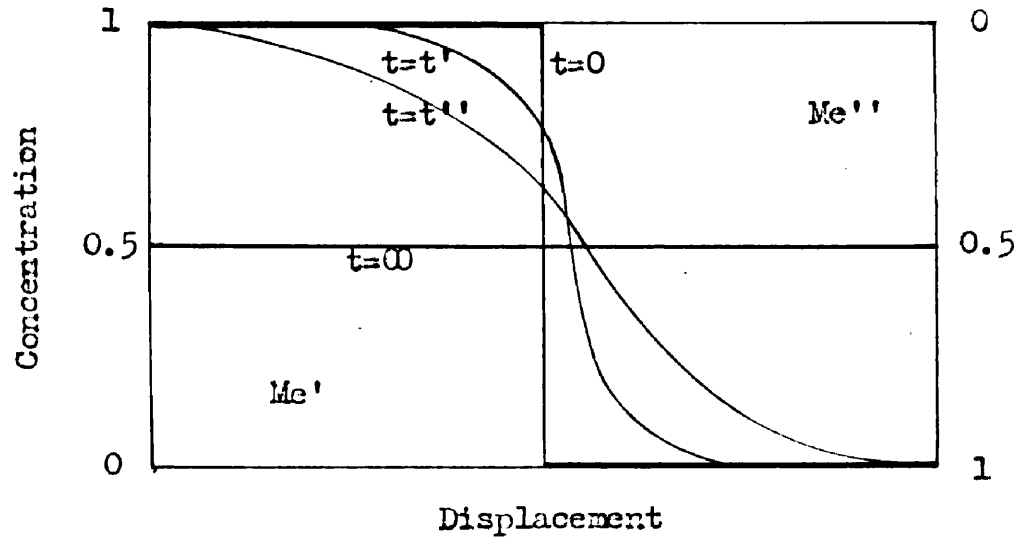

Fig.39. Diffusion of two Metals across a Boundary

Single Phase System

$D_I \neq D_{II}$

graphically in Fig. 39. For a system such as this the diffusion equation

$$\frac{\partial c}{\partial t} = \frac{\partial}{\partial x}\left(D \frac{\partial c}{\partial x}\right)$$

cannot be replaced by the more familiar form

$$\frac{\partial c}{\partial t} = D \frac{\partial^2 c}{\partial x^2}$$

as the so-called diffusion constant D is concentration dependent.

For these simple systems we assume that the parent metals are completely miscible, and in a finite time we would obtain a perfect gradation of structure elements. In such a system as this there could be little age-hardening, but there will be some hardness increase due to the presence of foreign atoms in the structure, as shown by Desch[12]. At the low temperatures considered here it would be practically impossible to obtain a perfectly homogeneous film, and the most likely structure to be obtained after ageing would be that of two practically pure layers of metal with a transition region between them.

When we consider the extension of this simple case, that is, where the two diffusion constants form one, or a number of distinct phases, we have to approach the

situation from a more approximate basis. It is known[55] that the diffusion constant D, which is generally not constant over a wide concentration range is least for metals that form a continuous series of mixed crystals, i.e. that are perfectly miscible, and is greater for systems of limited solubility. Thus it follows that for a system of only two phases the overall diffusion constant would be less than that for one having a large number of phase regions. From the work of Wagner as reported by Jost[56], pure phase regions will tend to grow at the expense of regions of mixed phases.

Let us consider the effect of these statements when applied to such a system as that shown in Fig. 40. Here we have six distinct phases, one of them, the ν, being unstable at low temperature. If the two pure metals are evaporated in succession then the concentration displacement across the boundary immediately after the evaporation of the films will be of the form shown in Fig. 41 (t=0). However, after the films have been allowed to interdiffuse the form of the graph might well[56,57] be that shown in Fig. 41 (t=t). Here we can distinctly see the effect of the concentration dependent, and the phase region dependent, diffusion constant. As we cannot determine the form of this curve with any accuracy we must

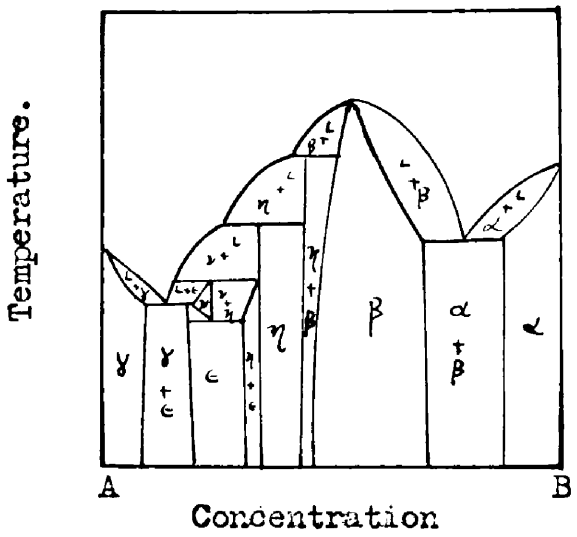

Fig.40. Equilibrium Diagram for Metals A and B.

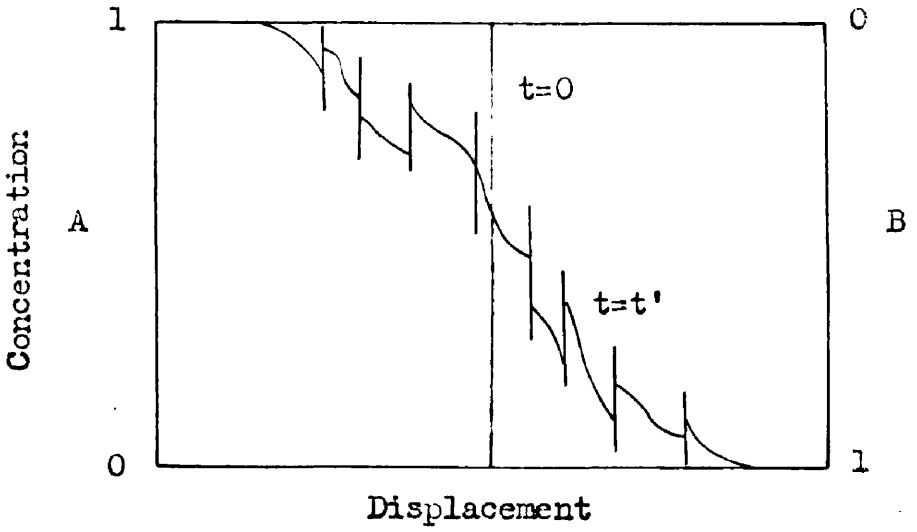

Fig.41. Diffusion in a Multiple Phase System

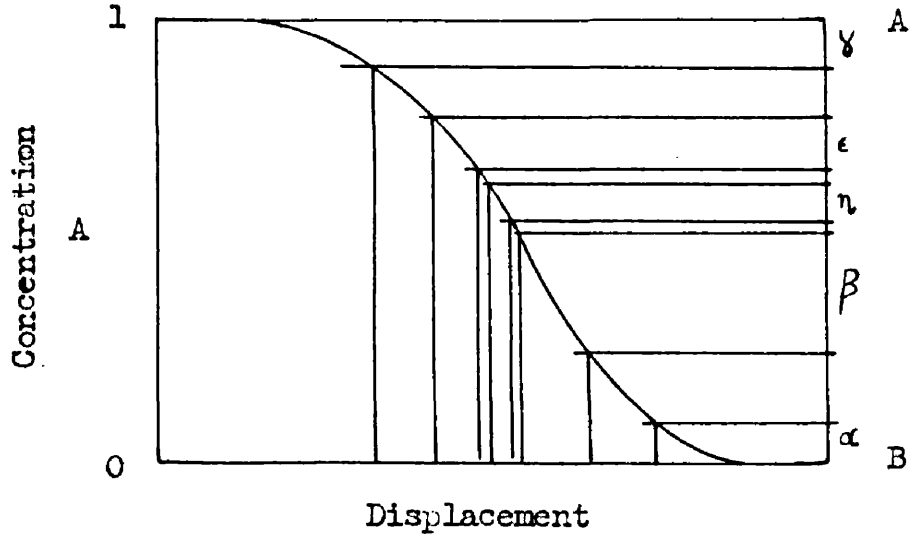

Fig.42. Simplified Diffusion in a Multiple Phase System

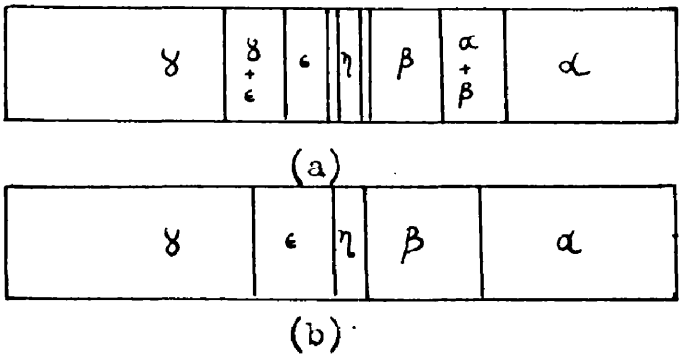

Fig.43. Transition region δx between the Metals A & B.

replace it with the simpler curve of Fig. 42. Then at a time 't' this would give a transmission region of width ∂x in which the stable phases were present in a regular manner. Applying Wagner's results to this system would give the transition structure represented in Fig. 43a. Further ageing will increase the width of transition region but not alter the relative compositions. If the pure phase regions grow at the expense of the mixed phases then the form of the transition band will become as shown in Fig. 43b.

We can thus say that for the interdiffusion of a metallic pair that form stable intermediate phases there will be formed at the interface a transition region. In this region will be precipitated all the thermally stable phases of the alloy system, and as the width of the region grows with time there will be a constant state of precipitation and re-precipitation due to the boundary movements. The relative widths of each region cannot be determined from the phase diagram as the form of the concentration displacement graph will not, in general, be readily available. However, the maximum number of stable phases can be obtained in this way and this gives a measure of the degree of complexity to be expected. The phase boundary movements will show age-hardening effects in the transition layer as the phases are precipitated. The

effect, however, will not be seen as sharply as in a perfectly homogeneous volume of alloy in which ageing takes place equally within every small particle. The effects obtained from the diffusion process will be additive over the whole transition region and only general changes in the hardness will be obtained.

(c) Limitations of the Method of Electron Diffraction

Electron diffraction is one of the simplest methods of determining the structure of the very thin metallic films prepared by the vacuum evaporation technique. Many investigations of metal and alloy films have been carried out using this technique, and some of the results obtained will be described later. For the purpose of this investigation, however, the method proved rather unsuitable. Two types of diffraction by thin films can be used, either transmission through the film or reflection from the surface. For the former the maximum thickness allowed in the specimens is about 300A. If thicker films are used the pattern becomes blurred and too few distinct rings can be obtained to give an accurate structure determination. Much thinner films, on the other hand, give too few diffractions.

The reflection technique requires a specimen holder possessing a large number of degrees of freedom.

As the instrument available was an electron microscope, and the diffraction mechanism was only subsidiary to the microscopical uses, this type of examination was not feasible. The reflection technique could only have supplied information for a very thin surface film which was not in accordance with the experimental technique. For this reason only a limited investigation was carried out using the transmission type of pattern.

As well as the type of orientations described in Chapter 3(e), thin films can also form another type of orientation. This is called fibre orientation and it is obtained when the metal atoms crystallise with one of their planes parallel to the condensing surface, and the other axes are distributed at random. By diffraction methods with the beam perpendicular to the specimen complete rings are obtained signifying that the specimen is randomly oriented: however, when the specimen is tilted these rings break up into arcs. In order to investigate for this type of orientation the specimens used were examined at normal incidence and again at 45° to the normal. In this way fibre orientation can be quite clearly detected. No trace of this type of growth was obtained in any of the specimens investigated.

The specimens were prepared under exactly the

same conditions as the films used for adhesion testing. Electron microscope copper grids covered with films of formvar were mounted alongside the microscope slides in the slide holder and presented to the same condensing beam of metal. Three specimens were evaporated at each preparation. One of each of the parent metals and a composite film of the two. Formvar was used as the condensing surface as it has been suggested[58] that this represented more nearly the structure of glass than the collodion films commonly used as supports. The grids were shielded from the gas discharge during the pumping cycle.

Due to the projector lens of the microscope the diffraction patterns, unless standardised for each lens setting, cannot be used to determine the absolute parameters of the structure being investigated. However, from the ratios of the radii of the patterns the type of structure of the unit cell can be obtained, for from the Bragg Law

$$n.\lambda = 2.d.\sin\theta \qquad (6.1)$$

where λ is the wavelength of the electron beam, d the lattice spacing, θ the angular deviation of the electrons, and n an integer, but for any one setting of the lens system

$$r \propto \sin\theta$$

where r is the radius of the ring on the photographic plate inserted into the diffracted beam. Thus

$$r^2 \propto \sin^2\theta = n^2\lambda^2/4d^2 \qquad (6.3)$$

for a cubic structure.

$$r^2 = (\lambda^2/4a^2).x\ (h^2 + k^2 + l^2) \qquad (6.4)$$

Thus $$r^2 = B.(N_C) \quad \text{or} \quad D^2 = B_i\ (N_C) \qquad (6.5)$$

where B and B_i are constants dependent on the wavelength of the electron beam, the side of the unit cube, and the projector lens setting, and D is the diameter of a ring. The quantity, N_C, which must be a whole number, can be determined from this equation and from the series of values of N_C the structure of the unit cell can be obtained if it is of a simple nature, for

$$N_C = h^2 + k^2 + l^2$$

where (h,k,l) are the Miller indices of the diffracting planes. Particular structures suppress some of the values of h, k or l and thus give different values for N_C. If the structure is not cubic the analysis is more difficult.

(d) Results of Electron Diffraction Investigation

Three investigations were carried out by means of electron diffraction. In the first of these the compound formed by the interdiffusion of nickel and aluminium was examined. Then two investigations were carried out on aluminium-chromium films. The first of the latter pair failed to show any useful information as the thickness of the films even although reduced from those normally used, was still too great to allow the transition layer to give an observable diffraction pattern. The film thicknesses were decreased in the last of the experiments and some information on the nature of the transition structure was then obtained.

Nickel-Aluminium. In order to obtain a perfectly homogeneous film that would aid the intermediate structure determination a compound film of the metals was prepared by evaporating onto the specimen grid of formvar a series of very thin films, alternately aluminium and nickel. The mean thickness of these films would be of the order of 10-20A by weight, and five layers of each were deposited. The film was allowed to age in a dessicator for three days and then investigated. Reproductions of the ring patterns obtained can be seen in Fig. 44. The positive prints are not very clear as the specimen thickness was small and thus

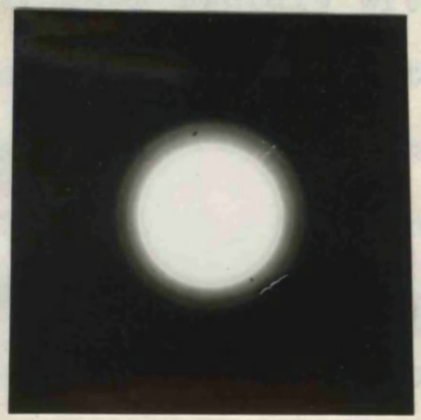

Aluminium-Nickel

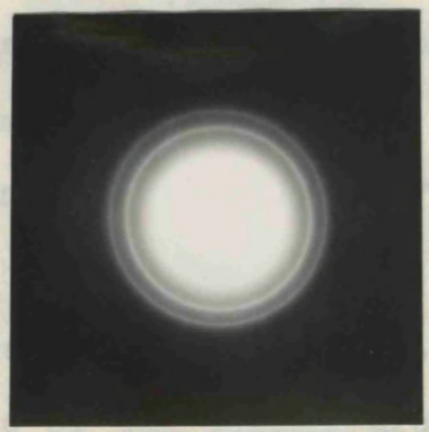

Nickel

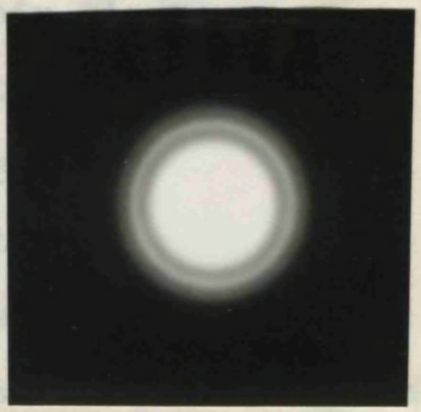

Aluminium

Fig.44. Electron Diffraction patterns from a compound specimen of Aluminium and Nickel.

the beam intensity fell off very rapidly with increasing radius. From the patterns it can be seen that the composite film has a different structure than either of the parent metals, whose diffraction patterns are also given. The ring diameters were measured by means of a low powered travelling microscope and the structure determination of the compound film is given in Table III. The structure was found to be cubic and there was some indication that nickel and aluminium were assisting the diffraction. The small degree of mismatch between their structures can be seen from the closeness of their lattice spacings for certain planes. Taking the F.C.C. rings of aluminium as standard, the size of the unit cell of the compound structure was calculated as 2.89A. The structure[59] of the β phase of the nickel-aluminium system is B.C.C. with lattice parameters 2.87A at 40 per cent nickel, 2.88A at 50 per cent and 2.86A at 60 per cent nickel. The examined structure could then be a distorted form of the β phase, and as that phase is formed with aluminium at the cube corners and nickel atoms at the cube centres the simple cubic structure obtained could be caused by the absence of some nickel atoms.

Aluminium-Chromium. The first specimens prepared for investigation by means of electron diffraction for the

TABLE III

STRUCTURE OF NICKEL-ALUMINIUM COMPOUND FILM

r	r^2	N_C	B	N_{IC}	N_{FC}
0.35	0.123	2	0.0615	-	-
0.455	0.208	4	0.052	2	
0.56	0.315	6	0.051	-	3
0.65	0.425	8	0.053	4	4
0.71	0.510	10	0.051	-	-
0.795	0.635	12	0.053	6	-
0.915	0.841	16	0.053	8	8
0.96	0.924	18	0.051	-	-
1.025	1.056	20	0.053	10	-

system aluminium-chromium consisted of an aluminium film 200A thick and a chromium film 100A thick. The rate of condensation of the chromium film was 3A/sec. and of the aluminium film 20A/sec. The films were examined 300 hours after preparation, and between evaporation and examination they were stored in a dessicator.

Positive prints of the diffraction patterns obtained are given in Fig. 45. Both the parent metal patterns are indicative of the bulk structures of the metals. The ring diameters of the double film are listed in Table IV, as are those of the parent metals. From the Table it can be seen that the pattern obtained for the compound film is a summation of the patterns of the parent metal films. This shows either the formation of a very thin transition structure layer as compared to the thickness of the other metals, or the absence of an interfacial layer of differing structure from that of the bulk metals.

A second specimen was prepared in which the thickness of the aluminium film was 70A and the chromium film was 30A. The investigation was carried out as before and the prints of the patterns are shown in Fig. 46. The patterns obtained did not agree with those of Fig. 45, although the period of ageing was about the same, 360 hours. In this case the aluminium appears to have oxidised

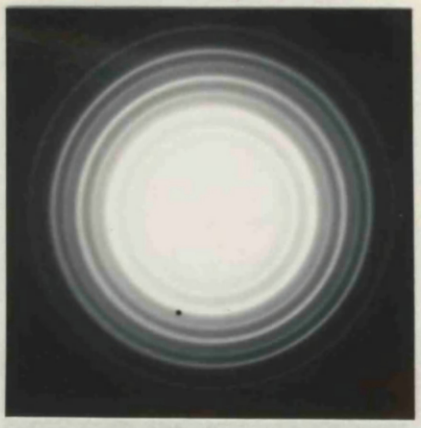

Aluminium-Chromium

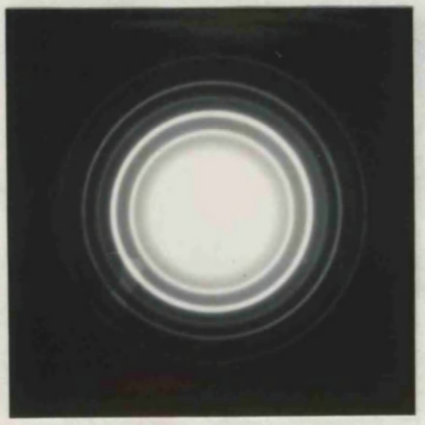

Chromium

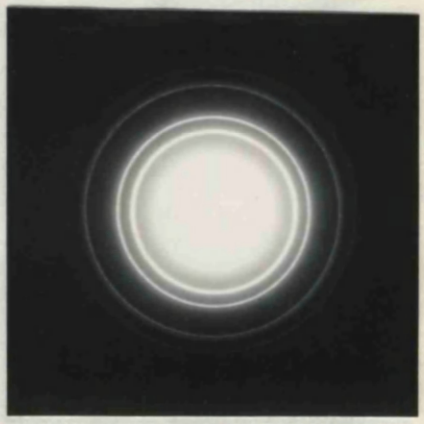

Aluminium

Fig.45. Electron Diffraction patterns from a thick specimen of Aluminium-Chromium.

Aluminium-Chromium

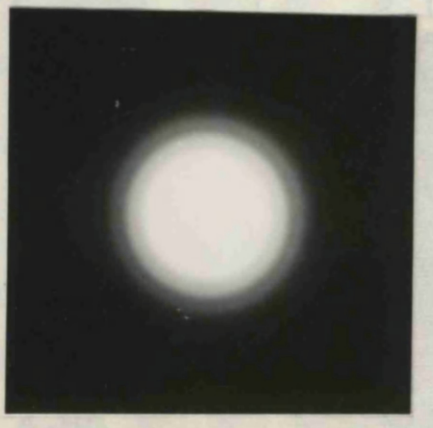

Chromium

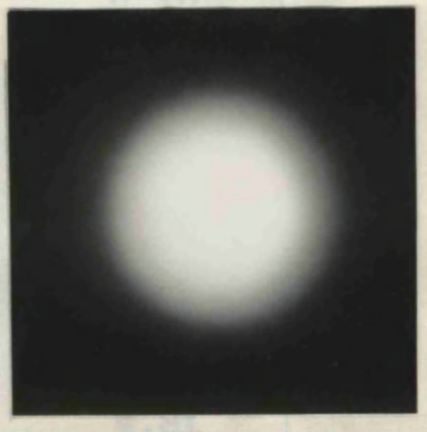

Aluminium

Fig.46. Electron Diffraction patterns from a thin specimen of Aluminium-Chromium.

TABLE IV

STRUCTURE OF CHROMIUM-ALUMINIUM COMPOUND FILM

Cr/Al	Al	Cr
D	D	D
1.08	1.11	-
1.26	1.29	1.24
1.79	1.77	1.78
2.13	2.10	-
2.19	2.15	2.17
2.56	2.65	-
2.85	2.81	2.84
2.89	2.88	-
3.18	3.20	3.15
3.43	3.41	3.39
3.71	3.75	3.68
3.93	3.84	3.90
4.16	4.27	4.15
4.40	4.42	4.36
4.63	-	4.60
4.85	4.85	4.81

Thickness of Aluminium - 200A

Thickness of Chromium - 100A

completely, giving a semi-amorphous pattern. The chromium film also shows the presence of an oxide, but some metal remains. Table V lists the measurable ring diameters and the film structure. The compound film, in this case, shows a structure that cannot be obtained directly from the parent metal films. From the investigation carried out on the structure of the film, Table VI, it can be seen that this corresponds to a cubic structure, either body-centred or simple. If the body-centred structure is preferred the length of unit cell is 2.92A, and if the simple cubic, 4.13A. The former could be a solid solution of aluminium in chromium[50] with an approximate concentration of 87 per cent. None of the other phases in the phase diagram is cubic. The possibility does exist that the structure might be the tetragonal β phase, which is composed of a stacking of three of the unit cells of the α solid solution with a rearrangement of some of the atoms.

Whichever structure is formed, it certainly is not either of the pure metals and thus represents a transition structure. From the phase diagram of the system, Fig. 10c, it would appear that the only phase that might grow thick enough to cause diffraction in this way would be the solid solutions.

TABLE V

INVESTIGATION OF STRUCTURE OF 30A THICK CHROMIUM FILM

D	D^2	N	B_i	d	Cr	Cr_2O_3
1.01	1.02	-	-	2.49A	-	2.49A (110)
1.23	1.51	2	0.755	2.04A	2.039A	2.17A (113)
1.71	2.92	4	0.730	1.47A	1.419A	1.47A (214) 1.431 (300)
2.07	4.29	6	0.714	1.21A	1.174A	1.096 (226)
2.85	8.12	10	0.812	0.88A	0.912A	0.948A(324)

TABLE VI

INVESTIGATION OF STRUCTURE OF

CHROMIUM-ALUMINIUM COMPOUND FILM

D	N	B_i	B_i'
1.26	1.59	1	2
1.79	3.20	2	4
2.13	4.54	3	6
2.50	6.25	4	8

The B_i structure is simple cubic and the B_i' body centred cubic.

(e) Previous Results using Electron Diffraction

Similar investigations by Electron Diffraction have been carried out by Trillat[61] and Michel[53]. Michel prepared the alloy films by a number of methods, including evaporation of alloys, sputtering of alloys, simultaneous evaporation of the components, and diffusion from electro-deposited and evaporated layers. The temperature range of preparation and ageing was maintained close to 20°C. By simultaneous evaporation complete alloy films were obtained, as we have shown for the discontinuous evaporation of nickel and aluminium, but by the diffusing technique no alloying could be detected for the systems silver-magnesium, copper-aluminium and copper-gold, whereas the systems silver-zinc and silver-tin gave spontaneous alloy formation. The latter two alloys form eutectic phase mixtures, the first two form an intermetallic compound directly from the liquid state, and the copper-gold system is completely miscible at high temperatures, but complex in the lower temperature range.

If, as in Chapter 3(d), the diffusion constant D is defined as

$$D = D_o \, e^{-E/RT} \qquad (6.6)$$

and we assume that this relationship is to some extent replaceable by a parabolic expression, the right hand side

can be replaced by

$$D = X^2/2t \qquad (6.7)$$

where X represents the mean penetration of the diffusing particles, and 't' is the time of diffusion. This type of equation which was evolved for gaseous diffusion[62] gives only an approximation in the present case. But the results obtained using this value can be taken qualitatively. For the systems that Michel investigated he obtained the results listed in Table VII. Examination of the values obtained for X shows that there is some degree of agreement between the depth of penetration as determined by the presence of an alloy layer and the magnitude of X. The first two systems listed in the Table giving alloy diffraction immediately after evaporation, and the latter two showing only the presence of the parent metals after some time of ageing at room temperature.

The results quoted by Michel are only approximate as the diffusion constant and activation energy values are extrapolated from values obtained at much higher temperatures and for limited concentration ranges. But this cannot altogether invalidate the degree of consistency obtained.

TABLE VII

System	D_o	E	D at 27°C.	t	X
Ag-Zn	2.1×10^{-4}	14,100	1.31×10^{-14}	1 day	4.75×10^{3} A.
Ag-Sn	7.8×10^{-5}	26,400	2.5×10^{-20}	...	6.6 A.
Cu-Au	5.8×10^{-4}	27,400	8.4×10^{-24}	...	1.2×10^{-1} A.
Cu-Al	2.3	34,900	1.45×10^{-25}	...	1.47×10^{-2} A.

(f) Discussion of Results of Investigation

For the systems that we have been investigating little research seems to have been carried out on the measurement of the diffusion constants. In an investigation[63] on the effect of vacancies on the diffusion of nickel in alloys of nickel-aluminium, results have been published for the value of D for a range of temperatures and concentrations, but no results are given for the activation energy. Using the relationship given in equation (6.6) the diffusion constant D_o and the activation energy E were calculated from the results given for one particular value of concentration, and two values of temperature. Similarly, values were obtained for the manganese-aluminium system, using the diffusion values[64] published for low concentrations of manganese in aluminium at temperatures of 600°C. and 650°C. Barrer[65] lists both the constants for the system silver-lead, and the values of X at 27°C. and 127°C. were easily calculated. The results given in Table VIII were obtained.

For the system cobalt-aluminium, only the change of diffusion constant at one temperature, but for a range of compositions were obtainable[66]; but as the system is extremely similar to the nickel-aluminium the activation energy calculated for the latter was used. It was found impossible to obtain results for the diffusion of chromium,

TABLE VIII

System	D_o	E	D at 27°C.	X_{27}	D at 127°C.	X_{127}
Ag-Pb	7.5×10^{-2}	15,200	7.75×10^{-11}	2.7×10^{4} A	4.32×10^{-10}	8.63×10^{5} A
Al-Ni	1.36×10^{-3}	47,300	5.46×10^{-34}	9.7×10^{-7} A	3.38×10^{-29}	2.42×10^{-4} A
Al-Co	3.0×10^{-3}	47,300	1.2×10^{-33}	1.4×10^{-6} A	7.4×10^{-29}	3.57×10^{-4} A
Al-Mn	2.68×10^{6}	66,000	4.6×10^{-42}	8.9×10^{-11} A	4.1×10^{-30}	8.4×10^{-5} A

Time of ageing, t = 1 day

which was unfortunate as this would have been very instructive.

From the results obtained in this investigation, and the work published elsewhere, it seems that undoubtedly there will be some phase precipitation at an interface between two evaporated films. It is impossible to say from either diffraction results or phase diagram constructions, exactly which phase will be precipitated, or the extent of the precipitation process. From the theory of diffusion it would appear that the pure phase regions grow at the extent of the mixed ones. No direct experimental evidence has been found either to support or contradict this. However, some agreement has been found between the mean penetration of the metal atoms, assuming a parabolic law to hold, and the degree of formation of interfacial alloy layers.

CHAPTER 7

OPTICAL METHODS OF INVESTIGATION

(a) Introduction

Two types of optical investigation were carried out. For a number of compound specimens the changes in reflectivity during ageing were measured using a reflectometer. The results of this examination are given in Chapter 10. Some information was obtained in this way of the rates, and extent, of the diffusion processes.

The other type of investigation was much more detailed. Using optical techniques the structure of chromium films was investigated over a thickness range. This type of examination is possible because the effective refractive index of the films is a function of the film structure. Many theories have been put forward as to the exact nature of the function, and some of these are described in section (c) overleaf. For this investigation it was necessary to include the measurement of the bulk refractive index of chromium from a number of metal samples. In this Chapter is outlined the theories used in these investigations and the equipment constructed for the reflectivity measurements.

(b) Optical Properties of a Reflecting Surface

In the theory of the reflection of light from an absorbing, but reflecting, surface two cases have to be considered according to whether the electric vector of the incident wave is parallel or perpendicular to the plane of incidence. Generally the phase shift and the reflection coefficients are different in the two cases. Drude[67] considered the case of an incident beam plane-polarised at $\pi/4$ to the plane of incidence, and showed that generally the reflected beam would be elliptically polarised and that the optical constants of the surface could be deduced from the degree of ellipticity.

The equations that Drude obtained for reflection at an angle of incidence ϕ to the normal were

$$n = \frac{\sin\phi \tan\phi \cos 2\chi}{1 + \cos\Delta \sin 2\chi} \qquad (7.1)$$

$$k = n \sin\Delta \tan 2\chi \qquad (7.2)$$

where the refractive index of the surface is given by

$$N = n - ik$$

and $\tan\chi$ = the ratio of the reflection coefficients for parallel and perpendicular incidence

Δ = the relative phase shift introduced between the two components.

This method has been widely used to obtain the optical constants of reflecting surfaces. The results obtained from it should be constants for all angles of incidence. Drude[68], however, extended his theory to cover the case in which a non-absorbing film is present on the reflecting surface. If χ and Δ remain as the ratio of the reflection coefficients and the phase shift for reflection at the clean metal surface of refractive index $(n - ik)$ and $\bar{\chi}$ and $\bar{\Delta}$ are the corresponding values for the same surface covered with the film of refractive index, n_1, and thickness, L, then

$$n_1^2 = \left[1 + \frac{2(\chi - \bar{\chi})(\cos^2\phi - a)}{(\Delta - \bar{\Delta})\, a' \sin 2\bar{\chi}}\right] \frac{1}{\cos^2\phi} \qquad (7.3)$$

$$L = - \frac{\Delta - \bar{\Delta}}{A(1 - 1/n_1^2).180} \qquad (7.4)$$

where $a = \dfrac{n^2 - k^2}{(n^2 + k^2)^2}$ and $a' = \dfrac{2nk}{(n^2 + k^2)^2}$

and where $A = \dfrac{4\pi}{\lambda} \dfrac{\cos\phi \sin^2\phi (\cos^2\phi - a)}{(\cos^2\phi - a)^2 + a'^2}$ (7.5)

Thus if the refractive index of the metal and the angles χ and Δ are known, or if measurements can be made on a clean surface of the metal in order to obtain

the quantities, by measuring the same quantities on the coated surface the refractive index and thickness of the film could be measured. If, however, it is impossible to take measurements on a clean surface then it appears that there is no solution to the above equations.

(c) Optical Properties of Thin Films

Thin evaporated films are known to have electrical and optical properties differing from the bulk metal. The changes in these properties cannot only be due to the limited thickness of the films and it has been shown, in many cases, that the films have an aggregated structure[35-7]. A number of investigations have been undertaken in order to correlate the theoretical optical properties of aggregated structures with the results obtained from actual measurements on thin films. If the aggregated structure particles in such a film behave in exactly the same way throughout the growth of the film then the film, though aggregated, is homogeneous. If, however, the properties of the aggregates change with the thickness of the film, due to structural changes within the aggregates, the film formed will be inhomogeneous. Generally the theoretical methods imply that the film must be homogeneous and application has only been made to metallic films that grow in this way.

The optical properties of small spherical particles embedded in a dielectric medium have been investigated by Maxwell-Garnett[69]. The problem he was considering was that of a thick layer of dielectric in which were present a number of particles whose diameters were all small compared to the wavelength of incident light. This approach has been applied to thin evaporated metal films as an aggregated structure is in some ways analogous to the spherical particles. Such a film will contain a large volume of voids if the particles are all assumed to have nearly the same diameters. Thus the effective density of the film will be decreased, and if the thickness of such a film, d_w, is measured by a gravimetric method, it will be found to be much less than the optical thickness, d_o. The ratio d_w/d_o, is called the packing factor of the film and given the symbol 'q'. The Maxwell-Garnett theory states that if the film can be represented by this volume fraction q of metal of refractive index, n_b', in a medium of refractive index unity, the effective refractive index n_e', is given by

$$\frac{n_e'^2 - 1}{n_e'^2 + 2} = q \cdot \frac{n_b'^2 - 1}{n_b'^2 + 2} \qquad (7.6)$$

Slight agreement with experimental measurements has been generally found using the Maxwell-Garnett theory.

It has, however, been extended to a more comprehensive form by David[70] and Schopper[71]. They assumed that the particles were more ellipsoidal than spherical, and that the ellipsoids were figures of rotation with the unique axis perpendicular to the condensing surface. Then if the film could be represented by a substance of dielectric constant ε_i, in a medium of dielectric constant, ε_a, and Madelung's[72] ellipsoidal coordinates were used in which (x,y,z) are replaced by (μ,ν,ϕ), where

$$\begin{aligned} x &= \alpha(\mu^2+1)^{\frac{1}{2}}(1-\nu^2)^{\frac{1}{2}}\cos\phi \\ y &= \alpha(\mu^2+1)^{\frac{1}{2}}(1-\nu^2)^{\frac{1}{2}}\sin\phi \\ z &= \alpha\,\mu\,\nu \end{aligned} \qquad (7.7)$$

then it follows that for this system μ = a constant defines the ellipsoidal surface. We consider such a surface and let the axes be a, b and b. Then

$$\begin{aligned} \tfrac{1}{2}a &= \alpha\,\mu_o \\ \tfrac{1}{2}b &= \alpha(\mu_o^2+1)^{\frac{1}{2}} \end{aligned} \qquad (7.8)$$

where α is a constant and $\mu = \mu_o$ defines the surface of the ellipsoid.

The ellipsoid is then considered to be placed in an electric field of value unity in the x direction. The solution of the Laplaceian equation for the potential

within the particle is

$$\phi_i = -x + Cx\left\{\frac{\pi}{2} - \tan^{-1}\mu_o - \mu_o/(1+\mu_o^2)\right\} \qquad (7.9)$$

and outside

$$\phi_a = -x + Cx\left\{\frac{\pi}{2} - \tan^{-1}\mu - \mu/(1+\mu^2)\right\}$$

where C is a constant dependent on the shape of the ellipsoid.

At the boundary the displacements must be equal across the boundary, i.e.

$$\varepsilon_i \frac{\partial \phi_i}{\partial \mu} = \varepsilon_a \frac{\partial \phi_a}{\partial \mu} \qquad (7.10)$$

On substitution for ϕ, one obtains the form

$$\varepsilon_i\left\{-\frac{\partial x}{\partial \mu} + C\frac{\partial x}{\partial \mu}\left(\frac{\pi}{2} - \tan^{-1}\mu_o - \mu_o/(1+\mu_o^2)\right)\right\} =$$

$$\varepsilon_a\left\{-\frac{\partial x}{\partial \mu} + C\frac{\partial x}{\partial \mu}\left(\frac{\pi}{2} - \tan^{-1}\mu - \mu/(1+\mu^2)\right) + Cx\left(-\frac{\partial}{\partial \mu}\tan^{-1}\mu - \frac{\partial}{\partial \mu}\left(\frac{\mu}{1+\mu^2}\right)\right)\right\} \qquad (7.11)$$

but $\dfrac{\partial x}{\partial \mu} = \dfrac{x\mu}{1+\mu^2}$; $\dfrac{\partial}{\partial \mu}\tan^{-1}\mu = \dfrac{1}{1+\mu^2}$; $\dfrac{\partial}{\partial \mu}\left(\dfrac{\mu}{1+\mu^2}\right) = \dfrac{1-\mu^2}{(1+\mu^2)^2}$

and as the equality is at the boundary $\mu = \mu_o$.

Thus, on substitution into equation (7.11) we

obtain

$$(\varepsilon_i - \varepsilon_a)\left\{-\frac{x\mu_o}{1+\mu_o^2} + C\frac{x\mu_o}{1+\mu_o^2}\left(\frac{\pi}{2} - \tan^{-1}\mu_o - \frac{\mu_o}{1+\mu_o^2}\right)\right\} =$$

$$\varepsilon_a Cx\left\{-\frac{1}{1+\mu_o^2} - \frac{1-\mu_o^2}{(1+\mu_o^2)^2}\right\} \qquad (7.12)$$

Thus

$$C = \frac{\varepsilon_i - \varepsilon_a}{\{(\varepsilon_i - \varepsilon_a)f + \varepsilon_a\}}\,\frac{\mu_o(1+\mu_o^2)}{2} \qquad (7.13)$$

where $f = \frac{1}{2}\mu_o(1+\mu_o^2)\left\{\frac{\pi}{2} - \tan^{-1}\mu_o - \mu_o/(1+\mu_o^2)\right\}$.

But the part of ϕ_a which is disturbed by the presence of the ellipsoids will tend for large values of x to the limit

$$Cx\left\{\frac{\pi}{2} - \tan^{-1}\mu - \mu/(1+\mu^2)\right\} \rightarrow Cx\mu^2(2/3) \longrightarrow Ca^3 2x/(3r^3) \qquad (7.14)$$

where $r^2 = a^2(\mu^2 - \nu^2 + 1)$.

This is the potential of a dipole of strength $Ca^3(2/3)$. From the relationship $D = E + 4\pi P$, we can see that the corresponding displacement will be

$$D = 4\pi\, Ca^3\varepsilon_a(2/3) \qquad (7.15)$$

But the total electric polarisation of a thin

layer is given by

$$P.Vs = (\varepsilon_i - \varepsilon_a)\varepsilon_o.EVs \qquad (7.16)$$

where Vs is the volume per unit area of surface of the layer. If the layer is made up of a number of droplets, each contributing to the polarisation, the total polarisation from each droplet is given by

$$p_a = D.V_k\varepsilon_o E \qquad (7.17)$$

where V_k is the total volume of the droplets, and D is the displacement per unit volume of the film material. If N is the number of droplets per unit area the total displacement is

$$N.p_a = D.N.V_k\varepsilon_o E = D.d_w\varepsilon_o E \qquad (7.18)$$

the weight thickness, d_w, being given by the product, $N.V_k$. Here we are assuming that the shape of the droplets is constant, then it follows that

$$(\varepsilon_i - \varepsilon_a)\varepsilon_o E.V_s = D.d_w.\varepsilon_o E \qquad (7.19)$$

and thus

$$D = (\varepsilon_i - \varepsilon_a).\, d_o/d_w \qquad (7.20)$$

Equating equations (7.15) and (7.20), we obtain the displacement relative to volume to be

$$\frac{\Delta\left\{(\varepsilon_i - \varepsilon_a)\,\frac{d_o}{d_w}\right\}}{\Delta V} = \frac{C\alpha^3\,\varepsilon_a.(8\pi/3)}{\Delta V} \qquad (7.21)$$

but the volume of an ellipsoid in these coordinates is

$$\Delta V = ab^2 \pi/6 = \pi a^2 \mu_o (1+\mu_o^2).4/3 \qquad (7.22)$$

Thus it follows that

$$C = \tfrac{1}{2}\mu_o(1+\mu_o^2).\frac{\Delta}{\Delta V}\left\{\frac{(\varepsilon_i - \varepsilon_a)}{\varepsilon_a}.\frac{d_o}{d_w}\right\} \qquad (7.23)$$

Therefore, equating equations (7.13) and (7.23)

$$\frac{\Delta}{\Delta V}\left\{(\varepsilon_i - \varepsilon_a)\frac{d_o}{d_w}\right\} = \frac{\varepsilon_i - \varepsilon_a}{\{(\varepsilon_i - \varepsilon_a)/\varepsilon_a\}f+1} \qquad (7.24)$$

If the system is considered to be representing a metal of refractive index (n - ik) in air, then the above equation resolves to give

$$\frac{\Delta}{\Delta V}\left\{((n_e - ik_e)^2 - 1)\frac{d_o}{d_w}\right\} = \frac{(n-ik)^2 - 1}{\{(n-ik)^2 - 1\}f+1} \qquad (7.25)$$

which is the form Schopper used.

For the films examined the volume is only changing by virtue of the change in thickness of the film. Change with respect to volume ΔV can then be replaced by the change relative to thickness Δt. Thus the right hand side of the equation should describe the changes in refractive index to be expected with varying thickness. The quantity f represents a function of the axial ratio of

the ellipsoidal particles, and is indicative of the shape of the particles. The form of the function is given in Fig. 47, where it can be seen that for $b \gg a$, f tends to zero and bulk values are obtained. For f about 0.3 the axial ratio is unity and the particles become spherical.

Schopper, however, considered that the particles in a film were not all the same shape, but distributed about a mean value in a Gaussian fashion. Assuming the mean value of f to be $\bar{f}$ the distribution function is then

$$g(f) \propto f.e^{(-f/\bar{f})^2}$$

and C in equation (7.9) is replaced by a mean value $\bar{C}$ where

$$\bar{C} = \frac{(n-ik)^2 - 1}{\{(n-ik)^2 - 1\}\bar{f}+1}$$

$$= \frac{\int C.g(f)\, df}{\int g(f)\, df} \qquad (7.26)$$

This form of the equation was applied by Schopper to the changes in refractive indices of gold films with thickness, with some success. He eliminated the problem of correlating the f function and the thickness by considering that as f was a function of the size of the particles, it could be used to replace the thickness function.

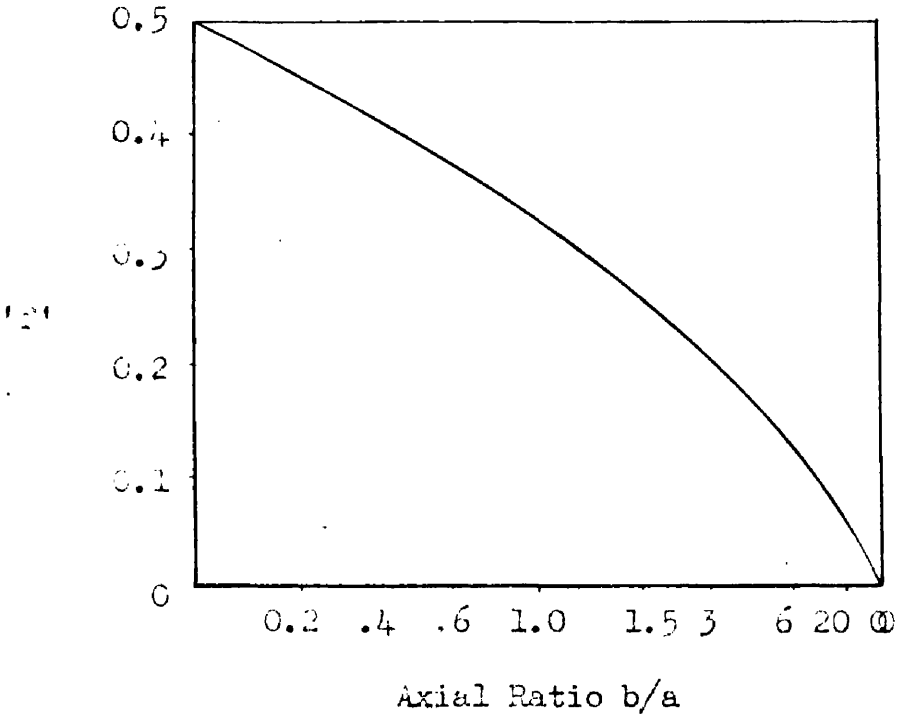

Fig.4.7. Graph of the function 'f' against axial ratio of ellipsoidal particles.

Graphs were constructed of the real and imaginary parts of $\bar{C}$ as functions of $\bar{f}$. The experimentally determined points were then fitted to the graph of the real function irrespective of the thickness of the specimens. It was found that $\bar{f}$ decreased with increasing thickness. The graph gave for each of the experimental points an $\bar{f}$ value. Onto the graph of the imaginary function were then plotted the corresponding experimental points, using the $\bar{f}$ values already obtained. The agreement between these points and the theoretical curve was taken as showing that the function described the changes in refractive indices of the gold films.

(d) The Wolter Relationship

Although inhomogenity can be described in a qualitative way it is very difficult to express either the degree of inhomogeneity in detail or to measure changes in the function. The most commonly used means of measuring the quantity is that due to Wolter[73], called the Wolter relationship. It was shown that for an absorbing film lying in air on a substrate of refractive index n_2, the absorption of light passing from the air side (A) could be related to that in the opposing direction (A') if the film was homogeneous. The relationship suggested was

$$n_2 A = A' \qquad (7.27)$$

This only holds where the transmission is measurable, that is, where the thickness of the film is very small compared to the wavelength of the incident light.

The absorptions of the films can be determined directly from measurements of the reflectivities and transmissions. If the reflectivities of the film on the air and substrate sides are respectively R and R', and the transmission of the film is T, then

$$A = 1 - R - T \quad \text{and} \quad A' = 1 - R' - T \tag{7.28}$$

The relationship only holds accurately for very thin homogeneous films[74].

(e) Reflectivity Measurements

Reflectivity measurements were made on two different types of reflectometers. One measured the reflectivity at an angle of incidence of 45°, using mercury green filters in conjunction with white light sources, and the other incorporated a monochromator and photomultiplier tube. The former was constructed using a long optical bench and a Brodhun-Lummer photometer. A diagram of the apparatus is given in Fig. 48. As the reflecting films had been evaporated onto 3" x 1" microscope slides a slide holder was constructed as shown.

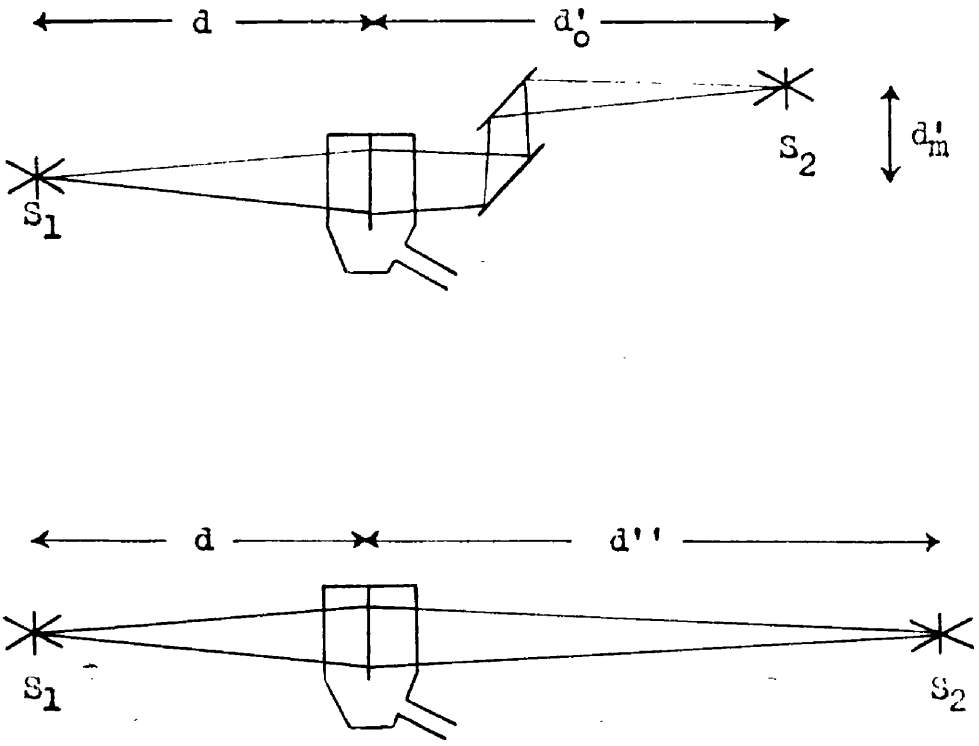

Fig.48. Fixed Wavelength Reflectometer.

This held the slides 7.4 cm. apart and parallel at an angle of 45° to the main axis of the bench. One of the reflecting films was mounted level with the photometer window, and the source, S_2, was displaced in the same direction as the other mirror, and by the same distance. Then when the reflectivities of the mirrors are R_1 and R_2, and d'_o is the horizontal position of the source S_2

$$S_1/d^2 = R^2(S_2/d'^2) \qquad (7.27)$$

where, if d'_m was the displacement of the mirrors and the source S_2

$$d' = d'_o + d'_m \qquad \text{and} \qquad R^2 = (R_1 \times R_2)$$

If the mirrors be removed and S_2 reset to its original position on the optical axis, and the source, S_1, kept in the same position, then on resetting the photometer the new position of S_2 will be d'', where

$$S_1/d^2 = S_2/d''^2$$

thus

$$R^2 = d'^2/d''^2 \qquad (7.30)$$

But if the mirrors were prepared under exactly the same conditions, then R_1 will equal R_2, that is, they will both be equal to R. Thus, for this particular case

$$R = d'/d'' \qquad (7.31)$$

This form of reflectometer was found very convenient for measuring the reflectivities of a number of films as they aged, and was used for this purpose.

The other reflectometer was constructed in order to measure the reflectivity coefficients of evaporated films over the complete visible spectrum. A highly stabilised photomultiplier cell was used as the measuring device. This could be mounted in either of two positions inside a light tight box. One position was used for measuring the transmissions of the films, and the other for reflectivities at an angle of 7^{o} to the normal.

The design of the monochromator is given in Fig. 49. Light from the filament strip source S was focussed to give an image of the filament along the slit T. The prism, p, mounted on the side of the body tube, was used to reflect the light from T through the lens, L_1, onto the prism P. As the slit T was in the focal plane of L_1, a parallel beam of light was thus obtained. The prism, P, was set so as to give minimum deviation of the beam, which would then have given a spectrum band at infinity, but for the mirror M. This mirror reflected the light back through the prism and focussed the doubly dispersed spectrum on the focal plane of L_1. The slit T' mounted in this plane then selected the pass-band of

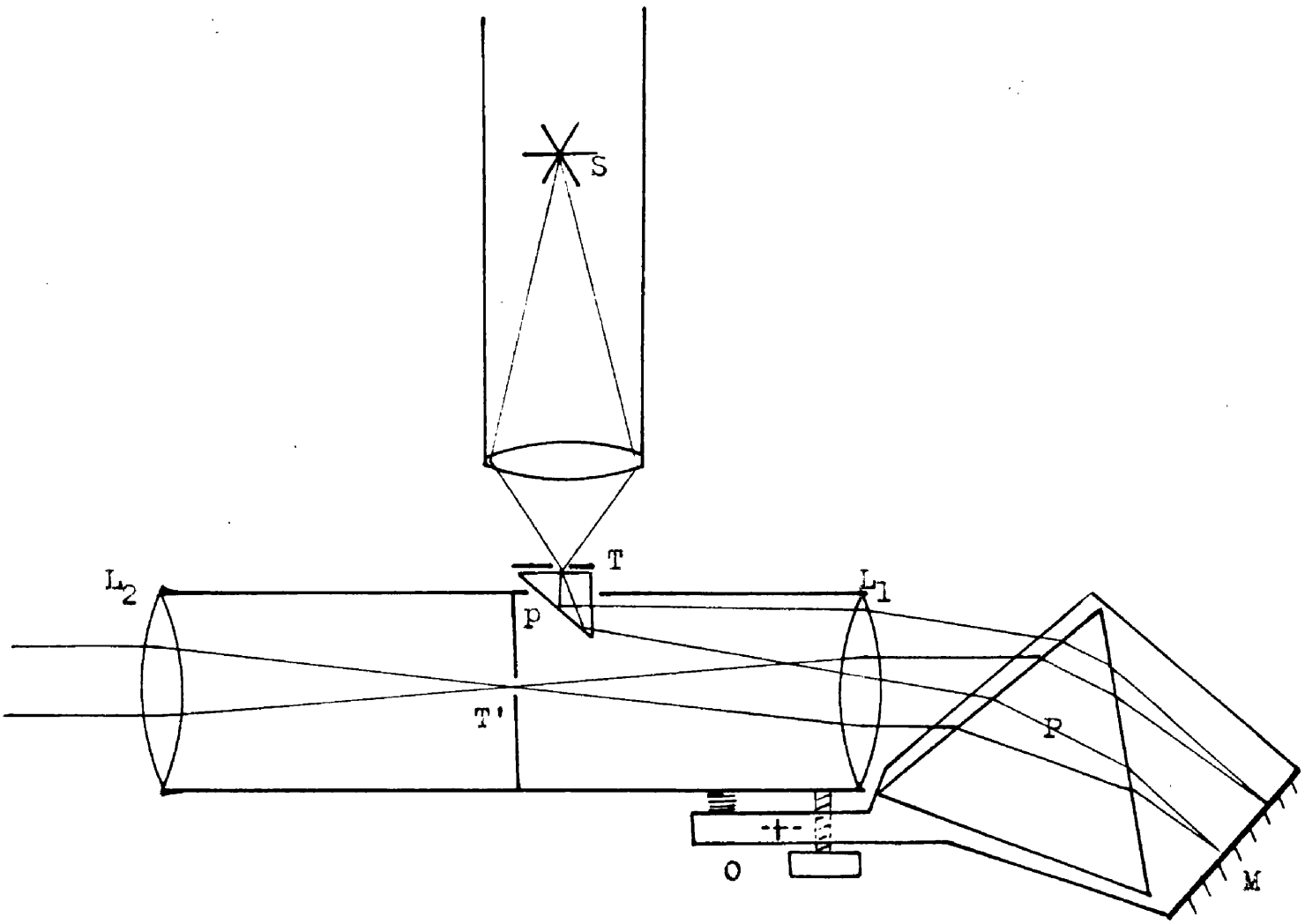

Fig.49. Design of Monochromator for the Variable Wavelength Reflectometer.

the instrument, as T' was also mounted in the focal plane of the lens, L_2, a parallel, semi-monochromatic beam was obtained. The wavelength of the pass-band could be altered by swinging the prism, P, and the mirror, M, about the axis at O. A calibrated drum and revolution counter were mounted on the body to measure the position of the swinging arm.

The monochromator was calibrated against a standard spectroscope, and the calibration and pass-band width graph is given in Fig. 50. The instrument was rigidly mounted outside the light tight box, and a light seal was interposed. The intensity of the incident beam was measured directly on a galvanometer, without the specimen and as the characteristics of the system were found to be linear the transmission and reflectivities were found by direct ratio of the corresponding readings. In front of the measuring cell a ground glass screen and narrow slit were fitted to reduce the effect of scattered light.

When the reflectivities and transmissions of the thinner chromium slides were being measured it was necessary to correct for multiple reflections within the condensing plate, and reflections at the metal glass interface. If the measured reflectivities were taken

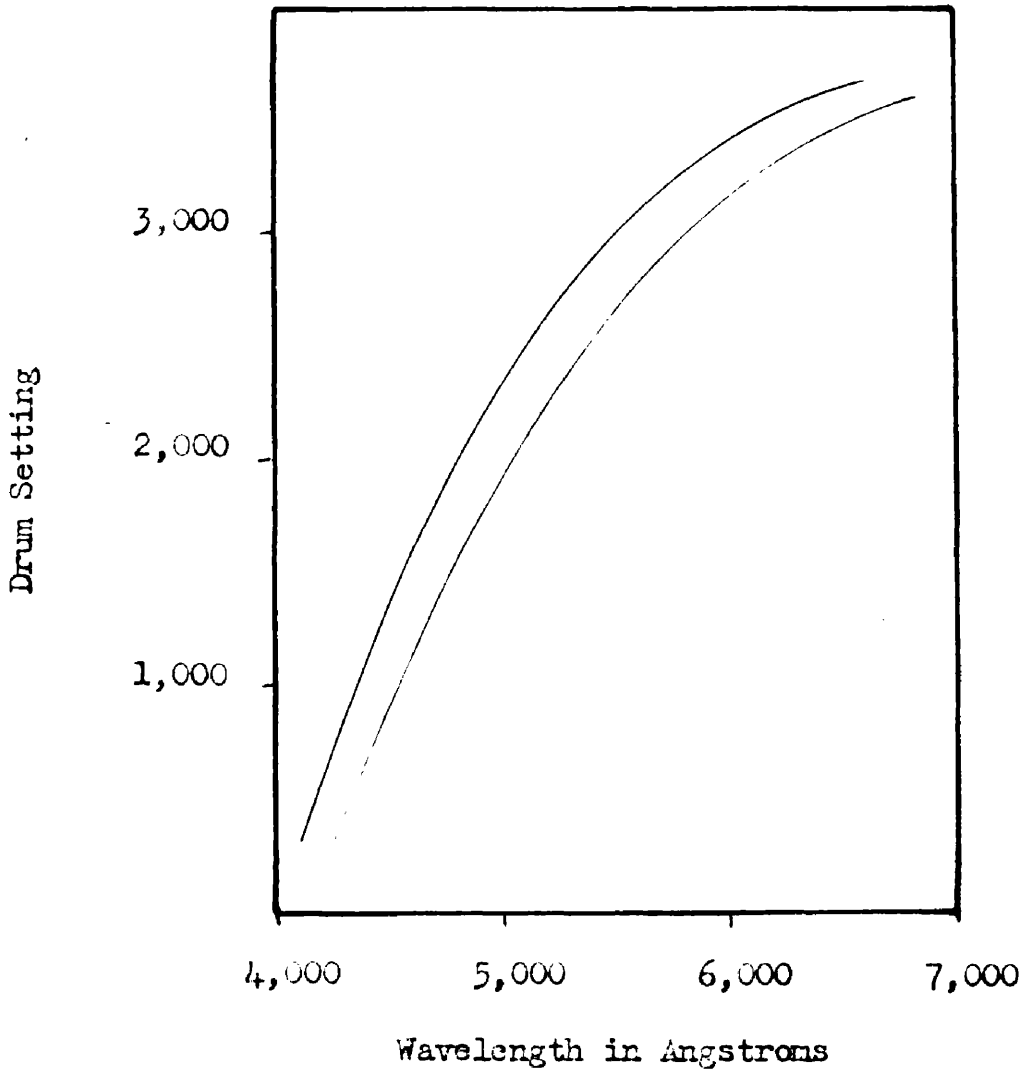

Fig. 50. Pass-band and Calibration Graph for the Monochromator.

as R_o and R'_o for reflection from the film side and from the glass side, respectively, and the transmission of the complete system was T_o, then it can be seen, where the absolute values are R, R' and T that, from Fig. 51a

$$R'_o = R_g + T_g^2 R' (1 + R_g R' + R_g^2 R'^2 + ...) \qquad (7.32)$$

where the reflectivity of one surface of the glass is R_g, and the transmission is T_g. In the case above we have neglected further reflections from the air side of the metal films. This is justified as, for these reflections, the film has to be traversed twice, and for such films, the absorption is high.

Thus

$$R'_o \doteq R_g + \frac{T_g^2 R'}{1 - R_g R'} \qquad (7.33)$$

and by simplifying for R'

$$R' \doteq \frac{R_g - R'_o}{R_g^2 - T_g^2 - R'_o R_g} \qquad (7.34)$$

$$= \frac{R'_o - R_g}{R_g R'_o - R_g + T_g} \quad \text{since } R_g + T_g = 1 \qquad (7.35)$$

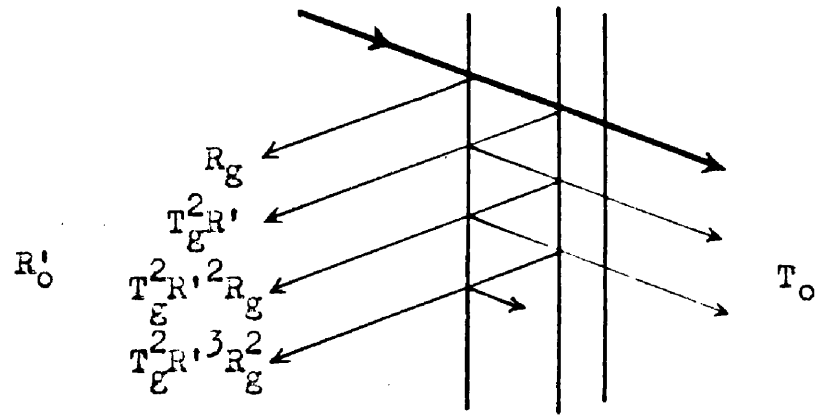

(a)

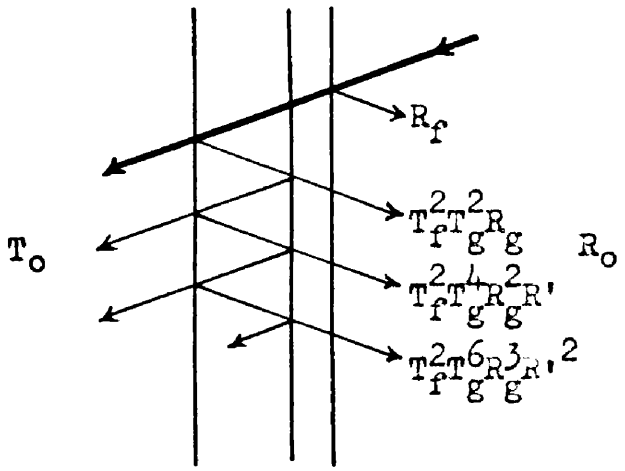

(b)

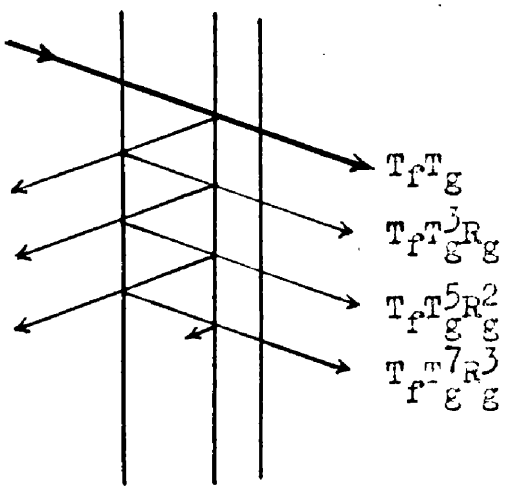

(c)

Fig. 51. Calculation of Correction Factors for Multiple Reflections within the Condensing Plate.

From Figs. 51b and 51c in a similar manner it can be seen that

$$R = R_o - \frac{T_o^2 R_g}{R_g R'_o - R_g + T_g} \; ; \quad T = \frac{T_o T_g}{R_g R'_o - R_g + T_g} \tag{7.36}$$

When the transmissions of the films are low, $R \doteq R_o$ and $T = T_o$, but a correction factor has still to be applied for the reflection coefficient R'.

CHAPTER 8

OPTICAL PROPERTIES OF BULK CHROMIUM

(a) Introduction

Some experimental work has already been undertaken on the measurement of the reflection and transmission coefficients of evaporated films of chromium[75,76], and sputtered films of chromium[76]. The earlier investigators were hoping to measure the refractive index of bulk chromium by measuring the optical constants of very thick films of the metal. The results that were obtained were very varied and did not compare with the published results for the bulk metal. These latter, however, when measured by different observers showed alarming variations (Table IX). As it was intended to measure the structure of chromium films by means of an optical investigation it was felt necessary to obtain the bulk refractive index of the metal with a fair accuracy. Thus three bulk metal specimens of the purest samples available, and the thickest chromium film used in the optical investigation, were examined. It was only possible to use this thickest sample as reflection from the glass backing plate would have interfered with the measurements of the degree of ellipticity.

TABLE IX

SUMMARY OF PUBLISHED VALUES FOR THE

OPTICAL CONSTANTS OF BULK AND EVAPORATED CHROMIUM

n	k	Wavelength	Source
2.97	4.87	5790A	Wortenburg[81]
3.53	4.41	5460A	Physikalisch Chemische Tabellen[82]
3.28	4.35	5460A	Sennett & Scott[83]
2.49	2.30+	5460A	Abeles[75]

+ This last specimen was vacuum evaporated.

(b) Experimental

The experimental measurements on the specimens were made using a modification of Drude's method due to Tronstad[72]. In this a compensator was placed in the light beam before the specimen but after the polariser, giving an incident beam that was elliptically polarised. The ellipticity of the beam could be adjusted to give plane polarised light after reflection at the specimen surface. The compensator used was a mica quarter-wave plate with its principal axis at $\pi/4$ to the plane of incidence, the ellipticity was adjusted by rotating the polariser. Plane polarised light was detected by obtaining an extinction position for the analyser. If P and A be the required angles of rotation of polariser and analyser from the zero position, taken parallel to the plane of incidence, then it can be shown that the relative phase shift Δ and the angle χ between the electric vector of the reflected beam and the plane of incidence are given by the relationships

$$\begin{aligned} \sin \Delta &= \cos 2P \\ \tan \chi &= \tan A \end{aligned} \qquad (8.1)$$

A diagram of the apparatus is given in Fig. 52. This is based on Tronstad's polarising spectroscope. In the original instrument a half shade device was used to detect the plane of polarisation of the reflected beam;

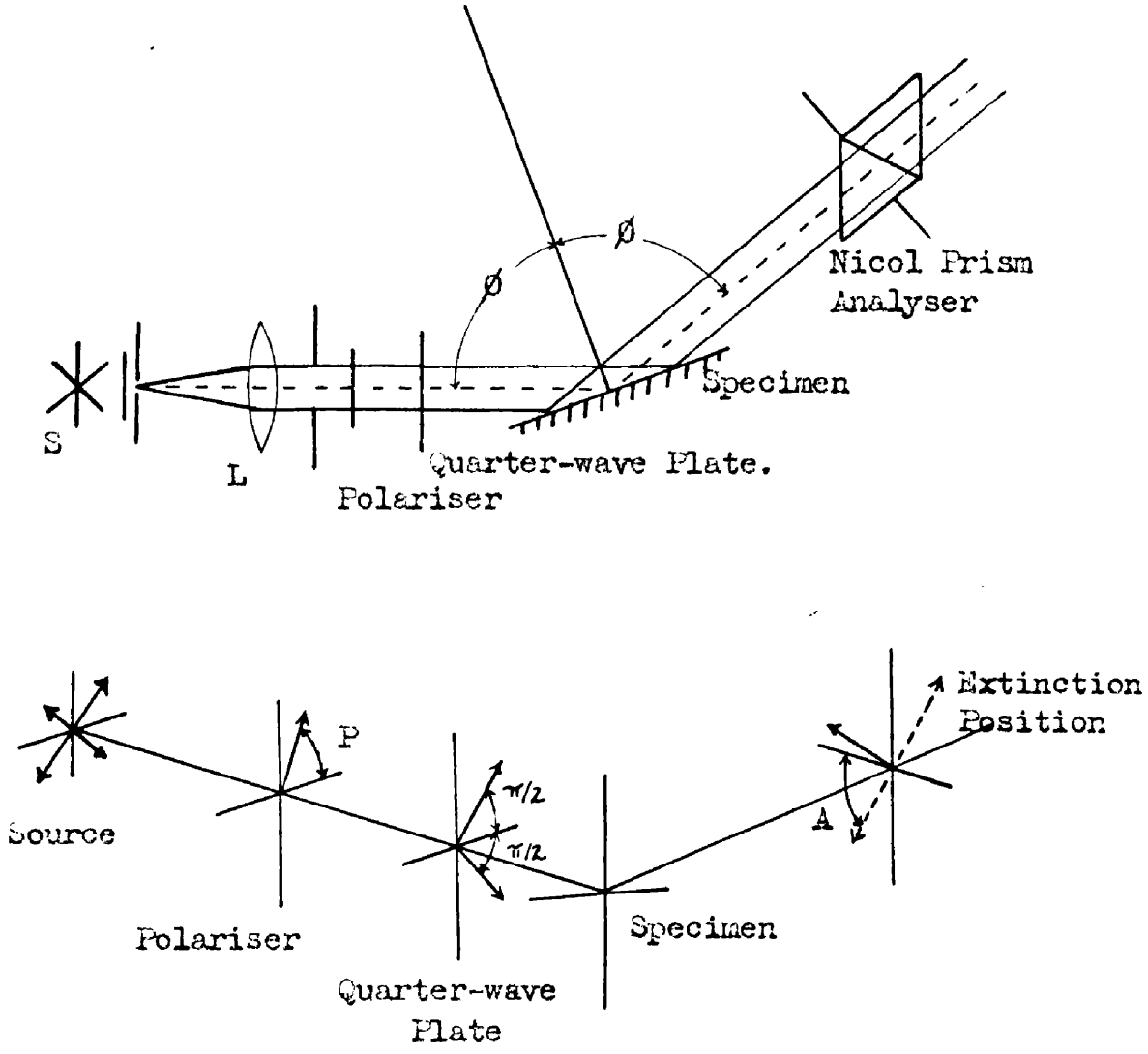

Fig.52. Polarising Spectroscope.

in our equipment this was not used but instead, the nicol analyser was adjusted to give, in conjunction with the polariser, an extinction position. This undoubtedly reduces the accuracy of the method, particularly for the higher angles of incidence, but it was found to be convenient.

A high pressure mercury lamp was used as the source, S, with a mercury green filter to obtain the 5461Å line. A diffusing screen and aperture were mounted in front of the lamp at the focal distance of the lens, L, from the lens. This gave a parallel beam of monochromatic light; a second aperture was introduced into the beam just before the polaroid polariser to reduce the scattered light. The polaroid sheet was mounted in a large ball race, carrying a 360° scale. After the polariser a quarter-wave plate was inserted with its principal directions at 45° to the plane of incidence of the specimen. A nicol prism was used as the analyser, being mounted in a $90^{\circ} - 0 - 90^{\circ}$ scale with a vernier attachment.

Three samples of bulk chromium were investigated and represented the purest specimen available. A visual spectrographic comparison of their purity with a sample of known purity is given in Table X. The fourth sample listed in that table was that of the chromium chips used for the evaporation of a vacuum prepared specimen. The

TABLE X

PURITY OF CHROMIUM SPECIMENS

Impurity	No. 1	No. 2	No. 3	No. 4	Standard
Iron	4	1	2	3	1 (2ppm)
Silicon	6	1	5	4	1 (1ppm)
Copper	2	2	4	5	1 (1ppm)
Manganese	2	1	4	3	1 (1ppm)
Magnesium	1	1	1	1	1 (1ppm)

Suppliers of Metal Samples:

No. 1.	Union Carbide Co.	America
No. 2.	Alreco Metal Corpn.	Germany
No. 3.	Henry Wiggin & Co.Ltd.	Birmingham, England.
No. 4.	Hopkin & Williams.	Essex, England.

impurities of the standard are listed in parts per million. The spectrographic comparison is only qualitative, i.e. where an impurity is listed as twice that in the standard it means that it is present to a greater extent, but not necessarily exactly double. The bulk metal specimens were polished to give a surface area of about two centimetres square, but a slight graininess was left on the surface due to the difficulty of polishing such a hard and brittle metal as chromium.

The evaporated specimen was prepared under exactly the same conditions as the adhesion tested samples. This particular specimen was evaporated at a rate of 10A/sec. in a vacuum of 4.10^{-4} mm.Hg. and the thickness of the specimen by weight was 537A.

(c) Results of Optical Measurements

Table XI shows the values obtained for the angles χ and Δ for the specimens. It can be seen that there is no constant deviations from a mean value for any of the bulk metal surfaces. The relatively larger scatter of results for the higher angles of incidence were due mainly to the difficulty of obtaining sharp extinction settings at those values of ϕ. For this reason the values obtained for these high angle values are treated with

TABLE XI

EXPERIMENTAL VALUES OBTAINED FOR THE ANGLES χ AND Δ FOR THE RANGE OF SPECIMENS

Angle of Incidence	Values of χ				
				Mean of Bulk	
ϕ	No. 1	No. 2	No. 3	Nos. 1, 2 & 3	No. 4
30°	43.2°	43.5°	43.13°	43.2°	42.0°
35°	42.4°	42.5°	42.3°	42.4°	40.9°
40°	41.3°	41.4°	41.65°	41.5°	39.17°
45°	40.4°	40.5°	40.2°	40.4°	38.2°
50°	39.1°	39.25°	38.6°	39.2°	36.69°
55°	37.3°	37.3°	37.2°	37.3°	34.65°
60°	35.5°	34.8°	35.9°	35.5°	32.22°
ϕ	Values of Δ				
30°	171.8°	171.0°	172.0°	171.7°	172.4°
35°	169.1°	168.1°	169.1°	168.8°	169.5°
40°	165.6°	165.1°	164.0°	165.1°	165.8°
45°	162.6°	160.9°	160.4°	161.3°	161.3°
50°	158.8°	156.0°	156.0°	156.5°	156.0°
55°	152.7°	151.0°	150.7°	151.5°	148.7°
60°	146.0°	143.8°	142.0°	143.8°	141.0°

caution. Complete agreement was not obtained between the evaporated specimen and the others but this was not unexpected as the optical constants of thin films usually differ from those of the bulk material[78]. The high angle settings for the evaporated specimen were much easier to obtain as the surface of the sample was much smoother than the others, but difficulty was still experienced in obtaining sharp settings.

The values of the constants n and k assuming a simple metal/air interface were calculated from equations (7.1) and (7.2), and are listed in Table XII. The wide range of these values was not expected from the theory of a simple reflector. If chromium does not reflect simply in this way, then the wrong theory has been applied. However, no allowances were made in the earlier published work for the presence of any form of surface film. As the published results do not appear to be consistent, see Table X, and as the surface of the evaporated film had received no polishing or abrading, it appeared reasonable that the disagreements were due to the presence of a surface, or polish, layer.

If we wish to investigate this layer, however, we need to obtain measurements on a perfectly pure metallic chromium surface, in order to measure Ψ and Δ and to calculate n and k. This, however, was found to be impossible.

TABLE XII

RESULTS OF CALCULATION OF REFRACTIVE INDICES

Angle of Incidence	Mean of Bulk Metal Values		Evaporated Specimen Values	
ϕ	n	k	n	k
30°	1.25	3.40	2.19	2.76
35°	1.45	3.38	2.17	2.63
40°	1.63	3.35	2.15	2.56
45°	1.78	3.43	2.12	2.63
50°	1.91	3.50	2.10	2.85
55°	2.01	3.51	2.15	3.40
60°	2.09	3.52	2.17	3.97

The difficulty can only be resolved by postulating for chromium a range of n and k. Then for each pair of these from equations (7.1) and (7.2) we can calculate the values of χ and Δ. The experimental measurements have already furnished us with values for $\bar{\chi}$ and $\bar{\Delta}$. In this way n_1 and L can be calculated from equations (7.3) and (7.4) for the range of angles of incidence. When a pair of (n,k) values had been obtained that gave constant values for n_1 and L for all ϕ we would have obtained at the same time the refractive index of the bulk metal, (n-ik), the refractive index of the surface film, n_1, and the thickness of the surface film, L. This calculation was carried out for the experimental values already obtained.

The method was at first calculated through for the evaporated specimen as the $\bar{\chi}$ and $\bar{\Delta}$ values obtained were more critical. The calculation was found to be rather laborious, and, at first, the refractive index of the surface layer was calculated for only four angles of incidence, ($\phi = 30^\circ, 40^\circ, 50^\circ$ and 60°). As the values for n_1 became more constant they were calculated for every five degrees of angle of incidence, and ultimately, the values listed in Table XIII were obtained. The finally acceptable values for this specimen were taken as

$$N = 1.18 - i0.944 \; ; \quad n_1 = 2.230 \; ; \quad L = 50\text{A}$$

TABLE XIII

CALCULATION OF REFRACTIVE INDEX AND THICKNESS OF THE SURFACE FILM FOR A RANGE OF (n,k) - EVAPORATED SPECIMEN

Angle of Incidence	n - ik					
ϕ	1.20 - i0.96		1.15 - i0.92		1.18 - i0.944	
	n_1	L	n_1	L	n_1	L
30^o	2.24	46A	2.16	40A	2.220	44A
35^o					2.225	44A
40^o	2.36	41A	2.15	48A	2.206	49A
45^o					2.238	48A
50^o	2.27	48A	2.31	37A	2.242	53A
55^o					2.240	65A
60^o	2.29	81A	2.25	83A	2.238	68A

The final stages of the above calculation were repeated using the experimental results of the third bulk metal specimen, and for this specimen the values obtained, Table XIV, were

$$N = 1.18 - i1.06 \quad ; \quad n_1 = 2.42 \quad ; \quad L = 50A$$

Some of the earlier results are listed in Table XV, and it can be seen that although the refractive index components show only slight variation the thickness values are extremely inconsistent.

(d) Discussion

The refractive index value obtained for the surface film agrees fairly well with that of 2.5 listed in the tables[79] as the refractive index of chromium oxide. The slightly lower value obtained for the evaporated specimen will indubitably be due to the presence of voids within the evaporated film. From the result for that specimen and the listed value, it would appear that about twelve per cent by volume of the film is in the form of voids. This is not unreasonable and higher values have been obtained in dielectric films[80]. Mechanical polishing does not appear to have had any pronounced effects upon the nature and thickness of the surface film. The thickness of about 50A obtained probably represents the maximum value for

TABLE XIV

CALCULATION OF REFRACTIVE INDEX OF THE SURFACE FILM FOR A RANGE OF (n,k), WITH THICKNESS VALUES FOR THE BEST FIT

BULK METAL SPECIMEN

Angle of Incidence	n - ik				
ø	1.18 - i0.826	1.18 - i0.944	1.18 - i1.00	1.18 - i1.062	
	n_1	n_1	n_1	n_1	L
30°	2.60	2.52	2.50	2.50	34A
35°				2.46	36A
40°	2.42	2.40	2.40	2.42	41A
45°				2.40	44A
50°	2.40	2.34	2.38	2.40	48A
55°				2.36	61A
60°	2.22	2.34	2.40	2.44	68A

TABLE XV

CALCULATION OF REFRACTIVE INDEX OF THE SURFACE FILM FOR A RANGE OF (n,k)

EARLY RESULTS FOR THE EVAPORATED SPECIMEN

Angle of Incidence	n - ik							
ϕ	0.5 - i1.4		0.5 - i1.0		1.0 - i1.0		1.5 - i1.0	
	n_1	L	n_1	L	n_1	L	n_1	L
30°	1.35	614A	1.62	513A	2.73	105A	2.94	45.2A
40°	1.37	402A	1.57	641A	2.06	146A	2.46	68.2A
50°	1.64	563A	1.84	662A	2.27	281A	2.48	112A
60°	1.72	352A	1.99	366A	2.36	311A	2.40	327A

growth of the oxide film at room temperature. This result is in agreement with the oxidation theories outlined in Chapter 3. The variation in thickness of the surface layer for different values of the angle of incidence are probably due to the lack of a clear cut metal-metal oxide interface. A transition region is normally set up at such a boundary and this will certainly affect the state of polarisation of a reflected beam of light. The more the beam approaches normal incidence the less should be the effect of the transition region.

CHAPTER 9

OPTICAL PROPERTIES OF EVAPORATED CHROMIUM FILMS

(a) Introduction

Electron microscope and electron diffraction[35-7] investigations have shown that the structure of thin films cannot be considered to be regular except in very exceptional circumstances. For a large number of metals aggregated particles have been found to form, and the sizes of these aggregates vary with the film material and thickness, from fractions of a millimetre in diameter down to the limit of resolution of the electron microscope. Chromium, when evaporated onto a condensing surface at room temperature, forms a very finely aggregated structure. In one microscopical investigation it was found that with the highest resolution possible, the films still presented a perfectly continuous appearance[36], but from electrical resistivity measurements[84] it was known that this could not be so. Thus the particles must be extremely small.

This present chapter describes an investigation carried out using optical techniques to ascertain the structure of such films. From the reflection and transmission coefficients the effective refractive index

and thickness of each film was determined. Then, by assuming a number of structural models attempts were made to correlate structure and the effective refractive index as they both varied with the thickness of the specimen considered. The best fit was obtained using a new type of structural model, based on the ellipsoid type of particle described by David[70] and Schopper[71]. The derivation of the theory and fitting of the experimental results are given in detail.

The films were all evaporated under the same conditions as those used in the adhesion investigation. The rate of evaporation was about 10A/sec., and at no time did the evaporating pressure exceed 5.10^{-5} mm. Hg. As little change in the optical reflectivities had been found, the films were allowed to age for three weeks before being measured. The reflection and transmission coefficients were measured on the apparatus described in Chapter 7(e). The correction factors calculated for the use of parallel sided glass condensing plates were carried out.

(b) Calculation of Refractive Index

Numerous methods have been evolved for the measurement of the refractive index of a thin absorbing film. Most of the methods assume that the film is

homogeneous, and bounded by two plane and parallel surfaces. Using these simplifying assumptions the refractive index of the film (n-ik), and occasionally the thickness, d_o, can be calculated if suitable measurements are made on the surfaces of the film. The commonest measurements to make are the changes in amplitude and phase of reflected light from either side of the film. In a method originated by Male[85] only three measurements are required, and each of these is a simple ratio of intensities. These are: the coefficient of transmission of a beam of light at normal incidence to the film; the coefficient of reflection of the reflected component, R; and the coefficient of reflection from the glass substrate side of the film, R'.

In this method of calculation, a range of refractive indices has to be assumed, where n and k are allowed to vary independently, together with a range of thicknesses, d_o. The reflection and transmission coefficients are then calculated and graphed as functions of δ for each pair of n,k values over the range of d_o, δ being given by $4\pi nd_o/\lambda$. The calculations can be made by a relatively simple graphical method also due to Male.[86] This gives a series of curves of R, R' and T respectively against δ, each curve corresponding to a pair of n,k values. Using the measured values of T for a given film, a horizontal line can be drawn to cross the theoretical

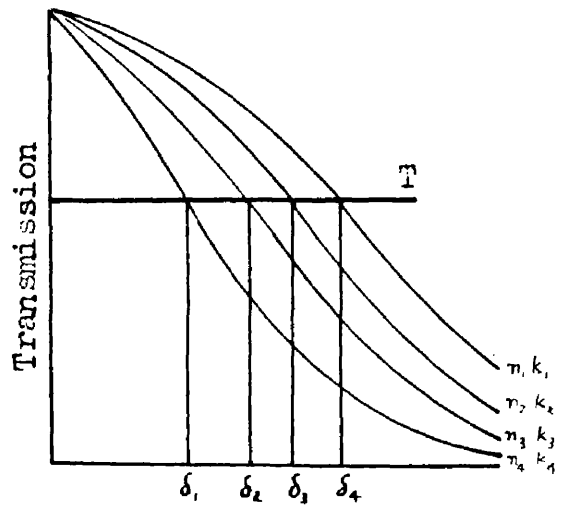

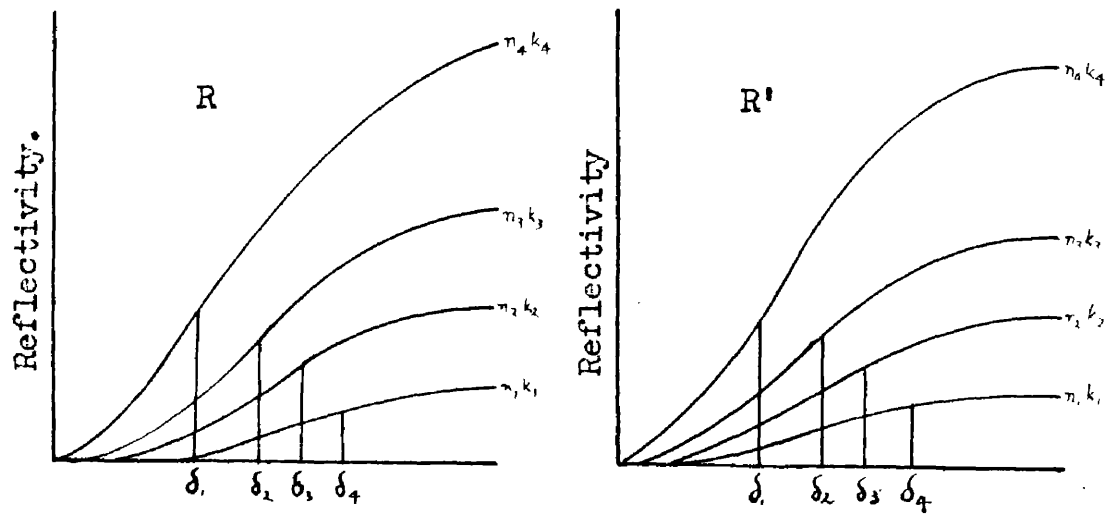

Fig.53(a). Graphs of R, R' and T against δ.

transmission curves, Fig. 53a. Each intersection with the curves giving a value of δ and values of n and k which would together satisfy the transmission condition.

Each set of n,k and δ associated with an intersection enables the corresponding values of R and R' to be obtained from the series of reflectivity curves already drawn. Using the figures thus obtained, R can be plotted against n for each given k value, and similarly for R'. This gives two sets of curves and from each set a series of n,k values can be obtained by drawing a horizontal line at a level corresponding to the observed reflection coefficients, Fig. 53b. The first series of n,k satisfy simultaneously the R and T conditions, and the second set the R' and T conditions. Using these two series of values two curves can be obtained by plotting k against n and the intersection of these two curves, Fig. 53c, gives unique n,k values which satisfy the observed values of R, R' and T. Knowing the refractive index (n_e-ik_e) of the film, the δ value can be readily obtained from plots of n against δ for the given k values. Hence the apparent thickness, d_o, can be obtained.

As a check on the accuracy of the determination, the reflectivities and transmissions were recalculated from the n_e and k_e values. This reverse calculation eliminated

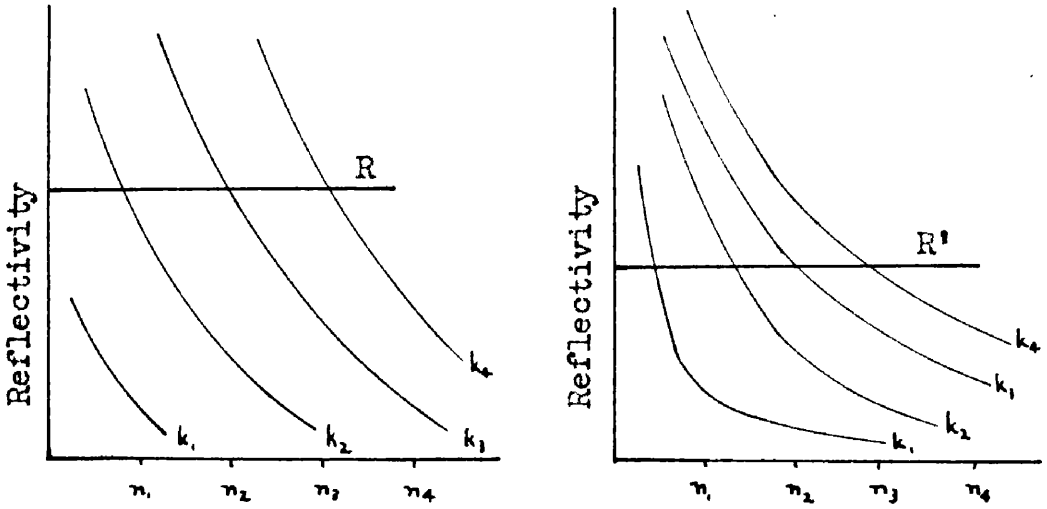

Fig.53(b). Graphs of Reflectivity against n for ranges of k.

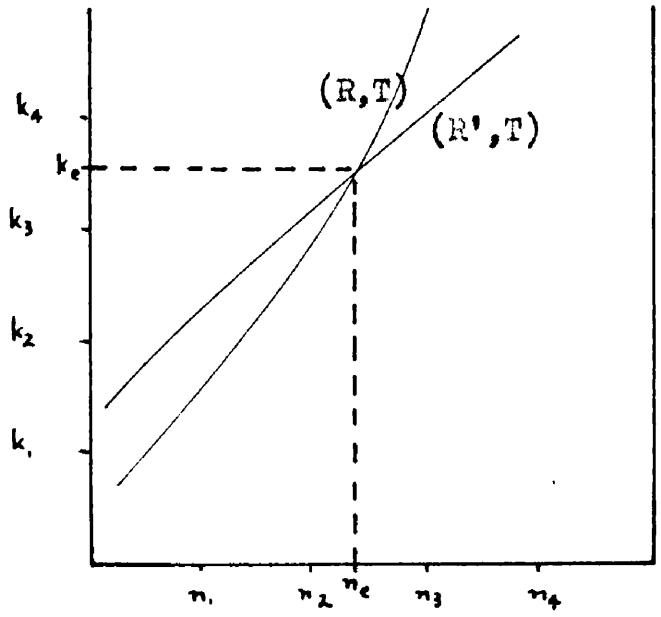

Fig.53(c). Graphs of n against k.

any possibility of errors and comparison between these and the experimental values gave an indication of the accuracy of the method. The recalculated values were found to agree closely with the experimental values.

These results, Fig. 54, are in general agreement with the published work of other authors for a number of different metal films[87-9], where the real part of the refractive index increases as the film thickness decreases and the imaginary part tends to zero with the thickness. These variations are not purely thickness effects of the type encountered in electrical conductivity[90], and indeed it has been found impossible to explain this type of experimental result by considering the film as continuous or homogeneous.

(c) Application of the Maxwell-Garnett Theory

The packing factor, q, of the Maxwell-Garnett equation[69]

$$\frac{n_e'^2 - 1}{n_e'^2 + 2} = q \cdot \frac{n_b'^2 - 1}{n_b'^2 + 2}$$

where n_e' is the effective refractive index of the film and n_b' the bulk refractive index was calculated for a number of films. For one or two of the films it was also

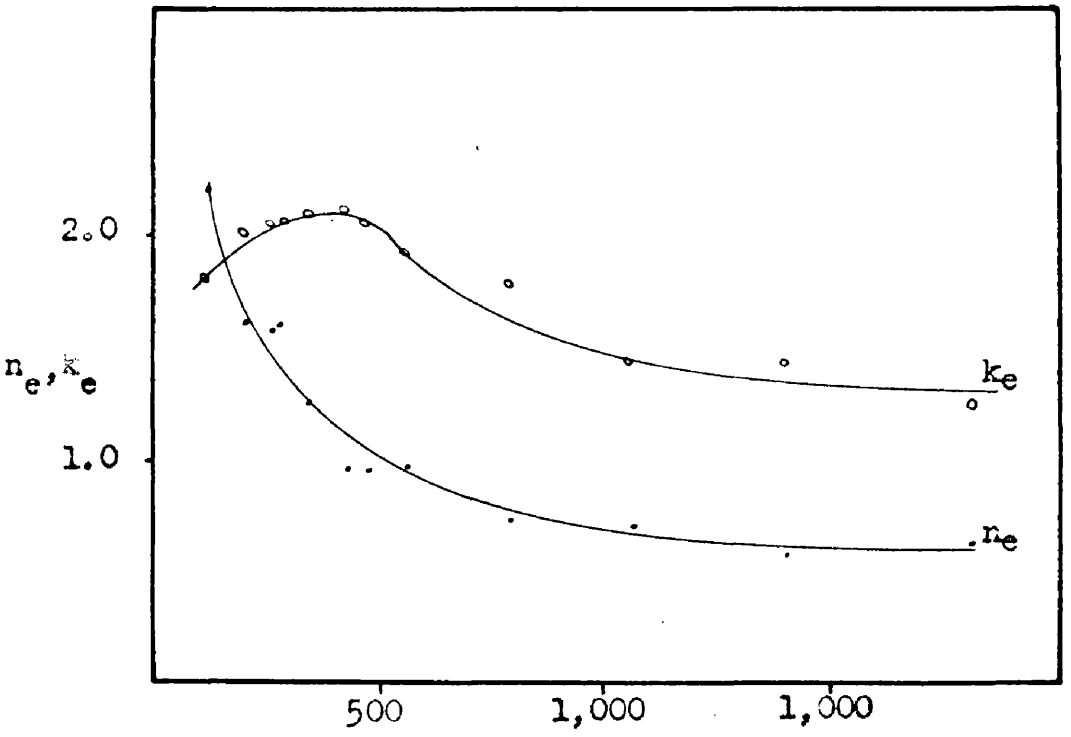

Fig.54. Optical Constants of Evaporated Chromium Films.

calculated for a number of the published values of the bulk refractive index, as well as the bulk value obtained in the previous chapter. Some of the results are given in Table XV. It can be seen that, in all cases, q was a complex number, and for one particular bulk value, q was greater than unity. For two particular values of refractive index the q values were calculated throughout the thickness range. Assuming that the bulk refractive index was 0.62 - i1.25 which was obtained by extrapolating the graph in Fig. 54 to infinite thickness, the value of the imaginary component was approximately constant, but the real component increased with thickness. Using Abeles' results the imaginery component increased with the thickness of the films. Even with the bulk value obtained in the earlier investigation the packing factor was always complex.

From the definition of the packing factor as the ratio of the actual amount of metal in the film to the volume of the film, q must be real and when the nature of the films is considered, q must be less than unity, and probably increases with thickness. Using the optical thicknesses obtained from the refractive index calculation, and the weight thicknesses obtained from the transmission calibration, an experimental value of q, q_e was obtained, Table XVI. It can be seen that the values of this function do not agree with the q values calculated earlier. Using

this packing factor, however, and the experimental refractive index values, no constant refractive index could be obtained. Thus it seems unlikely that the Maxwell-Garnett theory supplies us with a suitable structural model, representing the films we are investigating.

(d) Application of Schopper Theory

Due to the failure of the Maxwell-Garnett form of structural model it became necessary to consider the more sophisticated form due to David[70] and Schopper[71]. The Schopper equation can be expressed, Chapter 7, for a film of material of bulk refractive index, n_b', and effective refractive index, n_e', as

$$\frac{\Delta}{\Delta t}\left\{\left[(n_e')^2 - 1\right]\frac{d_o}{d_w}\right\} = \frac{(n_b')^2 - 1}{\left\{(n_b')^2 - 1\right\} f+1} \qquad (9.1)$$

where f is a function of the shape of the particles, which are generally assumed to be ellipsoids of resolution with the unique axis perpendicular to the substrate. If $n_e' = n_e - ik_e$ and $n_b' = n_b - ik_b$, then it follows that

$$n_e'^2 = (n_e^2 - k_e^2 - 2in_ek_e) \text{ and } n_b'^2 = (n_b^2 - k_b^2 - 2in_bk_b).$$

If we now let $(n_b^2 - k_b^2 - 1) = A$, and $(2n_bk_b) = B$, it

follows from equation (9.1) that

$$\frac{\Delta}{\Delta t}\left\{(n_e^2 - k_e^2 - 1 - 2in_ek_e)\frac{d_o}{d_w}\right\} = \frac{A - iB}{Af - iBf + 1} \qquad (9.2)$$

$$= \frac{(A^2 + B^2)f + (A - iB)}{(Af + 1)^2 + B^2f^2} \qquad (9.3)$$

This function was found considerably easier to handle than the form given in equation (9.1) in the calculation of the change of the optical constants with varying f values. Using the bulk values of chromium, calculated earlier values of Schopper's function were calculated for the range of f from zero to 0.5. The graphs obtained are given in Fig. 55. The results shown do not agree with the experimental functions given in Table XVII and Fig. 56.

From the electron diffraction investigation, Chapter 6, results, it was deduced that the chromium films contained not only the pure metal, but some oxide as well. The system then might be better represented by Schopper's theory if we were to consider the metal particles suspended in a dielectric medium formed by the oxide of the metal. The form of Schopper's theory to use in this case is, from equation (7.23)

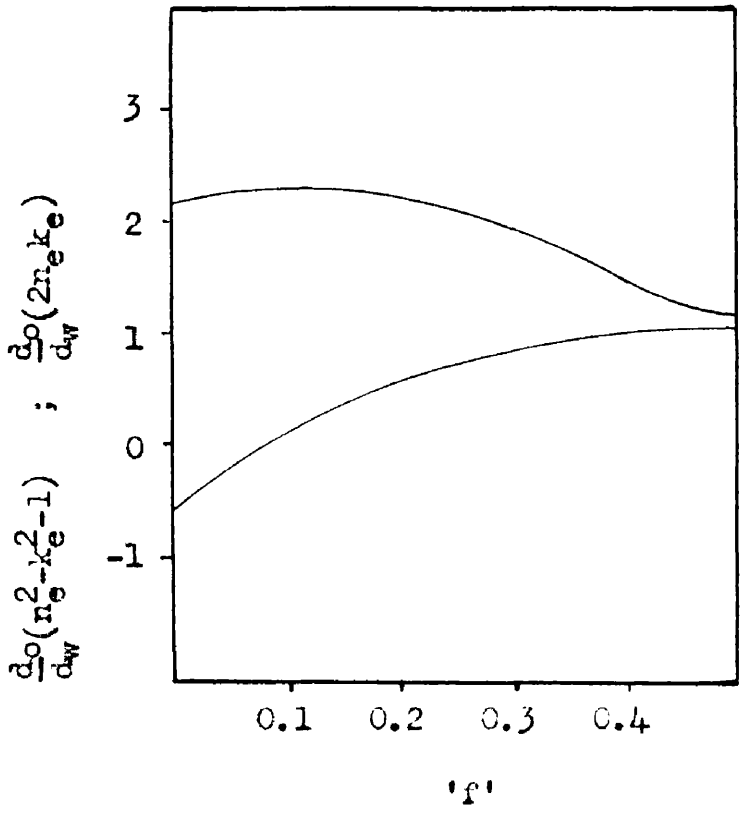

Fig.55. Substitution of the bulk refractive index of Chromium into Schopper's function.

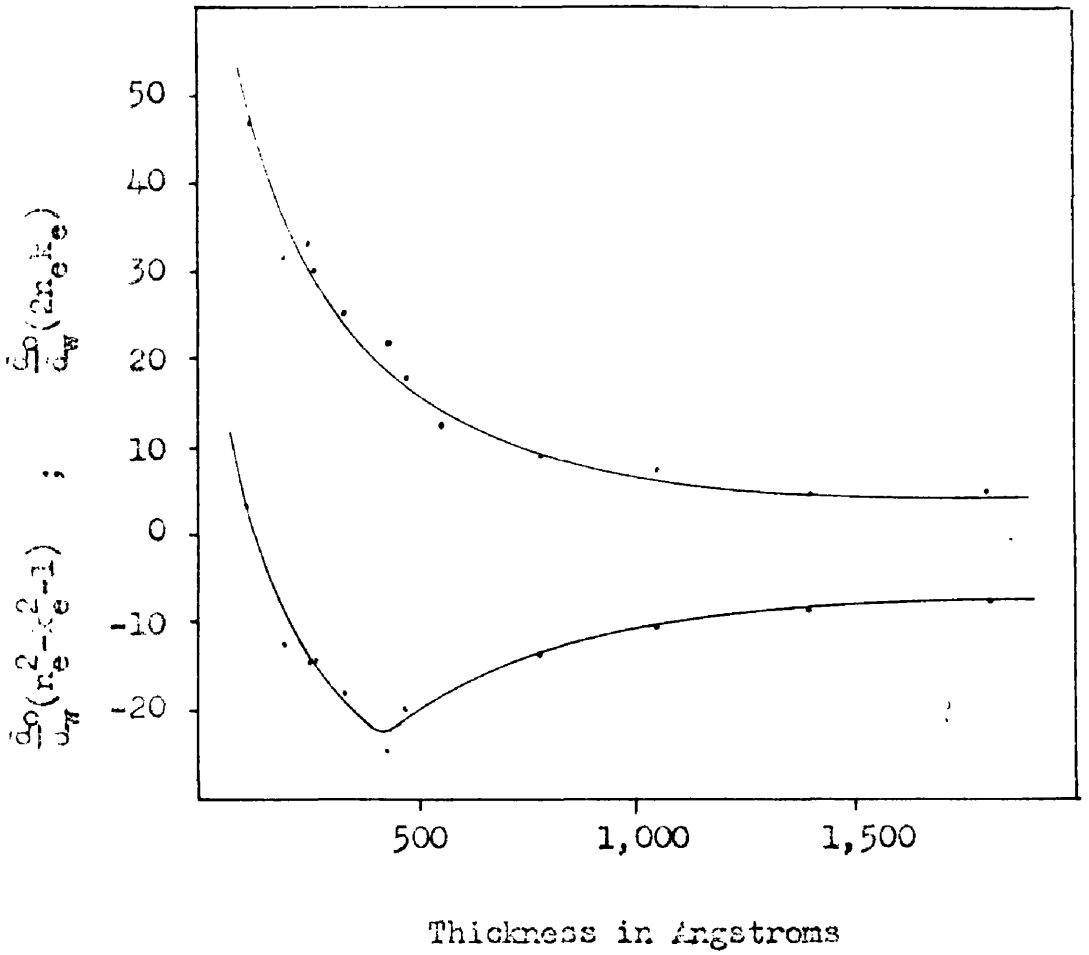

Fig. 36. Experimental values for Schopper's functions.

TABLE XVII

n_e	k_e	d_o in A	d_w in A	q_e	$\frac{d_o}{d_w}(n_e^2 - k_e^2 - 1)$	$\frac{d_o}{d_w}(2n_e k_e)$	n_2A-A'
2.20	1.80	119	20	0.17	+3.07	47.1	0.037
1.60	2.00	200	40	0.20	-12.2	32.0	0.022
1.57	2.05	260	50	0.19	-14.3	33.5	0.098
1.60	2.05	272	50	0.19	-14.4	30.2	0.106
1.25	2.10	340	72	0.21	-18.2	25.8	0.203
0.96	2.12	436	80	0.18	-24.9	22.2	0.123
0.95	2.05	476	100	0.21	-19.9	18.05	0.139
0.97	1.93	561	168	0.36	-12.63	12.6	0.148
0.72	1.77	796	220	0.28	-13.1	9.25	0.157
0.70	1.45	1055	273	0.26	-10.1	7.84	-
0.58	1.45	1400	480	0.34	-8.61	5.24	-
0.64	1.25	1810	537	0.30	-7.5	5.64	-

$$\frac{\Delta}{\Delta t}\left\{\left[(n'_e)^2 - v^2\right]\frac{d_o}{d_w}\right\} = \frac{(n'_b)^2 - v^2}{\left\{\frac{(n'_b)^2 - v^2}{v^2}\right\}f+1} \qquad (19.4)$$

where v is the refractive index of the oxide. If we now let $A = n_b^2 - k_b^2 - v^2$, and $B = 2n_bk_b$, we obtain the form

$$= \frac{v^2\left\{(A^2 + B^2)f + v^2(A - iB)\right\}}{(Af + v^2)^2 + B^2f^2} \qquad (9.5)$$

In this form, in order to obtain a peak in the imaginary curve it is necessary for A to be extremely large and negative. For the values of A and B obtained from the experimental refractive index values no peaks in either curve were obtained.

Films of chromium, however, unlike those of gold, used by Schopper have been said to be inhomogeneous[75]. The degree of inhomogeneity of the films investigated here was measured by the Wolter relationship. The discrepancies obtained are listed in Table XVII. The values tended towards a maximum for the thicker films and to zero as the thickness decreased. This is what would be expected from a range of inhomogeneous films. For the thinnest values there will be no absorption, so n_2A will be equal to A', and for the thicker films the reflection factors are constant

so the absorptions will tend towards the constant maximum values giving a constant difference.

Table XVII shows conclusively that the films are inhomogeneous and very different from those considered by Schopper. If the basis of the inhomogeneity is due to a widely changing particle shape, that is, the f function differs for each layer that is deposited, and varies regularly from layer to layer through the film, we would be wrong in applying a statistical distribution to the value of f. A more consistent, though not perhaps perfect, distribution function would be to consider the distribution as so small that it could be neglected. This would certainly aid us in attempting to obtain peaked curves, for the presence of a distribution of any sort tends to act as a summation factor and smooth out rapidly changing values.

(e) Calculation of Effective Refractive Index

If this is the case, then as chromium forms extremely small particles[51], we would expect scattering from the particle surfaces[91] and we could hardly expect the Schopper theory to hold for the thinner films. In an attempt to obtain the effective bulk refractive index of the particles curves were constructed of the functions

$$\frac{(A^2 + B^2)\, f + A}{(Af + 1)^2 + B^2 f^2} \quad ; \quad - \frac{iB}{(Af + 1)^2 + B^2 f^2}$$

for the range of f, and a range of values of A and B in such a way that the curves would fit both sets of experimental points at the same time. In order to reproduce the peaked effect of the experimental curves, Table XVII, it was found to be necessary that A should be negative and B numerically much smaller than A. No curves were obtained that fitted all the experimental points but emphasis was placed more directly on the fit of the lower thickness values as these correspond more directly to the theoretical assumption of a number of individual particles. The best fit was obtained, Fig. 57, for the values

$$A = -9.0 \quad ; \quad B = 2.0$$

This fit was obtained without the aid of a distribution function. If statistical distribution of any width is considered then it becomes impossible to reproduce the peaks in the curves, without A and B respectively increasing and decreasing out of all proportion. These values for A and B gave for the effective refractive index of the bulk metal of the ellipsoid particles

$$n' = 0.36 - i2.80$$

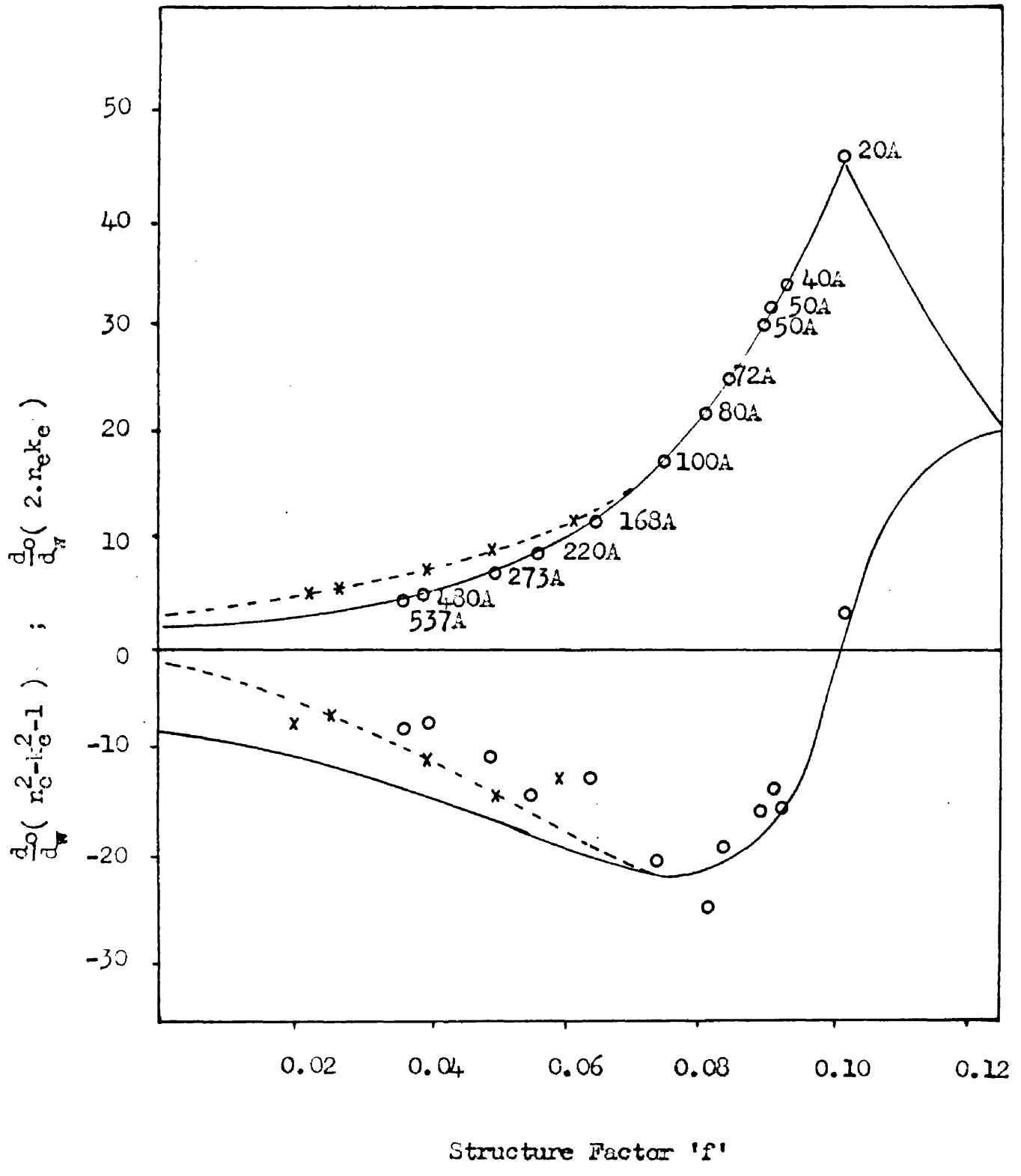

Fig.57. The best fit of the experimental points to Schopper's type of theoretical curves.

a result that is in complete diagreement with any of the previously determined values of the refractive index of chromium.

We had, however, already obtained for this particular film from the calculation of the refractive index by Male's method

$$n''' = 0.64 - i1.15$$

and for the same film from the polarimetric investigation

$$n'' = 1.18 - i0.944$$

It would appear, then, that we have obtained for one film of chromium, by three distinctly different methods of measurement, three completely different values of refractive index. If we assume that each of them is correct within the limitations imposed by the methods of measurement then it should be possible to correlate the three values.

As Male's method uses the reflection coefficients from both surfaces of the film as well as the transmission coefficient through the film, it could possibly represent a mean value of the refractive index of the film if the refractive index changed with the thickness of the film. The polarimetric technique, on the other hand, is mainly dependent on the properties of the layer that is finally

deposited, whereas the effective refractive index of the material composing the reflecting surface on the substrate side is given by the result of fitting Schopper's curves to the experimental values for the thinner films. If we consider that the film can be represented by a structure consisting of two distinct homogeneous layers, one the reflecting surface on the substrate side, and the other the reflecting surface on the air side, and that the relative thickness of the former is s, then it follows that the relationship

$$n''' = s.n' + (1 - s)n'' \qquad (9.6)$$

should hold where n', n'' and n''' are the refractive index values given above. The fraction s must be real and less than unity. If the fraction is real then equating the real parts of equation (9.6) should give the same value for s as equating the imaginary parts. Perfect agreement would not be expected as the simplifying assumptions made in obtaining equation (9.6) are probably not fully justifiable. Upon substituting into the equation for n', n'' and n''', equating the real parts gave for s, 0.659, and the imaginary, 0.154. This disagreement is too great to be considered as only caused by the simplifying assumptions.

Examination of n', n'' and n''' shows that the result most likely to be in error is that obtained from

fitting the curve to the experimental points by Schopper's theory. The polarimetric results have been shown, Chapter 8(d), to be similar to values obtained for the bulk refractive index of chromium and the result obtained from the reflectivity measurements is supported by the continuity of the graph of the change in refractive indices with thickness, Fig. 54.

We considered that the inhomogeneities of the chromium films were only due to the absence of a distribution factor, and indeed have found that the presence of a distribution factor is incompatible with the peaked experimental curves of the changes in Schopper's functions with thickness. However, there is another difference between the properties of the films studied by Schopper and those we are considering. Gold is a very passive metal, while chromium oxidises readily forming a very thin tough protective coating. Evidence of the presence of the oxide in very thin layers of chromium was found by electron diffraction in Chapter 6(b), and during the polarimetric investigation of this particular film we are considering. If the chromium metal particles oxidise as they are formed, and even under vacuum this has been shown to be quite possible, then the assumption of a number of ellipsoidal particles lying in air is in error and cannot be used to describe the system we are investigating.

(f) Extension of David and Schopper's Theory

A more accurate representation of the state of the chromium films would be given, then, by considering a number of metal particles, ellipsoidal in shape, of dielectric constant, ε_i, surrounded by a very thin layer of oxide of dielectric constant, ε_o, in a dielectric medium, ε_a. Then following David and Schopper the potential equations for these three media when the particles are placed in unit electric field in the x-direction are

$$\begin{aligned} \phi_i &= -x + Cx\left\{\frac{\pi}{2} - \tan^{-1}\mu_o - \mu_o/(1+\mu_o^2)\right\} \\ \phi_o &= -x + Cx\left\{\frac{\pi}{2} - \tan^{-1}\mu_o - \mu_o/(1+\mu_o^2)\right\} \\ \phi_a &= -x + Cx\left\{\frac{\pi}{2} - \tan^{-1}\mu - \mu/(1+\mu^2)\right\} \end{aligned} \qquad (9.7)$$

Here we are assuming that the surface layer is so thin that μ, which defines the surface of our ellipsoid, is constant throughout and equal to the value defining the boundary of the metallic particle. At each of the two boundaries the displacement will be equal, and if the layer is very thin the displacement will be continuous through the oxide layer, i.e.

$$\varepsilon_i \frac{\partial \phi_i}{\partial \mu} = \varepsilon_o \frac{\partial \phi_o}{\partial \mu} = \varepsilon_a \frac{\partial \phi_a}{\partial \mu} \qquad (9.8)$$

and thus

$$2\varepsilon_i \frac{\partial \phi_i}{\partial \mu} = \varepsilon_o \frac{\partial \phi_o}{\partial \mu} + \varepsilon_a \frac{\partial \phi_a}{\partial \mu} \qquad (9.9)$$

If we substitute for the appropriate values of ϕ and differentiate, we obtain

$$(2\varepsilon_i - \varepsilon_o - \varepsilon_a)\left\{ - \frac{x\,\mu_o}{1+\mu_o^2} + C\,\frac{x\,\mu_o}{1+\mu_o^2}\left(\frac{\pi}{2} - \tan^{-1}\mu_o - \frac{\mu_o}{1+\mu_o^2}\right)\right\}$$

$$= \varepsilon_a\, Cx\left\{ - \frac{1}{1+\mu_o^2} - \frac{1-\mu_o^2}{(1+\mu_o^2)^2}\right\} \qquad (9.10)$$

Thus

$$C = \frac{(2\varepsilon_i - \varepsilon_o - \varepsilon_a)}{(2\varepsilon_i - \varepsilon_o - \varepsilon_a)f + \varepsilon_a} \cdot \frac{\mu_o(1+\mu_o^2)}{2} \qquad (9.11)$$

where $f = \frac{1}{2}\mu_o(1+\mu_o^2)\left\{\frac{\pi}{2} - \tan^{-1}\mu_o - \mu_o/(1+\mu_o^2)\right\}$

For large values of x the equation (7.14) still holds and thus

$$\frac{\Delta}{\Delta t}\left\{(\varepsilon_i - \varepsilon_a)\frac{d_o}{d_w}\right\} = \frac{(2\varepsilon_i - \varepsilon_o - \varepsilon_a)}{\left\{(2\varepsilon_i - \varepsilon_o - \varepsilon_a)/\varepsilon_a\right\} f + 1} \qquad (9.12)$$

If we consider that this equation applies to a system consisting of a metal of refractive index (n-ik), surrounded

by a very thin oxide layer of refractive index, v, and that the system is lying in air, then the equation becomes

$$\frac{\Delta}{\Delta t}\left\{\left[(n_e - ik_e)^2 - 1\right]\frac{d_o}{d_w}\right\} = \frac{2(n-ik)^2 - v^2 - 1}{\left\{2(n-ik)^2 - v^2 - 1\right\}f + 1} \qquad (9.13)$$

where as before $(n_e - ik_e)$ is the value for the effective refractive index of the film and d_w/d_o the packing fraction. If we now let

$$A' = 2(n^2 - k^2) - v^2 - 1 \qquad (9.14)$$

and $$B' = 4nk$$

then it follows that

$$\frac{\Delta}{\Delta t}\left\{\left[(n_e^2 - k_e^2 - 1) - 2in_e k_e\right]\frac{d_o}{d_w}\right\} = \frac{A' - iB'}{A'f + 1 - iB'f}$$

$$= \frac{(A'^2 + B'^2)f + (A' - iB')}{(A'f + 1)^2 + B'^2 f^2} \qquad (9.15)$$

which is the same form as equation (9.3).

We now have to substitute into the values for A' and B' to get n and k, where as before the best fit is given by $A' - iB' = -9.0 - i2.0$.

The refractive index of the oxide, v, formed on the evaporated films has been already measured as 2.230, giving, after substitution into equation (9.14)

$$n' = 0.49 - i1.32$$

If it is assumed that this represents the true refractive index of the first layers of the film, and that the structure of the film could again be represented, to a first approximation, as composed of two layers only, with the upper layer having as before the refractive index

$$n'' = 1.18 - i0.944$$

then we can recalculate the relative thickness factor, s. This was carried out and by equating the real parts a value of s was obtained of 0.308, and from the imaginary, 0.295. These figures are in remarkable agreement and show that the refractive index, as obtained by Male's method appears to be an accurate average of the refractive indices of the first and last layers of the film.

(g) Discussion

The modified ellipsoidal structure model that we have used appears to be true for film thicknesses less than 100Å. For any type of homogeneous film of this order of

thickness the Wolter relationship should hold accurately and the change in the relationship for the film is indicative that the growth process is taking place in layers and that the f value varies from layer to layer. The changes in f value do not appear to be continuous above 100A and it has already been shown, in Chapter 8, that the refractive index of the surface of the thicker films do not differ greatly from that of the bulk material. This is in agreement with the existing evidence on film growth.

The transition at approximately 100A from an aggregated structure to a continuous metal film would explain the success of our approximation regarding a thicker film as being composed of two layers only. For transmission properties this would certainly hold as the properties of the underlayer would be determined mainly by the layer of larger aggregates, and very little by the much thinner layer of smaller aggregates.

The value ultimately obtained for the refractive index of the bulk material comprising the small particles certainly shows little agreement with the earlier results for the bulk metal. It has been suggested that this is primarily due to electron scattering at the surface of the ellipsoidal particles. It could, however, be caused by the metallic particles existing within each aggregate in

a more open structure than in the bulk metal. This would account for the decreased values of the real part of the refractive index and for the increased absorption coefficient, by having a higher initial resistivity[92]. It can be seen from Fig. 54 that the absorption of the films increase up to a thickness value of about 400A which corresponds, Table XVII, to a weight thickness of 100A. This is in accordance with previous results[83] and for thickness greater than this value the absorption decreases as one would expect.

The theoretical treatment is still imperfect though such good agreement has been obtained for this thin range. At the limiting value of $f = 0$, Schopper's theory gave bulk metal values for aggregates which can be considered as extending infinitely in the plane of the film; our theory, however, does not give the bulk metal optical constants for $f = 0$, or even the bulk constants obtained by any of the other investigators. This is caused by the presence of the thin oxide layer around each particle, and it is doubtful if even for the thickest of our films the conductivity reached the value of that of the bulk metal.

The results suggest that chromium films are highly aggregated only up to a limiting thickness of 100A, and that subsequent layers are continuous and denser, approximating

to the bulk metal structure. The theoretical curve, Fig. 57, has been modified by drawing a continuous curve between the results we obtained for the thinner films to the point on the axis corresponding to the measured value of the real part of the refractive index of the metal. Upon the fitting of our experimental points to this new curve it was found that each point was displaced towards the bulk value, as the averaging would lead us to anticipate. The corresponding imaginary points now fell upon a new continuous curve joining the results for the thinner films to the intercepts on the vertical axis which corresponded with the imaginary part of the refractive index of bulk chromium when substituted into equation (9.15).

CHAPTER 10

REFLECTIVITY MEASUREMENTS

(a) Introduction

For industrial uses as a reflecting film the high reflectivity of silver in the visible spectrum has made this metal particularly suitable. However, where resistivity to atmospheric corrosion is a necessity, aluminium is to be preferred, for during the initial stages of ageing the reflecting surface grows a very thin, transparent oxide coating, Chapter 3(f), which is of a protective nature. Silver tends to tarnish readily forming black compounds and the reflectivity steadily deteriorates with time. It is for these reasons that we have concentrated mainly on the use of aluminium as the reflecting film material.

In order for an adhesion promoting film to be considered as suitable it is necessary that, as well as increasing the adhesion of the film to the condensing plate, the presence of the film as an underlayer should not affect the reflecting properties of the surface film. For the majority of the systems investigated the underlayer had little effect upon the reflecting power of the surface. In one or two cases, after the films had been ovened, some

drop in reflectivity was noted that did not appear when the same type of film had been aged at the lower temperature. This was taken as indicative that if the films had been kept at room temperature for an indefinitely long period there might have been a slight deterioration in the reflective properties.

(b) Experimental

The reflectivities of a number of reflecting films prepared with and without substrate layers were measured during the normal ageing periods on the two reflectometers described in Chapter 7(e). In the bench reflectometer, white light sources were used in conjunction with Ilford Mercury Green filters to give a limited pass-band. The specimens were prepared under the same conditions as before, but the rotating slide holder was removed from the vacuum chamber and the glass blanks were mounted on the lower shield in such a way that both films could be deposited over practically the whole area of the slide. Two specimens were prepared at each evaporation and these were always mounted together in the photometer bench instrument. This aided the calculation of the reflection coefficients, Chapter 7(e), and made the results more representative as a larger effective specimen area was being used than if some standard surface was used

as one of the reflecting plates, as the reflectivity of the standard would also have to be measured.

(c) Results

(i) Pure Metal Films. The changes in reflectivity obtained for the pure metal films are given in graphical form in Fig. 58. The tarnishing action upon the silver surface can be easily seen from the larger decrease obtained for this metal as compared with aluminium. Copper oxidises more readily than either of the other two metals, but the oxide formed at room temperature appears to be fairly thin and does not affect the reflectivity as much as when the films were ovened. Ovening at 120°C. caused a relatively thick film of oxide to form on the copper surface, which by interference gave a bright blue reflection. This indicates that the film was about 500Å thick[93]. The reflectivity of this specimen in the green region was, of course, zero. The higher temperature ageing curves for both the other metal samples are given in Fig. 60, and show a decrease in the final value of reflectivity with increasing temperature. The results are collected together in Table XVIII as the percentage decrease in reflectivity over the ageing period.

For each of these three films the reflectivity

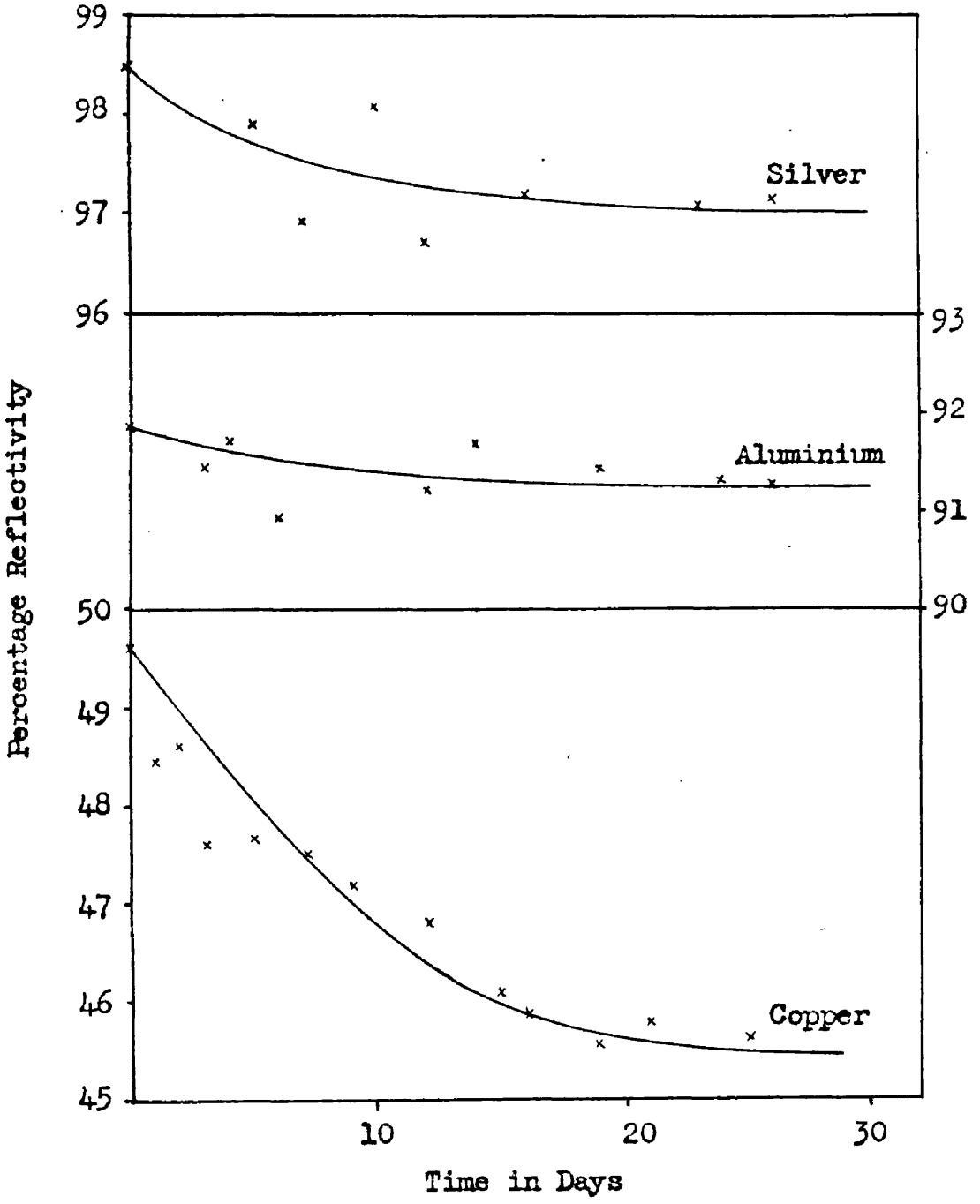

Fig.58. Ageing of Evaporated Metal Films at Room Temperature

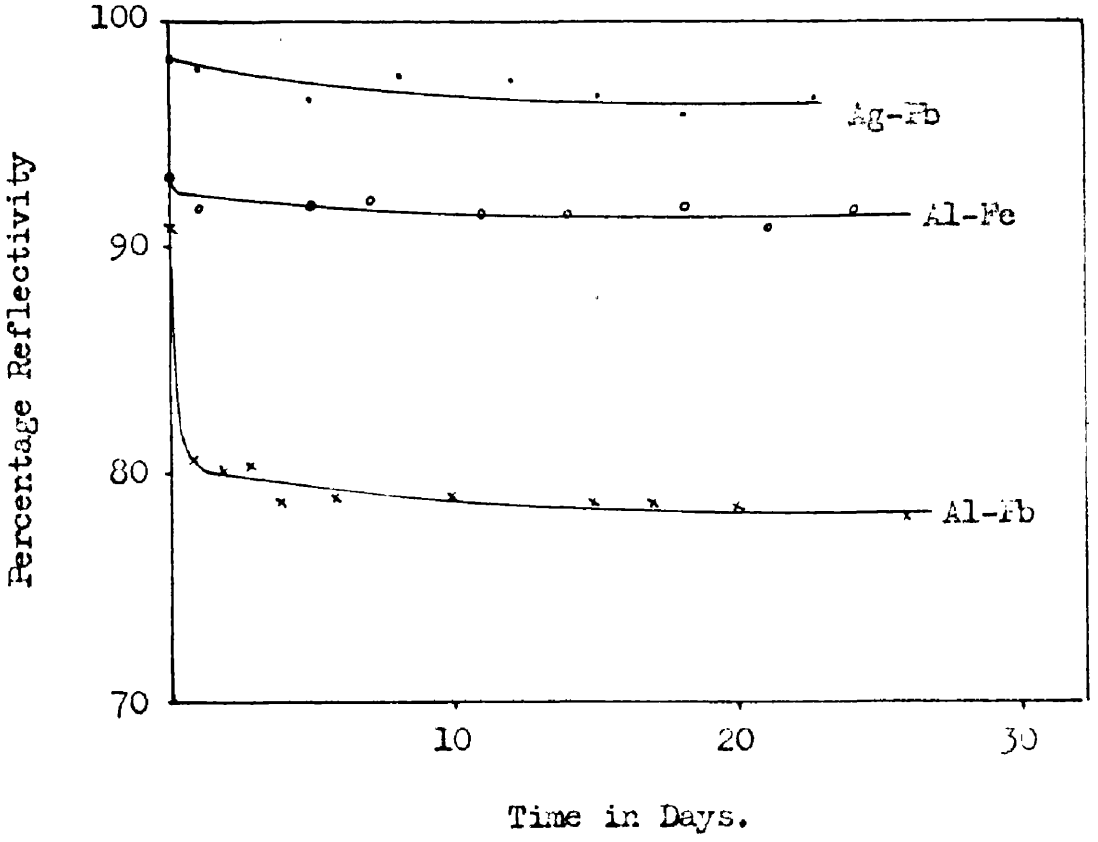

Fig.59. Ageing of Compound Films at Room Temperature.

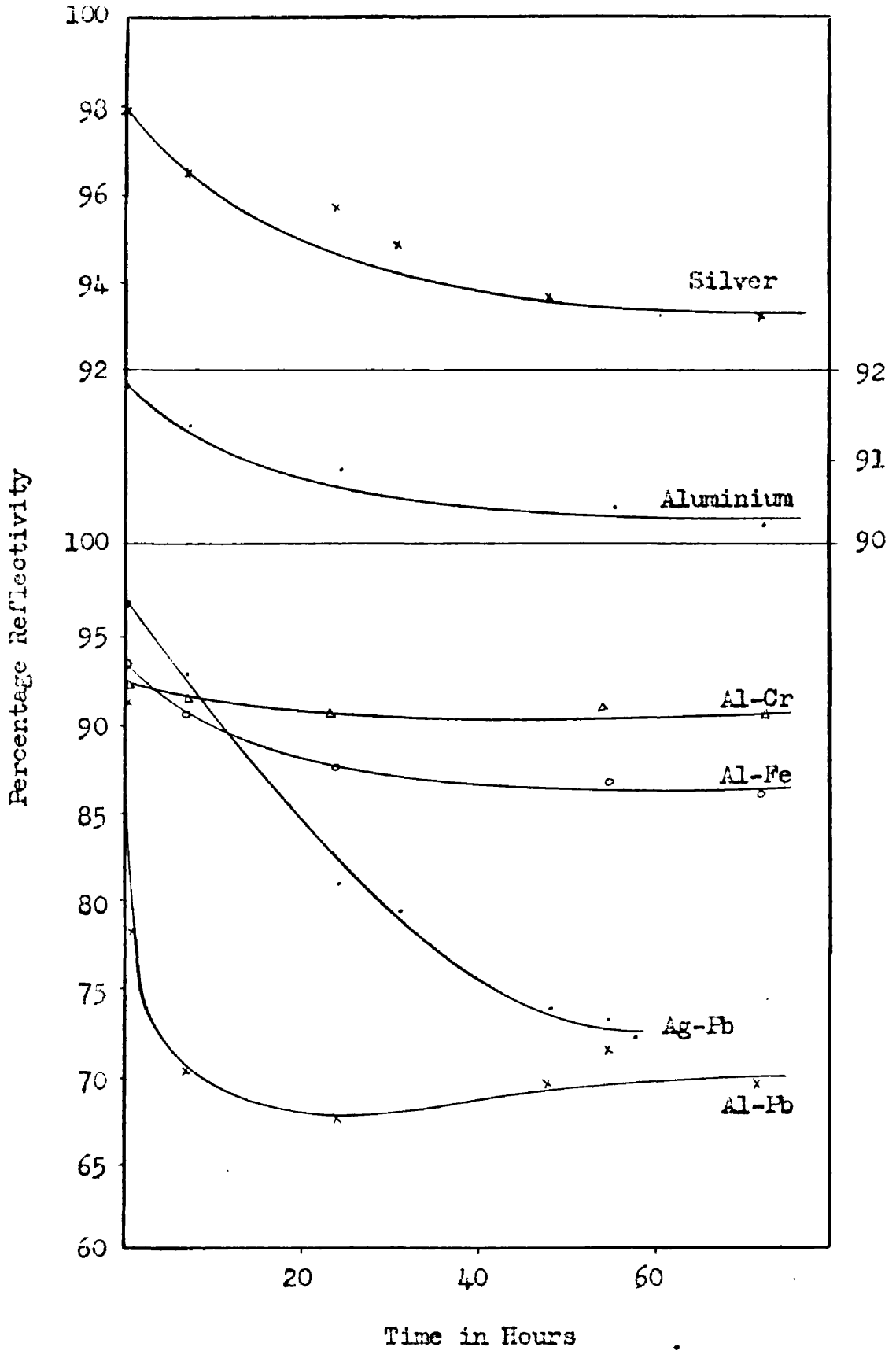

Fig.60. Ageing of Single and Compound Metal Films at 120°C

coefficient was measured over the visual spectral region, 4,000A - 7,000A. As Fig. 61 shows, aluminium and silver gave almost constant values, but the copper film was much more efficient as a reflector in the red region than in the blue. Very slight changes were obtained with ageing and the curves are representative of the reflectivity of the specimens after ageing at room temperature for three days.

(ii) Compound Metal Films. For most of the metal systems an underlayer made very little difference to the reflectivity of the upper film. The only major exception to this was lead films when used as underlayers to silver and aluminium. The results of the low temperature ageing are given in Fig. 59, and of ageing at 120°C. in Fig. 60. The higher temperature ageing appears to affect the aluminium film evaporated onto an iron substrate layer but no deviation was experienced when a similar film was aged at 20°C. The aluminium-chromium specimen is included in Fig. 60 for comparison between the other graphs given there and a film that showed the normal ageing changes.

As for the single metal films, the percentage decrease in reflectivity on ageing for each of the metal pairs investigated is given in Table XVIII. The accuracy within which measurements could be made was of the order of a half of one per cent., and within this error the

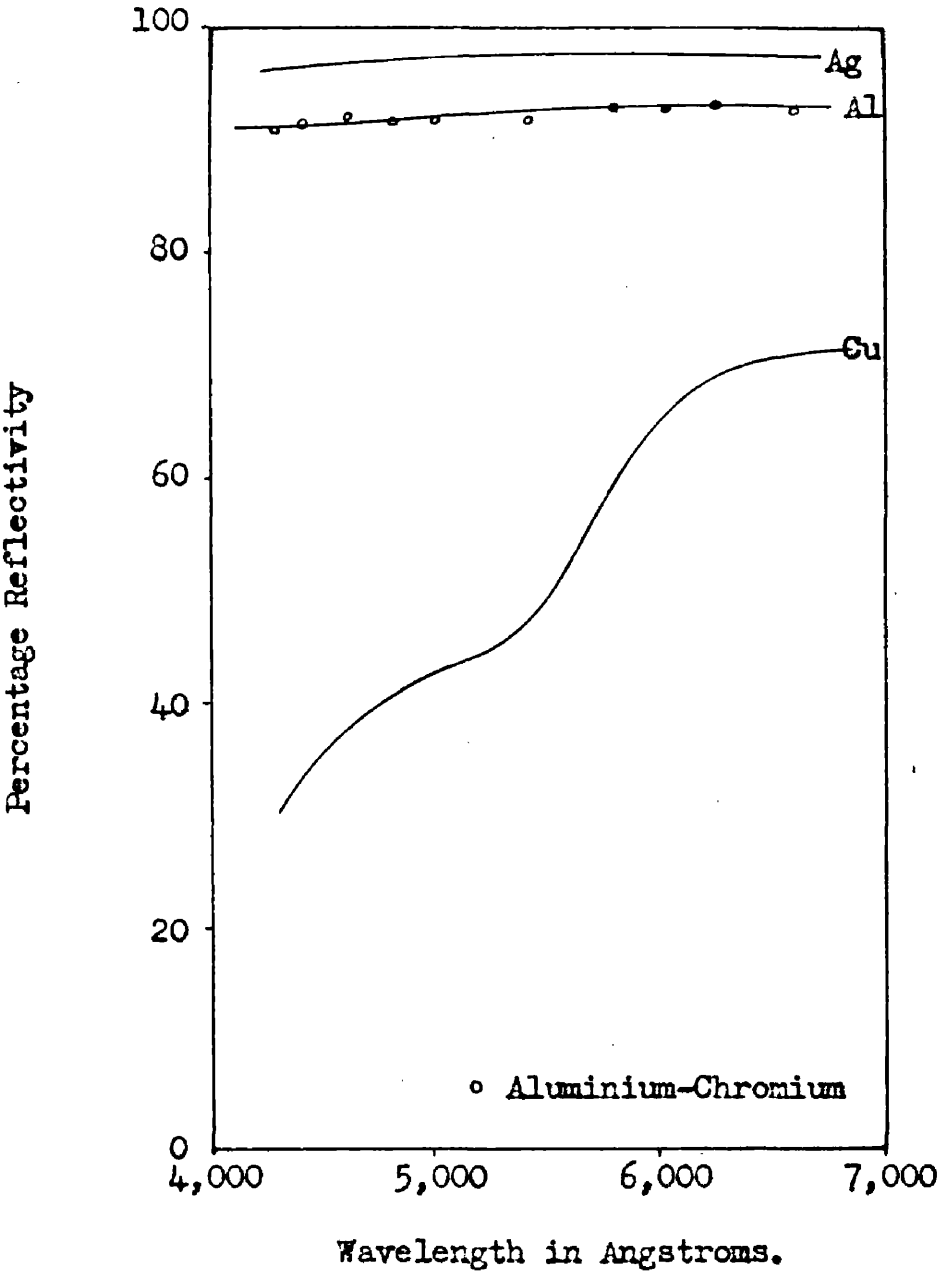

Fig. 61. Reflectivity in the Visible Spectrum of Evaporated Metal Films.

TABLE XVIII

CHANGES IN REFLECTIVITIES OF SPECIMENS AFTER AGEING

MERCURY GREEN LIGHT

Metal	Substrate	Change in Reflectivity in per cent. after ageing.	
		3 weeks at 20°C.	3 days at 120°C.
Aluminium	-	-0.5	-1.5
Silver	-	-1.5	-4.5
Copper	-	-4.0	-
Aluminium	Lead	-12.0	-33.0
Silver	Lead	-2.4	-25.0
Aluminium	Chromium	-1.4	-1.3
Silver	Chromium	-0.9	-3.8
Copper	Chromium	-3.6	-
Aluminium	Manganese	0	-0.7
Aluminium	Iron	-1.2	-7.3
Aluminium	Nickel	-0.3	-0.6
Aluminium	Cobalt	-1.7	-0.6

results for the majority of the systems are fairly consistent. From the results, lead would appear to be the most readily diffusable substrate material as it diffused through the aluminium layer almost immediately after evaporation. For both the specimens the drop in reflectivity given in Table XVIII has been calculated by assuming that the initial reflectivity of the aluminium surface was the same as that of the bulk metal, for even when measured within five minutes of evaporation the reflectivity had fallen to almost eightyper cent.

(d) Discussion on Results

Considering the suitability of the substrate materials used in this investigation from a purely reflective point of view we must reject outright the use of lead as a substrate material. All the reflecting films for which it was used to form a substrate layer showed large decreases in reflectivity, due to the migration of lead through to the reflecting surface. For a similar reason iron would have to be regarded with caution, for although no loss in reflectivity was obtained for the low temperature hardened film the ovened film showed a definite decrease in reflectivity.

All the other substrate materials appeared to

be quite suitable from the evidence obtained here. The decreases in reflectivity obtained for these substrated films, and for the pure metal films, is in agreement with the results of Kuhn and Wilson[94] on reflecting films of aluminium and silver, and is almost certainly due to the formation of surface oxide or tarnish layers. The form of the reflectivity ageing curves for these metals and copper closely resemble the oxidation curves obtained earlier. The apparent penetration of the diffusing substrate atoms is in agreement with the results obtained using Michel's method in Chapter 6, and with Barrer's[95] statement that the rate of diffusion is greater the lower the melting point of the solute.

CHAPTER 11

GENERAL CONCLUSIONS ON THE USE OF A SUBSTRATE FILM

From the results of the adhesion investigation it can be seen that one would be unwise to state sweeping general conclusions that could be applied to any particular pair of metals. It is obvious, however, that the nature of the substrate film is of primary importance and for high durability it requires to show not only good adhesion to the condensing plate but to possess a fair hardness. Chromium and manganese appear to be, from the metals examined, the most suitable materials. The transition metals, as a group, were used as substrate materials as they possessed larger cohesional energies than most of the other metals[96]. Lead was chosen from outside the group, not only because it gave the simpler phase diagrams but because the cohesional energy was about half of that of the other metals.

Although an increase in the hardness of the transition layer can be associated with the presence of intermetallic compounds it appears that if the composition range of the compound is very wide, or if it possesses a

large free energy, then the ageing process is one of decreasing hardness. This, it was suggested, was due to the precipitation of the alloy phase, and the subsequent release of strain. However, where the concentration range of the compound is small, or where no preferential compound is formed, the stresses set up by the solid solution cannot reach the critical value for precipitation. An excellent example of this type of reaction was seen in the system aluminium-nickel, where ageing at 120°C. allowed precipitation to be nucleated and the hardness of the transition region fell. However, when a similar film was aged at room temperature nucleation could not take place and high adhesion values were recorded for the specimen.

The high initial adhesions, however, are more difficult to describe. Heavens' suggestion of oriented overgrowths may well be true for some of the systems but just as good values were obtained for systems in which overgrowth of this type would not be expected. In particular, manganese possesses a highly irregular structure in any of its three forms[97] and yet acted as a very suitable substrate material for aluminium. If, however, the initial adhesion was caused by an action similar to that giving the ageing effects then the adhesion values become more realistic when compared with the increases

and decreases in adhesion obtained after ageing. In order to obtain such adhesion values there would need to be a fair penetration of the condensing atoms of the reflecting film into the substrate film. The energy for this process would need to come from the kinetic or thermal energies of the condensing atoms. On an amorphous substrate the condensing atoms would have a mobility which would cause them to form three-dimensional aggregates, and the films would grow in a similar manner to the chromium films. If, however, the condensing surface is not smooth, but covered with hills and dales, formed by actual surface irregularities due to aggregates, the physical movement of the condensing atoms will be limited and the energy will pass to the substrate material. This will cause local heating and assist the interpenetration of the reflecting film material into the substrate layer.

The most suitable substrate film for this form of growth would be one in which the growth process formed a large number of very small aggregates. This system, however, would also require for thicker substrates, which cause a further increase in adhesion, an even more finely divided surface. From the theories of growth of thin films[83], this would appear to be an impossibility. But if the increased adhesion using thicker films was due to diffusion into the body of larger aggregates within the films, and not to diffusion through the grain boundaries,

a larger particle size in the thicker films would be required. The increased size of aggregates would give an enhanced area of contact between metal and substrate film which would cause the further increase in adhesion.

Excellent increases in adhesion were obtained using a nickel-chromium alloy as the substrate material. Dushman's theory[9] of the evaporation of alloys showed that the chromium should evaporate off perferentially, but Banning[98] has obtained films, evaporated at 10^{-4} mm. of mercury, in which the nickel was detectable. The adhesion values for the specimens that were prepared distinctly showed that the substrate material was not pure chromium.

The work presented in this thesis is, as far as the author can determine, the first attempt to obtain the structure of optically inhomogeneous films from optical measurements. It is certainly the first using purely reflective and transmissive coefficients. The results obtained are quite consistent with previous experimental work, both on chromium films, and films of other materials. It has been recognised, for a number of years, that evaporated films tended to grow in an aggregated structure, and from electron microscopic investigations it was known that in the plane of condensation the particles showed no apparent preferential growth direction[38]. For a number

of years the Maxwell-Garnett theory has been applied to this type of film with some, but not complete, success[99]. The new theories, based on the assumption that the aggregates form ellipsoidal particles, appear promising. The degree of emphasis that can be placed on the calculation of the relative thickness fraction 's' is difficult to assess, but the close fit between the experimental points and the theoretical curve obtained is interesting in view of the deviation of refractive index from bulk metal values. It would suggest that the aggregates themselves have a loose, more open structure when the thickness of the film is below 100A. The electron scattering within such a structure would affect not only the optical properties but the electrical properties of the films. Using electron diffraction methods, Lafourcade[51] has estimated that the size of the particles in a film of this thickness were of the order of 15A - 20A.

It was considered that the non-homogeneity in the films might be due to the presence of the oxide coating around the metal particles, but this was finally decided not to be so. For if we were to consider two elemental volumes in a film some distance apart along a normal to the condensing plane, then from the theory of the method the value of 'f', the structure factor, will be different in the two volumes. The function 'f', however, not only

describes the size of the particles but their shape, and as the oxide coatings are assumed to be uniformly thin the oxide coatings around the particles within each of the elemental volumes will only differ in as much as 'f' changes. Thus 'f', as well as defining the ellipsoidal surfaces, describes the oxide coating. The only true variable then, between the two elements, is the structure factor 'f'.

In presenting the theory some wide approximations have been made, but it is felt that a more penetrating analysis would give similar results.

The limited diffusion of the substrate materials, as suggested by Michel, is shown by the results of the reflectivity investigation. Of the substrate materials used lead is certainly the most mobile in either aluminium or silver. The slight deterioration in the reflectivities of the single metal films, and the compound films in which the depth of penetration at the interface was limited, is undoubtedly due to the formation of the surface oxide layers similar to those detected on chromium by the optical investigations using the polarising spectroscope. The close agreement between the values obtained using that instrument for the evaporated metal sample and the bulk samples is quite unusual and must be due to the strong cohesive energy of the metal in resisting the formation

of a polish, or Beilby, layer at the surface. The constants obtained, do nevertheless, show some agreement with those determined by Abeles who also used an evaporated metal specimen.

CHAPTER 12

FUTURE WORK

It is considered that certain lines of investigation arising out of this work could be tackled and might lead to interesting results.

(1) Adhesion and Hardness of Thin Films

The nature of the adhesion of a single metal film to a glass or ionic condensing plate is already being investigated[100]. It would be of interest, however, to obtain results for the adhesion of reflecting films, such as these used here when substrated with metallic layers not showing such strong cohesional energy values as the transition series of metals, nor the much poorer value of lead. Metals showing a poor adhesion could not be expected to increase the adhesion of the reflecting film by a large amount, but it should be possible to obtain results for a film which had a poor adhesion to the substrate, but a good cohesional energy. Similarly magnesium would be worth investigating as it possesses a heat of sublimation less than that of lead[96], but is readily oxidisable, a quality that appears to be necessary for good adhesion.

(2) Investigation of Transition Structure

Perhaps the most fruitful method of investigating both the transition structure in the initial deposit and during ageing would be by preparing the specimens directly in a reflection electron diffraction camera. The complete range of substrate layer thicknesses could be used with a very thin deposit of the reflecting film material. This type of apparatus has already been used[61] to investigate the change in the structure of films of alloy materials as temperature changes were imposed on the specimens.

(3) Optical Inhomogeneity

If the results obtained in Chapter 10 are consistent with the normal growth process in thin films then the changes observed with thickness should be obtainable for other materials. Metals that follow the same type of growth process as chromium are, according to Levinstein[36], iron, nickel, cobalt, manganese, titanium, beryllium, lead, tin, palladium and platinum. However, nickel, beryllium and platinum are considered as not being readily oxidisable, and no information can be obtained on the oxidising properties of palladium and tin at room temperatures[45]. Iron, cobalt and manganese are readily evaporated and could be investigated without much difficulty.

No comprehensive investigation appears to have been undertaken on any of these metals which could indicate that they have been regarded as optically inhomogeneous and thus suitable for an examination using the method carried out on chromium.

Lead, however, might be the best metal to choose, for the lead films are generally regarded as highly aggregated, and the degree of aggregation can be increased with thickness. In this way, large enough aggregates could be formed, with an oxide layer on the surface, to have bulk conductivity inside the particles. Alternatively, with a suitably heated condensing plate it might be possible to grow larger aggregates of chromium, possessing a structure more akin to the bulk metal than we obtained by condensing onto a plate at room temperature.

REFERENCES

1.	O.S. HEAVENS.	J. Physique Rad. 11. 1950. p.355.
2.	L.E. COLLINS.	Ph.D. Thesis, Univ. of Reading. 1954.
3.	O.S. HEAVENS & L.E. COLLINS.	J. Physique Rad. 13. 1952. p.658.
4.	M.G. TOWNSLEY.	Rev. Sci. Inst. 16. 1945. p.143.
5.	S. BATESON.	Vacuum. 2. 1952. 375.
6.	R. BEECHING.	Phil. Mag. 22. 1936. p.938.
7.	S. TOLANSKY.	'An Introduction to Interferometry', Longmans, London, 1955. p.154.
8.	S. BATESON.	Vacuum. 2. 1952. p.365.
9.	S. DUSHMAN.	'Scientific Foundations of Vacuum Technique.' 1st Ed. John Wiley & Sons, Inc., New York. 1949.
10.	A.H. COTTRELL.	'Theoretical Structural Metallurgy.' 2nd Ed. Arnold, London, 1955. p.147.
11.	T. ISAHARA.	Tohoku Imp. Univ. Science Rept. 11. 1922. p.207.
12.	C.H. DESCH.	'Intermetallic Compounds.' Longmans Green & Co. 1914. p.15.
13.	M. HANSEN.	'Der Aufbau der Sweistofflegierungen.' J. Springer. Berlin. 1936.
14.	A.H. COTTRELL.	'Theoretical Structural Metallurgy.' Arnold. London. 2nd Ed. 1955. p.129.
15.	L. PAULING.	J. Amer. Chem. Soc. 49. 1927. p.765.
16.	W.L. FINK & D.W. SMITH.	Trans. A.I.M.M.E. I28. 1938. p.223.

17.	R.F. MEHL & L.K. JETTER.	'Age-hardening of Metals'. Amer. Soc. Met. 1940. p.342.
18.	M.L.V. GAYLER.	J. Inst. Metals. 73. 1947. p.581.
19.	A.H. GEISLER, C.S. BARRETT & R.F. MEHL.	Trans. A.I.M.M.E. 152. 1943. p.182.
20.	W.L. FINK & D.W. SMITH.	Trans. A.I.M.M.E. 137. 1940. p.95.
21.	A.H. COTTRELL.	'Theoretical Structural Metallurgy.' 2nd ed. Arnold, London. 1955. p.50.
22.	M.L.V. GAYLER.	J. Inst. Metals. 60. 1937. p.249.
23.	G.I. FINCH & C.H. SUN.	Trans. Faraday Soc. 32. 1936. p.852.
24.	G.P. THOMSON.	Proc. Roy. Soc. 133A. 1931. p.1.
25.	J.H. VAN DER MERWE.	Faraday Soc. Disc. 5. 1949. p.201.
26.	G.W. JOHNSON.	Nature. 166. 1950. 189.
27.	T.N. RHODIN.	Faraday Soc. Disc. 5. 1949. p.215.
28.	A. WELLEMS.	Naturwiss. 31. 1943. p.232.
29.	F.C. FRANK & J.H. VAN DER MERWE.	Proc. Roy. Soc. 198A. 1949. p.305.
30.	G.P. THOMSON.	Proc. Physic. Soc. 16. 1948. p.403.
31.	R. WOOD.	Phil. Mag. 32. 1926. p.365.
32.	K. ESTERMANN.	Z. Elektrochem. 31. 1926. p.441.
33.	N. SEMENOFF.	Z. Physik. Chem. 7. 1930. p.471.
34.	E.T.S. APPLEYARD.	Proc. Physic. Soc. 49. 1932. p.118.
35.	R.G. PICKARD & O.S. DUFFENDACK.	J. Appl. Physics. 14. 1943. p.291.

36. H. LEVINSTEIN. J. Appl. Physics. 20. 1949. p.306.

37. T.A. McLAUGHLIN, R.S. SENNETT & G.D. SCOTT. Can. J. Res. 28A. 1950. p.530.

38. W. COCHRANE. Proc. Physic. Soc. 48. 1936. p.723.

39. U.R. EVANS. Nature. 157. 1946. p.732.

40. N.F. MOTT. Trans. Faraday Soc. 43. 1947. p.429.

41. E.J.W. VERWEY. Physica. 2. 1935. p.1059.

42. G.H. HASS & N. SCOTT. J. Physique Rad. 11. 1950. p.394.

43. G.H. HASS. Optik. 1. 1946. p.134.

44. W.H.J. VERNON. Trans. Faraday Soc. 23. 1927. p.156.

45. O. KUBACHEWSKI & E.E. HOPKINS. 'Oxidation of Metals and Alloys.' Butterworths, London. 1953. p.131.

46. J.S. HALLIDAY & W. HIRST. Proc. Physic. Soc. 68B, 1955. p.178.

47. E.A. GULBRANSEN & K.F. ANDREW J. Electrochem. Soc. 104. 1957. p.334.

48. R.W. HOFFMAN & H.S. STORY. J. Appl. Phys. 27. 1956. p.193.

49. J. MORET BAILLY. J. Physique Rad. 16. 1955. p.695.

50. P. BENJAMIN. Private communication.

51. L. LAFOURCADE. Theses No. 104 L'Universitie de Toulouse. 1954. p.85.

52. H.S. COLEMAN & H.L. YEAGLEY. Trans. Amer. Soc. Metals. 31. 1943. p.105.

53. P. MICHEL. Theses No. 31 L'Universitie de Strasbourg. 1955. p.22.

54. A.A. BARR, H.S. COLEMAN & W.P. DAVEY. Trans. Amer. Soc. Metals. 33. 1944. p.73.

55. R.M. BARRER. 'Diffusion in and through Solids.' Cambridge Press. 1951. p.285.

56. C. WAGNER. See W. Jost 'Diffusion'. Academic Press. New York. p.70.

57. J.S. KIRKALDY. Can. J. Physics. 35. 1957. p.435.

58. A. VAN ITHERBECK, L. DE GREVE, G.F. VAN VEELEN & C.A.F. TUGNEEM. Nature. 170. 1952. p.795.

59. A.J. BRADLEY & A. TAYLOR. Proc. Roy. Soc. 159A. 1937. p.56.

60. A.J. BRADLEY & S.S. LU. J. Inst. Metals. 60. 1937. p.319.

61. J-J. TRILLAT. Cahiers de Physique. 49. 1954. p.44.

62. W. SEITH. 'Diffusion in Metallen.' J. Springer. Berlin. 1939.

63. R. SMOLUCHOWSKI & H. BURGES. Physic. Rev. 76. 1949. p.309.

64. C.J. SMITHELLS. 'Metals Reference Book'. Butterworths, London. 1949. p.394.

65. R.M. BARRER. 'Diffusion in and through Solids.' Cambridge Press. 1951.

66. F.C. NIX & F.E. JAUMONT JR. Physic. Rev. 83. 1951. p.1275.

67. P. DRUDE. Weid. Ann. 1890. 36. p.865; 1890. 39. p.481.

68. P. DRUDE. Weid. Ann. 43. 1891. p.126.

69. J.C. MAXWELL-GARNETT. Phil. Trans. 203. 1904. p.385.
do. 205. 1906. p.238.

70. E. DAVID. Z. Physik. 114. 1939. p.389.

71. H. SCHOPPER. Z. Physik. 130. 1951. p.565.

72. E. MADELUNG. 'Die Mathematischen Hilfsmittel des Physikers.' Dover Press. New York. 1943. p.148.

73. H. WOLTER. Z. Physik. 105. 1937. p.269.

74. D. MALE. Comptes Rendus. 235. 1952. p.1630.

75. F. ABELES. J. Opt. Soc. Amer. 47. 1957. p.473.

76. M. PERROT. Theses No. 24 L'Universitie de Marseille. 1943.

77. L. TRONSTAD & C.G.P. FEACHEM. Proc. Roy. Soc. 145A. 1934. p.115.

78. O.S. HEAVENS. 'Optical Properties of Thin Solid Films.' Butterworths, London. 1955. p.206.

79. Handbook of Chemistry and Physics. Chemical Rubber Publishing Co. 37th Ed. 1955-56.

80. L.G. SCHULZ. J. Chem. Phys. 17. 1949. p.1153.

81. H. VON WORTENBURG. 'International Critical Tables.' 1929. 1st Ed. Vol. 5. p.248.

82. Physikalish Chemische Tabellen. 5th Ed. 1923. p.403.

83. R.S. SENNETT & N.W. SCOTT. J. Opt. Soc. Amer. 40. 1950. p.201.

84. P. BENJAMIN. Private communication.

85. D. MALE. Comptes Rendus. 230. 1950. p.1369.

86. D. MALE. J. Physique Rad. 11. 1950. p.332.

87. G. ESSERS-RHEINDORF. Ann. Physik. 28. 1937. p.297.

88. F. GOOS. Z. Physik. 106. 1937. p.297.

89. P. COTTON & P. ROUARD. J. Physique Rad. 11. 1950. p.657.

90. N. MOSTOVITCH & B. VODAR. 'Semi-conducting Materials.' Butterworths, London. 1951. p.260.

91. V. VAND. Proc. Physic. Soc. 55. 1943. p.222.

92. K. KREBS, H. NELKOWSKI & R. WINKLER. Z. Physik. 144. 1956. p.509.

93. H.A. MILEY. J. Amer. Chem. Soc. 59. 1937. p.2626.

94. H. KUHN & B.A. WILSON. Proc. Physic. Soc. 63B. 1950. p.745.

95. R.M. BARRER. 'Diffusion in and through Solids.' Cambridge Press, London. 1951. p.285.

96. F. SEITZ. 'Modern Theory of Solids.' McGraw-Hill. New York and London. 1940. p.3.

97. R.W.G. WYCKOFF. 'Crystal Structures.' Butterworths, London. 1949. Vol. 1. Chapter 2.

98. M. BANNING. J. Opt. Soc. Amer. 37. 1947. p.686.

99. O.S. HEAVENS. 'Optical Properties of Thin Solid Films.' Butterworths, London. 1955. p.177.

100. P. BENJAMIN. Ph.D. Thesis, University of Glasgow. In preparation.

101. R.M. HILL & C. WEAVER. Trans. Faraday Soc. To be published.

GENERAL REFERENCES AND BACKGROUND READING

BARRER, R.M. 'Diffusion in and through Solids'. Cambridge. 1951.

Cambridge University Press - 1st Ed.

BARRETT, C.S. 'Structure of Metals.' New York & London. 1943.

McGraw-Hill. - 1st Ed.

COTTRELL, A.H. 'Theoretical Structural Metallurgy.' London. 1955.

Edward Arnold - 2nd Ed.

HEAVENS, O.S. 'Optical Properties of Thin Solid Films.' London. 1955.

Butterworths - 1st Ed.

HOLLAND, L. 'Vacuum Deposition of Thin Films.' London. 1956.

Chapman & Hall - 1st Ed.

PINSKER, Z.G. 'Electron Diffraction.' London. 1953.

Butterworths - 1st Ed.

SMITH, G.C. 'Age Hardening of Metals.' Vol. 1. 1949. p.163.

Progress in Metal Physics Series.

LETTRES A LA RÉDACTION

VIEILLISSEMENT DES COUCHES D'ALUMINIUM DÉPOSÉES PAR ÉVAPORATION

Par C. WEAVER et R. M. HILL,
Dept. of Natural Philosophy, Royal Technical College, Glasgow.

Les couches d'aluminium déposées sur verre par évaporation sous vide élevé sont fréquemment utilisées comme surfaces réfléchissantes de miroirs. L'adhérence de ces couches au verre du support est malheureusement assez faible et c'est devenu une pratique courante de condenser une fine couche de chrome sur le verre aussitôt avant d'y déposer l'aluminium. Le chrome semble accroître la dureté et l'adhérence de la couche finale d'aluminium.

Heavens [1, 2] a suggéré que cette action pouvait être due à un effet de « sensitisation » ou d'orientation induite dans la couche d'aluminium. Pour étudier l'effet d'une variation de l'épaisseur de la sous-couche de chrome, il mesurait l'adhérence des couches en les égratignant avec une aiguille de gramophone chargée, et en cherchant la charge juste nécessaire pour arracher le film. L'accroissement d'adhérence était faible tant que les sous-couches de chrome avaient des épaisseurs inférieures à 300 Å, mais une augmentation nette de l'adhérence apparaissait pour des épaisseurs plus grandes de chrome.

Nous avons observé sur ces couches des effets de vieillissement qui accroissent l'adhésion. Celle-ci tend à atteindre une valeur constante après 14 jours environ à la température ambiante ou 3 jours à 120 °C. L'adhérence a été mesurée, par la méthode de Heavens, pour des films parvenus à un état stable. En portant la charge de l'aiguille juste nécessaire pour arracher le film en fonction de l'épaisseur de la sous-couche de chrome, on obtient un graphique à deux échelons : il faut un premier accroissement de charge de 200 g environ au moment où l'épaisseur de chrome atteint 20 Å, et un second quand elle dépasse 200 à 300 Å. De son côté, Heavens a obtenu 100 à 150 g pour des épaisseurs de chrome supérieures à 350 Å, mais ses mesures étaient probablement faites peu de temps après le dépôt, ce qui expliquerait la divergence.

Collins a examiné par diffraction électronique des couches d'aluminium déposées sur du chrome [2, 3], mais n'a pas pu mettre en évidence d'orientation de la couche. Le chrome lui-même ne présentait aucune orientation si on le déposait lentement et une orientation (110) pour un dépôt très rapide. La couche superposée d'aluminium ne présentait d'orientation en aucun cas, bien que l'aluminium déposé sur verre prenne une certaine orientation (100) [4].

On a suggéré que le vieillissement pouvait venir de la formation d'une pellicule dure d'oxyde qui résisterait à la pénétration. Des pesées à la microbalance n'ont montré aucune augmentation de poids après les 15 premières minutes, la formation de la couche d'oxyde étant presque complètement terminée au bout de ce temps. Cela s'accorde avec les courbes d'oxydation en fonction du temps obtenues par Mott [5], mais pas avec le vieillissement de longue durée observé.

Les diagrammes d'équilibre du système chrome-aluminium sont incomplètement connus, mais ces métaux donneraient 9 composés intermétalliques distincts [6]. On a cependant des diagrammes complets pour les systèmes nickel-aluminium et cobalt-aluminium, et dans les deux cas un sommet accusé indique la formation d'un composé stable à haute température de fusion. On sait que ces composés sont durs et tenaces, et qu'ils ont une grande énergie de formation. Les grandes analogies entre le chrome et les métaux en question, conduisent à supposer que l'un au moins des composés chrome-aluminium serait aussi très stable, de point de fusion élevé, et aurait une grande énergie de formation [7].

Lorsque nous déposons de l'aluminium sur du chrome, nous devons donc nous attendre à ce qu'une réaction intervienne à la surface de contact et forme une couche de composé intermétallique. Les courbes de vieillissement obtenues, tant à 120° qu'à température ordinaire, le confirment, car leur forme est caractéristique d'un processus de diffusion-précipitation. On suggère donc que la dureté et l'adhérence observées sont dues à une couche intermédiaire de ce composé intermétallique dur et tenace, adenté et trouvant prise dans l'aluminium plus tendre qui le recouvre. Ce composé renforcerait assez la pellicule pour lui permettre de résister à la distorsion produite par le test d'égratignure utilisé.

Nous poursuivons et étendons nos recherches, dont nous publierons plus tard un compte rendu détaillé.

Manuscrit reçu le 12 mai 1956.

BIBLIOGRAPHIE

[1] HEAVENS, (O, S.), *J. Physique Rad.*, 1950, **11**, 335.
[2] HEAVENS, (O. S.) et COLLINS (L. E.), *J, Physique Rad.* 1952, **13**, 658.
[3] COLLINS (L. E.), *Ph. D. Thesis*, University of Reading, 1954.
[4] RHODIN (T. N.) Jnr., *Farad. Soc. Disc.*, 1949, **5**, 215.
[5] MOTT (N. F.), *Trans. Far. Soc.*, 1947, **43**, 429.
[6] BRADLEY (A. J.) et LU (S. S.), *J. Inst. Metals*, 1937, **60**, 319.
[7] HANSEN (M.), Der Aufbau der Zweistofflegierungen, Springer, Berlin, 1936.

THE OPTICAL PROPERTIES OF CHROMIUM

by

Robert M. Hill and Charles Weaver

Department of Natural Philosophy

The Royal College of Science and Technology,

Glasgow.

One illustration in text

Short title - The Optical Properties of Chromium

Accepted for publication by The Faraday Society.

Abstract

An investigation into the optical properties of chromium is described, using the polarimetric technique. The results obtained show disagreement with the previously published values. It is suggested that this may be due to the presence of a polish, or oxide, layer on the specimens' surfaces. The refractive index of bulk chromium was measured as 1.13 - i1.06 for light of wavelength 5461 A. The surface film on a polished bulk metal sample was found to have a refractive index of 2.42, and a thickness of 50A. A thick evaporated specimen of the same metal was found to give similiar metallic values, and to sustain a surface film of the same thickness but of refractive index 2.23.

Introduction

In the theory of the reflection of light by a metal surface, two cases have to be considered, according to whether the electric vector of the incident wave is parallel or perpendicular to the plane of incidence, generally the phase shift and reflection coefficients are different in the two cases. Drude[1] considered the case of an incident beam plane-polarised at $\pi/4$ to the plane of incidence, and showed that in general the reflected beam would be elliptically polarised and that

the optical constants of the metal could be deduced from measurements of the ellipticity.

The method has been widely used to obtain the optical constants of metal surfaces, and the results should not depend on the angle of incidence, but measurements we have made upon chromium for a range of angles of incidence gave results which were not consistent but varied in a regular manner. Assuming the validity of the method, this casts doubts upon the assumption of a clean metal surface. If, however, the chromium metal is always covered with a surface film, probably oxide, it would naturally follow that measurements made upon such a surface would never yield directly the correct optical constants of the metal. Measurements made at different angles of incidence are quite likely in this case to give inconsistent results since the calculations ignore the presence of a surface film.

Drude[2] did extend his theory to cover the case where a thin, non-absorbing, surface film is present and showed that the refractive index and thickness of such a film could be calculated from polarimetric measurements, provided that similiar measurements could be made on a clean metal surface, or the optical constants of the underlying metal were known. This is not possible, however, in the case of chromium due to the rapid nature of the oxidation process.

A direct measurement of the refractive index of chromium does not appear to be feasible, but useful results have been obtained by

calculating the refractive index and thickness of the surface film upon a given specimen using approximate values of the optical constants(n,k) for the bulk metal and then varying these (n,k) values assumed for the metal until the calculated film index and thickness were the same for all angles of incidence.

Drude[1] has shown that for reflection from a plane metal surface at angle of incidence ϕ

$$n = (\sin\phi \tan\phi \cos 2\psi)/(1 + \cos\Delta \sin 2\psi) \quad \ldots\ldots\ldots\ldots(1)$$

$$k = n.\sin\Delta \tan 2\psi \quad \ldots\ldots\ldots\ldots(2)$$

where the refractive index of the bulk metal is given by

$$N = n - ik$$

and $\tan\psi$ = the ratio of the reflection coefficients R_p/R_s for the two components

Δ = the relative phase shift induced between the two components.

If, however, there be a film of refractive index n_1 on the metal, and its thickness is L, where the metal's bulk constants are still(n,k) then

$$(\Delta - \bar{\Delta}) = -\frac{4\pi L}{\lambda} \frac{\cos\phi \sin^2\phi}{(\cos^2\phi - a)^2 + a'^2} (1 - \frac{1}{n_1^2})(\cos^2\phi - a) \quad \ldots\ldots\ldots(3)$$

and

$$2(\psi - \bar{\psi}) = \frac{4\pi L}{\lambda} \frac{\sin 2\psi \cos\phi \sin^2\phi\, a'}{(\cos^2\phi - a)^2 + a'^2} (1 - n_1^2\cos^2\phi)(1 - \frac{1}{n_1^2}) \quad \ldots\ldots\ldots(4)$$

where $a = (n^2 - k^2)(n^2 + k^2)^{-2}$ $\quad a' = 2nk(n^2 + k^2)^{-2}$

and $(\Delta - \bar{\Delta})$ is the difference between the relative phase shifts on reflection with the film and without the film, and $(\psi - \bar{\psi})$ is the corresponding difference in reflection ratios, the measurements being made in air.

These equations have been rewritten[3] to give n_1 and L directly as functions of $(\Delta - \bar{\Delta})$, $(\psi - \bar{\psi})$, (n,k) and the angles $\bar{\psi}$ and ϕ.

i.e. $$n_1^2 = \left[1 + \frac{2(\psi - \bar{\psi})}{\Delta - \bar{\Delta}} \cdot \frac{\cos^2\phi - a}{a' \sin 2} \right] \frac{1}{\cos^2\phi} \qquad \ldots\ldots\ldots\ldots(5)$$

$$L = - \frac{\Delta - \bar{\Delta}}{A(1 - 1/n_1^2).180} \qquad \ldots\ldots\ldots\ldots(6)$$

where $(\Delta - \bar{\Delta})$ is measured in degrees and A is given by

$$A = \frac{4\pi}{\lambda} \frac{\cos\phi \sin^2\phi (\cos^2\phi - a)}{(\cos^2\phi - a)^2 + a'^2}$$

In order to calculate n_1 and L it is necessary to obtain values for the other quantities. Where there is no possibility of stripping the surface film to leave clean metal only Δ and ψ can be measured directly. However by postulating values for (n,k) the angles $\bar{\Delta}$ and $\bar{\psi}$ for the pure metal surfaces can be calculated. From equations (1) and (2) it can be seen that

$$\cos 2\bar{\psi} = 2ny (n^2 + k^2 + y^2)^{-1} \quad ; \quad \sin\bar{\Delta} = k(n \tan 2\bar{\psi})^{-1}$$

$\ldots\ldots\ldots\ldots(7)$

where $y = \sin\phi \tan\phi$

Upon substitution into equations (5) and (6), values can be obtained for n_1 and L. If the correct values have been chosen for (n,k) then n_1 and L will be constant for all the range of the angle of incidence.

Experimental

The experimental measurements were made using a modification of Drude's method, due to Tronstad[4]. Tronstad placed a compensator before the specimen, but after the polariser, giving an incident beam that was elliptically polarised. The ellipticity of this beam could then be adjusted to give plane polarised light after reflection at the specimen surface. The compensator used was a quarter-wave plate with its principal directions at $\pi/4$ to the plane of incidence, and the ellipticity was adjusted by rotation of the polariser. Plane polarised light was detected by obtaining an extinction position for the analyser. If P and A be the required angles of rotation of polariser and analyser respectively from the zero position taken parallel to the plane of incidence then it can be readily shown[4] that the relative phase shift between the two components and the angle between the electric vector of the reflected beam and the plane of incidence are given by the relationships

$$\sin\Delta = \cos 2P$$
$$\tan\chi = \tan A \qquad \text{.....(8)}$$

A diagram of the apparatus is given in fig.1. This is based on the polarising spectroscope of Tronstad. A half shade device was not used but instead the analyser was adjusted for extinction. This decreases the accuracy of the settings for the higher angles of incidence, but was found to be quite convenient.

A high pressure mercury lamp was used as the source S, with a mercury green filter F to obtain the 5461A line. A diffusing screen and aperture were mounted in front of the lamp at the focal distance of the lens L from the lens. This gave a parallel beam of monochromatic light and a second aperture was introduced just before the polaroid polariser to reduce any effect of scattered light. The polaroid sheet was mounted in a large ball race, carrying a 360° scale. After the polariser a mica quarter-wave plate was inserted with its principal directions at 45° to the plane of incidence of the specimen. A nicol prism was used as analyser, being mounted in a 90°-0-90° scale with a vernier attachment.

Polariser and analyser were adjusted alternately until an extinction position was found for the reflected light. At this position the angles of rotation of the polariser and analyser from the zero azimuth were measured.

Three samples of chromium bulk metal were investigated. A visual spectrographic comparison of their purity with a sample of known purity is given in Table I. The fourth sample listed in the table is that of the chromium chips used for the evaporation of a vacuum prepared

specimen. The impurities of the standard are listed in parts per million. The spectrographic comparison is only qualitative, i.e. where an impurity is listed as twice that in the standard then it is present to a greater amount, but not necessarily exactly double. The bulk metal specimens were polished to give a surface area of about 5 sq.cm. but a slight graininess was left on the surface due to the difficulty of polishing such a brittle metal as chromium.

The evaporated specimen was prepared in a vacuum of 5.10^{-5} mm. of mercury from the chromium chips whose purity is listed as specimen No.4. in Table I. The chips were packed into a tungsten helix so as to give as much surface contact betweem the metal and heater as possible. By this means a fairly thick film could be obtained with a constant evaporation rate, and without burning out the tungsten basket. The specimen used here was evaporated at 10 Angstroms/sec., and the thickness, measured by the Tolansky interferometric technique, was 580A. The optical transmission of the specimen was low, about $\frac{1}{2}$ per cent, and it showed a brownish tinge.

The evaporating chamber was pumped out by means of a rotary pump and a water cooled oil diffusion pump. At the evaporation pressure the metal charge was outgassed at a temperature just below the evaporating temperature with the condensimg slide well concealed by a shutter. As condensing plate a microscope slide was used. The slide had been washed in hot water and Teepol and polished with a lens tissue before mounting in the chamber. Before using the diffusion pump the slide was subjected

to a glow discharge for 15 minutes. The chamber was then pumped down by the diffusion pump. During the evaporation process no attempt was made to heat or cool the slide. After evaporation the slide was allowed to age in air for three months. The chromium film was a good reflector and no difficulty was experienced in the optical measurements.

Results of Optical Measurements

Table II shows the values obtained for the angles ψ and Δ for the specimens, assuming that there was no surface layer and applying the formula given in equation (8). It can be seen that there are no constant deviations from the mean for any of the bulk metal specimens. The scatter obtained at the larger angles of incidence was due mainly to the difficulty of obtaining sharp settings of the polariser and analyser. Without a half shade device the sensitivity is low at these angles and the extinction positions not sharp peaks as for the smaller values of ϕ. For this reason the results obtained from the larger angles are treated with caution. Complete agreement is not obtained between the evaporated specimen and the others, but this is not expected since the optical constants of thin films usually differ from those of the bulk material[5]. The settings for this specimen were much easier to obtain as the surface of this sample was much smoother than the others.

The values of (n,k) assuming a simple metal/air interface were calculated and are given in Table III. The wide range of values was not expected from the simple theory of an absorbing reflector. If

chromium is not a simple reflector and supports an absorbing film then the wrong theory has been applied. No allowance for surface films have been made in earlier published works and some of the results which have been obtained are listed in Table IV.[6-9]

As the published results do not appear to be consistent, and as the surface of the evaporated specimen had received no polishing or burnishing it appeared reasonable that in applying equations (5), (6) and (7) the first approximations to the bulk constants of chromium should be taken near to the values obtained for that specimen. In the early approximations using the evaporated specimen results, and a range of (n,k) values the refractive index of the surface layer n_1 was calculated for four values of angle of incidence (ϕ = 30°, 40°, 50°, 60°). Later results were calculated every five degrees and the results given in Table V were obtained. The finally accepted values for this specimen were taken as:

$$N = 1.18 - i0.944 \quad ; \quad n_1 = 2.230 \quad ; \quad L = 50 \text{ A.}$$

This was repeated with the results for the bulk metal specimen Number 3., as shown in Table IV, and for this the values obtained were:

$$N = 1.18 - i1.06 \quad ; \quad n_1 = 2.42 \quad ; \quad L = 50 \text{ A.}$$

In both cases we have taken our results to try to obtain maximum consistency in the refractive index values. The thickness value representing a further stage in the calculation and Tables V and VI

show only the final approximations. Some idea of the wide variations we have encountered may be obtained from Table VII. This table gives some of the earlier results obtained using a series of widely spaced values for the refractive index of the metal. Some general trends may be observed in the refractive index values but the variations in thickness are more irregular and it is thus more difficult to use these as a guide. The degree of agreement on the thickness values of our final results is comparatively good, particularly since the measurements at high angles of incidence are subject to a larger error in our experimental measurements Such variations as still exist may be due to the fact that there will not be a sharp boundary between oxide and metal but a transition region where oxide and metal are intermingled. The effect of such a transition layer would vary with angle of incidence.

Conclusions

We have assumed a surface film and attempted to choose the optical constants of the underlying metal so as to obtain consistency in the constants of the surface film, but the degree of consistency obtained simultaneously in the results for both the refractive index and the thickness appears to provide some indication of the validity of the method. Further confirmation is obtained from the agreement between the refractive index figures for surface films on polished metal and evaporated films respectively.

The refractive index figures in both cases compare favourably

with the tabulated value of 2.5 for chromium oxide.[10] This suggests that the surface film is chromium oxide and the thickness of 50 Å obtained is probably the ultimate value for complete coverage of a perfectly smooth surface according to the theories of oxide formation at room temperature.[11] The effect of mechanical polishing does not appear to have any pronounced effect upon the nature and thickness of the surface film, and the measured optical constants of the metal do not appear to be affected by pure flow of the type suggested by Beilby although the burnishing and compacting may partially account for the slightly higher figures obtained for the optical constants of both the bulk metal and its oxide layer. It is, however, common for evaporated films to have densities which are lower than those of the bulk material and to have correspondingly lower refractive indices. In our results, if we assume that the refractive index of the film on the evaporated specimen is lower due to the presence of voids which are not present in oxide films on bulk metal, it would appear that about 12 per cent., by volume,[12] of the film may be in the form of voids. This is not unreasonable and higher figures have been obtained by Schulz[13] for voids in evaporated dielectric films. High purity chromium was used for our bulk specimens but small amounts of impurity appear to have little effect on the optical properties.

We wish to acknowledge the help given by the Union Carbide Co., Ltd., the Alreco Metal Corporation, Ltd., and Henry Wiggin & Co., Ltd. in providing specimens and by the research Dept., Babcox & Wilcox, Ltd.

in preparing and polishing the surfaces used, and for the spectrographic analysis.

One of us (R.M.H.) wishes to thank the Caird Trust, Dundee for provision of a post-graduate scholarship to allow this work to be undertaken.

REFERENCES

1. Drude. Weid. Ann. 1890, 36, 885 ; 1890, 39, 481.

2. Drude. Weid. Ann. 1891, 43, 126.

3. Tronstad. Trans. Faraday Soc. 1935, 31, 1151.

4. Tronstad & Feachem. Proc. Roy. Soc. 1934, A145, 115.

5. Heavens. 'Optical Properties of Thin Solid Films' Butterworth London 1st. Ed. 1955 p206.

6. Wortenburg. 'International Critical Tables' 1st. Ed. 1929 Volume 5, p248.

7. Physikalisch Chemische Tabellen, 5th. Ed. 1923, p403.

8. Sennett & Scott. J. Opt. Soc. Am. 1950, 40, 201.

9. Abeles. J. Opt. Soc. Am. 1957, 47, 473.

10. Handbook of Chem. & Phys. Chemical Rubber Publishing Co. 37th. Ed. 1955-6

11. Gulbransen & Andrew. J. Electrochem. Soc. 1957, 104, 334.

12. Heavens. 'Optical Properties of Thin Solid Films' Butterworth London 1st. Ed. 1955 p128

13. Schulz. J. Chem. Phys. 1949, 17, 1153.

TABLE I

Purity of Chromium Specimens

Impurity	No.1	No.2	No.3	No.4	Standard
Iron	4	1	2	3	1(2ppm)
Silicon	6	1	5	4	1(1ppm)
Copper	2	2	4	5	1(1ppm)
Manganese	2	1	4	3	1(1ppm)
Magnesium	1	1	1	1	1(1ppm)

Suppliers of metal samples:

No.1 Union Carbide Co.

No.2 Alreco Metal Corpn. Ltd.

No.3 Wiggin Nickel Co.

No.4 Hopkin and Williams

TABLE II

Experimental values obtained for the angles

χ and Δ for the range of specimens

Angle of Incidence	Values of χ				
ϕ	No.1	No.2	No.3	Mean of Bulk Nos.1,2 & 3	No.4
30°	43.2°	43.5°	43.13°	43.2°	42.0°
35°	42.4°	42.5°	42.3°	42.4°	40.9°
40°	41.3°	41.4°	41.65°	41.5°	39.17°
45°	40.4°	40.5°	40.2°	40.4°	38.2°
50°	39.1°	39.25°	38.6°	39.2°	36.69°
55°	37.3°	37.3°	37.2°	37.3°	34.65°
60°	35.5°	34.8°	35.9°	35.5°	32.22°
ϕ	Values of Δ				
30°	171.8°	171.0°	172.0°	171.7°	172.4°
35°	169.1°	168.1°	169.1°	168.8°	169.5°
40°	165.6°	165.1°	164.0°	165.1°	165.8°
45°	162.6°	160.9°	160.4°	161.3°	161.3°
50°	158.8°	156.0°	156.0°	156.5°	156.0°
55°	152.7°	151.0°	159.7°	151.5°	148.7°
60°	146.0°	143.8°	142.0°	143.8°	141.0°

TABLE III

Results of calculation of refractive indices

Angle of Incidence	Mean of bulk metal samples		Evaporated specimen values	
ϕ	n	k	n	k
30°	1.25	3.40	2.19	2.76
35°	1.45	3.38	2.17	2.63
40°	1.63	3.35	2.15	2.56
45°	1.78	3.43	2.13	2.63
50°	1.91	3.50	2.10	2.85
55°	2.01	3.51	2.15	3.40
60°	2.09	3.52	2.17	3.97

TABLE IV

Summary of published values for the

optical constants of bulk and evaporated chromium

n	k	Wavelength	Source
2.97	4.87	5790 A	Wortenburg[6]
3.53	4.41	5460 A	Physikalisch Chemische Tabellen[7]
3.28	4.35	5460 A	Sennett & Scott[8]
2.49	2.30+	5460 A	Abeles[9]

+ This last specimen was vacuum evaporated.

TABLE V

Calculation of refractive index and thickness of the surface film for a range of (n,k) - Evaporated specimen

Angle of Incidence	n - ik					
ø	1.20 - i0.96		1.15 - i0.92		1.18 - i0.944	
	n_1	L	n_1	L	n_1	L
30°	2.24	46 A	2.16	40 A	2.220	44 A
35°					2.225	44 A
40°	2.36	41 A	2.15	48 A	2.206	49 A
45°					2.238	48 A
50°	2.27	48 A	2.31	37 A	2.242	53 A
55°					2.240	65 A
60°	2.29	81 A	2.25	83 A	2.238	68 A

TABLE VI

Calculation of refractive index of the surface film for a range of (n,k) with thickness values for the best fit.

Bulk metal specimen

Angle of Incidence	n - ik				
ϕ	1.18 - i0.826	1.18 - i0.944	1.18 - i1.00	1.18 - i1.062	
	n_1	n_1	n_1	n_1	L
30°	2.60	2.52	2.50	2.50	34 A
35°				2.46	36 A
40°	2.42	2.40	2.40	2.42	41 A
45°				2.40	44 A
50°	2.40	2.34	2.38	2.40	48 A
55°				2.36	61 A
60°	2.22	2.34	2.40	2.44	68 A

TABLE VII

Calculation of refractive index and thickness of the surface film of the evaporated specimen

Initial values

Angle of Incidence	n - ik							
∅	0.5 - i1.4		0.5 - i1.0		1.0 - i1.0		1.5 - i1.0	
	n_1	L	n_1	L	n_1	L	n_1	L
30°	1.35	614A	1.62	513A	2.73	105A	2.94	45.2A
40°	1.37	402A	1.57	641A	2.06	146A	2.46	68.2A
50°	1.64	563A	1.84	662A	2.27	281A	2.48	112A
60°	1.72	352A	1.99	366A	2.36	311A	2.40	327A

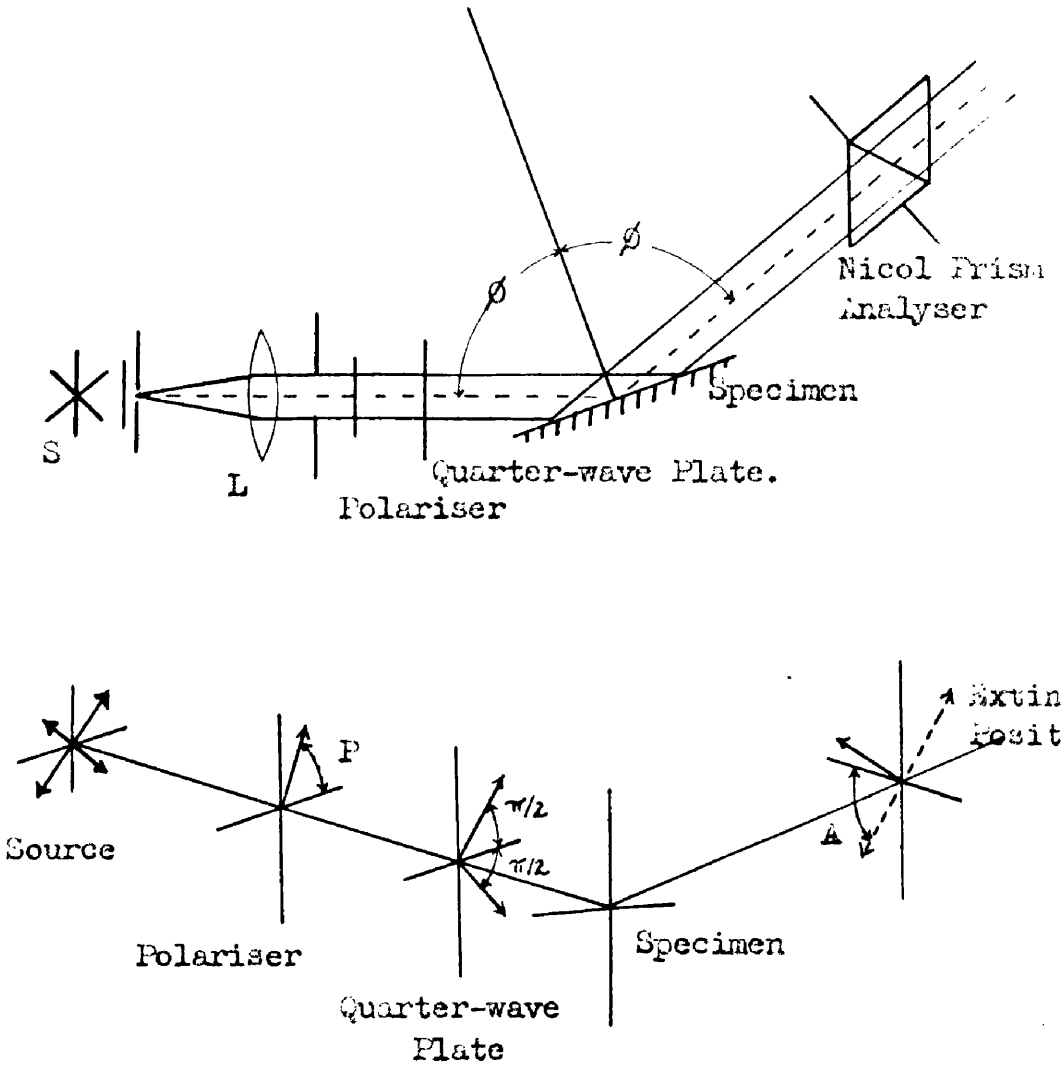

Fig.1 . Polarising Spectroscope, with Vector Diagram.

THE OPTICAL PROPERTIES OF EVAPORATED CHROMIUM FILMS.

by

Robert M. Hill & Charles Weaver

The Royal College of Science and Technology, Glasgow, C.1.

Short Title

Optical Properties of Chromium Films

Six Diagrams in text

One Table in text

Recommended for publication

by the Faraday Society - April, 1958.

ABSTRACT

The structures of very thin, vacuum evaporated, films of chromium are investigated by optical methods. The optical constants for a series of films of varying thicknesses are calculated from reflectivity and transmission measurements, and the films are found to be inhomogeneous. The changes in the optical constants with thickness are found to be inconsistent with either the Maxwell-Garnett theory of spherical particles or with Schopper's theory of ellipsoidal aggregates. It is suggested that the anomalous refractive index values are due to the presence of a very thin layer of oxide around each individual metal particle. Assuming that the particles have an ellipsoid shape, results are obtained which agree with the experimental values. It is found that the thickest film can be considered as consisting of two separate layers of different refractive indices, the surface layer exhibiting bulk optical properties, and the first deposited layer having the optical properties of the metal and oxide particles described above.

INTRODUCTION

The optical properties of thin metallic films of a homogeneous nature have been investigated by a number of authors[1-4]. In the earliest works the films were regarded as possessing bulk optical constants and the changes in reflectivities and transmission with thickness were calculated. Little agreement was found with the experimental measurements. It was suggested that this was due to aggregation within the films, and theoretical investigations were undertaken assuming at first spherical, then later ellipsoid particles of the bulk material. Considerable agreement has been found with the latter with the results from the experimental investigations.

Inhomogeneous films, however, have not been subjected to such investigations, as it was felt that such films would be practically impossible to consider from a theoretical viewpoint. Measurements[5] of the optical constants of the surface of a thickly evaporated inhomogeneou film material, using chromium as an example, have shown that the refractive indices were apparently different from those of the bulk material. However, a similar investigation, taking into account the effect of a surface oxide layer, has shown that agreement can be obtained for certain cases.

EXPERIMENTAL

Thin films of chromium were prepared by evaporation under high vacuum conditions in a demountable vacuum system consisting of a glass bell-jar, evacuated by a metal vacuum system with an oil diffusion pump and a rotary backing pump. The evaporations were carried out at pressures in the range $4 - 6.10^{-5}$ mm. Hg. The chromium metal was evaporated from a tungsten heater wound in a helical spiral to form a small cup, the chromium metal being in the form of very small chips. During the evaporation the rate of deposition was maintained at about 5A/sec. A shutter, operated through a Wilson seal was used to cover the heater until it had been brought up to the operating temperature and the chromium outgassed. The deposition was started by swinging the shutter to one side, and terminated by swinging the shutter back into position. This reduced the possibilities of impurities being present. The films were deposited on microscope slides which were thoroughly cleaned before use. The slides were scrubbed with cotton wool dipped in Teepol; once this had been washed off with hot water the slides were partially dried with more cotton wool. The drying process was completed with the aid of a well-washed linen duster, and immediately before mounting in the chamber, the slides were polished with lens tissue and subjected to

the breath figure test. During the process of pumping out the chamber the slides were subjected to a glow discharge for 15 minutes.

The film thicknesses were monitored during deposition by measuring the transmission of the film using white light. A barrier type photocell was mounted behind the slide and its output was measured directly on a sensitive galvanometer. A collimated beam of white light was reflected from a shielded prism inside the vacuum chamber onto the specimen slide, and through it onto the cell. The final reading of the galvanometer gave a measure of the film thickness and the photocell was calibrated by weighing a number of test slides of different transmissions. This was carried out on a microbalance immediately after removal from the vacuum chamber. The weight thicknesses, d_{wt}, of these slides were then calculated, assuming the bulk density for chromium to apply to the films. A calibration curve was constructed by plotting these weight thicknesses against the transmission.

The microscope slides were removed from the chamber immediately after evaporation and the films were allowed to age for a period of three weeks before the optical measurements were made. A few of the slides were measured immediately after evaporation, and again after the

ageing period, but negligible changes in the measured quantities were found. The refractive indices of the films were calculated using Male's method[1] which requires that the reflectivity of the metal-air face, R, that of the substrate-metal interface, R', and the transmission, T, be known. These reflectivities and transmission were measured on a reflectometer consisting of a monochromator and a photo-multiplier cell. The monochromator gave a parallel beam of light of the desired wavelength $\pm$ 50A and was designed to cover the whole of the visible spectrum, but measurements were only undertaken at 5460A. The intensity of the incident beam was measured by placing the photo-multiplier opposite the monochromator and then a specimen slide was introduced into the beam to obtain the transmission. The reflectivities were measured by swinging the photo-multiplier round so that light reflected off the specimen's surface at an angle of 7^{o} was measured. Precautions were taken so that the cell should not be overrun, but ageing and fatigue effects were quite noticeable and the system had to be constantly checked and zeroed. The results obtained were, however, very consistent and repeatable.

As the films were evaporated onto a non-absorbing, parallel-sided substrate the measured reflectivities and

transmission, R_o, R'_o and T, respectively, had to be corrected to give the values for the metal films alone. The quantities R, R' and T were calculated from the measurements R_o, R'_o, and T_o by means of the equations

$$R = R_o - (T_o^2.R_g)/(T_g + R'_o.R_g - R_g)$$

$$R' = (R'_o - R_g)/(T_g + R'_o.R_g - R_g)$$

$$T = (T_o.T_g)/(T_g + R'_o.R_g - R_g)$$

where R_g and T_g are the reflectivity and transmission of the substrate material.

Male's method of calculation of refractive indices requires that a range of refractive indices (n - ik) be assumed, where n and k are allowed to vary independently, together with a range of thickness, d_o. The reflection and transmission coefficients, R, R' and T, are then calculated and graphed as functions of δ for each pair of n,k values over the range of d_o, δ being given by $4\pi nd_o/\lambda$. The calculations can be readily made by a graphical method also due to Male[2]. This gives a series of curves of R, R' and T respectively against δ, each curve corresponding to a given pair of n,k values. Using the measured value of T for a given film, a horizontal line can be drawn to cross the theoretical transmission curves, each intersection with these curves giving a value of δ and values of n and k

which would together satisfy the transmission condition.

Each set of values of n,k and δ associated with an intersection enables the corresponding R and R' to be obtained from the series of reflectivity curves already drawn. Using the figures thus obtained, R can be plotted against n for each given k value, and similarly for R'. This gives two sets of curves and from each set a series of n,k values can be obtained by drawing a horizontal line at a level corresponding to the observed reflection coefficient. The first series of values of n,k satisfy simultaneously the R and T conditions, and the second series satisfy simultaneously the R' and T conditions. Using these two series of values two curves can be obtained by plotting k against n and the intersection of these curves gives unique n,k values which satisfy the observed values for R, R' and T. Knowing the refractive index $n_e - ik_e$ for the film the δ value can readily be obtained from plots of n against δ for given k values. Hence, the apparent thickness, d_o, can be obtained.

As a check on the accuracy of the determination the reflectivities and transmissions were recalculated from the $n_e - ik_e$ values. This reverse calculation eliminates the possibility of any gross error, and comparison with the experimental values give an indication of the inaccuracies

of the method. The recalculated values were found to agree closely with the experimental results.

The values of n_e and k_e obtained in this way were found to vary with the thickness of the films in the manner shown in Fig. 1. These results are in good agreement with those obtained by other authors for a number of metal films[3] wherein the real part of the complex refractive index increases as the film thickness decreases, whilst the absorption coefficient tends towards zero as the thickness becomes zero. It must be admitted that, in general, the refractive index of a metallic film cannot readily be measured directly and that the values are deduced from measurements of reflectivity and transmission. Repeated attempts to explain the observed reflectivity and transmission coefficients whilst assuming films to have the same optical constants as the bulk metal have been unsuccessful. The variations in the calculated values of refractive index cannot be explained in terms of thickness phenomena in the same manner as restriction of mean free path of electrons can be used[6] to explain the rapid rise in resistivity of very thin metal films. Indeed it does not appear to be possible to explain the experimental results as long as it is assumed that the films are continuous and homogeneous.

Examination of the structure of thin films using

the electron microscope[7-8] has shown that, in most cases, metallic films have a granular structure and that this is most pronounced for the thinner films, but persists even for large thicknesses. This has led to attempts to interpret experimental observations in terms of an aggregated structure and the simplest model is obtained by assuming that the aggregates can be regarded as approximately spherical particles.

The optical properties of spherical particles embedded in a dielectric medium have been investigated by Maxwell-Garnett[9]. He tried to explain the properties of coloured glasses by considering a thick layer of dielectric in which were embedded a number of particles whose diameters were much smaller than the wavelength of incident light. His theory has been applied to thin evaporated films, for most metals do not form continuous films even for thicknesses of several atomic layers, but grow in the form of aggregates which have a roughly spherical shape. Such a film will contain a large volume of voids if the particles are presumed to have almost the same diameters. This reduces the effective density and if the density of the bulk metal has been used to calculate the thickness of such a film from the weight as determined by some gravimetric method, thus giving the weight thickness, d_w; this will be found

to be much less than the actual thickness, d_o, which was obtained by optical measurements. The ratio, d_m/d_o, gives the ratio of the metal content to the actual volume and is called the packing factor of the film and being given the symbol 'q'.

The Maxwell-Garnett theory states that if the film can be represented as containing this volume fraction q of metal of refractive index, n'_b, in a medium of refractive index unity, the effective refractive index, n'_e, is given by

$$\frac{n'^2_e - 1}{n'^2_e + 2} = q \cdot \frac{n'^2_b - 1}{n'^2_b + 2} \quad \ldots\ldots\ldots\ldots (1)$$

For a number of the films investigated, q was calculated using for n'_e the experimentally determined values, and for n'_b the bulk optical constants of chromium that had been measured previously[10]. In every case the quantity q was found to be complex. Thus it can be said that the results did not agree with the Maxwell-Garnett theory and the films could not be represented as being composed of particles, possessing the bulk refractive index.

The Maxwell-Garnett theory has been extended to a more sophisticated form by David[11] and Schopper[12]. They assumed that the particles were not spheres but ellipsoids

of revolution, having the unique axis perpendicular to the substrate. David considered that the films could be represented by a substance of dielectric constant, ε_i, in a medium of dielectric constant, ε_a. Madelung's[13] ellipsoidal coordinates were used in which the coordinates (x,y,z) are replaced by (μ,ν,ϕ) where

$$\begin{aligned} x &= \alpha\,(\mu^2+1)^{\frac{1}{2}}\,(1-\nu^2)^{\frac{1}{2}}\cos\phi \\ y &= \alpha\,(\mu^2+1)^{\frac{1}{2}}\,(1-\nu^2)^{\frac{1}{2}}\sin\phi \qquad \ldots\ldots\ldots (2) \\ z &= \alpha\,\mu\,\nu \end{aligned}$$

For this system, μ = a constant, defines an ellipsoid surface. We let the particle have axes a, b and b, then

$$\begin{aligned} \tfrac{1}{2}a &= \alpha\,\mu_o \\ \tfrac{1}{2}b &= \alpha(\mu_o^2+1)^{\frac{1}{2}} \end{aligned}$$ where α is a constant.

This ellipsoid is then considered to be placed in an electric field of value unity in the x direction. The solution of the Laplaceian equation for the potential within the particle is

$$\phi_i = -x + Cx\left\{\frac{\pi}{2} - \tan^{-1}\mu_o - \mu_o/(1+\mu_o^2)\right\}$$

and outside $\ldots\ldots\ldots (3)$

$$\phi_a = -x + Cx\left\{\frac{\pi}{2} - \tan^{-1}\mu - \mu/(1+\mu^2)\right\}$$

the surface of the ellipsoid being defined by $\mu = \mu_o$, and C is a constant dependent on the shape of the particle.

At this boundary the displacements must be equal across the boundary

$$\varepsilon_i \frac{\delta \phi_i}{\delta u} = \varepsilon_a \frac{\delta \phi_a}{\delta u}$$

on substituting for ϕ one obtains the form

$$\varepsilon_i \left\{ - \frac{\delta x}{\delta \mu} + C \frac{\delta x}{\delta \mu} \left(\frac{\pi}{2} - \tan^{-1} \mu_o - \mu_o/(1 + \mu_o^2) \right) \right\} =$$

$$\varepsilon_a \left\{ - \frac{\delta x}{\delta \mu} + C \frac{\delta x}{\delta \mu} \left(\frac{\pi}{2} - \tan^{-1} \mu - \mu/(1+\mu^2) \right) + Cx \left(- \frac{\delta}{\delta \mu} \tan^{-1} \mu - \frac{\delta}{\delta \mu} (\mu/(1+\mu^2 \right.\right.$$

..... (4)

but $\frac{\delta x}{\delta \mu} = \frac{x\mu}{1+\mu^2}$; $\frac{\delta}{\delta \mu} \tan^{-1} \mu = \frac{1}{1+\mu^2}$; $\frac{\delta}{\delta \mu} \left(\frac{\mu}{1+\mu^2} \right) = \frac{1 - \mu^2}{(1+\mu^2)^2}$

and as the equality is at the surface, $\mu = \mu_o$.

Thus, on substituting into equation (4) we obtain

$$(\varepsilon_i - \varepsilon_a) \left\{ - \frac{x\mu_o}{1+\mu_o^2} + C \frac{x\mu_o}{1+\mu_o^2} \left(\frac{\pi}{2} - \tan^{-1} \mu_o - \frac{\mu_o}{1+\mu_o^2} \right) \right\}$$

$$= \varepsilon_a \, Cx \left\{ - \frac{1}{1+\mu_o^2} - \frac{1 - \mu_o^2}{(1+\mu_o^2)^2} \right\}$$

$$C = \frac{\varepsilon_i - \varepsilon_a}{\{(\varepsilon_i - \varepsilon_a)f + \varepsilon_a\}} \cdot \frac{\mu_o(1 + \mu_o^2)}{2} \qquad \ldots\ldots\ldots (5)$$

where $f = \frac{1}{2}\mu_o(1 + \mu_o^2)\left\{ \frac{\pi}{2} - \tan^{-1} \mu_o - \mu_o/(1 + \mu_o^2)\right\}$.

But the part of ϕ_a which is disturbed by the presence of the ellipsoids will tend for large values of x to the limit,

$$Cx\left\{\frac{\pi}{2} - \tan^{-1} \mu - \mu/(1 + \mu^2)\right\} \longrightarrow \quad Cx\ \mu^2(2/3) \rightarrow C\alpha^3\ 2x/(3r^3) \qquad \ldots\ldots\ldots (6)$$

where $r^2 = \alpha^2(\mu^2 - \nu^2 + 1)$.

This is, however, the potential of a dipole of strength $C\alpha^3(2/3)$. From the relationship $D = E + 4\pi P$, we can see that the corresponding displacement will be

$$D = 4\pi C\alpha^3\ \varepsilon_a(2/3) \qquad \ldots\ldots\ldots (7)$$

But the total electric polarisation of a thin layer of material is given by

$$P.Vs = (\varepsilon_i - \varepsilon).\ \varepsilon_o.E.Vs \qquad \ldots\ldots\ldots (8)$$

where Vs is the volume of the film per unit surface area. If the layer is made up of an assembly of droplets, each contributing to the polarisation, the total polarisation from each droplet, p_a, will be

$$p_a = D.V_k.\varepsilon_o.E$$

where V_k is the total volume of the droplets and D the displacement per unit volume of film material. If N is the number of droplets per unit area, the total displacement is

$$N.p_a = D.N.V_k.\varepsilon_o.E = D.d_w.\varepsilon_o.E$$

the weight thickness, d_w, being given by the product $N.V_k$. Here we are assuming that the shape of the droplets is constant, then it follows that

$$(\varepsilon_i - \varepsilon_a)\ \varepsilon_o.E.Vs = D.d_w.\varepsilon_o.E$$

and thus

$$D = (\varepsilon_i - \varepsilon_a).d_o/d_w \qquad \ldots\ldots\ldots (9)$$

When equations (7) and (9) have been equated we obtain the displacement relative to volume to be

$$\frac{\Delta(\varepsilon_i - \varepsilon_a)\frac{d_o}{d_w}}{\Delta V} = \frac{C\alpha^3.\varepsilon_a\ (8\pi/3)}{\Delta V}$$

but the volume of an ellipsoid in these coordinates is

$$V = a.b^2.\pi/6 = \pi.\alpha^3.\mu_o(1 + \mu_o^2).4/3$$

Thus it follows that

$$C = \tfrac{1}{2}\mu_o(1 + \mu_o^2) \cdot \frac{\Delta}{\Delta V}\left\{\frac{(\varepsilon_i - \varepsilon_a)}{\varepsilon_a} \cdot \frac{d_o}{d_w}\right\} \qquad \ldots\ldots\ldots (10)$$

Therefore, on equating equations (5) and (10)

$$\frac{\Delta}{\Delta V}\left\{(\varepsilon_i - \varepsilon_a)\cdot\frac{d_o}{d_w}\right\} = \frac{\varepsilon_i - \varepsilon_a}{\left\{(\varepsilon_i - \varepsilon_a)/\varepsilon_a\right\} f + 1}$$

If the system is considered as representing a metal of refractive index (n - ik) in air then the above equation resolves to

$$\frac{\Delta}{\Delta V}\left[\left\{(n_e - ik_e)^2 - 1\right\}\frac{d_o}{d_w}\right] = \frac{(n - ik)^2 - 1}{\left\{(n-ik)^2 - 1\right\} f + 1} \quad \ldots (11)$$

which is the form that Schopper obtained.

For the films examined the volume is only changing by virtue of a change in thickness. The quantity $\Delta/\Delta V$ can then be replaced by the change relative to thickness $\Delta/\Delta t$. The right hand side of the above equation thus represents the changes in refractive index to be expected for the system as the thickness of the film increases. The quantity, f, represents a function of the axial ratio of the particles and gives an indication of the shape of the ellipsoids. The form of the function with varying axial ratio is given in Fig. 2, where it can be seen that for bulk material, $b \gg a$, the function f tends to zero. This result, it can be seen, is in accordance with equation (11), where for f = 0, the right hand side gives

the bulk value of refractive index.

Schopper tried to apply this theory to his measurements on evaporated gold films, having already tried the simpler Maxwell-Garnett theory without success. However he was still unable to obtain very good agreement as long as he assumed that all the particles in a given film had approximately the same shape. He therefore suggested that there was a statistical distribution and assumed that the mean value of f was $\bar{f}$. The distribution function is then

$$g(f) \propto f.\exp(-f/\bar{f})^2$$

and the quantity, C, in equation (5) has to be replaced by a mean value $\bar{C}$ where

$$\bar{C} = \frac{(n - ik)^2 - 1}{\{(n - ik)^2 - 1\}\bar{f} + 1}$$

$$= \frac{\int C.g(f)df}{\int g(f)df} \qquad \ldots\ldots\ldots\ldots\ldots (12)$$

This form of the equation was applied to the change in refractive index for gold films, by Schopper, with some success. He eliminated the problem of correlating the f function and the thickness by stating that as f was a function of the size of the particles it could be used to replace the thickness and graphs of the

real and imaginary parts of $\bar{C}$ were constructed directly as functions of $\bar{f}$ instead of d. The experimentally determined points were then fitted to the graph of the real function irrespective of their thickness, as can be seen in Fig. 3a. This gave values of $\bar{f}$ for each set of experimental results. Then on to the graph of the imaginary function were plotted the corresponding points, using the $\bar{f}$ values obtained earlier. The proximity of the points in Fig. 3b to the curve shows the agreement Schopper obtained.

We have tried to apply this theory to our observations on chromium films. The optical constants of the surface of our thickest evaporated film of chromium had already been obtained by polarimetric measurements[10] and found to agree closely with values obtained for the bulk metal. These values were substituted into equation (11) and plotted against f which is approximately inversely proportional to thickness, as can be seen in Fig. 3, thus giving the graph shown in Fig. 4. This does not in any way compare with the experimental values of

$$\frac{d_o}{d_w}\,(n_e^2 - k_e^2 - 1) \quad ; \quad \frac{d_o}{d_w}\,(2n_e k_e)$$

which are calculated in Table I. Schopper's assumption of a statistical distribution does not make any improvement whatever.

In an attempt to find a theoretical curve which would agree with our experimental points, it was found convenient to replace the bulk optical constants n and k by two other functions A and B, where

$$A = n^2 - k^2 - 1$$
$$B = 2.nk \qquad \ldots\ldots\ldots\ldots (13)$$

Then the equation (11) can be replaced by the equation

$$\frac{\Delta}{\Delta V}\left\{\left[(n_e - ik_e)^2 - 1\right]\frac{d_o}{d_w}\right\} = \frac{A - iB}{Af + 1 - iBf}$$

$$= \frac{(A^2 + B^2)f + (A - iB)}{(Af + 1)^2 + B^2f^2} \qquad \ldots\ldots\ldots\ldots (14)$$

A series of graphs were constructed for a range of (A,B) values to try and obtain a fit between the experimental points and a theoretical curve. A few of the curves obtained are shown in Fig. 5. In order to reproduce the peaked effect of the experimental curves it was found to be necessary to have A negative and B numerically much smaller than A. The best fitting curve for the thinner films was obtained with the values

$$A = -9.0 \quad ; \quad B = 2.0$$

In this attempt to find a theoretical curve which

would, even approximately, agree with our experimental results we have used Schopper's equation without assuming a statistical distribution. When we used equation (12) employing an assumed Gaussian distribution we found that it was completely impossible by any choice of A and B values to reproduce the peaked effects which were observed in the experimental curves.

Chromium films, however, unlike those of gold have been said to be inhomogeneous. The inhomogeneity of our films was calculated using the Wolter relationship[14] as a measure of the degree of inhomogeneity. Wolter has shown that for a perfect film lying in air on a substrate of refractive index, n_2, the absorption of light passing from the air side (A) can be related to that in the opposing direction (A') by the relationship

$$n_2 \cdot A = A'$$

where the thickness of the film is small compared to the wavelength of the incident light. This forms a convenient test and was applied to those of our chromium films whose thicknesses were less than 1,000A.

The absorptions of the films were obtained from the reflectivities and transmission coefficients for

$$A = 1 - R - T \quad ; \quad A' = 1 - R' - T$$

The values obtained are listed in Table I as a numerical

fraction given by $(n_2A - A')$. It can be seen that the relationship holds only for the thinnest of our films and tends towards a maximum as the thickness increases. This is exactly what we would expect for a series of inhomogeneous films, for the relationship must hold at zero thickness, where both A and A' are negligible, and as T decreases both A and A' will tend to constant values. These results then show conclusively that the films studied were inhomogeneous and very different from the films of gold studied by Schopper.

In applying his theory to evaporated gold films, Schopper was unable to obtain good agreement when he assumed that all particles in a given film had the same shape factor and he therefore suggested that there would be a distribution of particles having different shape factors and assumed a statistical distribution as the most probable. There will almost inevitably be a distribution of some nature but at any given stage of film deposition, the particles in the lower layers are most unlikely to be affected. This means that the variation of f value with thickness must be due to the formation of new surface layers in which particles are predominantly of lower f and greater axial ratio than the underlying particles.

There is no observable variation in surface

properties across a film surface and this leads us to suggest that the particles being formed at any given stage of film growth are of approximately the same size and shape factor but the size and axial ratio both increase with successive layers. This change from layer to layer would account for the lack of homogeneity which has been shown by the Volter relation.

In any given film the larger and more recently formed particles will account for the bulk of the thickness and the earlier, small particles will have little effect and could, in a first approximation, be neglected and a single f value used for a given film.

Assuming the values of A and B used to obtain the theoretical curve shown in Fig. 6, the refractive index of the metal forming the aggregates was calculated by substitution into equation (13) giving

$$n' = 0.36 - i2.80$$

a result that is in total disagreement with the previously determined bulk constants of chromium. We had already obtained, in the earlier work, by polarimetric reflection methods from the reflecting surface of the thickest film

$$n'' = 1.18 - i0.944$$

and for the same film by Male's method

$$n''' = 0.64 - i1.25$$

We have thus obtained for one film three independent and dissimilar results for the optical constants by three different methods. If each of these is correct within the limitations imposed by the method of measurement, then it should be possible to interrelate them. Male's method measures a mean optical constant, being based on the three quantities reflection at each surface and transmission through the film. If we consider that the film is composed of a number of strata planes parallel to the substrate, then the properties of the last layer were measured by the surface reflection method, and by fitting the experimental results for the thinnest films to the (A,B) curve, we should have from the A and B values the refractive index of the first strata. If we then simplify the problem to consider only the first and last levels, and we let the relative thickness of the first be s, and of the last 1 - s, we should have the relationship

$$n''' = s.n' + (1 - s).n'' \quad \ldots\ldots\ldots\ldots (15)$$

holding at least approximately.

For the above results equating the real parts gave s = 0.659, and the imaginary s = 0.154. These

evidently divergent figures were disappointing but the degree of fit obtained in Fig. 6 for the films below 100A suggested that the general lines of the theory were correct, and gave correct values of A and B. An attempt was made to extend the theory to make it more suitable for the films under examination.

In the statement of David's and Schopper's theory it was accepted that the metal was in a simple dielectric. But while investigating the optical properties of bulk and evaporated chromium in the earlier work it was found that the metal sustained a very thin oxide film. This suggests that each particle may carry a thin film of oxide and, in this case, the theory is inadequate. We must postulate that the metallic particles of dielectric constant, ε_i, are surrounded by a thin layer of oxide of dielectric constant, ε_o, which then is placed in the dielectric media, ε_a.

We can give the potential equations for these three media in unit field in the x direction as

$$\begin{aligned}
\phi_i &= -x + Cx\left\{\frac{\pi}{2} - \tan^{-1}\mu_o - \mu_o/(1+\mu_o^2)\right\} \\
\phi_o &= -x + Cx\left\{\frac{\pi}{2} - \tan^{-1}\mu_o - \mu_o/(1+\mu_o^2)\right\} \quad \ldots\ldots (16) \\
\phi_a &= -x + Cx\left\{\frac{\pi}{2} - \tan^{-1}\mu - \mu/(1+\mu^2)\right\}
\end{aligned}$$

Here we are assuming that the surface layer is so thin that μ is constant throughout its width and equal to the value defining the boundary of the metallic particle. At each boundary the displacements must be equal and, as the layer is so thin, we let the displacement be continuous, i.e.

$$\varepsilon_i \frac{\delta\phi_i}{\delta\mu} = \varepsilon_o \frac{\delta\phi_o}{\delta\mu} = \varepsilon_a \frac{\delta\phi_a}{\delta\mu}$$

$$\text{i.e.} \quad 2\varepsilon_i \frac{\delta\phi_i}{\delta\mu} = \varepsilon_o \frac{\delta\phi_o}{\delta\mu} + \varepsilon_a \frac{\delta\phi_a}{\delta\mu}$$

If we substitute for the appropriate values of ϕ and differentiate, we obtain

$$(2\varepsilon_i - \varepsilon_o - \varepsilon_a) \left\{ - \frac{2\mu_o}{1+\mu_o^2} + C \frac{x\,\mu_o}{1+\mu_o^2} \left(\frac{\pi}{2} - \tan^{-1}\mu_o - \frac{\mu_o}{1+\mu_o^2} \right) \right\}$$

$$= \varepsilon_a Cx \left\{ - \frac{1}{1+\mu_o^2} - \frac{1-\mu_o^2}{(1+\mu_o^2)^2} \right\}$$

thus

$$C = \frac{2\varepsilon_i - \varepsilon_o - \varepsilon_a}{\{(2\varepsilon_i - \varepsilon_o - \varepsilon_a)/\varepsilon_a\} f + 1} \qquad \ldots\ldots\ldots (17)$$

where the function f has the same value as before.

For large values of x the limit of equation (6)

still holds, and thus

$$\frac{\Delta}{\Delta V}\left\{(\varepsilon_i - \varepsilon_a)\frac{d_o}{d_w}\right\} = \frac{(2\varepsilon_i - \varepsilon_o - \varepsilon_a)}{\{(2\varepsilon_i - \varepsilon_o - \varepsilon_a)/\varepsilon_a\} f + 1}$$

If we consider that this equation is to apply to a metal of refractive index $(n - ik)$, having an oxide of refractive index (ν) in air, then the above equation will become

$$\frac{\Delta}{\Delta V}\left[\left\{(n_e - ik_e)^2 - 1\right\}\frac{d_o}{d_w}\right] = \frac{2(n-ik)^2 - \nu^2 - 1}{\left\{2(n-ik)^2 - \nu^2 - 1\right\} f + 1} \quad \ldots (18)$$

If we now let

$$A' = 2(n^2 - k^2) - \nu^2 - 1$$

$$\text{and} \quad B' = 4.nk \quad \ldots\ldots\ldots (19)$$

then

$$\frac{\Delta}{\Delta V}\left\{\frac{d_o}{d_w}\left[(n_e^2 - k_e^2 - 1) - 2in_ek_e\right]\right\} = \frac{A' - iB'}{A'f + 1 - iB'f}$$

$$= \frac{(A'^2 + B'^2)f + (A' - iB')}{(A'f + 1)^2 + B'^2 f^2} \quad \ldots\ldots\ldots\ldots (20)$$

which is in the same form as equation (14).

We now have to substitute for A' and B', where as before the best fit is given by Fig. 7 and

$$A' - iB' = -9.0 - i2.0$$

The refractive index of the oxide formed on evaporated films had already been measured as 2.230, giving, after substitution, into equation (19)

$$n' = 0.49 - i1.32 \quad .$$

Assuming that this represents the refractive index of the first layers and that the film could again, to a first approximation, be regarded as made up of two layers only, the upper layer having the refractive index

$$n'' = 1.18 - i0.944$$

the relative thicknesses were recalculated as before giving for the real part of s, 0.308, and for the imaginary, 0.295. These figures are in remarkable agreement and this means that the refractive index, as obtained by Male's method, appears to be an accurate average of the refractive indices of the first and last layers of the film.

DISCUSSION

The picture originally presented by David and Schopper was of a thin film composed of a number of aggregates having a shape approximating to an oblate spheroid with the short axis perpendicular to the substrate. We have modified this theory by assuming that each aggregate is surrounded by a thin layer of oxide which could be

produced by the residual gas in the vacuum chamber during evaporation. Formation of an oxide film is certainly to be expected with a metal such as chromium. The modified picture certainly seems to be true for film thicknesses below 100A.

The change in the Wolter relationship, even for weight thicknesses below 100A, suggests that the growth takes place in layers, and the variations of the f value over this range leads us to suggest that the first layer of a chromium film may be composed of small aggregates. These aggregates would be almost spherical in shape and they are overlaid by successive layers of larger aggregates having higher axial ratios and lower f values. The progressive change in f values does not appear to continue above 100A and our measurements on a thick film showed that the top layers differed very little from bulk chromium values. It would appear that above 100A the individual aggregates are growing so large that they touch and the structure approximates to a continuous metal structure. This would be in general agreement with existing evidence on film growth. Electron microscope studies by McLaughlan, Sennett and Scott[15] on silver films show that the interstices between aggregates finally become very small and many disappear.

This transition at approximately 100A weight thickness from an aggregated structure to a continuous metal film would explain the success of our approximation in regarding a thick film as composed of two layers only. For transmission properties this would certainly hold, for the properties of the underlayer would be determined mainly by the layers of large aggregates, and very little by the much thinner layers of small aggregates.

The value of 0.49 - il.32 obtained for the refractive index of the material forming the aggregates certainly does not agree with any value previously determined for bulk chromium, but this is hardly to be expected. Even within the aggregates themselves the metal probably has a looser, more open structure than bulk metal, and this would account for the real part of the refractive index being lower. Such a structure would also account for an increased absorption coefficient as the internal resistivity would be higher and there would be considerably more scattering than for a continuous structure.

Going back to our original results as given in Fig. 1, it will be noticed that the absorptive coefficient increases up to a thickness value of d_o = 400A, which from Table I corresponds to a weight thickness of about 100A. Further layers having a continuous, denser structure would

have a much lower absorption and would therefore cause the overall absorption for thicker films to fall steadily as observed experimentally.

Our theoretical treatment is still imperfect even though such good agreement was obtained for the films below 100A in thickness. It assumes that there exists a continuous range of f values, or shape factors, for the aggregates up to a limiting value f = 0, at which the aggregates would be infinitely extended in the plane of the film to form a continuous thin uniform sheet. The f value being inversely related to the thickness, this means that the top layers of a thick film should have the same structure as bulk metal. The axis intercepts at f = 0 made by our theoretical curve, as shown in Fig. 6, do not agree with the measured constants for the bulk metal or even with the measured constants observed by polarised light methods for the surface layer of a very thick film.

Our results suggest that chromium films are aggregated only up to a limiting thickness of about 100A and that subsequent layers are continuous and denser, approximating to the bulk metal structure, the constants obtained by Male's method being an average between these two structures in the ratio of their respective thicknesses.

We have therefore tried to modify our curve as given in Fig. 6 by drawing a continuous curve joining our results for thin films to a point on the axis which corresponded to the measured value of the real part of the refractive index for the bulk metal. Upon fitting our experimental points to this new curve we found that each point was displaced considerably to the left of its original position, towards f = 0, or bulk values as our averaging would lead us to anticipate. The corresponding imaginary points fell upon a continuous curve. The new graph of the imaginary function was continuous with our results for the thinner films and made an intercept on the vertical axis which corresponded with the measured imaginary part of the refractive index for the bulk metal. The points (corresponding to films of 80A and 168A thickness) which deviated most from our new curves are the same results that deviated most from the general trend of the packing fraction or q values given in Table I.

One of us, R.M.H., would like to thank the Caird Trust for the provision of a post-graduate grant to allow this work to be undertaken.

TABLE I

n_e	k_e	d_o in A	d_w in A	$\frac{d_o}{d_w}(n_e^2 - k_e^2 - 1)$	$\frac{d_o}{d_w}(2n_e k_e)$	n_2A-A'	q
2.20	1.80	119	20	+3.07	47.1	0.037	.17
1.60	2.00	200	40	-12.2	32.0	0.022	.20
1.57	2.05	260	50	-14.3	33.5	0.098	.19
1.60	2.05	272	50	-14.4	30.2	0.106	.19
1.25	2.10	340	72	-18.2	25.8	0.203	.21
0.96	2.12	436	80	-24.9	22.2	0.123	.18
0.95	2.05	476	100	-19.9	18.05	0.139	.21
0.97	1.93	561	168	-12.63	12.6	0.148	.30
0.72	1.77	796	220	-13.1	9.25	0.157	.28
0.70	1.45	1055	273	-10.1	7.84	-	.26
0.58	1.45	1400	480	-8.61	5.24	-	.34
0.64	1.25	1810	537	-7.5	5.64	-	.30

REFERENCES

1.	MALE.	Comptes Rendus. 1950. 230. 1369.
2.	MALE.	J. Physique Rad. 1950. 11. 332.
3.	ESSERS-RHEINDORF.	Ann. Physik. 1937. 28. 297.
4.	GOOS.	Z. Physik. 1937. 106. 606.
5.	ABELES.	J. Opt. Soc. Amer. 1957. 47. 473.
6.	FUCHS.	Proc. Camb. Phil. Soc. 1938. 34. 100
7.	SENNETT & SCOTT.	J. Opt. Soc. Amer. 1950. 40. 203.
8.	LEVINSTEIN.	J. Appl. Physics. 1949. 20. 306.
9.	MAXWELL-GARNETT.	Phil. Trans. 1904. 203. 385.
10.	HILL & WEAVER.	Trans. Faraday Soc. To be published.
11.	DAVID.	Z. Physik. 1939. 114. 389.
12.	SCHOPPER.	Z. Physik. 1951. 130. 565.
13.	MADELUNG.	'Die Mathematischen Hilfsmittel des Physikers'. Dover Press. New York. 1st Ed. 1943. p.148.
14.	WOLTER.	Z. Physik. 1937. 105. 269.
15.	McLAUGHLAN, SENNETT & SCOTT.	Can. Jour. Res. 1950. A28. 530.

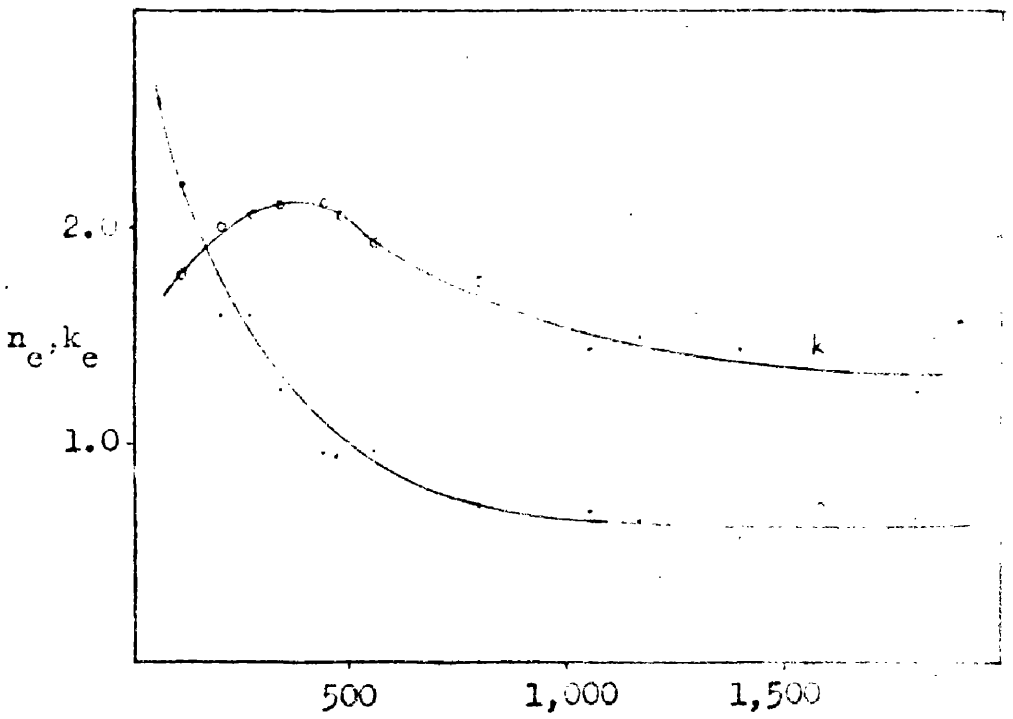

Fig.1. Variation of refractive index of Chromium films with thickness

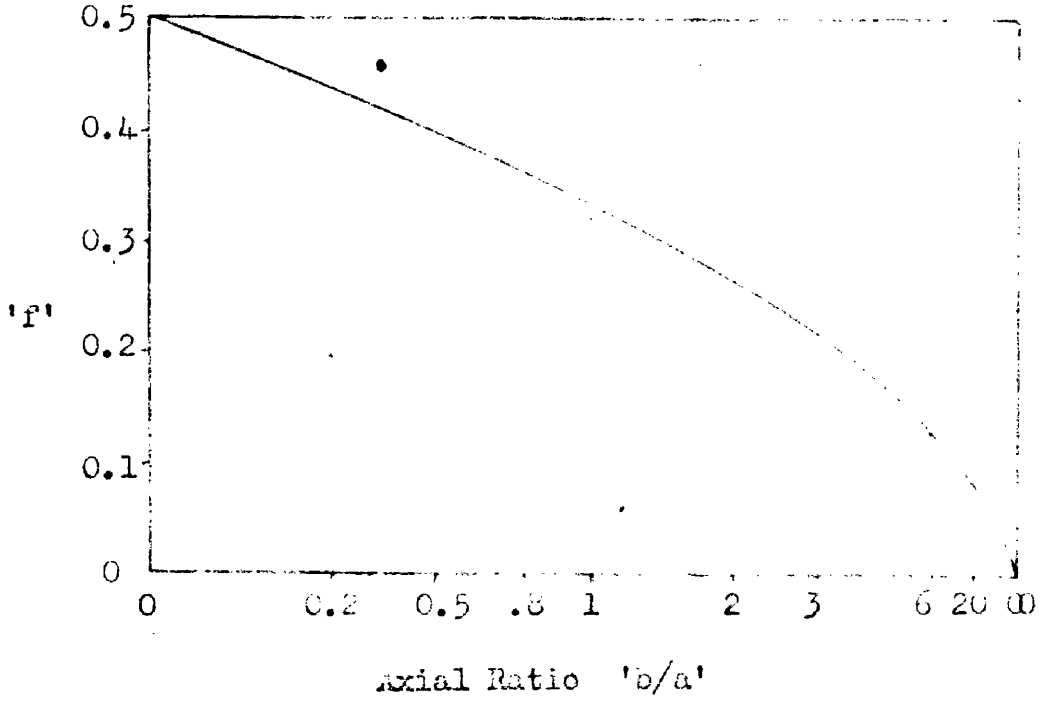

Fig.2. Variation of David's function 'f' with axial ratio.

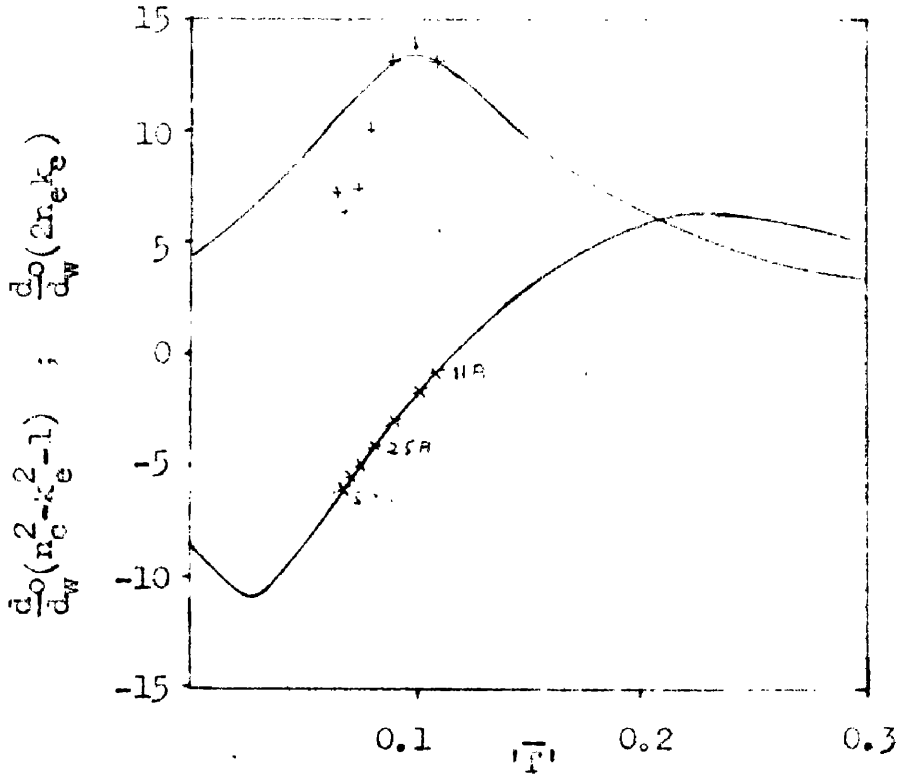

Fig.3. Variation with $\bar{f}$ of the optical constants of Gold particles, and Schopper's experimental results.

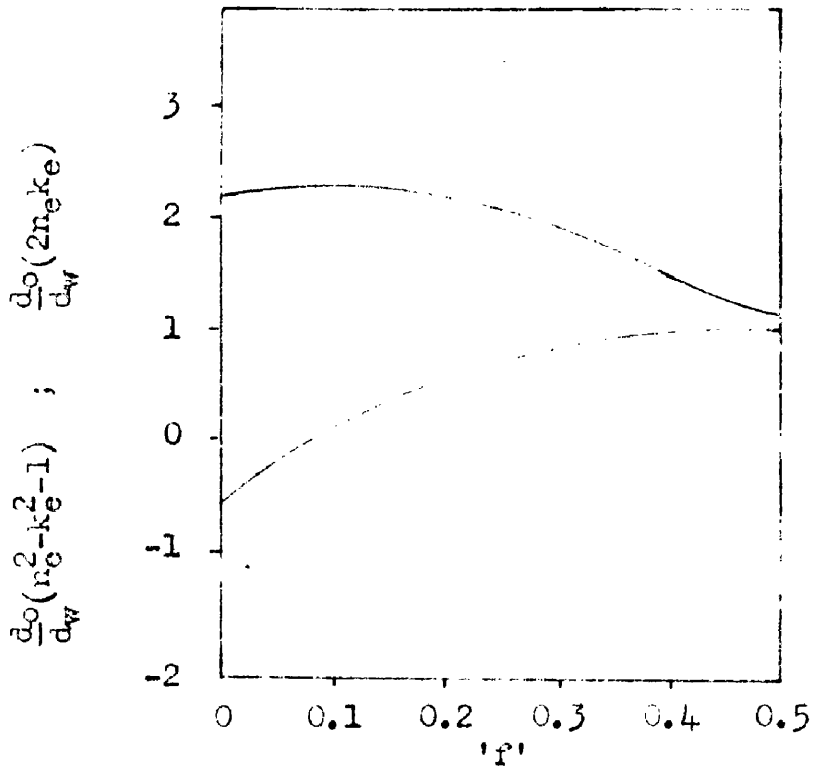

Fig.4. Variation with f of the optical constants of Chromium particles, assuming bulk refractive index.

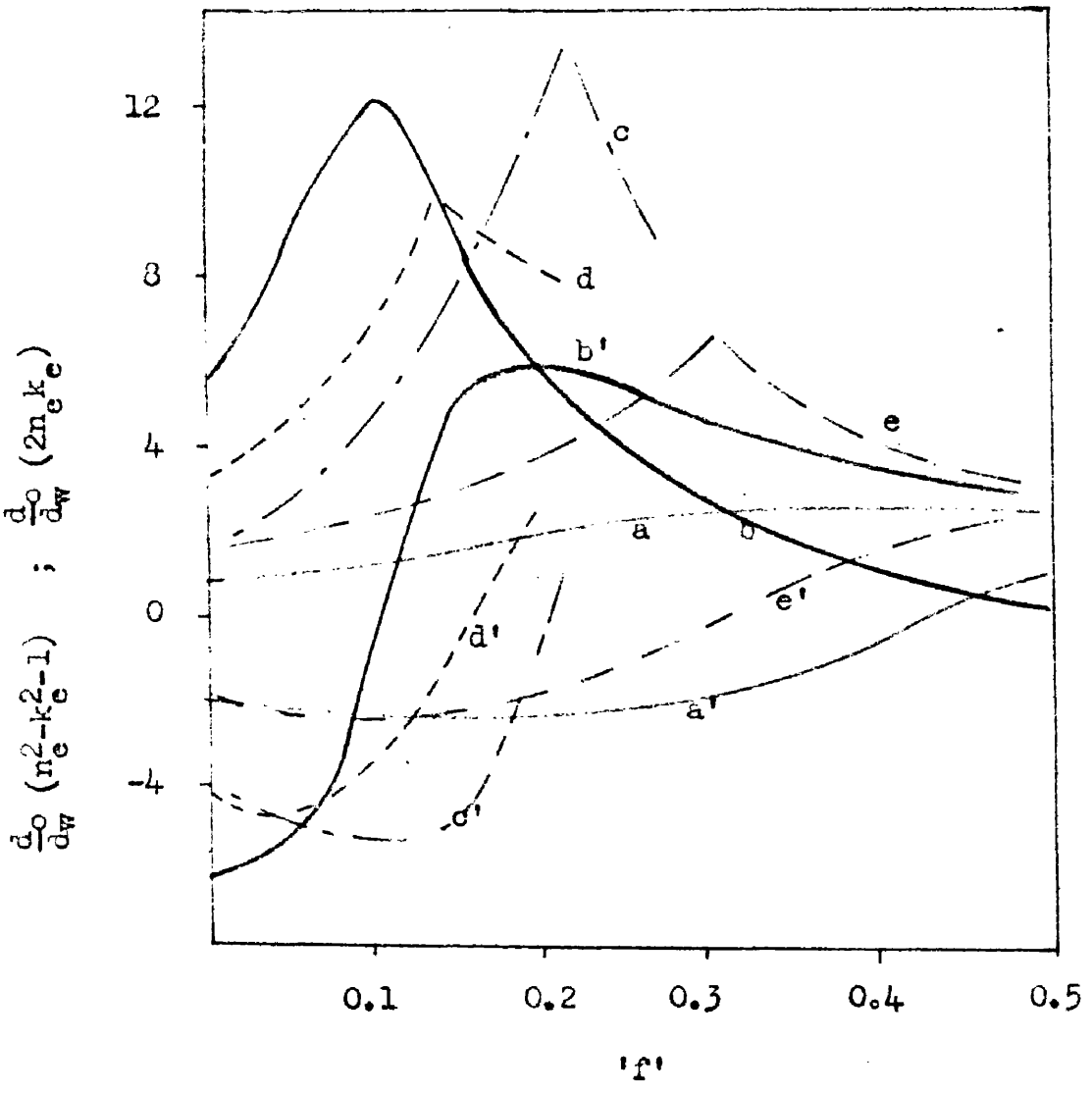

Fig.5. Form of a series of A - iB graphs for varying f functions.

(a) A - iB = -2.0 - i0.8

(b) A - iB = -6.0 - i5.0

(c) A - iB = -4.1 - i1.6

(d) A - iB = -4.2 - i3.0

(e) A - iB = -2.15 - i1.5

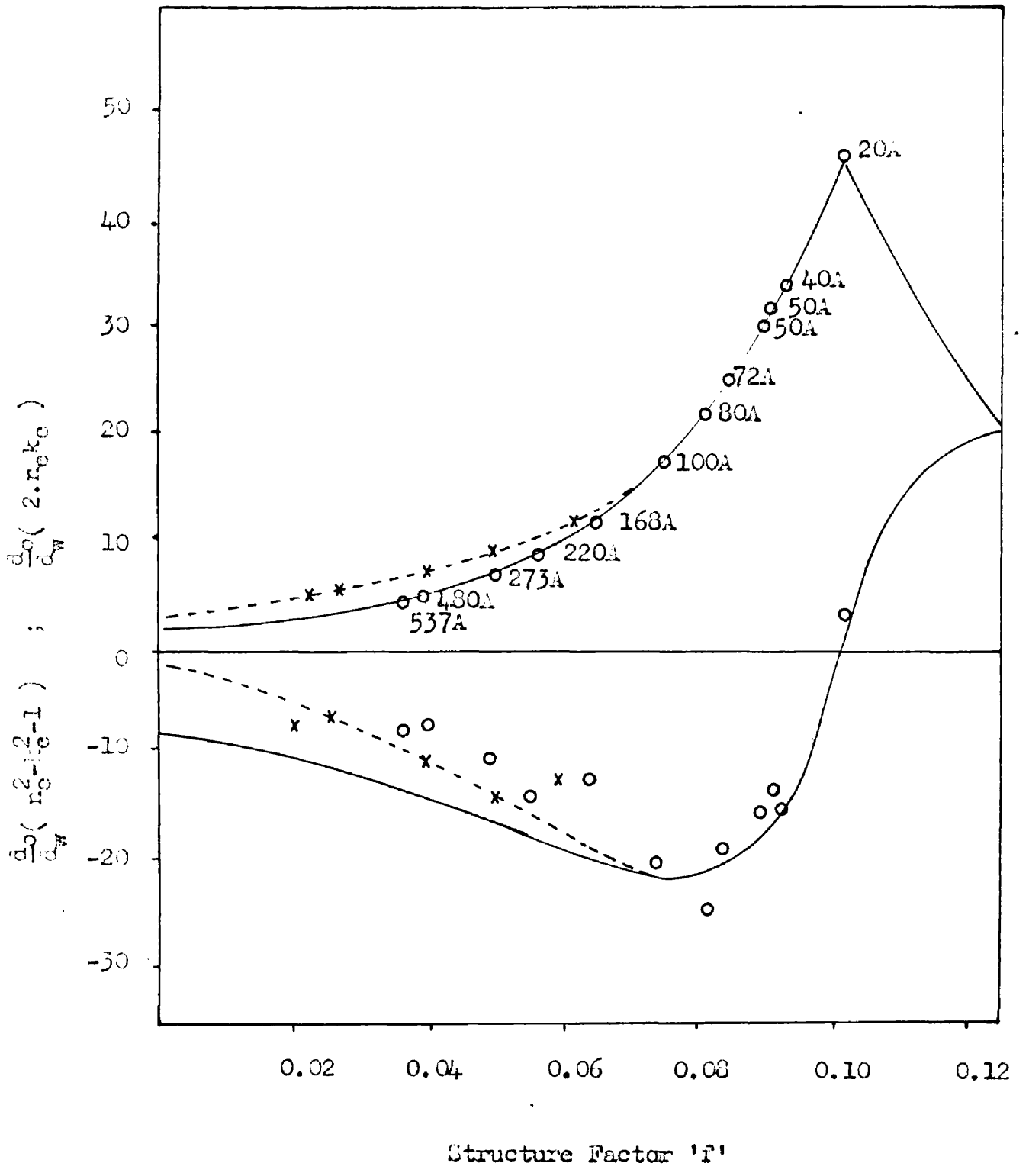

Fig. 6. The best fit of the experimental points for chromium films to an A - iB curve.